University of Alberta

Investigation of CT beneath MFT Deposition for Oil Sands Tailings Disposal

By

Gengxin Luo 

A thesis submitted to the Faculty of Graduate Studies and Research in partial fulfillment of the requirements for the degree of Master of Science

In

Environmental Engineering

Department of Civil and Environmental Engineering

Edmonton, Alberta

Fall 2004

Your file Votre référence
ISBN: 0-612-95808-6
Our file Notre référence
ISBN: 0-612-95808-6

Acknowledgements

I would first like to thank Syncrude Canada Ltd., Suncor Energy Inc., and Canadian Natural Resources Ltd., for their generous funding to this project. Without the companies' initiative and financial support, this project would not be a reality.

Despite the many difficulties and problems from the project planning to realisation, as my supervisors, Dr. Selma Guigard and Dr. Phillip Fedorak have shown their relentless support, instruction, and great effort to make this project move forward. Their knowledge and thoughts were among the key factors in making this project run in the right way. The study of this project also benefited very much from Dr. Fedorak's previous experiences of working with oil sands tailings.

Special thanks are to Dr. Mike MacKinnon, from Syncrude Canada Ltd., whose desire to better understand the tailings disposal of CT beneath MFT scheme initiated this project. His expertise, experience, and novel ideas set the general direction for this project.

Without the support of many technical staffs in Environmental Engineering, Biological Sciences, and Geotechnical Engineering groups at the University of Alberta, and Syncrude Research Centre in Edmonton, it would be impossible to make this project run smoothly. Particular thanks are to Debra Long, Garry Solonynko, and Nick Chernuka (Environmental Engineering group) for their routine technical supports in my laboratory work; to Debbi Coy

(Biological Sciences group) for her enthusiasm and commitment in the MPN analysis, and her technical coaching on the MPN analysis for me; to Gerry Cyre and Steve Gamble (Geotechnical Engineering group) for their support in column preparation and frozen column cutting; to Betty Fung (Syncrude Research Centre in Edmonton) for the demonstration in handling the oil sands tailings samples in her laboratory. Also, the supports for sample analyses provided by the Syncrude Analytical Group at the Edmonton Research Centre are much appreciated.

Many students in the Environmental group have given me a timely hand in the need of support, especially the help provided by the students from Dr. Selma Guigard's research group at the time of column filling and assembly.

I appreciate the work completed by Jianmin Pang, who conducted the laboratory work from June 2003, in the Environmental Engineering Laboratory, at the University of Alberta.

Finally, thanks are to all the authors referenced in the thesis.

Gengxin Luo

May 2004

Table of Contents

List of Tables

List of Figures

List of Abbreviations

AVS	acid volatile sulphide
BDL	below detection limit
CT	composite tailings or consolidated tailings
CT-L	lower zone of the CT layer
CT-U	upper zone of the CT layer
d	day
EC	electrical conductivity
Eh	redox potential
g	gram or gravity
GC	gas chromatography
H	height
He	Helium
h	hour
ID	inside diameter
L	litre
M	mole per litre
MFT	mature fine tailings
MFT-L	lower zone of the MFT layer
MFT-U	upper zone of the MFT layer
mg	milligram
mL	millilitre
MPN	most probable number
ms	millisecond
NA	not available
nd	non-detectable
nL	nanolitre
NST	non-segregating tailings
OD	outside diameter
ORP	oxidation - reduction potential
s	second
SRB	sulphate-reducing bacteria
t_{incu}	incubation time
t_R	retention time
USEPA	United States Environmental Protection Agency
wk	week
y	year

1.0 Introduction

The two original commercial oil sands companies, Syncrude Canada Ltd. and Suncor Energy Inc., have used a caustic-based Clark Hot Water Extraction process to recover bitumen from oil sands in Alberta, Canada, since the late 1960's. This process produces large quantities of aqueous slurry, called extraction tailings. The extraction tailings are a mixture of solids, water, salts, and unrecovered bitumen (MacKinnon 1989). The tailings are not released to the environment, but are stored in large settling basins (also called tailings ponds). Once in the tailings ponds, the fast-settling coarse sands fraction settles out on the beaches and is used to construct dikes for the tailings ponds. The remaining muddy liquids make up the fine tailings, which consist of slow-settling clay and silt particles, dissolved inorganic and organic substances, residual bitumen, and water.

The fine tailings are allowed to dewater and densify over time in the tailings ponds. After 2 to 3 y of relatively rapid densification a dense mature fine tailings (MFT) zone will be produced at the bottom of the tailings ponds. The released water on the top layer of the tailings ponds is reused for extraction process (List and Lord 1997). The MFT has a solids content of greater than 30 wt%. The dewatering and densification of MFT under natural conditions are very slow, with consolidation into a trafficable consistency expected to take hundreds of years (FTFC 1995).

The large volume of MFT poses a big challenge to oil sands companies. To increase the MFT densification rate and reduce the inventory of existing

MFT, the oil sands companies (Syncrude and Suncor) have proposed the CT (Composite Tailings in Syncrude and Consolidated Tailings in Suncor) technology (FTFC 1995). In CT production, the MFT, coarse solids, and gypsum are mixed together. The addition of gypsum causes the clay particles to aggregate and the slurry viscosity to increase. Thus, the fine solids and coarse solids would stay together at deposition, creating non-segregating tailings (NST) (Matthews *et al.* 2000). The initial solids content of CT is approximately 60 wt%. When the CT slurry is deposited, the CT deposit starts dewatering immediately. The CT deposit will densify to a solids content of approximately 75 wt% within a few weeks or months. CT will become trafficable within a few years, leading to a dry landscape at site restoration. The CT release water has to be recycled back to the plant, primarily for the extraction process. It is essential that this CT water not to be detrimental to bitumen recovery efficiency and plant integrity. The CT technique has been under research since 1990 (List and Lord 1997).

In the CT process, the optimum dosage of gypsum would be around 1000 mg/L (i.e. 1 kg gypsum per m^3 of CT slurry) (Matthews *et al.* 2000). As a result of the high gypsum dosage, the CT release water contains a high concentration of calcium (Ca^{2+}) and sulphate (SO_4^{2-}) (MacKinnon *et al.* 2000). These high concentrations of Ca^{2+} and SO_4^{2-} could decrease bitumen recovery and cause other process problems when reused for process recycling. To address this issue, the oil sands companies have been examining various treatment options, among which is the co-disposal of CT and MFT, with the CT being

placed beneath MFT. It is expected that this CT beneath MFT deposition will take advantages of physical, chemical, and anaerobic microbiological processes occurring in the CT and MFT layers to remove or reduce the high concentrations of Ca^{2+} and SO_4^{2-} in the CT release water. At Syncrude Canada Ltd., a pilot-scale field demonstration test was conducted in 1995 to study this CT beneath MFT deposition. The purposes of this CT beneath MFT deposition study were to improve the CT release water quality and MFT densification rate, and to see if the CT densification rate will be adversely affected (Shaw *et al.* 2001). The field demonstration test indicated that the CT beneath MFT deposition initiated changes that were beneficial to tailings disposal, with respect to the release water quality and densification rates of both MFT and CT (Shaw *et al.* 2001). However, prior to recommending this CT beneath MFT deposition scheme as a viable full-scale tailings disposal and management option, it is necessary to conduct a controlled laboratory experiment, to understand the physical, chemical, and microbiological processes that occur in this co-disposal tailings option as the CT release water goes through the MFT layer (Shaw *et al.* 2001).

The purpose of this project is thus to demonstrate whether the placement of CT beneath MFT is a feasible and beneficial disposal technology in tailings management under the laboratory conditions, with respect to the cap water quality and densification rates of both the MFT and CT.

2.0 Review of relevant literature

2.1 The oil sands industry in Alberta

Oil sands are geological units that consist of a mixture of bitumen, formation water, coarse sands, and fine particles (clays and silts). The oil sands deposits in Alberta contain an estimate of over 1.7 trillion barrels of bitumen, of which approximately 300 billion barrels are recoverable with existing technologies. These currently recoverable reserves are similar in size to the proven reserve of Saudi Arabia (ACR 1995).

There are four major reserves of oil sands in the province of Alberta: Athabasca, Peace River, Wabasca, and Cold Lake reserves. The Athabasca oil sands deposit is located in northeastern Alberta, and by itself is the largest petroleum resource in the world. Crude oil from oil sands currently accounts for over 30% of Canada's domestic oil production, and is expected to grow to more than 50% by year 2005 (Syncrude 2000a). Canada's energy supply can be secured for more than 200 years if Alberta's oil sands are fully developed (Syncrude 2000b).

Serious exploration of oil sands began in the early 1920s by the Alberta Government. Various entrepreneurs have explored the commercial potential of the vast oil sands. In 1967, Suncor Energy Inc. opened the first commercial-scale surface oil sands processing facility for mining the oil sands and extracting and upgrading the bitumen at its Lease 86 at the Tar Island site on the Athabasca River, about 30 km north of Fort McMurray in northern Alberta (MacKinnon and Sethi 1993). In the same area, Syncrude Canada Ltd. started production in

1978 at its Leases 17 and 22, located about 1.5 km west of the Athabasca River. Syncrude Canada Ltd. is now the world's largest producer of crude oil (known as Syncrude Sweet Blend) from oil sands. Syncrude Canada Ltd. and Suncor Energy Inc. are currently mining the oil sands using the surface mining operation, and extracting and upgrading the bitumen at the Athabasca oil sands deposit. The two companies produce over 500×10^3 barrels of crude oil daily from about 1.0×10^6 tons of ore processed (Dr. MacKinnon, Syncrude Canada Ltd., personal communication).

2.2 The bitumen extraction process of oil sands

Oil sands can vary in grade, fines or clay content, mineralogy, and salt content. The typical oil sands contain an average of approximately 10 wt% of bitumen; the remainder contains coarse sands (>22μm in diameter), fine particles (<22μm in diameter), and water (FTFC 1995).

The Athabasca oil sands are water-wet. The bitumen is not in direct contact with the sands or clay surface, but is separated by a thin layer of water. Hot water extraction has been proven to be a suitable method for removing and recovering the bitumen from the oil sands.

Bitumen is extracted from the oil sands in the extraction plant. The extraction process used by Syncrude and Suncor is based on the Clark hot water extraction process, which was developed by Dr. Karl Clark in the 1920s.

In the Clark hot water extraction process, the oil sands are slurried and conditioned for bitumen separation in large horizontally rotating tumblers by

mixing with hot water, steam, and caustic soda (NaOH). The introduction of steam is to raise the temperature of the slurry in the mixing tumbler to about 80°C. The addition of the caustic soda will raise the pH of the mixture to the range of 9.0 to 11.0. The slurry usually stays in the tumblers for less than 10 min. At this conditioning stage, bitumen is dislodged from the sand particles, resulting in a loose association of bitumen, sand, and water.

The slurry from the tumblers is then discharged onto vibrating screens to remove large size particles, such as rocks and lumps of undigested oil sands and clay. The slurry produced at this stage is further diluted with additional quantities of hot water and pumped to the primary separation vessels.

In the primary separation vessels, the bitumen floats to the surface as primary froth, while the coarse sands settle out to the bottom as primary tailings. The middlings (from the central portion in the primary separation vessels) and the primary tailings are combined and pumped to the tailings oil recovery vessels (the secondary separation vessels) to further recover most of the remaining bitumen, as the secondary froth.

The secondary froth is combined with the primary froth. This froth mixture is first deaerated and heated, then is fed to the froth treatment plants. Both Syncrude and Suncor's bitumen froth products contain large quantities of water and fine solids (mainly clays), which must be removed before proceeding to the upgrading process. Froth treatment minimises the water and solids going to the upgraders.

During the upgrading process, bitumen is converted from a viscous, tar-like material to a low-sulphur synthetic crude oil (a light gold-coloured liquid), using a coking and hydrocracking process. The resulting synthetic crude oil is then transported by pipeline to the conventional refineries for further refining.

Figure 2-1 shows the schematic flow diagram of the oil sands processes from open surface mining to synthetic crude oil production (FTFC 1995).

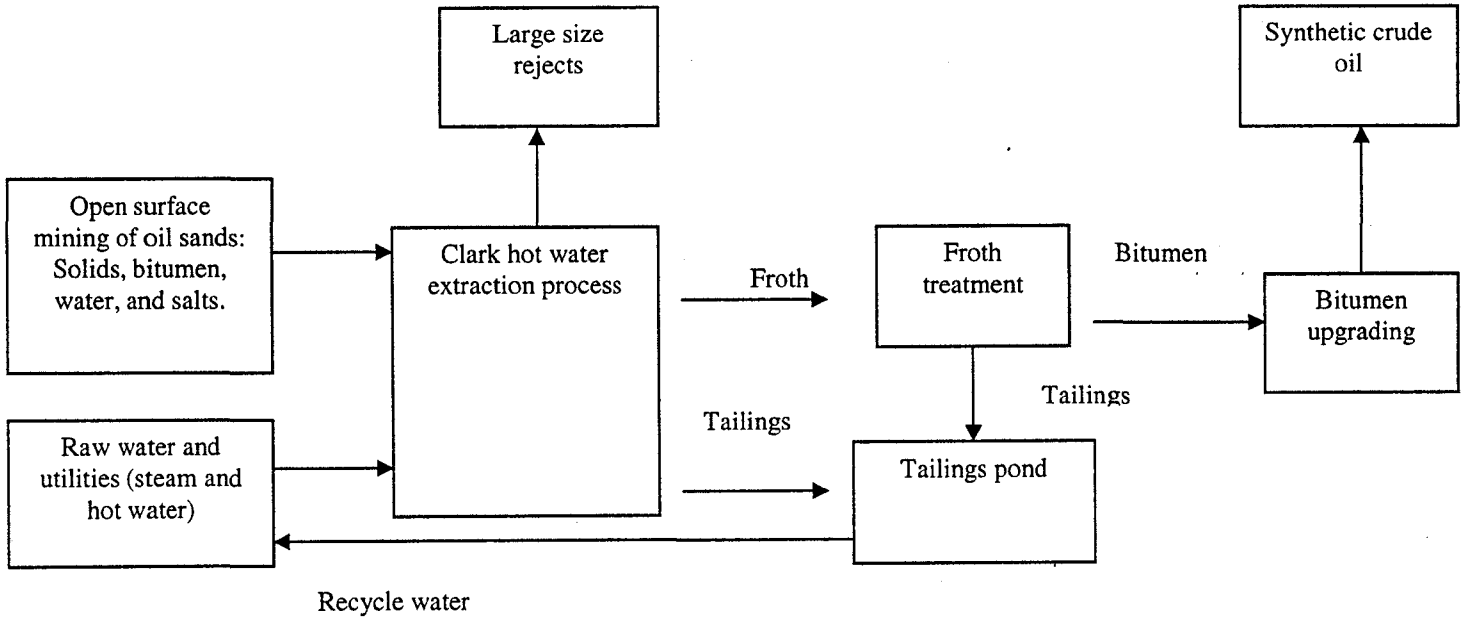

Figure 2-1. Schematic of oil sands processes at Syncrude and Suncor (adapted from FTFC 1995).

2.3 The fine tailings management

One of the main disadvantages of the aqueous digestion processes is its by-product of a large quantity of slurry tailings, which contain water, a coarse sands fraction, a fines fraction, and unrecovered bitumen (FTFC 1995). Neither the tailings solids nor the released water can be discharged into the environment, so that the present development is operating under a "zero discharge" policy in tailings management.

All the tailings from the primary and secondary separation vessels and the froth treatment plant are discharged into large settling basin (i.e. tailings ponds), as the "total extraction tailings" with solids content between 40 and 55 wt% (Dr. MacKinnon, Syncrude Canada Ltd., personal communication). Upon deposition, most (>95%) of the coarse solids (the sands fraction with particle diameter >22 μm, so is also called tailings sands) segregate and settle out from the fines fraction (<22 μm in particle diameter) and are used to build dykes that surround the tailings ponds. A large fraction (about 50%) of the fines are entrained with the coarse solids and settle out with them. The remainder of fines (fine tailings), consisting mainly of slow-settling fine silt and clay particles, water, and residual bitumen, are carried into the tailings ponds as thin fine tailings, with a solids content of about 3 to 8 wt% (MacKinnon and Sethi 1993). The "total extraction tailings" from the oil sands extraction process are thus segregated into tailings sands and fine tailings, which are disposed of separately.

In the tailings ponds, the thin fine tailings settle rapidly to about 20 wt% solids content over a period of several months, and then densify slowly over 2 to

3 years to approximately 30 wt% solids content (Mikula *et al.* 1996). The fine tailings with solids content larger than 30 wt% are termed "mature fine tailings", i.e. MFT (FTFC 1995). The produced surface water (i.e. the released water) in the tailings ponds is low in suspended solids (from 0.1 to 1 wt% at Syncrude and Suncor) and is reused as the recycle water in the extraction plant (MacKinnon and Sethi 1993).

2.3.1 The challenges of fine tailings management

In tailings management, technologies for handling coarse solids (the tailings sands) exist. The biggest difficulty in tailings management is the disposal of fine tailings.

In the fine tailings disposal and management, there are two major challenges. One is the slow self-weight densification rate of the fine tailings. Unlike the tailings sands, which segregate and settle out quickly from the tailings slurry, the fine tailings densify at a slow rate due to the nature of the fine particles (mainly kaolinite and illite clays) and the chemistry of the porewater. The high Na^+ content of the fine tailings porewater will cause clay particles to repel each other and remain in suspension in the tailings water, thus preventing the fine tailings from settling (Dr. MacKinnon, Syncrude Canada Ltd., personal communication). After 2 to 3 y of relatively rapid initial settling and densification, the fine tailings will reach a solids content of approximately 30 wt% and become MFT. Further densification of the MFT is very slow. It is

estimated that the natural densification of MFT to a trafficable surface would take hundreds of years (FTFC 1995).

Based on Syncrude's tailings pond data, an empirical equation for describing the solids content increase of fine tailings over time under self-weight conditions is given below (Mikula *et al.* 1996):

$$S_c = 18.6 + 6.35 \ln y \quad \text{.....(2-1)}$$

where S_c is the solids (<22 μm in particle diameter) content (wt%); y is the number of years of settling.

The production and accumulation of large volumes of fine tailings is another challenge. The Clark hot water extraction process uses large volumes of water and thus results in the production of large quantities of fluid wastes, i.e. the fine tailings. Because of the high water content in the fine tailings, the fine tailings retain fluid characteristics and must be stored behind geotechnically secure dikes with little possibility of being used as a solid substrate for plant establishment (FTFC 1995). The accumulation and disposal of the fine tailings have been on going since 1967 at Suncor and since 1978 at Syncrude. It is not allowed to discharge the fine tailings and its released water to the surrounding environment. All the fine tailings are stored in on-site large tailings ponds. Consequently, a large inventory (more than 500 million m^3) of fine tailings has been accumulated in the tailings ponds at Syncrude and Suncor, in Fort

McMurray, Alberta (Xiaomei and Yongsheng 1995). The Mildred Lake Settling Basin is Syncrude's largest settling basin and covers about 25 km^2, with a water surface area of about 12 km^2. Suncor's four tailings ponds cover a total area of about 13 km^2, with a water surface area of about 7 km^2 (FTFC 1996). Fine tailings are being accumulated at a rate of approximately 20 million m^3/y (Xiaomei and Yongsheng 1995).

Storage and disposal of the large volumes of fine tailings are considered to be the major environmental challenge facing the surface mining oil sands industry (AERCB 1984). For this reason, considerable efforts have been made by the oil sands companies, government, and research institutions to identify suitable technologies for reclaiming the existing fine tailings inventories and for reducing the future volumes of fine tailings that are being continuously produced (FTFC 1995).

2.3.2 The characteristics of MFT

MFT are mainly comprised of fine mineral solids, water, and residual bitumen. The solids content of MFT is larger than 30 wt%. The majority of fine mineral solids are clays (<2 μm in particle diameter), the remainder being silts (from 2 to 22 μm in particle diameter) and fine sands (FTFC 1995). Residual bitumen content (defined as weight of bitumen divided by weight of minerals) is typically in the range of 2 to 10 wt% (FTFC 1995).

There are two models to explain the slow densification rate of MFT: the bitumen model and the mineral model. In the bitumen model, the slow densification of MFT slurry is attributed to the presence of residual bitumen and soluble organic surfactants. They bind the clay particles into a stable aggregate structure that is slow to dewater and consolidate. In the mineral model, the water holding capacity and stability of MFT are attributed to the presence and interaction of fine mineral clays. The clay particles interact with each other and form a three-dimensional gel-like network structure (a "card house-like" structure) in the presence of electrolytes. Other MFT components (bitumen, water, coarser solids) are trapped in the network. Investigations using cryogenic electron microscopy show a definite structure of the clay mineral flocs or aggregates (Mikula *et al.* 1996). The densification rate of MFT is controlled by the permeability and compressibility of its structure. Studies since 1991 have favoured the mineral model in accounting for the MFT stability (Mikula *et al.* 1996).

According to the mineral model of MFT structure and stability, the bulk volume and water holding capacity of MFT are determined by the mineral components (FTFC 1995). The amount of ultra-fines in the particle diameter range of 0.2 to 0.3 μm (which comes from the original oil sands ores) in MFT will account for more than 90% of its water holding capacity (FTFC 1995). Furthermore, the bulk properties of MFT are a function of the chemistry of the porewater (FTFC 1995). The MFT from Clark hot water extraction process is a

weakly flocculated suspension of sodium-rich clays that densifies slowly by self-weight settling.

Tang (1997) reviewed and examined the MFT microstructures using scanning electron microscope (SEM). The MFT has a highly dispersed three-dimensional card-house structure (also called gel structure) with clay particles aligned in edge-to-edge and edge-to-face patterns. The porewater chemistry of MFT, including pH, alkalinity, salinity, ionic content, and organic matter, may contribute to the formation and stability of the MFT structure. The residual bitumen in MFT could also reduce the MFT hydraulic conductivity, and hence reduce the MFT densification rate. The high water holding capacity and slow densification rate of MFT may be explained by this gel structure.

Chemical, physical, and toxicological properties of the fine tailings and its porewater are a function of the source and composition of the oil sands ores. In addition, both the make-up water used for plant process and the chemicals added as process aids during hot water extraction can add extra inorganic and organic compounds to the fine tailings stream (FTFC 1995). The composition of the water in the tailings ponds is not static. As all the process water and wastes are stored in the tailings ponds and the released water is recycled, the ions in the water of tailings ponds accumulate. Over time, the recycle water from the tailings ponds becomes more brackish (Mikula *et al.* 1996).

The major anions (Cl^-, SO_4^{2-}, HCO_3^-) and cations (Na^+, K^+, Mg^{2+}, Ca^{2+}) account for most of the dissolved fraction in the MFT porewater. Sodium is the predominant cation, accounting for approximately 95% of the cation equivalents

(defined as ion concentration divided by ion equivalent weight) in the MFT water fraction. Most of the sodium comes from the process chemicals. The other cations (K^+, Mg^{2+}, Ca^{2+}) are minor components that represent only about 5% of the total cation equivalents (MacKinnon 1989).

Bicarbonate is the most abundant anion and accounts for 50 to 75% of the anion equivalents. The pH of the MFT porewater ranges from 7.3 to 8.3 (Dr. MacKinnon, Syncrude Canada Ltd., personal communication). In this pH range, the dissolved inorganic carbon is present predominantly as HCO_3^-, which determines the pH in the MFT slurry. Sulphate concentration is affected by microbial processes in anaerobic environment, where the SO_4^{2-} is reduced to S^{2-} by sulphate-reducing bacteria (SRB). The Na^+ and Cl^- ions are conservative species and are little affected by microbiological or chemical interactions (MacKinnon 1989).

The major hydrocarbon components of fine tailings include unrecovered bitumen and the naphtha. The concentrations of water-soluble organics released during the hot water extraction process in both the surface water and pore water of the tailings ponds are fairly low (55 to 85 mg/L) (FTFC 1995). Fine tailings and the associated water are toxic to aquatic biota. Acid-extractable organics account for most of the acute toxicity in tailings pond recycle water. Up to 95% of the total acid fraction extractable from fine tailings is composed of naphthenic acids (FTFC 1995).

The concentrations of oxygenated nutrients (such as nitrite, nitrate, and orthophosphate) in the MFT porewater and produced cap water are low. Most of

the nitrogen is present as ammonia in the range of 2 to 6 mg/L (MacKinnon 1989).

The concentrations of dissolved trace metals in fine tailings water are low relative to regulatory guidelines for the protection of freshwater aquatic biota and have been maintained quite constant over time. Usually only aluminum (Al), barium (Ba), boron (B), iron (Fe), molybdenum (Mo), strontium (Sr), and zinc (Zn) have concentrations above 0.1 mg/L. The trace metal level in the fine tailings does not appear high enough to be detrimental to the environmental acceptability of water quality (MacKinnon 1989).

The anaerobic tailings ponds are rich in microorganisms. Methanogens are active in the Mildred Lake Settling Basin (operated by Syncrude Canada Ltd.) (Holowenko 2000). The production of methane may have detrimental effects on the reclamation of the tailings ponds by affecting the tailings settling behaviour, producing fugitive emission of low molecular hydrocarbons, and leading to anaerobic conditions in the cap water (Fedorak *et al.* 2000). SRB are an important group of microorganisms in anaerobic ecosystems that have sulphate as the terminal electron acceptor. Methanogens and SRB are two important microorganisms affecting the reclamation of the tailings ponds and MFT slurry (Fedorak *et al.* 2000).

The typical strength values of vane shear test of MFT are in the range of 0.2 to 2.5 kPa (FTFC 1995). These values are very low relative to the typical geotechnical range for consolidated solids. Therefore, MFT is too weak to

support a trafficable surface (FTFC 1995). Dewatering of MFT occurs slowly, taking hundreds of years to develop into a structure of solid soil (FTFC 1995).

2.3.3 The CT

The majority of the fine minerals (mainly clays) in the oil sands tailings stream segregates from the coarse sands fraction and form the slurry fine tailings in the tailings ponds. After 2 to 3 y of relatively rapid settling, the fine tailings become a slow settling MFT. Because of the large volumes and the fluid character that requires geotechnically stable enclosure, the fine tailings and MFT pose the biggest environmental challenge to the oil sands companies in reclaiming the disturbed areas and tailings ponds.

It is thus a desirable option for the oil sands industry to prevent the segregation of coarse sands and fine minerals as the extraction tailings are deposited into the tailings ponds, such that the fines are incorporated in the sands deposit as they were in the original ore body (FTFC 1995). To prevent fines segregation, it is necessary to modify the tailings stream by increasing the coarse sands content, increasing the fines content, and adding a chemical coagulant (FTFC 1995). The floc structure of untreated MFT from Clark hot water extraction process is not strong enough to support a load or stress that would allow rapid densification by gravity. A chemical treatment can change the weak floc structure of the MFT into a stronger floc structure that would support some surcharge and enhance the densification (FTFC 1995).

Non-segregating tailings (NST) are a tailings mixture in which the fines and coarse sand particles settle simultaneously to form a uniform deposit. The introduction of coarse solids imparts an internal stress that significantly enhances the densification rate of the NST. The mixture of coarse sands tailings and fine tailings requires the presence of chemical additives (coagulants) to produce a non-segregating behaviour. With the addition of polyvalent cations (e.g. Ca^{2+} from gypsum), the fine particles (clays) in oil sands tailings will coagulate, resulting in the possibility to produce a MFT floc structure that is strong enough to support a surcharge and hence to create a non-segregating tailing (NST). Calcium ion has been known to be an effective coagulant in modifying the MFT properties. The addition of calcium can be achieved by the addition of gypsum ($CaSO_4 \bullet 2H_2O$) (FTFC 1995).

The term of CT has gained its wide use in replace of NST since 1995 (Shaw *et al.* 1996). Large-scale field testings of CT approach were started in 1993/1994 at Suncor and in 1995 at Syncrude (List and Lord 1997). In 1996, Suncor began to use CT technology based on gypsum treatment on a commercial scale to reduce the large volume of fine tailings in its tailings ponds. Suncor plans to use the CT process as the basis for future tailings management. In 1997/1998, Syncrude successfully demonstrated a full-scale prototype operation of CT test, also utilising gypsum as the coagulant. Under the present plans, a large portion of the extraction tailings will be handled using the CT process in Syncrude (MacKinnon *et al.* 2000).

In the CT process at Syncrude Canada Ltd., the densified coarse tailings sands (obtained by hydrocycloning the extraction tailings) are combined with MFT and a chemical coagulant aid to form a type of NST. Unlike the conventional extraction tailings, when the CT is deposited, the fines will stay and settle together with the coarse sands fraction. The coarse sands act as a stress or load that enhances the settling of the deposit. CT deposit has a higher permeability than MFT, resulting in more rapid dewatering (MacKinnon *et al.* 2000).

Factors affecting the segregation of CT mixture include total solids content (density), fines content (a fraction of the total solids), particle size gradation, and type and dosage of coagulant aids. These factors can be manipulated individually or in combination to shift the segregation boundaries (Matthews *et al.* 2000).

Three means of slurry manipulation have been evaluated in the course of the CT development; these are increase in solids content by hydrocyclone densification of the extraction tailings, increase in fines content through enrichment with MFT, and chemical adjustment by addition of coagulants (Matthews *et al.* 2000).

Without the addition of chemical coagulants, the tailings would exhibit a gap-graded particle size distribution and lead to the segregation of the fines from the coarse solids during the discharge and deposition. The addition of coagulant aids to the CT mixture (consisting of coarse tailings and MFT) is an essential component of the CT process. The coagulants produce changes in the properties

of clays in the CT mixture and cause the colloidal particles to aggregate. This phenomenon has the effect of changing the particle size distribution of the solids in the CT mixture to provide a more uniformly graded mixture that can suppress or eliminate segregation (Matthews *et al.* 2000).

During the development of the CT process, various coagulant aids were assessed, including sulphuric acid, lime (CaO, $Ca(OH)_2$), acid-lime (H_2SO_4-CaO), gypsum, sodium aluminate ($Na_2Al_2O_3$), alum (48% $Al_2(SO_4)_3 \cdot 14.3H_2O$), and organic polymers (polyacrylamides). The segregation characteristics, deposit dewatering and densification rates, released water quality, and economics are the factors in the assessment and selection of coagulants. Based on on-going research efforts, gypsum has proven to be a robust, effective, easy to handle, and readily available coagulant aid to the CT process. As a result, Syncrude used gypsum as the coagulant for the 1995 field demonstration and the 1997/1998 prototype CT test. Through these evaluations, Syncrude, as well as Suncor, have chosen gypsum as the base coagulant for the future commercial application of CT. The optimum gypsum dosages are in the range of 1000 to 1200 g/m^3 of tailings (Matthews *et al.* 2000).

In the CT mixture, most of the fines and porewater come from the MFT component. This is an important factor when predicting the quality of CT release water. The optimum solids content of CT is about 60 wt% (Dr. MacKinnon, Syncrude Canada Ltd., personal communication). When the CT slurry is deposited and starts settling, the CT deposits experience two stages of densification: the first stage of initial settling and the second stage of long-term

self-weight consolidation. The initial settling starts immediately upon deposition of the CT mixture. During this initial settling period, the CT deposit undergoes a substantial volume reduction as its porewater being released. As the CT deposit densifies to a solids content of 75 wt% in weeks or months, approximately 50% of the initial water can be released. The rate of the initial settling depends on the amount and type of fines, chemical addition, mixing procedure, and the hydraulic conductivity of MFT. The long term consolidation of CT begins as the sand grains become in contact with one another and form a sand matrix. Excess water is slowly released from the CT as it consolidates over a long-term (MacKinnon *et al.* 2000; Tang 1997). If allowered to dewater and drain, the CT deposit will become trafficable in a few years.

In the CT process, the gypsum dosage at about 1000 g per m^3 of CT mixture would result in approximately 1000 mg/L of sulphate (SO_4^{2-}) in the CT porewater (MacKinnon *et al.* 2000). With the high SO_4^{2-} concentration in the CT porewater, the CT will inhibit methane production by creating an environment that is more suitable for SRB and so that the SRB would out-compete the methanogens. Fedorak *et al.* (2002) has shown that the addition of sulphate to fine tailings decreased methane production, and the methanogenesis appeared to have started to a large extent only after the sulphate concentration has dropped to approximately 20 mg/L.

The purpose of CT process is to retain and consume the MFT with the coarse solids to eventually create a sustainable and acceptable dry or wet landscape (MacKinnon *et al.* 2000). Technologies like CT give the oil sands

companies the ability to create broadly diverse landscapes that help fulfill the commitment to the reclamation of the disturbed areas.

2.3.4 The options for fine tailings management

The fine tailings management and reclamation programme must ensure that (FTFC 1995): (i) the direct contact of fine tailings with the environment and the release of contaminants into the environment are restricted; (ii) the reclaimed area is stable, productive, and biologically self-sustaining.

To date, no single reclamation option can handle the huge volumes of fine tailings in a technically, environmentally, and economically acceptable manner. The reclamation of the fine tailings requires an integrated approach. The reclamation of the fine tailings will be accomplished through a combination of so called "dry" and "wet" landscape techniques (FTFC 1995).

The dry approach involves dewatering the fine tailings or incorporation of the fine tailings with a solids material and being reclaimed as a land surface. Some of the various dry landscape options include: (i) dewatering of the fine tailings through processes such as evaporation and freeze-thaw; (ii) incorporation of fine tailings with overburden clays; and (iii) creating NST or CT (FTFC 1995).

The wet approach involves a lake system, whereby the fine tailings are capped with a layer of water to be isolated from direct contact with the surrounding environment (FTFC 1995). The wet landscape option disposes of

MFT as a fluid or non-trafficable deposit. The objective of this reclamation option is to produce a stable, productive, and self-sustaining cap water zone, which can support viable aquatic ecosystems shortly after water capping and is free of long-term maintenance. The surface mining practice of the oil sands industry leaves large mined-out pits, which may be used as the geotechnically secure areas for long-term containment of the fluid fine tailings (FTFC 1995).

Each approach in fine tailings management has its advantages and disadvantages. The final strategy will depend on detailed technical and environmental assessments, economic consideration, and the stakeholder's acceptance (FTFC 1995).

2.4 SRB and methanogens

2.4.1 The SRB

SRB are a diverse group of strictly anaerobic bacteria that share the ability to use sulphate as the terminal electron acceptor and conduct dissimilatory sulphate reduction in the oxidation of organic matters. In the dissimilatory sulphate reduction, sulphate is reduced to sulphide according to Equation 2-2 (Levett 1991):

$$CH_2O + SO_4^{2-} \longrightarrow HCO_3^- + S^{2-} \quad \text{.....(2-2)}$$

where CH_2O represents the organic substrates.

The substrates used by SRB include lactate, pyruvate, and acetate, among many others. Lactate and pyruvate are all converted to acetate and CO_2 as the major end products by acetate-producing organisms. In the acetate-utilising species, CO_2 is a major product (Postgate 1984).

Sulphide is a normal metabolic product of dissimilatory sulphate reduction and can render soluble iron insoluble by converting it to FeS. Thus, the SRB colonies can be identified by the precipitation of black FeS (Levett 1991).

SRB are adaptable to almost any anaerobic environment. SRB need anaerobic and reducing conditions for growth. The redox potential (Eh) of the growth media should be around –100 mV (Levett 1991; Postgate 1984). However, some SRB can survive long exposure to oxygen and become active again if the environment becomes anaerobic. SRB can tolerate temperatures from –5 to +75 °C and pH values ranging from 5 to 9.5 (Postgate 1984).

The activity of SRB in a given environment will change the chemical and physical nature of that environment. Due to the release of CO_2 and accumulation of carbonate and bicarbonate, the aqueous environment will have elevated alkalinity and metal ions will precipitate as insoluble metal sulphides (e.g. FeS). If no metals are present or pH is low enough, the sulphide could be converted to hydrogen sulphide (H_2S) and escape into the water phase or the atmosphere (Gray 1989). Sulphate reduction will consume a substantial amount of organic substrates and produce, sometimes via acetate, CO_2 (Postgate 1984).

Given a high ratio of metabolisable carbon to sulphate, SRB can deplete an environment of sulphate almost completely (Postgate 1984).

Sulphite and thiosulphate are intermediates in the normal sulphate reduction process, and can also be used as substitute electron acceptors for the growth and carbon metabolism of some SRB species (Levett 1991; Postgate 1984).

The disappearance of sulphate in nature over time may be used as an index of the SRB activity (Levett 1991; Postgate 1984).

2.4.2 The methanogens

Methanogens are a morphologically diverse group of anaerobic bacteria unified by their ability to produce methane (CH_4) (Levett 1991).

Methanogens utilise a limited number of simple carbon compounds as carbon and energy sources for methanogenesis, including CO_2, formate, methanol, and acetate (Levett 1991). More than half of the biogenic methane in nature is believed to originate from acetate (Postgate 1984). Methanogens are usually considered to be the last players in the decomposition of organic matters in anaerobic ecosystems. That is, they consume the metabolic end products (mainly acetate and H_2) of other strictly anaerobic bacteria as energy sources and produce CH_4 as their waste product. CO_2 and HCO_3^- serve as the terminal electron acceptors during anaerobic respiration by methanogens (Fedorak *et al.* 2000).

Methanogens are found in a variety of anaerobic habitats including sediments, sludge, and animal waste digesters. They require an Eh in the range of –150 to –220 mV to thrive (Fedorak *et al.* 2000). In general, methanogens get inactivated by the presence of oxygen, although not every species is rapidly killed by oxygen (Levett 1991).

The most common method used to enumerate specific types of methanogens is the most probable number (MPN) technique, where the sample is serially diluted and inoculated into a suitable broth medium with a specific substrate (Levett 1991).

Methane, being a gas, diffuses from anaerobic zones and can also become subject to aerobic mineralisation by methanotrophic bacteria (Postgate 1984).

2.4.3 The competition between SRB and methanogens

SRB have long been known to be incompatible with methanogens, although both of them are strict anaerobes. Indeed, they seem in nature to have a somewhat competitive relationship. The methanogens take over when the SRB have done what they can (Postgate 1984).

A widely accepted view about the incompatibility of methanogenesis and sulphate reduction by SRB suggests that the SRB can out-compete methanogens for common substrates, H_2 and acetate, except in some particular environments with sulphate deficiency (Postgate 1984). It has long been known that methane production in marine sediments occurs only after sulphate has been depleted

from the pore water. This is due to the competition between methanogens and SRB for some electron donors. Based on thermodynamic considerations, the utilisation of H_2 or acetate by SRB yields more energy than the utilisation of these substrates by methanogens. When sulphate is depleted, methanogens carry out the terminal steps in the anaerobic environment (Fedorak *et al.* 2000). In most environments there is little or no overlap between the zone of methanogenesis and the zone of sulphate reduction by SRB in sediments. Methanogenesis begins when sulphate is depleted (Schlesinger 1997).

Like methanogens, SRB can also use acetate and H_2 as energy sources. However, SRB use a wider range of organic compounds as their energy sources compared to methanogens and produce sulphide as their waste product (Fedorak *et al.* 2000).

Sediments in which sulphate reduction is active often lie over sediments in which methane production is taking place. Methane can be a substrate for sulphate reduction by SRB as shown in Equation 2-3 (Schlesinger 1997; Postgate 1984):

$$CH_4 + SO_4^{2-} \longrightarrow HS^- + HCO_3^- + H_2O \quad \text{.....(2-3)}$$

Acetate is known to be a good substrate for methane formation. Therefore, the product of sulphate reduction by the acetate-producing organisms would be expected to favour methanogenesis, indicating the complex relationship between SRB and methanogens (Postgate 1984).

3.0 Problem statement and the objective of this project

3.1 Problem statement

As discussed in Section 2.3, as a tailings management option in the oil sands industry, CT is a type of NST and is made up of coarse sands, MFT, and gypsum. Upon deposition, the CT slurry releases its porewater quickly and the deposit becomes denser. The released water will be recycled as the process water.

The integration of CT into tailings disposal and management will affect the water properties in the oil sands operation. The CT release water must be suitable for recycle and not limit reclamation options. The addition of chemical coagulants in CT process can lead to the direct shifts in pH, alkalinity, salinity, as well as the cations and anions associated with the coagulants (MacKinnon *et al.* 2000). In addition, changes in the water quality will occur after deposition through exchanges and interactions with the atmosphere and clays, and bio-chemical reactions. Some of the possible water quality issues associated with the use of CT process are increase in salinity, scaling potential from increased Ca^{2+} content, change in pH, corrosion potential, potential effect on bitumen recovery, and impact on reclamation (MacKinnon *et al.* 2000).

In the gypsum-treated CT mixture, the main water quality change is the increase in Ca^{2+} and SO_4^{2-} contents. The CT release water will have Ca^{2+} content in the range of 70 to 120 mg/L and SO_4^{2-} content more than 1000 mg/L (MacKinnon *et al.* 2000). Excess Ca^{2+} in the recycle water can decrease bitumen recovery (FTFC 1995; Kasperski 1992). Bitumen recovery will be significantly

affected when the calcium concentration exceeds 3 mM (i.e. 120 mg/L) (FTFC 1995). The increased Ca^{2+} content will also raise issues regarding scaling and corrosion in the process units (MacKinnon *et al.* 2000). The elevated concentration of SO_4^{2-} from CT in the recycle water stream may also pose adverse effects on bitumen recovery (FTFC 1995). The high concentration of SO_4^{2-} content in the CT water is the main factor causing the increase in salinity. In studies on potential terrestrial impacts of CT water on vegetation, it has been shown that the salinity is the major factor that needs to be addressed (MacKinnon *et al.* 2000).

At Syncrude Canada Ltd., a preliminary pilot-scale field test (Shaw *et al.* 1996) was carried out from 1995 to 2000 for studying whether the co-disposal of CT placed beneath MFT is a feasible disposal technology. The main objectives of that test were to determine if CT would flow under MFT without segregation, if CT would dewater under MFT and the dewatering rate, and if and how the CT release water would affect the physical and chemical properties of the overlying MFT and cap water.

The main findings of this field demonstration test were as follows (Shaw *et al.* 2001; Shaw *et al.* 1996).

(i) The CT and MFT layers maintained their distinct characters during and after the placement of fresh CT slurry below a lay of MFT.

(ii) The CT layer densified with its solids content increasing from approximately 60 wt% to 78 wt% during the period from 1995 to 1999.

(iii) Enhanced densification through dewatering was observed in the MFT layer with the solids content increasing from 33 wt% to 41 wt% during the study period.

(iv) The produced surface water (i.e. cap water) showed a decrease in conductivity and in particular in SO_4^{2-} and Ca^{2+} concentrations, most likely due to the microbiological activities, dilution of the CT release water with the displaced MFT porewater, or precipitation reactions.

The field demonstration test indicates that the co-disposal of CT beneath MFT deposition initiates beneficial changes for tailings disposal with respect to the release water quality and both the MFT and CT densification rates. However, prior to recommending this co-disposal scheme as a viable full-scale tailings management alternative, it is necessary, under controlled laboratory conditions, to understand the physical, chemical, and microbiological processes that will occur in this deposit.

3.2 Objective of this project

The overall objective of this project is to demonstrate whether the co-disposal of CT beneath MFT is a feasible technology in tailings disposal and management under controlled experimental conditions, with respect to the cap water quality for recycle and the densification rates of both the MFT and CT layers. More specifically the objective is to:

(i) determine the effects of this CT beneath MFT deposition scheme on the produced cap water quality, mainly in terms of hardness (Ca^{2+} + Mg^{2+}) and SO_4^{2-} concentration in the cap water;

(ii) observe the physical, chemical, and microbiological changes that occur in the MFT zone under anaerobic conditions as the CT release water interacts in the MFT layer, including the sinks of SO_4^{2-} and Ca^{2+}, and the densification rate of MFT;

(iii) observe the physical, chemical, and microbiological changes that occur in the CT layer under anaerobic conditions, including the sinks of SO_4^{2-} and Ca^{2+}, and the densification rate of CT.

As the CT release water, rich in Ca^{2+} and SO_4^{2-} ions, percolates through the MFT layer, it is expected that the Ca^{2+} may be exchanged and sequestered on MFT clay surface, while the SO_4^{2-}, through microbiological activity, will be converted into sulphide, particularly iron sulphide. Lowered Ca^{2+} and SO_4^{2-} contents in the release water of this co-disposal deposit will be beneficial for re-using the water in oil sands extraction process. Increased densification rates of both the MFT and CT will also be beneficial in reducing the volumes that these deposits occupy in the tailings ponds.

4.0 Methods and materials

4.1 Methodology

This research used static column mesocosms to study and monitor the physical, chemical, and microbiological changes occurring in this CT beneath MFT co-disposal system, as detailed below.

The static column mesocosms consisted of four different deposit systems, as described in Table 4-1.

Table 4-1. Static column mesocosm systems.

System	Column configuration during incubation	Deposit at column filling	Number of columns
1	Cap water/MFT/CT	A 27-cm height of MFT on the top of a 54-cm height of CT.	20
2	Cap water/MFT/CT	A 27-cm height of MFT on the top of a 54-cm height of CT.	6
3	Cap water/MFT	Only a 54-cm height of MFT.	12
4	Cap water/CT	Only a 54-cm height of CT.	12

System 1 was the main system to be studied. Systems 3 and 4 served as controls for System 1. At column filling, System 1 contained a 27-cm height of MFT layer on the top of a 54-cm height of CT layer, while Systems 3 and 4 contained only a 54-cm height of MFT or CT layer. No extra water was added to the cap of the columns at column filling. All the cap water produced during the ensuing incubation was the released water from the deposit.

For Systems 1, 3, and 4, the columns were incubated for a maximum of 1 y under dark and temperature controlled conditions. After a certain incubation period, the columns were sacrificially sampled. For each column at its sacrificial

sampling, the column headspace gas, cap water, and MFT or CT samples were analysed. The analyses might include:

(i) the column headspace gas analysis for CH_4, O_2, N_2, CO_2, H_2S, and C_2H_4;

(ii) water (cap water and MFT or CT porewater) analysis for pH, electrical conductivity (EC), HCO_3^-, major cations of Ca^{2+}, Mg^{2+}, Na^+, K^+, NH_4^+, and major anions of SO_4^{2-}, S^{2-}, PO_4^{3-}, NO_3^-, NO_2^-, Cl^-;

(iii) MFT or CT analysis for trapped gases of CH_4, O_2, N_2, CO_2, H_2S, and C_2H_4, redox potential, the contents of oil, water, and solids (O/W/S), particle size distribution, acid volatile sulphides (AVS), and the quantification of microbial populations of methanogens and SRB using MPN method.

Also, the volume changes of the various zones (cap water, MFT, or CT) and the dewatering rates of MFT and CT were followed by visually recording the changes in the interface positions of cap water and MFT (in Systems 1 and 3), cap water and CT (in System 4), or MFT and CT (in System 1). For System 1, the interface position of MFT and CT was measured only at the time of sacrificial column sampling.

System 2 had the same deposit configuration as System 1, but it was designed in particular to regularly conduct headspace gas and cap water sampling and analysis, and to regularly record the position change in the interface of MFT and CT in an in-situ manner without sacrificing the columns. Furthermore, the columns in System 2 were sacrificially sampled only at the end of 1 y of incubation.

The details of the design and analysis for these static column Systems 1, 2, 3, and 4 are presented in the following protocol development Section 4.2.

4.2 Protocol development

Previous research (Fedorak *et al.* 2000) on oil sands tailings in the Department of Biological Sciences, at the University of Alberta, involved extensive physical, chemical, and microbiological investigations of the MFT and CT materials using a variety of innovative experimental methods. Fedorak *et al.* (2000) also developed and adopted many proven protocols for column setup and analyses to evaluate the CT and MFT under anaerobic conditions. In developing the protocols for this current project, the protocols used by Fedorak *et al.* (2000) were frequently referenced.

4.2.1 Number of columns in static column mesocosms

The planned incubation time was 1 y. The number of columns for Systems 1, 3, and 4 was determined to allow for a minimum of one column to be sacrificially sampled every month in each system. For System 2, no sacrificial sampling was designed until the end of the planned incubation periods, and therefore a reasonable number of columns were chosen. Table 4-1 shows the number of columns used in each system.

4.2.2 Column design for Systems 1, 2, 3, and 4

Systems 1, 2, 3, and 4 used a "12.1 ID × 12.7 OD × 91.4 H" cm clear acrylic column as their mesocosms. The top of the columns was covered with a 15×15×6 mm square acrylic plate, and the bottom of the columns was covered with a 22×22×12 mm square acrylic plate.

The fabrication of the pieces needed for assembly of the static columns was completed in the Geotechnical Engineering Laboratory in the Department of Civil and Environmental Engineering, at the University of Alberta. The pre-fabricated acrylic pieces were bonded using "Weld-On 16#" acrylic glue (from Johnston Industrial Plastics, Edmonton, Alberta) and assembled in Environmental Engineering Laboratory, University of Alberta, at the time of column filling. The designs of the column pieces are detailed below.

4.2.2.1 Design of the top covers

For Systems 1, 3, and 4, there were 2 holes placed in the top cover. A 3.2-mm NPT threaded hole was used for connecting a 1-L Tedlar bag (catalog Number 231-01, purchased from Safety Instruments Ltd., Edmonton, Alberta) through a 25-cm length of 3.2 ID × 6.4 OD mm Tygon tubing to collect the evolved headspace gas in the columns. A 10-mm diameter straight hole was used for fitting a rubber septa, which would allow for cap water sampling in an in-situ manner by using syringe if needed.

For System 2, there were four holes placed in the top cover. A 3.2-mm NPT threaded hole was used for connecting a 1-L Tedlar bag through a 25-cm

length of 3.2 ID × 6.4 OD mm Tygon tubing to collect the evolved headspace gas in the columns. A 3.2-mm NPT threaded hole was used for fitting a 3.2-mm OD stainless steel tubing to regularly monitor the position change in the interface of MFT and CT in an in-situ manner. A 3.2-mm NPT threaded hole was used for fitting a 3.2-mm OD stainless steel tubing to regularly sample the cap water in an in-situ manner. A 1.6-mm NPT threaded hole was used for fitting a 40-cm length of 1.6-mm OD stainless steel tubing to regularly conduct the head space gas analysis by gas chromatography (GC) in an in-situ manner.

4.2.2.2 Design of the bottom covers

For Systems 1 and 2, there were two 1.9-cm diameter straight holes placed in the bottom cover. One hole was used to finally fill the column with CT through a funnel, and the other hole was used to exit the trapped air before sealing the bottom cover. The two holes were plugged at the end of column filling using 1.9 mm diameter acrylic rods. For Systems 3 and 4, the bottom cover did not contain any hole design.

4.2.2.3 Reinforcement of the seals

Several triangular pieces of acrylic (two for the top cover and four for the bottom cover) were used to reinforce the seals between the column and covers.

4.2.2.4 Column stopper for Systems 1 and 2

Systems 1 and 2 contained a layer of MFT on the top of a layer of CT. Because of the special column filling procedures in these two systems, a column stopper was used to fill the columns of Systems 1 and 2, as detailed in the following Section 4.2.4.

4.2.2.5 Monitoring the interface position of MFT and CT in Systems 1 and 2

The major purpose of monitoring the interface position between MFT and CT layers in Systems 1 and 2 was to determine the densification rates of individual MFT and CT layers in these co-disposal deposition systems. To monitor the position change in the interface of MFT and CT in Systems 1 and 2, a piece of Geo-grid with a mesh hole size of approximately 0.5 × 0.5 cm (from Nilex Inc. Edmonton, Alberta) was placed at the interface of MFT and CT during column filling. The Geo-grid piece physically separates the MFT and CT layers, but does not interfere with the transport of the CT release water. Thus, by monitoring the position of the Geo-grid piece, the position change in the interface of MFT and CT could be obtained. For System 1, the Geo-grid position was only measured at the time of sacrificial column sampling. For System 2, the Geo-grid position was regularly monitored by using a stainless steel tubing in an in-situ manner. The stainless steel tubing was to be contacted to the Geo-grid piece at the time of measuring the Geo-grid position.

4.2.3 The MFT and CT materials

About 800 kg each of CT and MFT slurries were delivered in 20-L plastic pails from Syncrude Canada Ltd. in December 2001. Both the CT and MFT were kept in a 4°C temperature controlled room until use.

At the time of column fillings, in order to reduce the heterogeneity of the CT and MFT materials among different columns, several pails of the MFT or CT materials were randomly selected and well mixed in containers of suitable size. The mixed MFT or CT materials were then used to fill the columns.

4.2.4 Procedures for column filling and assembly in Systems 1, 2, 3, and 4

Prior to filling column with MFT and CT, each column was flushed with N_2 for 2 to 3 min. N_2 flushing continued during column filling. After column filling, the column headspace was flushed with N_2 for 2 to 3 min. The top cover of the columns was then bonded to the column using "Weld-On 16#" acrylic glue and temporarily clamped together to ensure a good seal. The 1-L Tedlar bag was flushed with N_2 three times prior to its connection to the column cover.

In the columns of Systems 1 and 2, both MFT and CT were to be layered in the same column, with a 27-cm height of MFT layer placed above a 54-cm height of CT layer. Due to the characteristics of the MFT and CT materials, the column filling for Systems 1 and 2 needed a special procedure.

In developing the protocol for column filling in Systems 1 and 2, two issues were considered. First, if the CT is placed first in the column, the CT will

start releasing its porewater quickly (in several hours after filling) and this porewater will accumulate at the surface of CT before placing the MFT in the column. Second, the freshly mixed MFT will have a very different structure from that of the field MFT, and thus some "maturing" of the MFT will be needed before being deposited above the CT. Considering these two factors, and after consultation with the industrial partner of this project, the column filling for Systems 1 and 2 used a procedure that involves filling the column with MFT first, letting the MFT "mature" for some time, then filling the column with CT, and finally inverting and sealing the column. This procedure required the column to be inverted at the time of filling with MFT and CT. A column stopper was designed for this purpose. Figure 4-1 shows the schematics of the side view of the column stopper as it stands inside the column at column filling.

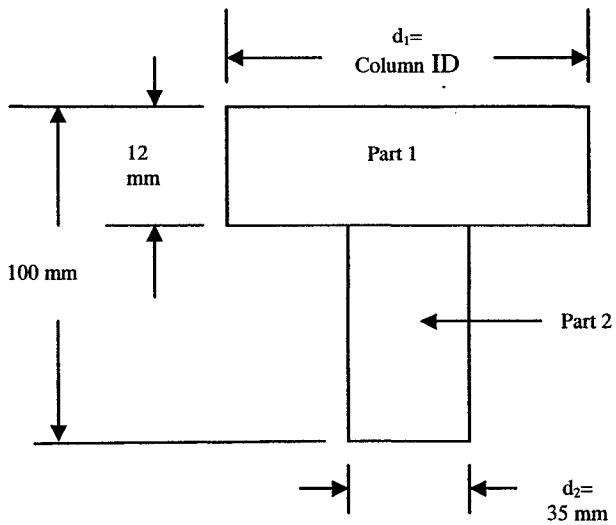

Figure 4-1. Schematics of side view of the column stopper used for filling columns in Systems 1 and 2 (not to scale)

The column stopper had a suitable external diameter, which was close to the column ID (inside diameter). Thus, the column stopper could minimise the MFT leaking during filling column with MFT and CT and be removed relatively easily after column filling. Four throughout holes of about 8 mm diameter were also designed in Part 1 of the column stopper to ease the removal of the column stopper after column filling. The four holes were stopped using nuts during column filling. The total height of the column stopper was approximately 10 cm. This 10 cm height of column stopper would create a 10 cm height of headspace after the column filling and stopper removal.

The protocol for column filling for Systems 1 and 2 can therefore be detailed as follows (see Figure 4-2).

(i) The column stopper was first installed onto one end of the column, and the column was filled with a 27-cm height of freshly mixed MFT under a N_2 atmosphere (see Figure 4-2a). After flushing the headspace of these MFT-filled columns with N_2 for a few minutes, the columns were temporarily covered with a plastic film to maintain the N_2 atmosphere in the column headspace. The MFT in the column was allowed to "mature" overnight to develop some structure, similar to that seen in the field.

(ii) On the second day, a piece of Geo-grid was first placed on the top of the MFT layer. The Geo-grid piece had a diameter close to the column ID. The purpose of using this Geo-grid is to physically separate the MFT and CT layers and provide a method to monitor the position change in the interface between

the MFT and CT during the ensuing incubation. After placing the Geo-grid, a 54-cm height of freshly mixed CT was placed on the top of MFT (see Figure 4-2b). Special caution was used when filling with CT to minimise the impact of the CT flow on the underlying MFT and to avoid disturbing or displacing the Geo-grid. After sufficient amount of CT was placed in the column, the acrylic bottom cover with two 1.9-cm diameter straight holes was used to seal the CT side of the column end, using "Weld-On #16" glue. The two 1.9-cm diameter straight holes were used for final column filling with funnel and to allow the trapped air to escape. The two holes were plugged using 1.9-cm diameter acrylic rods at the end of column filling with CT.

(iii) After filling with CT, the column was turned over, so that the CT layer was at the bottom and the MFT layer was at the top. The column stopper was then removed, creating a 10-cm height of headspace. The headspace was then flushed with N_2 for several minutes and the column was finally sealed with the acrylic top cover of suitable design (see Figure 4-2c).

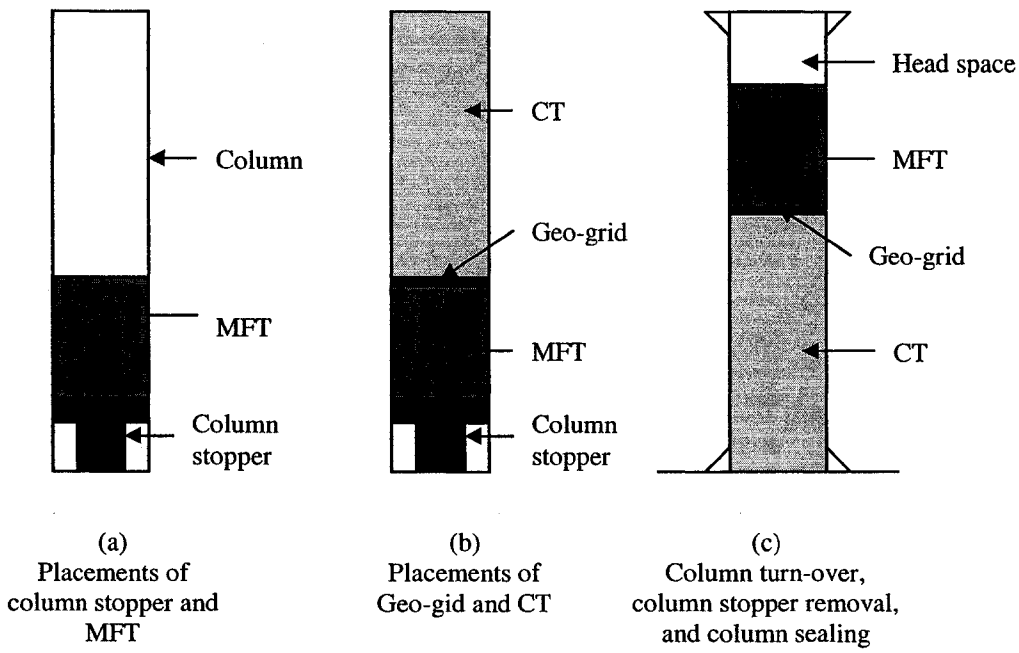

Figure 4-2. Schematics of column filling procedures for Systems 1 and 2 (not to scale)

4.2.5 Incubation and regular monitoring of the columns

After filling, all static columns were moved to the incubation room. The columns were maintained at 18 to 20°C, under dark conditions during incubation.

For all columns in Systems 1, 2, 3, and 4, at suitable intervals of several days at the beginning of incubation to longer periods at later incubation, the height of the produced cap water and the interface position between the cap water and MFT or cap water and CT layers were measured. These data would be used to determine the water release rate of the deposit and the MFT and/or CT

densification rates. Gas bubble evolution and other possible visual changes in the MFT and CT layers were also recorded.

For System 2, the columns were not sacrificially sampled during the incubation period. At suitable time intervals, the cap water extraction, Geo-grid position monitoring, and headspace gas analysis by GC were regularly performed in an in-situ manner. The order for these analyses was to first conduct the Geo-grid position recording, then conduct the headspace gas GC analysis, and finally perform the cap water extraction under N_2 atmosphere. Particular attention was paid to the cap water extraction. The cap water was extracted using a 60-mL syringe through the 3.2-mm OD stainless steel tubing, which was fixed to the top cover. At every cap water extraction, the existing cap water was completely removed. This complete removal of the cap water sample ensures that every time the sampled cap water represents only the water released since the last sampling. This practice can produce a time series of cap water composition change. The void volume created in the column headspace by the removal of cap water was filled with N_2 gas. Because an adequate volume of cap water was needed at every sampling, the sampling intervals for System 2 were based on the volume of produced cap water and were short at the beginning of incubation and long at the later incubation.

The Tedlar bags were checked regularly. If the Tedlar bag was fully filled with evolved gas, the existing Tedlar bag would be replaced with an empty Tedlar bag. The GC analysis and gas volume measurement of the Tedlar bag gas were conducted for every removed Tedar bag.

4.2.6 Sacrificing and freezing procedures of the columns

At the end of the planned incubation period, the columns were sacrificed for sampling and analysis. Prior to sacrificing the column, the Tygon tubing (which connected the Tedlar bag to the column top cover) was first clamped and the Tedlar bag was removed for gas analysis by GC and gas volume measurement using a 60-mL syringe (from Labcor Inc., Anjou, QC). Then, under a N_2 atmosphere, the top cover of the column was removed and the cap water was sampled.

For System 1, the microbial MPN analyses of SRB and methanogens were conducted at a frequency of usually once every 60 d. The sampling for MPN analysis was completed before the column freezing. The sampling used a core-sampling method (with a 6.4-mm diameter hole) under a N_2 atmosphere. The samples for MPN analysis were taken from the centre of the column using a stretch of suitable size rigid plastic tubing. The samples were then transported in a 60-mL syringe or a 90-mL plastic jar (made of clarified polypropylene) filled with N_2 to the Biological Sciences Laboratory at the University of Alberta. All materials used for MPN sampling (plastic tubing, syringe, and jar) were autoclaved at 121°C for 20 min prior to use.

For MFT, two samples were taken for MPN analysis. One sample was taken from approximately 4 cm below the interface of the cap water and MFT, and the other was taken from approximately 4 cm above the MFT and CT

interface, which was indicated by the position of the Geo-grid. For CT, only one sample was used for MPN analysis. This sample was taken from the middle of the CT layer.

The columns in Systems 1, 3, and 4 were sacrificed at a required interval. After the samplings of Tedlar bag gas, cap water, and MPN samples, the columns were placed in a freezer at a temperature of about –20°C and left for several days to reach a complete frozen state. The columns in System 2 were sacrificed only at the end of 1 y of incubation.

4.2.7 Frozen column cutting and sampling

Figure 4-3 shows the scheme of frozen column cuttings for Systems 1, 2, 3, and 4, with the shaded areas to be cut off.

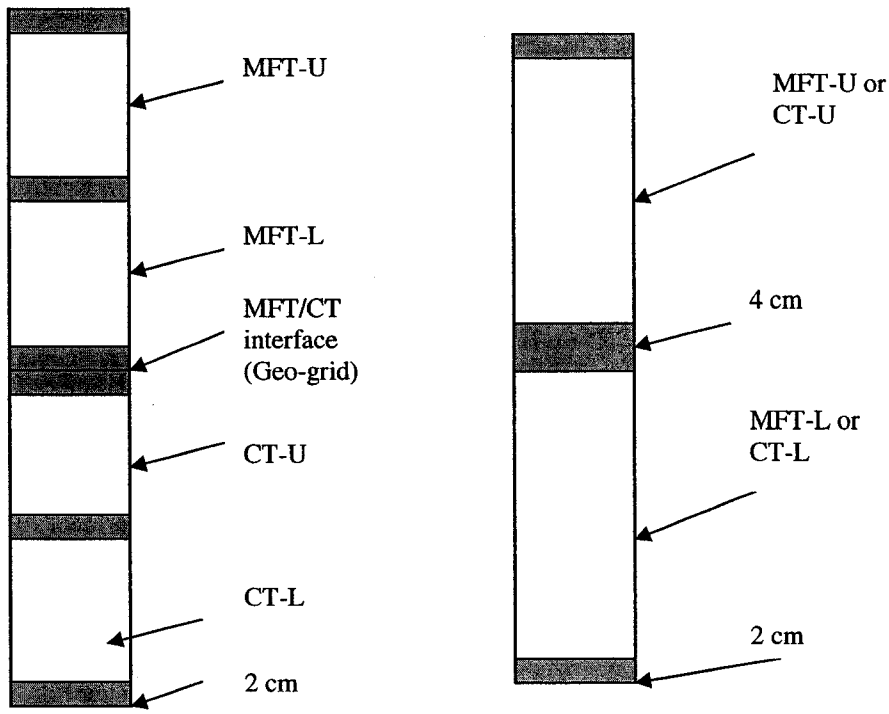

(a). For Systems 1 and 2

(b). For Systems 3 and 4

Figure 4-3. Scheme of frozen column cuttings with the shaded areas to be cut off (not to scale)

4.2.7.1 Frozen column cutting and sampling for columns in Systems 1 and 2

As shown in Figure 4-3a, two MFT and two CT samples from the upper and lower zones of MFT or CT were equally taken in Systems 1 and 2, using the following procedures. First, cut at the Geo-grid position to separate the MFT and CT layers. Then cut off 2 cm from either side in both MFT and CT layers. Further, cut off 2 cm in the middle of the remaining MFT and CT layers to

separate the individual MFT and CT into two samples, respectively. The two MFT and two CT samples were denoted as MFT-U, MFT-L, and CT-U, CT-L, respectively, where U refers to samples from the upper half zone and L refers to samples from the lower half zone of the MFT or CT layer.

4.2.7.2 Frozen column cutting and sampling for columns in Systems 3 and 4

As shown in Figure 4-3b, two MFT or CT samples from the upper and lower zones of MFT or CT were equally taken in Systems 3 and 4, using the following procedures. First cut off the MFT or CT in the middle to separate the MFT or CT into two equal parts. Then cut off 2 cm from either side of the MFT or CT layer to produce two MFT or CT samples. The two MFT or CT samples were denoted as MFT-U, MFT-L, and CT-U, CT-L, respectively, where U refers to samples from the upper half zone and L refers to samples from the lower half zone of the MFT or CT layer.

4.2.8 Subsampling of frozen MFT and CT

The frozen MFT or CT samples were brought to room temperature in 4-L glass jars (filled with N_2) overnight. Then, subsamplings were performed on the MFT or CT samples in a N_2 chamber. The following samples were prepared.

The porewater extraction was completed using a combination of centrifugation and filtration procedures. For centrifugation of the MFT and CT samples, a Sorvall RC-5B centrifuge with SS-34 rotor and eight Teflon tubes of

50 mL each was used at a relative centrifugal force of 12,100 g for 30 min. Immediately after the centrifugation, pre-filtration using AP 15 Millipore glass fiber filter and vacuum filtration under a N_2 atmosphere was performed to remove coarse solids and bitumen. A second filtration was conducted using a disposable 0.45 μm Millipore Millex syringe filter (Millipore, Billerica, Massachusetts, USA).

The MFT and CT subsamples for trapped gas, redox potential, oil/water/solids contents, particle size distribution, and AVS analysis, among others, were also taken at this time under a N_2 atmosphere. These subsamplings were conducted by first homogenizing the MFT or CT under N_2 atmosphere.

4.2.9 Eh measurement on MFT and CT samples

The instrument used for Eh measurement was an Accumet Model 50 pH/Ion/Conductivity Meter with a Cole-Parmer Ag/AgCl ORP electrode. The ORP electrode was calibrated against a standard ORP solution (from Orion Research Inc. Beverly, MA, U.S.A.) both before and after the Eh measurements.

For Eh measurement, the MFT or CT samples were contained in a 120-mL glass jar. During the Eh measurement, the headspace of the jar was filled with N_2. In some samples, the Eh would require a long time to reach a stable point. In order to obtain accurate and consistent results, the Eh readings after 1 and 2 h of measuring time were recorded. The Eh readings at 2 h of measuring time were used for data analysis.

4.2.10 Sulphide analysis in water sample

The S^{2-} analysis in the cap water and porewater samples was performed using "CHEMetrics sulfide test kit" (from CHEMetrics Inc., Calverton, Virginia, U.S.A.). The CHEMetrics test kit employs a methylene blue colorimetric method, and will measure total acid soluble sulphides, including dissolved H_2S, HS^-, and acid-soluble metallic sulphides in suspension. Results are expressed as mg of S/L.

Based on the previous sulphide analysis results in MFT and CT porewaters (Fedorak *et al.* 2000), a sulphide test kit with two ranges of 0 to 1 and 1 to 10 mg/L each (catalogue number K-9510) was used. The minimum detection limit of this test kit was 0.05 mg/L.

The water samples for S^{2-} analysis were first filtered using a 0.45-μm syringe filter. To avoid or minimise the oxidation of sulphides, water samples were prepared with minimum aeration under a N_2 atmosphere and were analysed immediately after the preparation.

4.2.11 MPN analysis on MFT and CT samples

Enumeration of viable microorganisms was accomplished by MPN technique. Only SRB and methanogens were enumerated as these are the most important groups of microorganisms in MFT and CT deposits (Fedorak *et al.* 2000).

The MPN analyses of SRB and methanogens on the MFT and CT samples were conducted using the 3-tube MPN method (Fedorak *et al.* 2000). Due to the laborious nature of the MPN analysis work, the MPN analyses were conducted only on the MFT and CT samples from System 1 at selected incubation times.

The result of MPN analysis used a unit of "MPN/g (of dry solids)" for the MFT or CT. Because the MPN samples for MPN analysis were dispensed as wet materials, the ratio of dry weight to wet weight of the CT and MFT samples was needed for the unit conversion. This ratio was determined in the Environmental Engineering Laboratory by drying the MFT and CT samples in a 104°C (103 to 105°C) oven overnight, following the procedures discussed in APHA (1995). The MFT and CT samples for this drying analysis were collected at the time of taking the MPN samples, using suitable glass containers. The weights of the MFT and CT samples were measured before and after the drying, and the ratio was then calculated.

4.2.12 Trapped gas analysis on MFT and CT samples

The term "trapped gas" in this thesis was used to describe the gas extracted from the MFT or CT samples. Thus, the trapped gas may include both trapped and dissolved gases in the MFT and CT. In this project, the purpose of the trapped gas analysis on MFT and CT was to qualitatively determine if CH_4 (and possibly H_2S and C_2H_4) was (or were) present in the MFT and CT. Due to

the high cost of trapped gas analysis on oil sands tailings in the commercial laboratory, with the consent of the industrial partner of this project, the trapped gas analyses of MFT and CT were completed in the Environmental Engineering Laboratory using a self-developed gas extraction and GC analysis method.

The aim of gas extraction method development for trapped gas was to maximise the release of the trapped gas. The following method was developed after some preliminary tests.

(i) In a 160-mL serum bottle, first placed 60 mL of MFT or CT sample, and then filled the serum bottle with 80 mL of N_2-degassed (degassing for about 1 h) deionised water.

(ii) Flushed the headspace of the serum bottle with helium (He) gas for a few minutes and then closed the bottle with a rubber septum. Shook the serum bottle thoroughly for 2 min using a wrist-action shaker.

(iii) Let the serum bottle sit overnight to reach equilibrium between the headspace gas and the slurried sample.

(iv) Using the GC to perform the headspace gas analysis in the serum bottle.

4.2.13 Physical and chemical analyses on water, MFT, and CT samples

These analyses include pH, EC, alkalinity, cations, anions, selected trace elements, residual bitumen, solids content, and particle size distribution. These analyses were performed by Syncrude Analytical Group at the Edmonton

Research Centre, using established company protocols and standard methods (Fedorak *et al.* 2000).

4.2.14 Gas analysis by GC

From Fedorak *et al.* (2000), the main gases detected in the headspace of column mesocosms containing MFT or CT deposit and the gases trapped in the MFT and CT were O_2, N_2, CH_4, and CO_2. In addition, some low quantities of H_2S and C_2H_4 might be present. Therefore, in this work, the GC analyses for Tedlar bag gas in Systems 1, 3, and 4, for in-situ column headspace gas in System 2, and for trapped gas in MFT and CT were focused on quantitatively measuring the O_2, N_2, CH_4, CO_2, H_2S, and C_2H_4.

A Varian CP-2003 portable Micro-GC with two channels of A and B was used for all the gas analyses. Channel A was installed with the CP-Mole Sieve column and a TCD detector. Channel A is suitable for the analyses of H_2, O_2, N_2, and CH_4. Channel B was installed with the HayeSep column and a TCD detector. Channel B is suitable for the analyses of CH_4, CO_2, C_2H_4, and H_2S. He was the carrier gas for both columns.

To maintain the Mole Seive column (in channel A) and HayeSep column (in channel B) in good working conditions, the GC columns were regularly "conditioned" at 170°C for Mole Seive column and at 140°C for HayeSep column for 2 to 4 h.

The Micro-GC instrument had an internal sampling pump to automatically retrieve the gas samples. Therefore, no syringe injection was needed for the GC sampling. The container of the gas sample (e.g. the Tedlar bag) was directly connected to the GC sampling port. A suitable sampling time was set to flush out the possible deadspace volume on the gas route between the GC and the gas sample container before the sample injection. The sample injection time was set to be 40 ms. This injection time results in an average injection volume of 200 nL (VCI 1999).

The flowrate reading of the carrier gas has to be measured at its flow-out ports at the back of the Micro-GC. This flowrate was too small to be measured using the available flowrate measuring instrument in this study. To keep the constant flowrate of the carrier gas, the GC was always connected to the carrier gas cylinder with constant 552 kPa outlet pressure. Thus, when running the GC, the carrier gas was always on and at constant flowrate.

Table 4-2 summarises the main parameters of the Micro-GC for GC calibration, Tedlar bag gas analysis in Systems 1, 3, and 4, in-situ column headspace gas analysis in System 2, and trapped gas analysis in MFT and CT.

Table 4-2. The main parameters for the Micro-GC gas analysis.

Channel name	TCD A	TCD B
Channel preference	Active	Active
Column preference	Hi temp.	Lo temp.
Column temperature (°C)	110	50
TCD offset	On	On
Sensitivity	Lo	Mid
Injection time (ms)	40	40
Injector heater	Yes	Yes
Injector temperature (°C)	110	110

According to Jason Dunbar from Varian Canada, the minimum detection limits of this GC for all the above listed gases are approximately 50 ppm (by volume).

4.2.14.1 GC calibration and verification

Based on the gas concentration ranges found in Fedorak *et al.* (2000), the expected concentration ranges for the gases in this project were determined. Four levels of external calibration were used for most of the gases, with the exception of H_2S, for which only three levels of external calibration were used. For preparing the desired standard concentrations, pure standard gas, helium gas (as balance gas), a 1-L Tedlar bag, a soap-film flowmeter, and a stopwatch were used.

For H_2S, only three level calibrations were used, because of the difficulty in preparing the standard concentrations. The three levels of standard H_2S gas were prepared by Aaron Gatzke in Maxxam Analytics Inc. (Edmonton, Alberta).

The GC calibration used the GC parameters as shown in Table 4-2. The Tedlar bag containing standard concentration gas was directly connected to GC

via a 4-cm long Tygon tubing. At the calibration, the sampling time was set to be 30 s.

After establishing the calibration curves, some verification runs were conducted using individual or mixed standard gases in the Environmental Engineering Laboratory. The verifications used the same method as the calibration. The calibration and verification of this GC are summarised at Tables A-1 and A-2 in Appendix A, respectively.

4.2.14.2 Gas analysis by GC for Tedlar bag gas in Systems 1, 3, and 4

The GC analysis on the Tedlar bag gas in Systems 1, 3, and 4 used the GC parameters in Table 4-2. The Tedlar bag was directly connected to the GC via a 4-cm long Tygon tubing. The sampling time was set to be 30 s. For each Tedlar bag gas, triplicate analysis was conducted.

4.2.14.3 Gas analysis by GC for in-situ column headspace gas in System 2

The GC analysis on the column headspace gas in System 2 used the GC parameters in Table 4-2. The column headspace was directly connected to the GC via a 40-cm long stainless steel tubing with 1.6-mm OD. The sampling time was set to be 60 s. For each headspace gas, triplicate analysis was conducted.

4.2.14.4 Gas analysis by GC for trapped gas in MFT and CT

The GC analysis on the trapped gas in MFT and CT for all systems used the GC parameters in Table 4-2. The serum bottle containing the MFT and CT samples for trapped gas analysis (see Section 4.2.12) was directly connected to the GC via a 10-cm long stainless steel tubing with 1.6-mm OD. The sampling time was set to be 30 s. For each trapped gas sample, triplicate analysis was conducted.

4.2.15 AVS analysis on MFT and CT samples

AVS are the sum of amorphous iron monosulphide (FeS), mackinawite (FeS_{1-x}), greigite (Fe_3S_4) (Duan *et al.* 1997; Morse *et al.* 1987), as well as sulphides of other metals such as ZnS and CdS (Gerard *et al.* 1998; Lasorsa *et al.* 1996). Because AVS species are metastable and reactive, either by oxidation or by subsequent reduction to FeS_2 (pyrite), it is reasonable to assume that the presence of AVS is an indicator of recent SO_4^{2-} reduction (Kennedy *et al.* 1999).

AVS are usually determined by first liberating H_2S from the sulphides using cold acid (1 to 6 M HCl), and then distillating and trapping of the released H_2S, which can be analysed by several methods. More severe acid treatment, often with heating or with the addition of other chemicals, releases sulphides from other compounds (e.g. pyrite).

In cold acid extraction, the amorphous FeS and mackinawite are quantitatively recovered, but the recovery of greigite is incomplete. Under

harsher conditions, such as hot HCl, or cold 6 M HCl plus $SnCl_2$, greigite and newly formed fine-grained synthetic pyrite are recovered. The presence of $SnCl_2$ in the HCl distillation is believed to help diminish the Fe(III) interference that may oxidize sulphide to elemental sulphur (S^0) in acid distillation (Duan *et al.* 1997).

Sampling, handling, and analytical techniques that minimise the effect of oxidation are critical for the accurate measurement of AVS. Sulphide is best maintained when samples are handled under a nitrogen atmosphere, stored at 4°C or frozen at –20°C and analysed within 2 wk after sample collection (Lasorsa and Casas 1996).

Through the discussions with the personnel at a commercial laboratory (ALS Environmental, Vancouver, British Columbia), the adopted AVS analysis method for this project was as follows. The AVS analysis used 6 M cold HCl plus $SnCl_2$ to digest the sample. Thus, it is assumed that the analysed sulphur pool is the AVS plus fine-graded (newly formed) synthetic pyrite. The sampling was completed under a N_2 atmosphere. The AVS samples were kept at 4°C in a N_2 atmosphere during storage and delivery, and were analysed within 14 d after sample collection.

4.2.16 Column and sample notations

Through discussions with Dr. MacKinnon, Syncrude Canada Ltd., the column and sample notations for this project were finalised, as shown in Tables A-3, A-4, and A-5 in Appendix A.

4.3 Some definitions and symbols for MFT and CT densifications

For simplifying the presentation and discussion, the following definitions are made and symbols are used throughout this thesis and the Appendices.

4.3.1 Total volume change (Vt, vol%)

The total volume is the combined volume of cap water and total tailings (MFT and/or CT) for Systems 1, 3, and 4. The total volume change (Vt) is defined in Equation 4-1.

$$Vt=((H_t-H_0)/H_0)\times 100 \quad \text{.....(4-1)}$$

where H_0 is the volume of "MFT and CT", of "MFT', and of "CT" for Systems 1, 3, and 4 at incubation time 0, respectively; H_t is the volume of "cap water and MFT and CT", of "cap water and MFT', and of "cap water and CT" for Systems 1, 3, and 4 at a specific incubation time, respectively. Note, at

incubation time 0, it is assumed there was no cap water in the columns of each system.

Based on the definition, a positive value of Vt indicates an increase in the total volume and a negative value of Vt indicates a decrease in the total volume, relative to the total volume at incubation time 0. The Vt is specifically denoted as Vt(1), Vt(3), Vt(4) (vol%) for Systems 1, 3, and 4, respectively.

4.3.2 Total tailings volume change (Vtt, vol%)

The total tailings volume is the volume of "MFT and CT" for Systems 1 and 2; the volume of "MFT" or "CT" for Systems 3 and 4, respectively. The total tailings volume change (Vtt) is defined in Equation 4-2.

$$Vtt=((H_{tt}-H_0)/H_0)\times 100 \quad \text{.....(4-2)}$$

where H_0 is the volume of "MFT and CT" for Systems 1 and 2, the volume of "MFT' or "CT" for Systems 3 and 4 at incubation time 0, respectively; H_{tt} is the volume of "MFT and CT" for Systems 1 and 2, the volume of "MFT" or "CT" for Systems 3 and 4 at a specific incubation time, respectively.

Based on the definition, a positive value of Vtt indicates an increase in the total tailings volume and a negative value of Vtt indicates a decrease in the

total tailings volume, relative to the total tailings volume at incubation time 0. The Vtt is specifically denoted as Vtt(1), Vtt(2), Vtt(3), and Vtt(4) (vol%) for Systems 1, 2, 3, and 4, respectively.

4.3.3 Individual MFT or CT tailings volume change (V_{MFT}, V_{CT}, vol%)

The individual MFT or CT tailings volume is the volume of individual "MFT" or "CT" for each system. The individual MFT or CT tailings volume change (V_{MFT} or V_{CT}) is defined in Equations 4-3 and 4-4, respectively.

$$V_{MFT}=((H_{MFT}-H_{MFT0})/H_{MFT0})\times 100 \quad \text{.....(4-3)}$$

$$V_{CT}=((H_{CT}-H_{CT0})/H_{CT0})\times 100 \quad \text{.....(4-4)}$$

where H_{MFT0} and H_{CT0} are the volumes of "MFT" or "CT" for Systems 1, 2, 3, and 4 at incubation time 0; H_{MFT} and H_{CT} are the volumes of "MFT" or "CT" for Systems 1, 2, 3, and 4 at a specific incubation time.

Based on the definition, a positive value of V_{MFT} or V_{CT} indicates an increase in the individual MFT or CT tailings volume and a negative value of V_{MFT} or V_{CT} indicates a decrease in the individual MFT or CT tailings volume, relative to the individual MFT or CT tailings volume at incubation time 0. The V_{MFT} or V_{CT} is specifically denoted as $V_{MFT(1)}$, $V_{CT(1)}$, $V_{MFT(2)}$, $V_{CT(2)}$, $V_{MFT(3)}$, and $V_{CT(4)}$ (vol%) for Systems 1, 2, 3, and 4, respectively.

It should be noted that by definition:

$V_{MFT(3)}$=Vtt(3);

$V_{CT(4)}$ =Vtt(4).

4.3.4 Cap water volume (Vcw, vol%)

The cap water volume (Vcw) is defined in Equation 4-5.

$$Vcw=(H_{cw}/H_0)\times 100 \quad (4\text{-}5)$$

where H_0 is the volume of "MFT and CT", of "MFT', and of "CT" for Systems 1, 3, and 4 at incubation time 0, respectively; H_{cw} is the volume of cap water for Systems 1, 3, and 4 at a specific incubation time, respectively.

The Vcw is specifically denoted as Vcw(1), Vcw(3), and Vcw(4) (vol%) for Systems 1, 3, and 4, respectively.

4.3.5 Cap water producing rate (Rcw, mL/d)

The cap water producing rate (Rcw) is defined in Equation 4-6.

$$Rcw = (H_{cw2}-H_{cw1})/(t_2-t_1) \quad (4\text{-}6)$$

where t_1 and t_2 are any two consecutive sampling times with $t_2 > t_1$; H_{cw1} and H_{cw2} are the accumulated volumes of cap water for Systems 1, 3, and 4 at the sampling times of t_1 and t_2, respectively.

Based on the definition, Rcw is the average cap water producing rate between any two consecutive sampling times. The Rcw is specifically denoted as Rcw(1), Rcw(3), and Rcw(4) (mL/d) for Systems 1, 3, and 4, respectively.

4.3.6 Headspace volume (Vhs, mL)

The headspace volume (Vhs) is the headspace volume of those sacrificed columns in Systems 1, 3, and 4. The Vhs is specifically denoted as Vhs(1), Vhs(3), and Vhs(4) (mL) for Systems 1, 3, and 4, respectively.

4.4 Column setup

4.4.1 Column setup in Systems 1, 3, and 4.

The MFT and CT placements for columns in Systems 1, 3, and 4 were conducted on November 4, 5, and 6, 2002. The procedures for column filling were discussed previously (Section 4.2.4).

The MFT and CT were stored in the dark storage room at 4°C before use. Because the CT had been in storage for quite a long time, the chemical and microbiological processes may have proceeded to some degree and lead to

lowered SO_4^{2-} and Ca^{2+} concentrations in the CT porewater. According to the suggestion from Dr. MacKinnon, Syncrude Canada Ltd., the CT was amended with Na_2SO_4 and $CaSO_4 \bullet 2H_2O$ salts at a suitable dosage to raise the SO_4^{2-} and Ca^{2+} levels comparable to those in the fresh CT.

A tracer ion, Br^-, was added to the CT in the form of NaBr. Because of its low degree of interactions with other species in the treat materials, Br^- was used as a tracer to follow the transit of the CT porewater release through the MFT layer in Systems 1 and 2. As the tracer in CT and MFT matrices, Br^- was selected over F^- after some preliminary tests.

No chemical amendments were applied to the MFT.

The chemical additions in CT were conducted at the time of column filling. The chemicals were well mixed with the CT. Table 4-3 lists the planned chemical dosages in the CT. The actual chemical additions might be slightly different from the planned dosages due to the errors in weighing the chemical dosages and measuring the CT volumes.

Table 4-3. The planned chemical dosages in CT for Systems 1 and 4.

Chemical	Planned dosage (g/L of CT)
NaBr	0.22
Na_2SO_4	0.56
$CaSO_4 \bullet 2H_2O$	0.06

Prior to column filling, CT mixing was conducted in a 100-L plastic container in the air and the MFT mixing was conducted in a 200-L plastic container under N_2 atmosphere. The CT and MFT materials for filling in

Systems 1, 3, and 4 were divided into several mixings. The baseline samples of all different mixings of MFT and CT were taken and analysed individually. Table 4-4 summarises the MFT and CT mixings and baseline sample notations for Systems 1, 3, and 4.

Table 4-4. MFT and CT mixings and baseline sample notations for Systems 1, 3, and 4.

Materials	Volume of each mixing (L)	Date of mixing and filling	Columns filled with	Baseline sample notation
MFT	135	4 Nov.-02	C1-1, ..., C1-20.	Base MFT 1
	135	6 Nov.-02	C3-1, ..., C3-12.	Base MFT 2
CT	70	5 Nov.-02	C1-1, ..., C1-11	Base CT 1
	70	5 Nov.-02	C1-12, ..., C1-20	Base CT 2
	80	6 Nov.-02	C4-1, ..., C4-12	Base CT 3

The column filling and incubation starting times for Systems 1, 3, and 4 are summarised in Table A-6 in Appendix A. Figure 4-4 shows the columns of Systems 1, 3, and 4 in the incubation room.

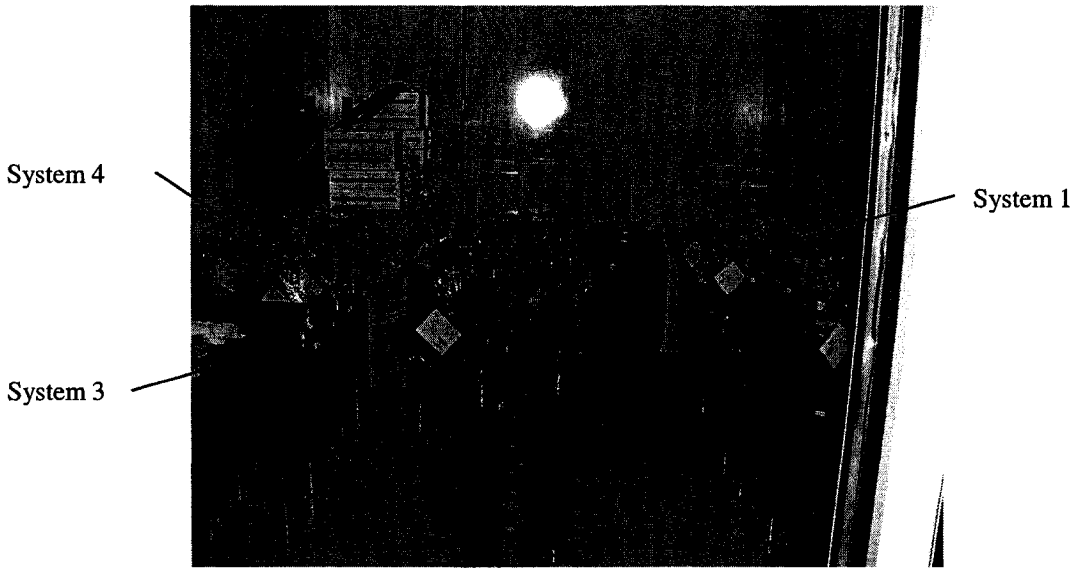

Figure 4-4. The columns of Systems 1, 3, and 4 in the incubation room.

4.4.2 Column setup in System 2

The MFT and CT placements for columns in System 2 were conducted on December 9 and 10, 2002. The procedures for column filling in System 2 were discussed previously in Section 4.2.4.

Chemical amendments and Br^- tracer addition in the form of NaBr in CT for System 2 were conducted. Table 4-5 shows the planned chemical dosages in the CT of System 2. The actual chemical additions might be slightly different from the planned dosages due to the errors in weighing the chemical dosages

and measuring the CT volumes. The six columns in System 2 were divided into three groups in terms of chemical dosage in CT.

Table 4-5. The planned chemical dosages in CT of System 2.

Column	Planned dosage (g/L of CT)			
	NaBr	Na_2SO_4	$CaSO_4 \bullet 2H_2O$	$CH_3COONa \bullet 3H_2O$
C2-1, C2-2, and C2-3	0.22	0.56	0.06	0
C2-4 and C2-5	0.22	1.11	0.22	0
C2-6	0.22	1.11	0.22	1.00

As shown in Table 4-5, The CT in columns C2-1, C2-2, and C2-3 had the same chemical amendments (Na_2SO_4, and $CaSO_4 \bullet 2H_2O$) as in System 1. The CT in columns C2-4 and C2-5 had higher chemical amendments of Na_2SO_4 and $CaSO_4 \bullet 2H_2O$ than in System 1. In column C2-6, the CT had the same dosages of Na_2SO_4 and $CaSO_4 \bullet 2H_2O$ amendments as in columns of C2-4 and C2-5, but with the addition of sodium acetate ($CH_3COONa \bullet 3H_2O$). The purpose of adding this $CH_3COONa \bullet 3H_2O$ was to see if it would stimulate the microbial (methanogens and SRB) activity and hence causing related physical and chemical changes in the MFT and CT.

Prior to column filling, the MFT and CT for System 2 were also well mixed in several mixings. The chemical amendments were applied to CT at CT mixing. The baseline samples of all different mixings of MFT and CT were taken and analysed individually. Table 4-6 summarises the MFT and CT mixings and baseline sample notations for System 2.

Table 4-6. MFT and CT mixings and baseline sample notations for System 2.

Materials	Volume of each mixing (L)	Date of mixing and filling	Columns filled with	Baseline sample notation
MFT	25	9 Dec.-02	C2-1, ..., C2-6	Base MFT 3
CT	25	10 Dec.-02	C2-1, C2-2, C2-3	Base CT 4
	25	10 Dec.-02	C2-4, C2-5	Base CT 5
	12	10 Dec.-02	C2-6	Base CT 6

The column filling and incubation starting times for System 2 are summarised in Table A-7 in Appendix A. Figure 4-5 shows the columns of System 2 in the incubation room.

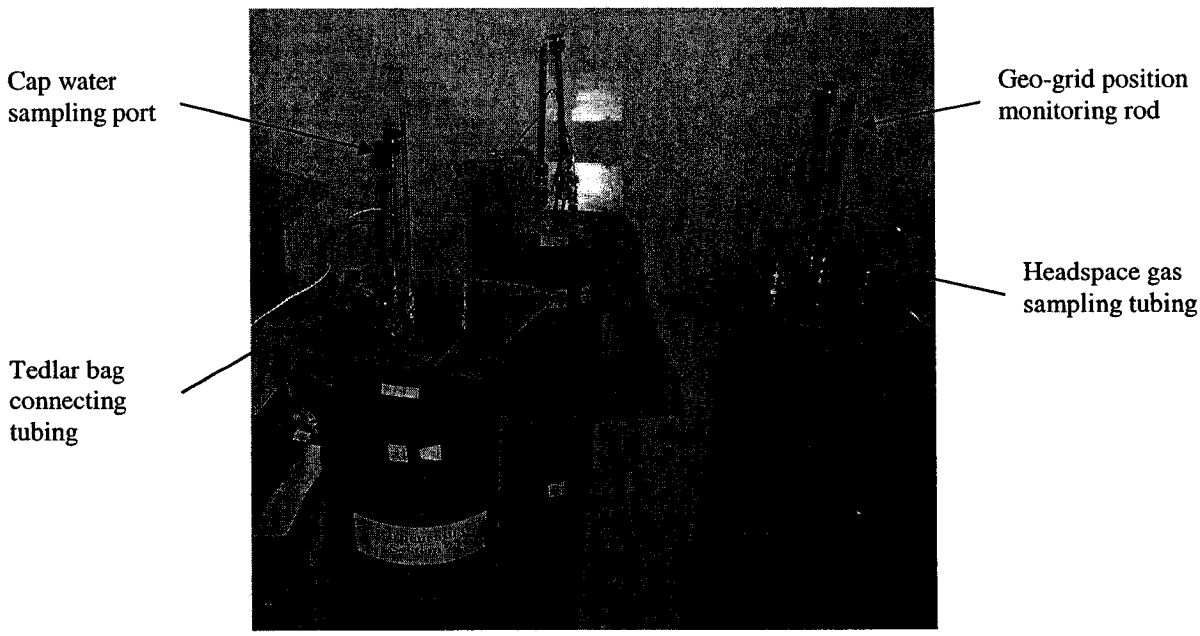

Figure 4-5. The columns of System 2 in the incubation room.

5.0 Results

Columns in Systems 1, 3, and 4 were sacrificially sampled on a regular basis. Columns in System 2 were sacrificed only at the end of 1 y of incubation. The incubation time and sacrificed columns for Systems 1, 2, 3, and 4 are summarised in Table 5-1. As an example for Table 5-1, 3 (C1-2) means the column C1-2 was sacrificed after 3 d of incubation.

Table 5-1. Incubation time and sacrificed columns for Systems 1, 2, 3, and 4.

System	t_{incu} (d) and sacrificed columns	Number of sacrificed columns
1 (Cap water/MFT/CT)	3 (C1-2), 15 (C1-3), 29 (C1-4), 62 (C1-5), 91 (C1-6), 121 (C1-12), 153 (C1-8), 182 (C1-9), 213 (C1-10), 244 (C1-11), 267 (C1-13), 303 (C1-14), 335 (C1-15), 366 (C1-16).	14
2 (Cap water/MFT/CT)	352 (C2-1, C2-4, C2-6)	3
3 (Cap water/MFT)	28 (C3-1), 61 (C3-2), 90 (C3-3), 120 (C3-4), 152 (C3-5), 181 (C3-6), 212 (C3-7), 243 (C3-8), 266 (C3-9), 302 (C3-10), 334 (C3-11), 365 (C3-12)	12
4 (Cap water/CT)	28 (C4-1), 61 (C4-2), 90 (C4-3), 120 (C4-4), 152 (C4-5), 181 (C4-6), 212 (C4-7), 243 (C4-8), 266 (C4-9), 302 (C4-10), 334 (C4-11), 365 (C4-12)	12

1). t_{incu}=incubation time.

The regular monitorings during incubation and analyses at sacrificial sampling for Systems 1, 2, 3, and 4 were given in Section 4.2.

5.1 MFT and CT densifications and water release

5.1.1 MFT densification and water release in System 3 (Cap water/MFT)

Figures B-1, B-2, B-3, and B-4 in Appendix B summarise the Vt(3), Vtt(3), Vcw(3), and Rcw(3) values over 1 y of incubation for the columns in System 3. Table 5-2 summarises the relevant parameters for the columns in System 3 at the end of specific incubation periods.

Table 5-2. Summary of relevant parameters at the end of specific incubation period in System 3.

Column	t_{incu} (d)	Vt(3) (vol%)	Vtt(3) (vol%)	Vcw(3) (vol%)	Rcw(3) (mL/d)	Vhs(3) (mL)
C3-1	28	4.4	1.3	3.1	7.5	3970
C3-2	61	10.6	2.7	7.9	6.6	3560
C3-3	90	13.0	3.7	9.3	0.9	3450
C3-4	120	9.3	-2.0	11.3	4.1	3690
C3-5	152	10.2	-3.3	13.5	3.2	3660
C3-6	181	10.1	-3.7	13.7	1.9	3650
C3-7	212	8.6	-5.1	13.8	1.1	3730
C3-8	243	8.6	-5.7	14.3	-0.7	3710
C3-9	266	8.1	-7.1	15.2	0.5	3740
C3-10	302	7.5	-8.0	15.5	0.9	3730
C3-11	334	7.9	-8.1	15.9	1.4	3730
C3-12	365	6.9	-8.8	15.7	0.8	3810

Table B-1 in Appendix B lists the absolute heights of cap water and MFT at time 0 and at column sacrificing for each sacrificed column in System 3. It is noted that the height of cap water at time 0 is zero. Based on Table B-1, Figure 5-1 shows the relative heights of cap water and MFT in the sacrificed columns of System 3 over 1 y of incubation.

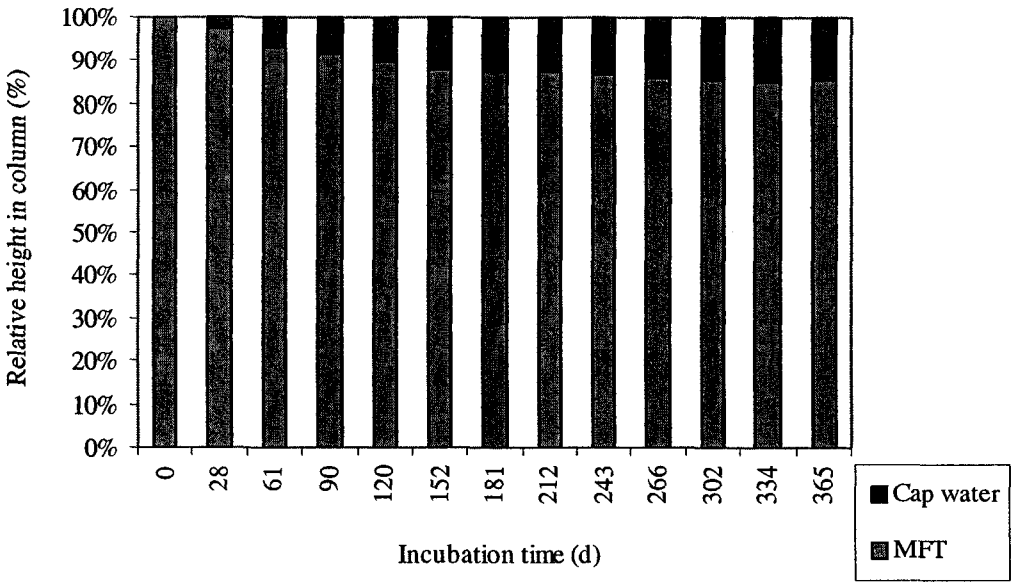

Figure 5-1. Relative heights of cap water and MFT in System 3.

5.1.2 CT densification and water release in System 4 (Cap water/CT)

Figures B-5, B-6, B-7, and B-8 in Appendix B summarise the Vt(4), Vtt(4), Vcw(4), and Rcw(4) values over 1 y of incubation for the columns in System 4. Table 5-3 summarises the relevant parameters for the columns in System 4 at the end of specific incubation periods.

Table 5-3. Summary of relevant parameters at the end of specific incubation period in System 4.

Column	t_{incu} (d)	Vt(4) (vol%)	Vtt(4) (vol%)	Vcw(4) (vol%)	Rcw(4) (mL/d)	Vhs(4) (mL)
C4-1	28	0.0	-22.5	22.5	15.1	4260
C4-2	61	-0.4	-28.2	27.9	6.6	4300
C4-3	90	0.0	-30.5	30.5	2.6	4270
C4-4	120	0.0	-31.0	31.0	1.1	4270
C4-5	152	0.0	-31.4	31.4	1.1	4220
C4-6	181	0.0	-31.8	31.8	0.8	4280
C4-7	212	0.0	-31.9	31.9	0.4	4350
C4-8	243	-0.4	-31.8	31.4	0.0	4310
C4-9	266	-0.7	-32.6	31.9	0.0	4340
C4-10	302	-0.4	-32.1	31.7	0.3	4270
C4-11	334	-0.7	-32.6	31.9	0.0	4410
C4-12	365	-0.4	-31.9	31.5	0.0	4360

Table B-2 in Appendix B lists the absolute heights of cap water and CT at time 0 and at column sacrificing for each sacrificed column in System 4. It is noted that the height of cap water at time 0 is zero. Based on Table B-2, Figure 5-2 shows the relative heights of cap water and CT in the sacrificed columns of System 4 over 1 y of incubation.

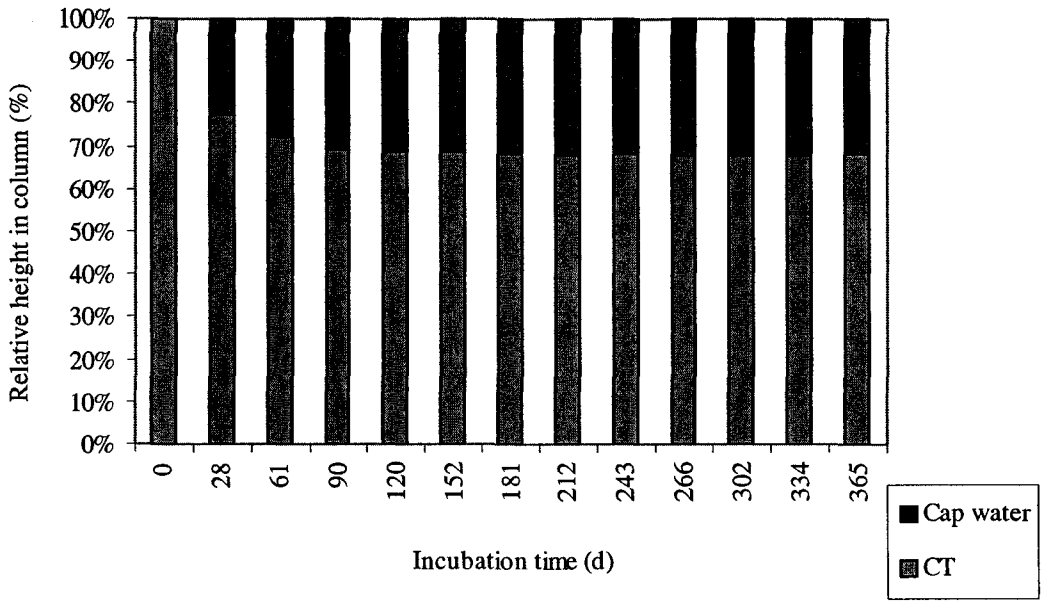

Figure 5-2. Relative heights of cap water and CT in System 4.

5.1.3 MFT and CT densifications and water release in System 1 (Cap water/MFT/CT)

Figures B-9, B-10, B-11, B-12 in Appendix B summarise the Vt(1), Vtt(1), Vcw(1), and Rcw(1) values over 1 y of incubation for the columns in System 1. Table 5-4 summarises the relevant parameters for the columns in System 1 at the end of specific incubation periods.

Table 5-4. Summary of relevant parameters at the end of specific incubation period in System 1.

Column	t_{incu} (d)	Vt(1) (vol%)	Vtt(1) (vol%)	Vcw(1) (vol%)	Rcw(1) (mL/d)	$V_{CT(1)}$ (vol%)	$V_{MFT(1)}$ (vol%)	Vhs(1) (mL)
C1-2	3	-0.1	-4.8	4.6	90.4	-7.3	0.4	1130
C1-3	15	-1.4	-11.8	10.5	28.3	-19.3	1.5	1330
C1-4	29	-0.6	-15.5	14.8	18.8	-23.4	0.0	1220
C1-5	62	0.2	-18.3	18.6	8.5	-29.7	4.8	1160
C1-6	91	-0.6	-20.1	19.5	5.2	-29.7	-1.8	1210
C1-12	121	0.7	-21.2	22.0	3.0	-30.7	-2.2	1100
C1-8	153	-2.8	-22.4	19.5	0.7	-33.1	-1.1	1410
C1-9	182	-3.4	-23.4	20.0	0.4	-32.6	-4.8	1450
C1-10	213	1.2	-20.3	21.6	0.7	-32.1	3.3	1040
C1-11	244	1.6	-20.0	21.6	0.4	-30.0	-0.4	995
C1-13	267	1.8	-22.0	23.8	-1.0	-32.6	-0.4	950
C1-14	303	1.7	-23.3	25.0	0.6	NA	NA	1010
C1-15	335	-2.1	-24.8	22.8	0.4	-34.9	-5.1	1310
C1-16	366	2.8	-22.1	24.9	1.5	-33.8	1.1	893
C1-1	366	-8.8	-26.2	17.4	0.0	NA	NA	NA
C1-17	366	-2.7	-24.6	21.9	1.5	NA	NA	NA
C1-18	366	2.3	-22.4	24.7	1.1	NA	NA	NA
C1-19	366	-3.4	-25.2	21.8	0.0	NA	NA	NA
C1-20	366	-6.4	-26.1	19.7	0.0	NA	NA	NA

1). NA=not available.

Table B-3 in Appendix B lists the absolute heights of cap water, MFT, and CT at time 0 and at column sacrificing for each sacrificed column in System 1. The separated MFT and CT heights of those sacrificed columns in System 1 are determined by measuring the position of Geo-grid at column sacrificing. It is noted that the height of cap water at time 0 is zero. Based on Table B-3, Figure 5-3 shows the relative heights of cap water, MFT, and CT in the sacrificed columns of System 1 over 1 y of incubation.

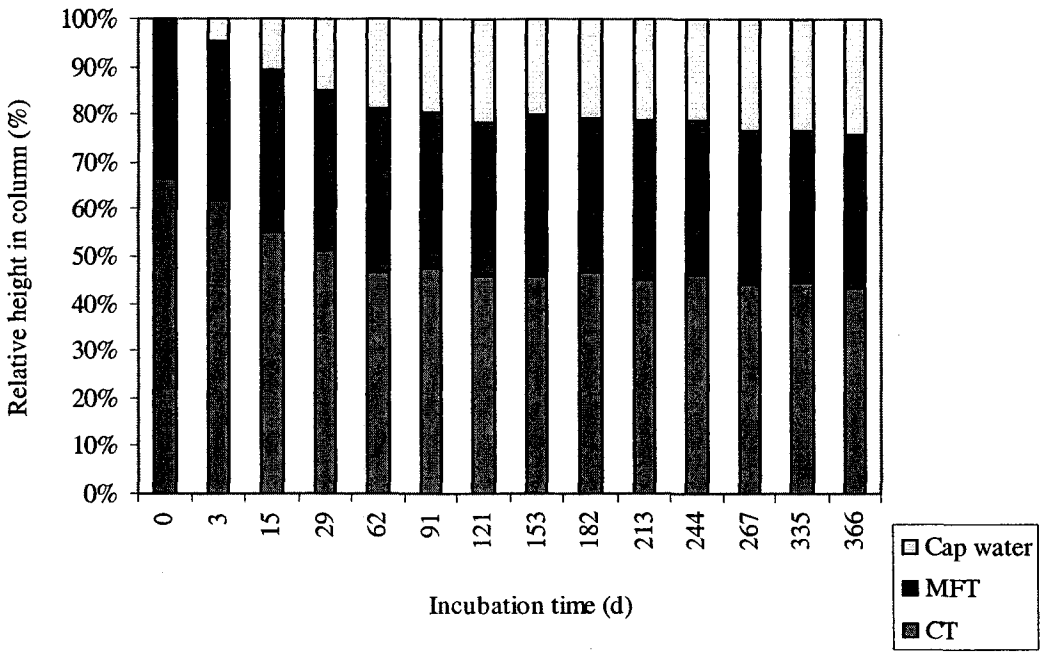

Figure 5-3. Relative heights of cap water, MFT, and CT in System 1.

5.1.4 MFT and CT densifications and water release in System 2 (Cap water/MFT/CT)

Figures B-13, B-15, and B-14 in Appendix B summarise the Vtt(2), $V_{CT(2)}$, and $V_{MFT(2)}$ values over 1 y of incubation for the columns in System 2. Table 5-5 summarises the relevant parameters for the columns in System 2 at the end of 1 y of incubation.

Table 5-5. Summary of relevant parameters at the end of 1 y of incubation in System 2.

Column	t_{incu} (d)	Vtt(2) (vol%)	$V_{CT(2)}$ (vol%)	$V_{MFT(2)}$ (vol%)
C2-1	352	-26.2	-31.8	-14.9
C2-2	352	-22.5	-32.8	-1.8
C2-3	352	-26.0	-34.4	-9.2
C2-4	352	-27.7	-36.9	-9.6
C2-5	352	-27.7	-37.8	-7.7
C2-6	352	-26.8	-37.4	-6.2

5.2 Headspace gas analysis

5.2.1 Tedlar bag gas volume and GC analysis in Systems 1, 3, and 4

Table B-4 in Appendix B summarises the Tedlar bag gas volume and GC analysis results for the major sacrificed columns in Systems 1, 3, and 4.

5.2.2 In-situ headspace gas GC analysis in System 2

Table B-5 in Appendix B summarises the frequent in-situ headspace gas analysis results for the columns in System 2, over 1 y of incubation.

5.3 Physical and chemical analyses

The physical and chemical analyses include pH, EC, cations (Ca^{2+}, Mg^{2+}, Na^{+}, K^{+}, NH_4^{+}), anions (SO_4^{2-}, S^{2-}, PO_4^{3-}, NO_3^{-}, NO_2^{-}, Cl^{-}), trace elements (Al, Fe), AVS, Eh, solids content, residual bitumen, particle size distribution, and S^{2-}. The Br^{-}, F^{-}, and SO_4^{2-} ions, and Al and Fe trace metals in some samples were non-detectable or below detection limits (BDL). The detection limits are 0.5

mg/L for Br^-, F^-, and SO_4^{2-}, and 0.01 mg/L for Al and Fe (Dr. MacKinnon, Syncrude Canada Ltd., personal communication).

5.3.1 Physical and chemical analyses on baseline MFT and CT

Table B-6 in Appendix B summarises the results of physical and chemical analyses on the baseline MFT and CT samples for Systems 1, 2, 3, and 4. The baseline MFT and CT samples were taken at the column fillings, and their data serve as the time 0 baseline data.

5.3.2 Physical and chemical analyses in System 3 (Cap water/MFT)

Table B-7 in Appendix B summarises the results of physical and chemical analyses on the cap water, MFT porewater, and MFT samples for all the sacrificed columns in System 3 over 1 y of incubation.

5.3.3 Physical and chemical analyses in System 4 (Cap water/CT)

Table B-8 in Appendix B summarises the results of physical and chemical analyses on the cap water, CT porewater, and CT samples for all the sacrificed columns in System 4 over 1 y of incubation.

5.3.4 Physical and chemical analyses in System 1 (Cap water/MFT/CT)

Table B-9 in Appendix B summarises the results of physical and chemical analyses on the cap water, MFT and CT porewaters, and MFT and CT samples for all the sacrificed columns in System 1 over 1 y of incubation.

5.3.5 Physical and chemical analyses in System 2 (Cap water/MFT/CT)

Table B-10 in Appendix B summarises the results of physical and chemical analyses on the cap water, MFT and CT porewaters, and MFT and CT samples for the columns in System 2 over 1 y of incubation.

5.4 Trapped gas analysis

5.4.1 Trapped gas analysis in baseline MFT and CT

Table B-11 in Appendix B summarises the results of trapped gas GC analysis on all baseline MFT and CT samples for Systems 1, 2, 3, and 4.

5.4.2 Trapped gas analysis in Systems 1, 2, 3, and 4

Table B-12 in Appendix B summarises the results of trapped gas GC analysis on the MFT and CT samples in major sacrificed columns of Systems 1, 2, 3, and 4.

5.5 MPN analysis in System 1

Table B-13 in Appendix B summarises the MPN analysis results on the MFT and CT samples for specific sacrificed columns in System 1.

6.0 Discussion

Systems 3 and 4 contained only MFT or CT, respectively, and served as controls for the main systems. Systems 1 and 2 contained a combination of overlying MFT and underlying CT, and were the main systems to be studied. System 2 was designed in particular to allow for regular in-situ cap water and headspace gas analyses, and Geo-grid position monitoring without sacrificial sampling.

6.1 MFT and CT densifications and water release

Figures 5-1, 5-2, and 5-3 visually shows the changes, over incubation time, of relative heights of cap water, MFT, and CT layers in the sacrificed columns of Systems 3, 4, and 1, respectively. The detailed discussions on the MFT and CT densifications and water release are presented as follows.

6.1.1 Total volume change (Vt) in Systems 3, 4, and 1

For System 3 (Cap water/MFT), Figure B-1 shows that over 1 y of incubation, the Vt(3) values among the columns were quite similar. The Vt(3) increased quickly from the beginning of the incubation and reached a maximum value in the range of 12.3 to 13.5 vol% in 90 d of incubation among the columns. The Vt(3) then decreased with time and reached 6.9 vol% at 365 d of incubation.

A similar total volume increase in Syncrude MFT in the early incubation was also noted by Fedorak *et al.* (2000).

Fedorak *et al.* (2000) proposed the production of biogenic gas as the possible cause for the total volume increase in MFT deposit, and had observed evident bubbles entrapped in MFT. The high volume of Tedlar bag gas accumulated in System 3 (see Table B-4) indicated that active gas production occurred in the MFT of System 3. Visual observations also showed obvious gas bubbles that rose to the surface of the cap water in columns of System 3.

For System 4 (Cap water/CT), Figure B-5 shows that over 1 y of incubation, the Vt(4) values among the columns were quite small and within 0 to -0.7 vol% (see Figure B-5). These small Vt(4) values during incubation may be due to the small evolved and entrapped gases and the uniform settling and densification in CT. The Tedlar bag gas volume measurement showed little gas production in System 4 (see Table B-4), and no gas bubbles were observed on the cap water surface of columns in System 4.

For System 1 (Cap water/MFT/CT), Figure B-9 shows that after 1 y of incubation, the Vt(1) values among the columns were in the range of -8.8 to 2.8 vol%, indicating a large variation of Vt(1) among different columns.

Possible explanations for the decrease in total volume are the densification of MFT and/or CT, and the release of entrapped gases from the MFT and/or CT layers. Densifications of MFT and/or CT will increase the tailings density and reduce the tailings volume. Gas entrapping into the MFT

and/or CT at column filling is possible. The release of the entrapped gas during incubation will reduce the tailings volume and thus the total volume.

One possible explanation for the increase in the total volume is the trapping and accumulation of newly evolved biogenic gases in the MFT and/or CT layers during incubation.

System 1 showed a large variation in Vt value among the columns over 1 y of incubation. Some columns have positive Vt values while others have negative Vt values over time (see Figure B-9). It is possible that this is in part due to the heterogeneity of MFT and CT materials in different columns. The heterogeneity of MFT and CT materials will lead to different solids densification, gas production and trapping.

6.1.2 Total and individual tailings volume changes (Vtt, V_{MFT}, and V_{CT}) in Systems 3, 4, 1, and 2

The total tailings volume change (Vtt) or individual tailings volume change (V_{MFT} and V_{CT}) can indicate the expansion or shrinkage of the volumes of total "MFT + CT" or individual MFT and CT tailings.

6.1.2.1 Total tailings volume change of MFT (Vtt(3)) in System 3 (Cap water/MFT)

Figure B-2 shows that the MFT tailings volume expanded steadily in the first 60 to 90 d of incubation and reached maximum values of Vtt(3) between 3.6 and 4.6 vol% among the columns of System 3 at 77 d of incubation. After

this time, the Vtt(3) dropped steadily and reached 0 vol% at about 110 d of incubation, and -8.8 vol% at 365 d of incubation.

Table 6-1 lists some Vtt(3) data among the columns of System 3 at specific incubation times, together with solids contents of MFT for the sacrificed columns in System 3 (from Table B-7).

Table 6-1. Tailings volume change and solids content of MFT in System 3 at specific incubation times.

t_{incu} (d)	Tailings volume change (vol%)	Solids content (wt%)	
	Vtt(3)	MFT-U	MFT-L
0	0	38.0	38.0
61	2.7 to 3.3	39.7	40.3
120	-1.6 to -2.4	41.8	41.9
181	-3.3 to -5.1	42.4	43.2
266	-6.4 to -7.1	46.8	43.0
334	-8.0 to -8.1	45.7	46.2
365	-8.8	44.3	45.6

1). NA=not available.
2). Incubation time 0 means baseline samples.

Both the Vtt(3) and solids content values showed densification trend of MFT over 1 y of incubation. However, during the early incubation times, Vtt(3) showed an expansion of MFT while the solids content still showed densification of MFT. The trapped gases in the MFT may be a factor to cause this difference. Gases present in the MFT will increase Vtt of MFT but will not affect the solids content results.

6.1.2.2 Total tailings volume change of CT (Vtt(4)) in System 4 (Cap water/CT)

Figure B-6 shows that over 1 y of incubation, the Vtt(4) decreased substantially in the columns of System 4. The most rapid volume reduction of CT tailings in System 4 occurred in the first 60 d of incubation. Among the columns of System 4, the CT volume reduction reached the Vtt(4) values between -27.7 and -28.6 vol% at 61 d of incubation, and -31.9 vol% at 365 d of incubation.

Table 6-2 lists some Vtt(4) data among the columns of System 4 at specific incubation times, together with the solids contents of CT for the sacrificed columns (from Table B-8).

Table 6-2. Tailings volume change and solids content of CT in System 4 at specific incubation times.

t_{incu} (d)	Tailings volume change (vol%)	Solids content (wt%)	
	Vtt(4)	CT-U	CT-L
0	0	56.6	56.6
61	-27.7 to -28.6	69.3	70.9
120	-30.6 to –31.3	71.3	73.3
181	-31.8 to -32.4	70.4	72.8
212	-31.4 to -32.6	75.7	74.1
266	-31.7 to -32.6	71.5	73.2
334	-31.9 to -32.6	74.9	75.9
356	-31.9	75.9	76.4

1). NA=not available.
2). Incubation time 0 means baseline samples.

It can be seen from Table 6-2 that the solids content in the sacrificed columns of System 4 increased over time, showing densification of CT over time. This is consistent with the Vtt(4) curve (see Figure B-6). It should be noted

that for both the solids content increase and tailings volume decrease, most of the change occurred in the first 60 d of incubation.

6.1.2.3 Total and individual tailings volume changes (Vtt(1), $V_{MFT(1)}$, $V_{CT(1)}$) in System 1 (Cap water/MFT/CT)

Figure B-10 shows that over 1 y of incubation, the Vtt(1) value among the columns of System 1 decreased steadily, with the most rapid decrease occurring in the first 60 d of incubation. The Vtt(1) values among the columns of System 1 were between –17.0 and -21.2 vol% at 62 d of incubation and between -22.4 and -26.2 vol% at 366 d of incubation (see Figure B-10).

Figure C-1 in Appendix C displays the values of Vtt(1), $V_{MFT(1)}$, and $V_{CT(1)}$ for those sacrificed columns in System 1 over 1 y of incubation. The $V_{MFT(1)}$ and $V_{CT(1)}$ were calculated by measuring the position of Geo-grid at the time of sacrificial sampling.

Figure C-1 shows that the MFT layer expanded slightly in the first 60 d of incubation, reaching a maximum $V_{MFT(1)}$ of 4.8 vol% at 62 d of incubation, and started shrinking thereafter. The MFT volume change reached a $V_{MFT(1)}$ of -4.8 vol% at 182 d of incubation. After this time, the $V_{MFT(1)}$ curve was fluctuating and showed no certain decreasing or increasing trend with time. One likely source of this fluctuation in $V_{MFT(1)}$ is the errors introduced in the measurement of Geo-grid position when sacrificing the columns. Because MFT settles more slowly than CT, the errors in measuring the Geo-grid position will have a greater effect on the accuracy of $V_{MFT(1)}$ data than on that of $V_{CT(1)}$ data.

Most of the CT volume decrease also occurred in the first 60 d of incubation, with $V_{CT(1)}$ at –30.0 vol% at 62 d of incubation and at -33.8 vol% at 366 d of incubation. The decrease in Vtt(1) was mainly caused by the tailings volume decrease in CT layer.

Table 6-3 lists some data of Vtt(1), $V_{MFT(1)}$, and $V_{CT(1)}$ in System 1 at specific incubation times, together with the solids contents of MFT and CT for the sacrificed columns. It should be noted that the Vtt(1) data were derived from all the columns under incubation, while the $V_{MFT(1)}$ and $V_{CT(1)}$ data were derived only from the sacrificed columns.

Table 6-3. Total and individual tailings volume changes and solids content at specific incubation times in System 1.

t_{incu} (d)	Total and individual tailings volume changes (vol%)			Solids content (wt%)			
	Vtt(1)	$V_{MFT(1)}$	$V_{CT(1)}$	MFT-U	MFT-L	CT-U	CT-L
0	0	0	0	37.9	37.9	57.2	57.2
62	-17.0 to -21.2	4.8	-29.7	38.3	38.8	71.4	69.2
121	-19.2 to -23.8	-2.2	-30.7	38.9	38.8	73.3	70.9
182	-19.4 to -24.0	-4.8	-32.6	40.1	41.3	73.1	73.8
267	-21.7 to -25.4	-0.4	-32.6	40.0	40.4	71.0	72.8
335	-21.7 to -25.9	-5.1	-34.9	43.0	43.9	75.6	76.3
366	-22.4 to -26.2	1.1	-33.8	42.5	42.9	73.2	73.5

1). Incubation time 0 means baseline samples.
2). The baseline solids content of MFT was 37.9 wt% for all samples in System 1(from 'Base MFT 1').
3). The baseline solids content of CT at 62 and 182 d of incubation was 57.2 wt% (from 'Base CT 1'), and at 121, 267, 335, and 366 d of incubation was 56.5 wt% (from 'Base CT 2').
4). NA=not available.

As shown in Table 6-3, the solids content of CT increased steadily over time and most rapidly in the first 62 d of incubation. This was well matched with the $V_{CT(1)}$ curve. The solids content of MFT also increased steadily over 1 y of incubation. This is not consistent with the fluctuating $V_{MFT(1)}$ data over time. As

discussed above, the fluctuation in $V_{MFT(1)}$ is likely caused by the errors introduced in the measurement of Geo-grid position when sacrificing the columns. The solids content data show that both MFT and CT in System 1 densified to a large extent over time.

6.1.2.4 Total and individual tailings volume changes (Vtt(2), $V_{MFT(2)}$, $V_{CT(2)}$) in System 2 (Cap water/MFT/CT)

Figure B-13 in Appendix B shows that during 352 d of incubation, the Vtt(2) values among the columns of System 2 decreased steadily over time. The data show that the most rapid settling and densification of the total "MFT + CT" in System 2 occurred in the first 60 d of incubation.

Figures B-14 and B-15 in Appendix B show the $V_{MFT(2)}$ and $V_{CT(2)}$ values in System 2 over 352 d of incubation. The $V_{MFT(2)}$ and $V_{CT(2)}$ were calculated by monitoring the Geo-grid position. The Geo-grid positions in the columns of System 2 were monitored in an in-situ manner. Therefore, the $V_{MFT(2)}$ and $V_{CT(2)}$ data of System 2 were determined without sacrificing the columns.

Figure B-14 shows that the MFT in System 2 expanded slightly in the first 30 d of incubation and started densification thereafter. This trend was similar to the trend observed in the MFT of System 3. In System 2, the largest MFT expansion was 2.9 vol% of $V_{MFT(2)}$ at 14 d of incubation among all six columns. The MFT densified slowly over time and, among the columns of System 2, reached a $V_{MFT(2)}$ range of 0.4 to -1.5 vol% at 49 d of incubation, and

-6.2 to -14.9 vol% at 352 d of incubation. These ranges do not include the data of column C2-2, because column C2-2 had $V_{MFT(2)}$ values deviated greatly from other columns over time. The exact reasons for the large deviation of $V_{MFT(2)}$ in column C2-2 were unknown. The columns in System 2 showed some difference in $V_{MFT(2)}$ values, but the $V_{MFT(2)}$ curve still indicates steady densification of MFT in System 2 with time after an initial expansion in the first 30 d of incubation. By comparison, the $V_{MFT(1)}$ of MFT layer in System 1 showed no obvious trend of densification (see Figure C-1). As in System 1, the $V_{MFT(2)}$ data were also determined by first monitoring the Geo-grid position, which separated the MFT and CT layers in the column. The Geo-grid position in System 2 was measured in in-situ manner without sacrificing the column, whereas the Geo-grid position in System 1 was determined by first sacrificing the column and removing the column cover. This practice of Geo-grid position measurement leads to more accurate Geo-grid position data in System 2 than in System 1. Therefore, the $V_{MFT(2)}$ in System 2 will be more reliable than $V_{MFT(1)}$ in System 1. A conclusion can thus be made that, from the $V_{MFT(2)}$ data of MFT in System 2, the MFT in the CT beneath MFT deposition system (Systems 1 and 2) will consolidate steadily after slight expansion in the first 30 to 60 d of incubation.

Figure B-15 shows that the CT in System 2 consolidated rapidly and to a larger extent than the MFT, similar to the CT in System 1 (see Figure C-1). Most of the $V_{CT(2)}$ decrease occurred in the first 60 d of incubation. The $V_{CT(2)}$ values among the columns in System 2 were between -28.3 and -31.7 vol% at 49 d of incubation, and between -31.8 and -37.4 vol% at 352 d of incubation.

Both the individual tailings volume change (V_{MFT}, V_{CT}) and solids content can be used to describe the densification behaviour of MFT and CT.

For the MFT in Systems 1 and 2, the $V_{MFT(1)}$ and $V_{MFT(2)}$ are calculated by first measuring the position of Geo-grid. Because the MFT settled and consolidated slowly, the errors caused by the Geo-grid displacement at column filling and by Geo-grid position measurement at column sacrificing will have substantial affect on the accurate calculation of $V_{MFT(1)}$ and $V_{MFT(2)}$. Therefore, the data of $V_{MFT(1)}$ and $V_{MFT(2)}$ should be used with caution. Furthermore, $V_{MFT(2)}$ will likely be more accurate than $V_{MFT(1)}$, due to the more accurate in-situ Geo-grid position monitoring in System 2. The solids content analysis will not be affected by the errors related to the Geo-grid position measurement. Therefore, for the MFT in Systems 1 and 2, it is believed that the solids content data will be more reliable than the tailings volume change (V_{MFT}) in characterising the densification behaviour of MFT.

Due to the substantial densification of the CT in both Systems 1 and 2, the $V_{CT(1)}$ and $V_{CT(2)}$ are large values. Thus, the $V_{CT(1)}$ and $V_{CT(2)}$ will be less affected by the errors in Geo-grid position determination. That is, the $V_{CT(1)}$ and $V_{CT(2)}$ are more accurate and reliable than the $V_{MFT(1)}$ and $V_{MFT(2)}$. Therefore, for the CT in Systems 1 and 2, both the solids content and tailings volume change (V_{CT}) can be used to characterise the densification behaviour of CT.

As shown in Table 4-5, the columns in System 2 had different chemical amendments (Na_2SO_4, $CaSO_4 \cdot 2H_2O$, and $CH_3COONa \cdot 3H_2O$). However, the data of Vtt(2), $V_{MFT(2)}$, and $V_{CT(2)}$ in System 2 over 1 y of incubation showed no

certain effects of these different chemical amendments on the MFT and CT densification rates.

Table 6-4 lists some data of Vtt(2), $V_{MFT(2)}$, and $V_{CT(2)}$ among the columns of System 2, at specific incubation times.

Table 6-4. Total and individual tailings volume changes at specific incubation times in System 2.

t_{incu} (d)	Total and individual tailings volume changes (vol%)		
	Vtt(2)	$V_{MFT(2)}$	$V_{CT(2)}$
49	-18.1 to -21.5	0.4 to -1.5	-28.3 to -31.7
77	-19.8 to -23.5	-1.1 to -2.6	-30.5 to -34.3
133	-21.0 to -25.7	-2.9 to -4.8	-31.9 to -36.3
352	-22.5 to -27.7	-6.2 to -14.9	-31.8 to -37.4

1). For the data of $V_{MFT(2)}$, column C2-2 is not included.

The comparison of V_{MFT} between System 2 (see Figure B-14) and System 3 (see Figure B-2) shows that the MFT in both systems had similar densification over time, and the CT water release had little affect on the densification rate of the overlying MFT in the CT beneath MFT deposition system.

The V_{CT} in Systems 1 and 2 (see Figures C-1 and B-15) had basically the same values as the V_{CT} in System 4 (see Figure B-6). This comparison shows that the overlying MFT layer had no adverse affect on the densification rate of the underlying CT in Systems 1 and 2.

Furthermore, all CT in Systems 1, 2, and 4 showed that most of the settling and densification occurred in the first 60 d of incubation with a slower densification thereafter (see Figures C-1, B-15, and B-6), indicating further densification of CT would be limited.

Tang (1997) discussed two stage CT densification: the first stage of initial settling and the second stage of long-term densification. The initial settling of CT starts immediately after deposition, and usually lasts several days or weeks. Initially, the CT has a strengthened MFT card-house structure within which the coarse sands particles are embedded. During the initial settling of CT, the self-weight force of the sands is transferred to the clay particles and the CT deposit undergoes significant volume reduction as the porewater is pushed out of the clay medium. The second stage of long-term densification begins when the sand grains come in contact with one another and form a sand matrix. The long-term densification of CT proceeds at a much slower rate.

Figure C-1 for System 1, Figure B-15 for System 2, and Figure B-6 for System 4 all show the two stages of densification of CT, that is, the first stage of rapid CT volume reduction which occurred in the first 60 d of incubation, and the second stage of CT densification where the CT consolidated slowly. This settling pattern is matched with the curve of cap water producing rates in Systems 1 and 4 (see Figures B-12 and B-8). The rate of CT dewatering and densification depends on many factors, including the deposit composition, density, and the permeability.

6.1.3 Cap water volume (Vcw) and cap water producing rate (Rcw)

6.1.3.1 Cap water volume (Vcw)

Figures B-3, B-7, and B-11 show the Vcw(3), Vcw(4), and Vcw(1) values over 1 y of incubation in Systems 3, 4, and 1, respectively. Comparing Figures B-3, B-7, and B-11, in Systems 1 and 4, most of the cap water was produced in the first 60 d of incubation, and this was matched well with the rapid total tailings volume reduction during the first 60 d of incubation (see Figures B-10 and B-6); whereas in System 3, the cap water was produced over a longer time period. In general, CT released more water than MFT over the 1 y of incubation as shown in Figure B-3 for System 3 and Figure B-7 for System 4.

6.1.3.2 Cap water producing rate (Rcw)

Figures B-4, B-8, and B-12 show the Rcw(3), Rcw(4), and Rcw(1) values over 1 y of incubation in Systems 3, 4, and 1, respectively. System 3 showed a relatively uniform cap water producing rate over the entire incubation period, whereas Systems 1 and 4 showed rapid cap water producing in the first 60 d of incubation.

For System 3 (Cap water/MFT), Figure B-4 shows that no initial rapid cap water producing was observed at the beginning of the incubation. The cap water producing rate was slow at the beginning of incubation and reached a maximum value of approximately 17.0 mL/d at 30 d of incubation. After that time, the cap water producing rate decreased slowly over time and reached 0.8

mL/d at 365 d of incubation. The slow cap water producing rate of MFT was well matched with the slow densification rate of MFT (see Figure B-2).

For System 4 (Cap water/CT), Figure B-8 shows that the cap water producing rate among the columns decreased from approximately 200 mL/d to between 7.5 and 9.4 mL/d at 61 d of incubation, and to approximately 0 mL/d by 212 d of incubation.

For System 1 (Cap water/MFT/CT), Figure B-12 shows that the cap water producing rate among the columns decreased from approximately 200 mL/d during the first day of incubation to between 6.4 and 9.4 mL/d at 62 d of incubation, and to approximately 0 mL/d by 244 d of incubation.

6.2 Headspace gas analysis

6.2.1 Tedlar bag gas analysis in Systems 1, 3, and 4

Tedlar bag gas analysis included the Tedlar bag gas volume measurement and the Tedlar bag gas GC analysis. Table B-4 summarises the volume measurement and the GC analysis results of the Tedlar bag gas for the major sacrificed columns in Systems 1, 3, and 4 over 1 y of incubation.

For comparison purpose, Figure C-2 in Appendix C summarises the Tedlar bag gas volume measurements in the three systems over 1 y of incubation. The Tedlar bag gas volume is the gas volume collected in the Tedlar bag of each sacrificed column.

System 3 (Cap water/MFT) showed high and large variation of gas production over time. Over 1 y of incubation, 20 to 2030 mL of Tedlar bag gas from one single column was collected among the sacrificed columns. Visual observations indicated obvious gas evolution from the columns of System 3. Fedorak *et al.* (2000) also reported large variations of Tedlar bag gas volume from Syncrude MFT. The different gas productions and gas holding capacities among MFT columns may cause this gas volume variation from column to column.

Compared with System 3, the Tedlar bag gas volumes in Systems 1 (Cap water/MFT/CT) and 4 (Cap water/CT) were quite low and relatively constant over time (see Table B-4). In System 1, over 1 y of incubation, only 10 to 60 mL of Tedlar bag gas from one single column was collected among the sacrificed columns. In System 4, 17 to 308 mL of Tedlar bag gas from one single column was collected over 1 y of incubation among the sacrificed columns. Visual observations indicated that no obvious gas evolution was seen from columns of Systems 1 and 4.

The Tedlar bag gas GC analysis for Systems 1, 3, and 4 is also presented in Table B-4. The gases identified by the GC analysis included CH_4, N_2, O_2, CO_2, H_2S, and C_2H_4.

For CH_4, the Tedlar bag gas from both Systems 1 and 3 showed an increase in CH_4 concentration over incubation time. In System 1, the CH_4 concentration increased steadily from 0.04 vol% at 29 d of incubation to 4.57 vol% at 213 d of incubation. In System 3, the CH_4 concentration increased

steadily from 0.39 vol% at 28 d of incubation to 20.7 vol% at 212 d of incubation, with 34.0 vol% at 334 d of incubation. Fedorak *et al.* (2000) also reported increase trend of CH_4 concentration in the headspace of MFT column. However, in some columns of Systems 1 and 3 (including columns C1-8, C1-11, C1-13, C1-14, C1-15, and C1-16 in System 1, columns C3-5, C3-8, C3-9, and C3-12 in System 3), the CH_4 concentrations were lower than the level expected from the increasing CH_4 concentration trend. These unusually low CH_4 concentrations corresponded to high O_2 concentrations in the Tedlar bag gas (see Table B-4). The high O_2 concentrations indicated column leaking and air intake in the Tedlar bag. This column leaking was also a possible source to cause these low CH_4 concentrations, due to the loss of CH_4 from the Tedlar bag to the air. The heterogeneity of MFT and CT materials among columns and the errors in GC analysis might also have a role in resulting in the unusually low CH_4 concentrations.

In System 4, the CH_4 concentrations in the columns were quite low and only between non-detectable concentrations to 0.29 vol% over 1 y of incubation.

Using Tedlar bag gas volume, the headspace volume at column sacrificing, and gas composition (see Table B-4), Figure C-3 summarises the total CH_4 volume in the Tedlar bag and column headspace of each sacrificed column in Systems 1, 3, and 4 over 1 y of incubation. By dividing the total CH_4 volume by the volume of baseline tailings, the CH_4 yield could be calculated. The baseline tailings volume for each system could be calculated based on the deposit dimension at column filling (see Table 4-1). The volume of baseline

tailings was approximately 9.2 L of "MFT+CT" for System 1, 6.1 L of MFT for System 3, and 6.1 L of CT for System 4. Table 6-5 summarises the CH_4 yield data.

Table 6-5. The CH_4 yield in Systems 1, 3, and 4.

System 1 (Cap water/MFT/CT)		System 3 (Cap water/MFT)		System 4 (Cap water/CT)	
t_{incu} (d)	mL of CH_4/L of baseline "MFT+CT"	t_{incu} (d)	mL of CH_4/L of baseline MFT	t_{incu} (d)	mL of CH_4/L of baseline CT
29	0.1	28	2.8	28	0.3
62	0.6	61	2.9	61	0.4
91	4.9	90	29.4	90	0.6
121	3.6	120	86.7	120	0
153	0.2	152	2.0	152	0.8
182	6.5	181	140	181	0.4
213	5.3	212	142	212	2.1
244	0.7	243	5.2	243	0.9
267	0.2	266	3.5	266	0
303	1.0	302	123	302	1.0
335	0.1	334	286	334	0.3
366	0	365	46.3	365	0.5

The results presented in Table 6-5 indicate that System 1 yielded more CH_4 than System 4, but still less than System 3. Fedorak *et al.* (2000) reported the CH_4 yield from Syncrude MFT after about 1 y of incubation was 130 mL of CH_4/L of MFT, which was comparable to some CH_4 yield data of System 3.

As discussed above, System 3 had higher Tedlar gas volume and CH_4 yield than either System 1 or 4. This high CH_4 yield can be explained by the activities of methanogens and low sulphate concentrations in the MFT.

Methanogens and SRB are active in Syncrude MFT and CT (Holowenko 2000; Fedorak *et al.* 2000). The methanogens and SRB will compete for substrates. Thermodynamically and kinetically, SRB have the advantage to compete over methanogens. In an anaerobic environment containing sulphate (as is the case in CT), methanogenesis will be inhibited and may be active again after the sulphate has depleted to a certain level. Fedorak *et al.* (2000) noted that both Syncrude MFT and CT have the potential to become methanogenic and methane production occurred substantially after the sulphate concentration has dropped to about 20 mg/L.

Figures C-4, C-5, and C-6 show the sulphate concentrations in the cap water and porewaters of MFT and CT in Systems 1, 3, and 4 over 1 y of incubation, respectively. It is clear that, in Systems 1 and 4, the SO_4^{2-} concentrations in most of the cap water and porewater were well above 20 mg/L over 1 y of incubation. Accordingly, the high concentrations of SO_4^{2-} in the cap water and porewater samples will favour the activity of SRB and inhibit the methane production. In System 3, however, the SO_4^{2-} concentrations in most of the cap water and porewater samples were well below 20 mg/L, thus favouring potential methanogenesis and methane production.

Although high concentrations of SO_4^{2-} will inhibit methane production, methane production does not always require low SO_4^{2-} concentrations (Fedorak *et al.* 2002). This observation may provide an explanation for the fact that in the Tedlar bag gases of Systems 1 and 4, there was still some measurable CH_4. With the decrease in SO_4^{2-} concentration, the methane production increased in System

1 (see Table B-4). System 4 had low methane production over the 1 y of incubation (see Table B-4), which was consistent with its high SO_4^{2-} concentration over that time period (see Figure C-6).

As shown in Table B-4, the main gas present in the Tedlar bag was N_2. Because the nitrate concentrations in all the cap waters and porewaters in Systems 1, 3, and 4 were low and mostly below the detection limits (<0.5 mg/L), it is unlikely that this high volume of N_2 was from the denitrification process. The most possible N_2 source was from the N_2 flushing at column filling, because all columns were flushed with N_2 before and during column filling for several minutes.

The air contains approximately 78 vol% N_2, 21 vol% O_2, and 0.03 vol% CO_2 (Hopp and Hennig 1983). The constant presence of O_2 in the Tedlar bag gas is believed to be mainly from air, due to either the incomplete N_2 flushing at column filling or the leaking of columns or Tedlar bags during incubation. Some columns (i.e. columns C1-4, C1-8, C1-13, C1-14, C1-15, C3-5, C3-8, C3-9, and C4-9) had approximately 20 vol% O_2 (see Table B-4), essentially the same O_2 concentration as in air. This high O_2 concentration may indicate severe column leaking during incubation. However, the sampling during GC analysis may also introduce O_2 into the results if handled improperly. Most of other columns maintained fairly low concentrations of O_2, indicating a good column sealing and anaerobic environment (see Table B-4).

Figure C-7 shows the CO_2 concentrations in the headspace of Systems 1, 3, and 4 over 1 y of incubation. It can be seen that, in the early incubation, the

CO_2 concentrations in Systems 1, 3, and 4 increased with time and reached 4 to 8 vol% in 180 d of incubation. This increase in headspace CO_2 concentration was likely from microbial activity that occurred in the MFT and CT. As stated in the literature (Maier 2000), in the process of microbial metabolism, the heterotrophic bacteria will utilise the naturally occurring organic materials as substrates and produce CO_2 in both aerobic and anaerobic environments. Under aerobic conditions, the heterotrophic bacterial activity will transform the carbon in the substrate to about 50% of CO_2 and 50% of new cell mass. Under anaerobic conditions, a smaller portion of the carbon is used for new cell mass and a larger portion goes to CO_2 and CH_4. Thus, the CO_2 in the Tedlar bag gas is believed to be the result of and an indicator of active microbial activity (either aerobic or anaerobic) occurring in the MFT and CT. The unusually low CO_2 concentrations in some columns (see Figure C-7) are likely due to the dilution by air or loss from leaking. This is supported by the O_2 analysis, which indicated generally high O_2 concentrations in those columns with unusually low CO_2 concentrations (see Table B-4).

The CO_2 concentrations in the Tedlar bag should be the same as in the column headspace. During long incubation time, the $CO_{2(g)}$ concentrations in the headspace gas are deemed to be in equilibrium with the $CO_{2(aq)}$ concentrations in the cap water, which is in direct contact with the headspace gas. Thus, Henry's law might be used to calculate the $CO_{2(g)}$ concentrations in the headspace gas based on the concentrations of $CO_{2(aq)}$ in the cap water. In applying the Henry's

law for the $CO_{2(g)}$ concentration calculations in the headsapce gas, the following Equations 6-1 to 6-6 are used (Sawyer, *et al.* 1994; Snoeyink and Jenkins 1980):

$$H_2CO_3^* \rightleftharpoons H^+ + HCO_3^- \quad \text{.....(6-1)}$$

$$[H_2CO_3^*] = ([H^+]\times[HCO_3^-])/K_{A1} = ([H^+]\times[HCO_3^-])/(4.3\times10^{-7}) \quad \text{.....(6-2)}$$

$$[H_2CO_3^*] = [CO_{2(aq)}] + [H_2CO_{3(aq)}] \quad \text{.....(6-3)}$$

$$[H_2CO_3^*] \approx [CO_{2(aq)}] \quad \text{.....(6-4)}$$

$$CO_{2(aq)} \rightleftharpoons CO_{2(g)} \quad \text{.....(6-5)}$$

$$K_H = 1.0\times10^{-1.5} = [CO_{2(aq)}]/Pco_{2(g)} \approx [H_2CO_3^*]/Pco_{2(g)} \quad \text{.....(6-6)}$$

where K_H is the Henry's law constant at room temperature; $Pco_{2(g)}$ is the partial pressure of CO_2 in the headspace gas with the unit of atm.

Thus, with the known concentrations of HCO_3^- and pH in the cap water at room temperature, by using the Equations 6-1 through 6-6, the partial pressure of CO_2 in the headspace gas can be calculated.

For System 1, Table C-1 in Appendix C provides a comparison of the measured CO_2 concentrations by GC and the calculated CO_2 concentrations

using Henry's law in the headspace. It can be seen that the calculated CO_2 concentrations in the headspace gas are comparable to the measured CO_2 concentrations in the headspace gas. The calculation of the CO_2 concentrations using the above equations confirms the results of measured CO_2 concentrations in the headspace gas or Tedlar bag gas.

As shown in Table B-4, in some columns, low concentrations (for the most part, <1.0 vol%) of H_2S and C_2H_4 were detected in the headspace. Both the H_2S and C_2H_4 are assumed to be the products of microbial activity, as detailed below.

As the result of SRB activity, sulphate will be reduced to sulphide. Depending on the pH of the environment, the sulphide will predominantly exist either as H_2S when pH<7.3 or as HS^- when pH>7.3 (Fedorak *et al.* 2000). As shown in Table B-7 for System 3, Table B-8 for System 4, and Table B-9 for System 1, most of the pH values in the cap water and tailings porewater in all three systems were between 7.6 to 8.3. This pH range will produce HS^- as the predominant form of sulphide. The HS^- will further most likely combine with heavy metals to precipitate as sulphide-containing minerals, also called acid volatile sulphides. The rare detection and low concentration of H_2S in column headspace was well matched with the alkaline pH range of 7.6 to 8.3. Furthermore, System 1 had similar H_2S release as in Systems 3 and 4.

Ethylene has been commonly found in the Syncrude MFT. Ethylene has adverse effects on plant growth. The presence of ethylene was attributed to the microbial activity of either aerobic or anaerobic microorganisms. (Fedorak *et al.*

2000). In this project, ethylene was occasionally detected in the headspace with concentrations between 9 and 3000 ppm by volume (see Table B-4).

6.2.2 In-situ headspace gas analysis in System 2

For the headspace gas analysis in System 2, the Micro-GC was directly connected to the headspace of columns via a piece of stainless steel tubing (see Section 4.2.2). Therefore, the headspace gas analysis in System 2 was performed in an in-situ manner to regularly monitor the headspace gas. Because any evolved headspace gas will quickly disperse into Tedlar bag, the results of in-situ headspace gas analysis should be the same as in the Tedlar bag gas analysis.

As discussed previously, in-situ cap water sampling was performed each time after completing the in-situ headspace gas analysis. The cap water was completely removed at each sampling. The void in the headspace created by removing the cap water was filled with pure N_2. This increased headspace volume and introduction of N_2 will dilute and decrease the concentrations of existing headspace gases (other than N_2), as compared to Tedlar bag gas analysis. Also, the frequent in-situ headspace gas analysis and cap water sampling could cause more air contamination in the headspace, thus leading to a higher O_2 concentration.

The headspace volume increased with each cap water sampling. The increased headspace volume can be estimated from the total tailings volume change (Vtt). Figure B-13 shows the Vtt(2) values with time in System 2. The

Vtt(2) is defined in Equation 4-2. At time 0, the columns in System 2 contained approximately an 81-cm height of "MFT+CT" and a 10-cm height of headspace. At 133 d of incubation (i.e. the 9th sampling), the six columns in System 2 had a Vtt(2) in the range of -21.0 to –26.0% (see Figure B-13). This level of Vtt(2) translates into a headspace volume 2.7 to 3.1 times that of the original headspace volume. At 352 d of incubation (i.e. the 10th sampling), the headspace volume in System 2 had increased even further.

For columns in System 2, there were 10 samplings for the in-situ headspace gas analysis over 1 y of incubation, as shown in Table B-5. In comparison to the Tedlar bag gas analysis in System 1 (see Table B-4), the in-situ headspace gas analysis in System 2 showed constantly low CH_4 and CO_2 concentrations, and a high O_2 concentration. The low CH_4 and CO_2 concentrations may be partially due to the dilution effect caused by the increased headspace volume and newly added N_2 gas with each cap water sampling and removal. As discussed above, at 133 d of incubation, the headspace volume in the six columns of System 2 was about 3 times the original headspace volume. It should be noted that the Tedlar bags in System 2 had little gas collected over time; therefore all of the gases were basically contained in the headspace. If the in-situ headspace CH_4 and CO_2 concentrations were multiplied by a factor of 3 to take into account the increased headspace, the CO_2 concentrations in System 2 had similar values as those in Tedlar bag gas of System 1, but the CH_4 concentrations still showed lower values than those in System 1. That is, the CH_4 yield in System 2 was lower than in System 1. The O_2 concentration in

System 2 increased with each sampling, indicating some possible contamination by air during headspace gas analysis and cap water sampling.

In the headspace of System 2, some low concentrations (<1.0 vol%) of H_2S and C_2H_4 were occasionally detected. As discussed above, both the H_2S and C_2H_4 are believed to be the products of microbial activity.

In characterising the evolved gases in Tedlar bag or headspace from the MFT and CT deposits, due to the interference and contamination caused by the frequent in-situ cap water sampling and headspace gas analysis, the in-situ headspace GC analysis in System 2 would appear to be less accurate than the Tedlar bag gas analysis in Systems 1, 3, and 4.

As mentioned above, the columns in System 2 had different chemical amendments in the CT at column filling (see Table 4-5). The in-situ headspace gas analysis of System 2 showed that the six columns in System 2 had similar levels of CH_4, CO_2, and H_2S detection, indicating that the different chemical amendments added to the CT had little effect on the headspace gas evolution and gas composition during 1 y of incubation.

6.3 Physical and chemical characteristics of cap water, MFT, and CT

Both MFT and CT are heterogeneous materials, so the physical, chemical, and microbiological data obtained from one location could vary to

some degree from the data obtained from other locations. Caution should be used in interpreting the data.

6.3.1 Physical and chemical characteristics in System 3 (Cap water/MFT)

6.3.1.1 Calcium and magnesium concentrations and the pH

According to Table B-6, the baseline Ca^{2+} concentration in MFT for System 3 (Base MFT 2) was 23 mg/L. Figure C-8 shows the Ca^{2+} concentrations in the cap water and MFT porewater of System 3 over 1 y of incubation. Both the cap water and MFT porewater in System 3 had quite constant Ca^{2+} concentrations over time, with the Ca^{2+} concentrations in the cap water ranging from 19 to 27 mg/L and the Ca^{2+} concentrations in the MFT porewater ranging from 15 to 21 mg/L over 1 y of incubation. These Ca^{2+} concentrations in the cap water and MFT porewater are close to 23 mg/L of the baseline Ca^{2+} concentration in the MFT, indicating that the MFT released Ca^{2+} without Ca^{2+} concentration abatement and that the Ca^{2+} release was stable over this incubation period. The upper and lower zones of MFT showed similar Ca^{2+} concentrations over time. The cap water had a consistently higher Ca^{2+} concentration than the MFT porewater over 1 y of incubation.

According to Table B-6, the baseline Mg^{2+} concentration in MFT for System 3 (Base MFT 2) was 16 mg/L. Figure C-9 shows the Mg^{2+} concentration in System 3 over 1 y of incubation. The Mg^{2+} concentrations in the cap water

and MFT porewater were constant over time. The Mg^{2+} concentrations in the cap water ranged from 13 to 18 mg/L, while the Mg^{2+} concentrations in the MFT porewater ranged from 11 to 15 mg/L over 1 y of incubation. The Mg^{2+} concentrations in the cap water and MFT porewater were close to 16 mg/L of the baseline Mg^{2+} concentration in MFT, indicating that the MFT released Mg^{2+} without Mg^{2+} concentration abatement and that the Mg^{2+} release was stable over this incubation period. The upper and lower zones of MFT showed similar Mg^{2+} concentrations over time. The cap water had a consistently higher Mg^{2+} concentration than the MFT porewater over 1 y of incubation.

Figure C-10 shows that the pH of cap water and MFT porewater were similar, and for the most part within the range of 7.7 to 8.3 over 1 y of incubation.

6.3.1.2 Sulphate concentration and methanogenesis

According to Table B-6, the baseline SO_4^{2-} concentration in MFT for System 3 (Base MFT 2) was 14 mg/L. Figure C-5 shows the SO_4^{2-} concentration in System 3 over 1 y of incubation. In both the cap water and MFT porewater, SO_4^{2-} concentrations decreased with time and reached a non-detectable level (<0.5 mg/L) after the first 90 d of incubation. Then the SO_4^{2-} concentrations in both the cap water and MFT porewater remained at non-detectable levels (<0.5 mg/L) until 243 d of incubation. These results may indicate that the SRB were still active under initially low SO_4^{2-} concentration and could reduce SO_4^{2-} in MFT. The reduction of the initially low concentration

of SO_4^{2-} in MFT will lead to a slight HCO_3^- concentration increase, as shown in Equation 2-2. A slight increase in HCO_3^- concentration over 1 y of incubation was observed (see Figure C-11). The SO_4^{2-} concentrations in the cap water at late incubation time were in the range of 10 to 11 mg/L. No certain explanations can be found to account for this increase in SO_4^{2-} concentration in the cap water.

Table B-7 lists the S^{2-} analysis results on the cap water and MFT porewater in System 3. All the S^{2-} concentrations in the cap water and MFT porewater were non-detectable (<0.05 mg/L). These essentially zero values may reflect the low quantity of S^{2-} resulting from reduction of initially a low concentration of SO_4^{2-} by SRB. It is also possible that the sulphide was trapped as minerals (e.g. FeS) in MFT.

As discussed previously in Section 2.4, with low SO_4^{2-} concentration (<20 mg/L), the condition in MFT will favour the methanogen activity when the environment becomes anaerobic. Figure C-12 shows the redox potential in the MFT of System 3 over 1 y of incubation. The suitable Eh for methanogen activity is in the range of –150 to –220 mV (Fedorak *et al.* 2000). Figure C-12 shows that, over 1 y of incubation, the Eh in MFT was mostly in the range of 21 to 77 mV. These high Eh values in MFT were unexpected. But the consistent Eh values in MFT may in some way justify the measurement results. The positive Eh in the MFT of System 3 should not favour the methanogen activity. However, the Tedlar bag gas analysis showed that high volume of CH_4 was detected in the headspace of System 3 (see Figure C-3). The trapped gas analysis in the MFT of System 3 also showed that CH_4 was detected in most of the MFT samples (see

Table B-12). Therefore, the methanogenesis was occurring in the MFT of System 3, despite the positive Eh values. Fedorak *et al.* (2000) suggested the presence of anaerobic microsites in the MFT and CT materials. The bulk Eh measurement may be not sensitive enough to the Eh in these anaerobic microsites, while the anaerobic microsites may have negative enough Eh for methanogensis to occur.

6.3.1.3 Solids content

Figure C-13 shows the solids content in the MFT of System 3 over 365 d of incubation. The solids content of MFT in System 3 showed a steady increase over this incubation period. This trend matches the steady water release from the MFT of System 3 (see Figure B-3). Over the 365 d of incubation, the solids content increased from baseline data of 38.0 wt% (Base MFT 2) to 44.7 wt% in the upper MFT zone and 45.6 wt% in the lower MFT zone. The upper and lower MFT zones showed similar solids content over time, indicating uniform densification throughout the MFT layer.

6.3.2 Physical and chemical characteristics in System 4 (Cap water/CT)

6.3.2.1 Bromide tracer analysis

The tracer Br^- was added to the CT at column filling in the form of NaBr. Approximately 0.22 g of NaBr was added to 1 L CT at column filling for

System 4 (see Table 4-3). The baseline Br^- concentration in the CT for System 4 (Base CT 3) was 260 mg/L (see Table B-6). This measured Br^- concentration of 260 mg/L in the baseline CT for System 4 is verified to be close to 258 mg/L. The figure 258 mg/L is the calculated Br^- concentration based on the planned NaBr dosage (Table 4-3). The verification will be presented at the end of this section.

Figure C-14 shows the Br^- concentration in the cap water and CT porewater of System 4 over 1 y of incubation. Figure C-14 shows that, over 1 y of incubation, the Br^- concentrations in the cap water and CT porewater were quite constant and in the range of 250 to 280 mg/L, close to 260 mg/L of the baseline Br^- concentration. The constant Br^- concentration at values close to the baseline data over 1 y of incubation shows that Br^- is a stable tracer in the CT material.

A mass balance of Br^- in the whole column of System 4 was attempted. System 4 contains CT only at time 0, and cap water plus CT during incubation. The Br^- concentrations in the cap water and CT porewater were measured for each sacrificed column in System 4 (Table B-8). By assuming that the Br^- is only present in the water (cap water and porewater), if the cap water and porewater volumes are known, the mass balance of Br^- in System 4 can be achieved. The cap water volume in each sacrificed column of System 4 can be calculated by using the absolute height of cap water at column sacrificing (see Table B-2) and the column ID. The column ID is 12.1 cm. The porewater volume can be determined from an empirical equation that relates the density of

MFT or CT materials to their solids contents, as shown in Equation 6-7 (Dr. MacKinnon, Syncrude Canada Ltd., personal communication):

$$\rho = (1/(1-0.0062 \times wt\%)) \times 1000 \quad \text{.....(6-7)}$$

where ρ is the density of MFT or CT (g/L of MFT or CT); wt% is the solids contents of MFT or CT.

From Equation 6-7, an estimation of the masses of solids and porewater per unit volume of MFT or CT as a function of solids content can be established. Table C-2 provides the estimations of the masses of solids and porewater per unit volume of MFT or CT at specific solids content. In establishing Table C-2, it is assumed that the total mass of MFT or CT is the sum of the mass of solids and the mass of porewater. Therefore, once the CT volume is known, the porewater volume can be determined by using Table C-2.

For each sacrificed column in System 4, the CT volumes at time 0 (baseline CT) and at column sacrificing can be calculated from the absolute heights of CT data listed in Table B-2 and the column ID. Thus, the porewater volume of CT can be obtained by together using Table C-2.

With the known Br^- concentrations in each water (cap water and porewater, see Table B-8) and the calculated cap water and porewater volumes, the mass of Br^- in the cap water and porewater can be calculated. Table 6-6 summarises the Br^- mass calculations in the baseline CT (Base CT 3), and in the

cap water and CT porewater from the sacrificed columns of System 4. It is seen that over 1 y of incubation, the Br^- recovery (relative to the Br^- mass at time 0) in System 4 was in the range of 93 to 104%. This mass recovery indicates that the Br^- is a stable and conservative tracer in CT material over the experiment time.

It should be noted that, based on the planned NaBr dosage of 0.22 g/L of CT in the baseline CT of System 4 (Table 4-3) and the typical CT volume of 6.1 L at time 0 (equivalent to a height of 54 cm in the column), the total mass of Br^- in the CT of each column of System 4 at time 0 is approximately 1053 mg, and the calculated baseline Br^- concentration in the CT of System 4 at time 0 is 258 mg/L. Here, 1053 mg $=(84/(23+84))\times0.22\times6.1\times1000$ mg, and 258 mg/L $=1053/(0.67\times6.1)$ mg/L, where 6.1 L is the volume of CT at time 0; 23 and 84 are atomic weights of sodium and bromine, respectively; 0.67 is the volume (L) of porewater per L of CT at solids content of 56.6 wt% (in Base CT 3) and is from Table C-2. The figure 1053 mg is quite close to the Br^- mass at time 0 obtained from the Br^- concentrations (see Table 6-6), and the figure 258 mg/L is quite close to the measured baseline Br^- concentration of 260 mg/L in the CT of System 4 (see Table B-6). This comparison in one way justifies the methods and calculation results of Br^- mass listed in Table 6-6, and also shows that the Br^- is a stable tracer in the CT material.

Table 6-6. The Br^- mass balance calculation in System 4.

Column	t_{incu} (d)	Total mass of Br^- in the whole CT at time 0 (mg)	Mass of Br^- at column sacrificing (mg)				Br^- mass recovery (%)
			In cap water	In CT-U	In CT-L	Total mass of Br^- in the whole column	
C4-1	28	1085	379	397	347	1123	104
C4-2	61	1083	469	313	302	1084	100
C4-3	90	1081	474	293	280	1047	97
C4-4	120	1083	502	287	274	1063	98
C4-5	152	1083	NA	287	259	NA	NA
C4-6	181	1075	511	277	261	1049	98
C4-7	212	1079	494	252	274	1020	94
C4-8	243	1081	508	265	272	1045	97
C4-9	266	1079	534	289	277	1100	102
C4-10	303	1083	534	290	278	1102	102
C4-11	334	1079	514	255	247	1016	94
C4-12	365	1083	511	251	248	1010	93

1). Br^- mass recovery (%) =((total mass of Br^- at column sacrificing)/(total mass of Br^- at time 0))×100%.
2). NA=not available.

6.3.2.2 Calcium and magnesium concentrations and the pH

According to Table B-6, the baseline Ca^{2+} concentration in CT for System 4 (Base CT 3) was 82 mg/L. Figure C-15 shows the Ca^{2+} concentration in System 4 over 1 y of incubation.

In the CT, Figure C-15 shows that most of the decrease in Ca^{2+} concentration occurred during the first 60 d of incubation. At 61 d of incubation, the Ca^{2+} concentration in CT decreased dramatically from the baseline concentration of 82 mg/L to 26 mg/L in CT-U and 25 mg/L in CT-L. After that time, the Ca^{2+} concentration was quite stable and in the range of 18 to 27 mg/L until the end of 365 d of incubation. The upper and lower zones of CT had similar Ca^{2+} concentrations over 1 y of incubation.

In the cap water, Figure C-15 shows that the Ca^{2+} concentration was in the range of 20 to 68 mg/L over 1 y of incubation, higher than in the CT porewater. The higher Ca^{2+} concentration in the cap water may be due in part to the pH difference. Figure C-16 shows that the cap water had a lower pH than the CT porewater. The lower pH in the cap water may contribute to a higher Ca^{2+} concentration, due to the effect of redissolution of $CaCO_3$ at lower pH conditions. Compared to the CT porewater, the cap water showed a large fluctuation of Ca^{2+} concentration over time (Figure C-15).

Using the same procedures as for the Br^- mass balance calculations in Section 6.3.2.1, a mass balance of Ca^{2+} in the whole column of System 4 was

attempted. Table 6-7 lists the results of Ca^{2+} mass balance calculations in System 4.

It can be seen from Table 6-7 that, over 1 y of incubation, only less than 50% of the original Ca^{2+} mass still exists in the water, suggesting that more than 50% of the original Ca^{2+} mass was removed from the water by some mechanisms, as detailed below.

The mechanisms leading to a change in Ca^{2+} concentration in System 4 may include ion exchange between Ca^{2+} and Na^{+} on the clays of CT, and precipitation or redissolution of $CaCO_3$ at high or low pH conditions.

Ion exchange between Ca^{2+} and Na^{+} on the clay surface will cause a change in Na^{+} concentration, leading to an increase in Na^{+} concentration in the porewater. Figure C-17 shows the Na^{+} concentration in System 4 over 1 y of incubation. In the early incubation, Figure C-15 shows a rapid decrease in the Ca^{2+} concentration in CT. This decrease in Ca^{2+} concentration was not accompanied by an increase in the Na^{+} concentrations of either the cap water or CT porewater during this period (see Figure C-17). This result indicates that ion exchange between Ca^{2+} and Na^{+} in CT most likely did not occur. The slight increase in the Na^{+} concentrations of the cap water and CT porewater at late incubation times may not result from the ion exchange between Ca^{2+} and Na^{+}, for the reason that the Ca^{2+} concentration in the CT porewater was quite constant during this late incubation period (see Figure C-15).

Table 6-7. The Ca^{2+} mass balance calculation in System 4.

Column	t_{incu} (d)	Total mass of Ca^{2+} in the whole CT at time 0 (mg)	Mass of Ca^{2+} at column sacrificing (mg)				Ca^{2+} mass recovery (%)
			In cap water	In CT-U	In CT-L	Total mass of Ca^{2+} in the whole column	
C4-1	28	342	84	50	44	178	52
C4-2	61	342	60	32	29	121	35
C4-3	90	341	74	26	24	124	37
C4-4	120	342	97	30	28	155	46
C4-5	152	342	NA	26	24	NA	NA
C4-6	181	339	109	29	25	163	48
C4-7	212	340	62	22	24	108	32
C4-8	243	341	38	24	24	86	25
C4-9	266	340	71	22	18	111	33
C4-10	303	342	88	26	23	137	40
C4-11	334	340	134	26	22	182	54
C4-12	365	342	113	25	24	162	47

1). Ca^{2+} mass recovery (%) =((total mass of Ca^{2+} at column sacrificing)/(total mass of Ca^{2+} at time 0))×100%.

2). NA=not available.

Therefore, the major mechanism causing the reduction in Ca^{2+} concentration in the CT of System 4 in the first 60 d of incubation may be due to the precipitation of $CaCO_3$. $CaCO_3$ has solubility product (Ksp) of 8.7×10^{-9} at 25°C (Nazaroff and Alvarez-Cohen 2001; AWWA 1999). At alkaline conditions, Ca^{2+} will precipitate as $CaCO_3$ if the ratio of $[Ca^{2+}]\times[CO_3^{2-}]$ to Ksp is greater than 1, according to the following reaction:

$$Ca^{2+} + CO_3^{2-} \rightleftharpoons CaCO_{3(s)} \quad \text{.....(6-8)}$$

This calcium carbonate precipitation usually takes place before pH level has exceeded 10 (Sawyer *et al.* 1994). The pH in the cap water and CT porewater of System 4 was within 7.7 to 8.2 (see Figure C-16), showing alkaline conditions. Because of the high concentration of Ca^{2+} and alkaline pH in the CT porewater, the reduction in Ca^{2+} concentration in the CT of System 4 might be due to this $CaCO_3$ precipitation.

Table 6-8 summarises the ratios of $[Ca^{2+}]\times[CO_3^{2-}]$ to Ksp in each zone of System 4 over 1 y of incubation, where $[Ca^{2+}]$ and $[CO_3^{2-}]$ are the molar concentrations (M) of Ca^{2+} and CO_3^{2-} in the cap water and porewater of System 4; Ksp is the solubility product of $CaCO_3$. The Ksp is 8.7×10^{-9} at 25°C (Nazaroff and Alvarez-Cohen 2001; AWWA 1999).

The calculation of this ratio of $[Ca^{2+}]\times[CO_3^{2-}]$ to Ksp is as follows. From the concentration of HCO_3^-, the concentration of CO_3^{2-} can be calculated based

on the Equations 6-9 and 6-10 (Sawyer, *et al.* 1994). Furthermore, the molar concentrations of $[H^+]$, $[HCO_3^-]$, and $[Ca^{2+}]$ (M) can be converted from the concentrations (mg/L) provided in Table B-8. Thus, the ratio of $[Ca^{2+}]\times[CO_3^{2-}]$ to Ksp can be obtained for System 4.

$$HCO_3^- \rightleftharpoons H^+ + CO_3^{2-} \quad \text{.....(6-9)}$$

$$K_{A2}=([H^+]\times[CO_3^{2-}])/[HCO_3^-]=4.69\times10^{-11} \quad \text{.....(6-10)}$$

Table 6-8 shows that the ratios of $[Ca^{2+}]\times[CO_3^{2-}]$ to Ksp in all zones of System 4 over 1 y of incubation are in the range of 4 to 13, indicating the precipitation of $CaCO_3$ is a possible route for the removal of Ca^{2+} in System 4.

Table 6-8. The ratios of $[Ca^{2+}]\times[CO_3^{2-}]$ to Ksp in the cap water and porewaters of System 4 at column sacrificing.

Column	t_{incu} (d)	The ratios of $[Ca^{2+}]\times[CO_3^{2-}]$ to Ksp at column sacrificing		
		In cap water	In CT-U	In CT-L
C4-1	28	6	12	12
C4-2	61	10	7	6
C4-3	90	9	7	7
C4-4	120	7	8	9
C4-5	152		6	7
C4-6	181	8	7	7
C4-7	212	7	6	9
C4-8	243	6	7	4
C4-9	266	6	4	5
C4-10	303	5	6	7
C4-11	334	13	9	10
C4-12	365	8	9	9

Figure C-18 shows the Mg^{2+} concentration in System 4 over 1 y of incubation. The CT for System 4 (Base CT 3) had a baseline Mg^{2+} concentration of 30 mg/L.

In the CT porewater of System 4, similar to the situation of Ca^{2+}, the Mg^{2+} concentration decreased most rapidly in the first 60 d of incubation and reached 13 mg/L in both CT-U and CT-L at 61 d of incubation. After that time, the Mg^{2+} concentration in CT porewater was stable and in the range of 11 to 14 mg/L for the remainder of the experiment. Both the upper and lower zones of CT had similar Mg^{2+} concentrations.

In the cap water of System 4, the Mg^{2+} concentration was quite constant and in the range of 22 to 30 mg/L over 1 y of incubation (see Figure C-18).

6.3.2.3 Sulphate concentration

Figure C-6 shows the SO_4^{2-} concentration in System 4 over 1 y of incubation. According to Table B-6, the baseline SO_4^{2-} concentration in the CT for System 4 (Base CT 3) was 1100 mg/L.

In the CT of System 4, Figure C-6 shows that the most decrease in SO_4^{2-} concentration occurred in the first 60 d of incubation. At 61 d of incubation, the SO_4^{2-} concentration in the CT decreased dramatically to 497 mg/L in CT-U and 413 mg/L in CT-L. After that time, the SO_4^{2-} concentration showed a slow decrease and reached 259 mg/L in CT-U and 178 mg/L in CT-L at 365 d of incubation. The upper and lower zones of CT had similar SO_4^{2-} concentrations over 1 y of incubation.

In the cap water of System 4, Figure C-6 shows that the SO_4^{2-} concentration was in the range of 490 to 1070 mg/L over 1 y of incubation, higher than in the CT porewater.

Using the same procedures as for the Br^- mass balance calculations in Section 6.3.2.1, a mass balance of SO_4^{2-} in the whole column of System 4 was attempted. Table 6-9 lists the results of SO_4^{2-} mass balance calculations in System 4.

It can be seen from Table 6-9 that, after 1 y of incubation, only less than 50% of the original SO_4^{2-} mass still exits in the water, suggesting that more than 50% of the original SO_4^{2-} mass was removed from the water by some mechanisms. As discussed previously in Section 2.4, with the high SO_4^{2-} concentration, the conditions in the CT of System 4 should favour SO_4^{2-} reduction by SRB when the environment becomes anaerobic.

The decrease in SO_4^{2-} concentration in the CT porewater of System 4 over time most likely indicates the SRB activity. As discussed in Section 2.4, the activity of SRB will produce HCO_3^- (according to Equation 2-2). Figure C-19 shows the HCO_3^- concentration in System 4 over incubation time, indicating a steady HCO_3^- concentration increase in both the cap water and porewater of the CT over incubation time. In CT porewater, the increase in HCO_3^- concentration was well matched with the decrease in SO_4^{2-} concentration (see Figure C-6), supporting SO_4^{2-} reduction by SRB in the CT layer.

Table 6-9. The SO_4^{2-} mass balance calculation in System 4.

Column	t_{incu} (d)	Total mass of SO_4^{2-} in the whole CT at time 0 (mg)	Mass of SO_4^{2-} at column sacrificing (mg)				SO_4^{2-} mass recovery (%)
			In cap water	In CT-U	In CT-L	Total mass of SO_4^{2-} in the whole column	
C4-1	28	4591	1500	1145	848	3493	76
C4-2	61	4583	1413	598	480	2491	54
C4-3	90	4574	1972	400	410	2782	61
C4-4	120	4583	1790	181	79	2050	45
C4-5	152	4583	NA	446	352	NA	NA
C4-6	181	4549	1716	386	64	2166	48
C4-7	212	4566	1388	291	314	1993	44
C4-8	243	4574	957	261	272	1490	33
C4-9	266	4566	1510	384	313	2207	48
C4-10	303	4583	1408	242	198	1848	40
C4-11	334	4566	1908	310	164	2382	52
C4-12	365	4583	1637	250	170	2057	45

1). SO_4^{2-} mass recovery (%) =((total mass of SO_4^{2-} at column sacrificing)/(total mass of SO_4^{2-} at time 0))×100%.
2). NA=not available.

Table B-8 shows that the Eh in the CT of System 4 was quite constant and in the range of –168 to –217 mV over 1 y of incubation. This Eh range should favour both SRB and methanogen activity. However, the high SO_4^{2-} concentration may inhibit methanogen activity. The trapped gas analysis on the CT samples of System 4 (see Table B-12) shows that trapped CH_4 in System 4 was only occasionally detected. The lack of trapped CH_4 seems to indicate that methanogenesis was inhibited by the high concentration of SO_4^{2-} in the CT of System 4.

As shown in Figure C-16, the pH of the cap water and of the CT porewater of System 4 was mostly in the range of 7.8 to 8.2. As discussed in Section 6.2.1, in this slightly alkaline pH range, the major form of the sulphide will be HS^- and the predominant sinks for sulphide will be as the minerals of FeS and FeS_2. Gaseous H_2S will not be a dominant sulphur species at these pH values. The trapped gas analysis (see Table B-12) only shows occasional H_2S detection (usually < 1 vol%) in System 4, supporting the above discussion.

Table B-8 shows the S^{2-} analysis results by CHEMetrics test kit on the cap water and the CT porewater of System 4 over 1 y of incubation. In comparison to the MFT in System 3, sulphide was detected more often in both the cap water and CT porewater of System 4. This sulphide most likely results from SO_4^{2-} reduction by SRB. The CT in System 4 had originally a high SO_4^{2-} concentration and thus will favour high SRB activity. However, the sulphide concentration in System 4 was still low, less than 1 mg/L for the most part.

The cap water of System 4 had a higher SO_4^{2-} concentration than the CT porewater over time. This higher SO_4^{2-} concentration in the cap water may be due to the initially rapid release of CT porewater at the beginning of incubation. This rapidly released CT water would not have been subject to as much SRB activity due to the insufficient time for SRB to reduce SO_4^{2-} before its release. The constantly high SO_4^{2-} concentration in the cap water of System 4 over 1 y of incubation may also suggest that SO_4^{2-} reduction by SRB in the cap water did not exist. The cap water had a redox potential of around +400 mV. This high Eh will inhibit the SRB activity.

6.3.2.4 Solids content

Figure C-20 shows the solids content in the CT of System 4 over 1 y of incubation. The baseline solids content in the CT for System 4 (Base CT 3) was 56.6 wt% (see Table B-6).

Figure C-20 shows that the solids content in the CT increased most rapidly in the first 60 d of incubation, and reached 69.3 wt% in CT-U and 70.9 wt% in CT-L at 61 d of incubation. After that time, the CT showed a slow increase in solids content over the remainder of the incubation, and reached 75.9 wt% in CT-U and 76.4 wt% in CT-L at 365 d of incubation. Over 65% of the solids content increase in the CT during 1 y of incubation occurred in the first 61 d of incubation. The CT solids content increase (see Figure C-20) was well matched with the CT tailings volume decrease (see Figure B-6). Both the solids

content increase and the tailings column change indicate rapid CT settling in the first 60 d of incubation and continuous but slow densification over the remainder of incubation time. Furthermore, Figure C-20 shows that the lower zone of CT had a slightly higher solids content than the upper zone of CT, indicating slightly higher densification rate in CT-L than in CT-U.

MacKinnon *et al.* (2000) state that it would take days or weeks for the CT deposit to densify from a solids content of 60 wt% up to 75 wt%. In this project, the CT solids content in System 4 increased from 56.6 wt% to approximately 76.0 wt% after 365 d of incubation.

6.3.3 Physical and chemical characteristics in System 1 (Cap water/MFT/CT)

The CT beneath MFT deposit is a complex system. Many physical, chemical, and microbiological reactions and interactions will occur among the multi-phases of water, MFT, and CT.

In this CT beneath MFT system, the water released from the CT will make its way upward through the overlying MFT. As this CT water passes through the overlying MFT layer, several effects will take place, including simple mixing between CT porewater and MFT porewater for both conservative and reactive components, chemical reactions (e.g. ion exchange, precipitation, and dissolution) and biochemical activities (e.g. sulphate reduction by SRB) for such components as Ca^{2+}, Mg^{2+}, SO_4^{2-}, HCO_3^-, pH, and Na^+. The anaerobic

microbial characteristics of the overlying MFT will also be changed due to the high SO_4^{2-} concentration from the CT release water.

6.3.3.1 Bromide tracer analysis and the estimation of dilution effect

The use of Br^- as a tracer in the CT of System 1 is expected to reveal information about the transit characteristics of CT release water through the MFT and whether the CT water is mixing or displacing the MFT water in the MFT layer, and to estimate the dilution effect at reducing the levels of major water components of Ca^{2+}, Mg^{2+}, SO_4^{2-}, and EC in the cap water. As in System 4, approximately 0.22 g of NaBr was added to 1 L CT at column filling for System 1 (see Table 4-3). As provided in Section 6.3.2.1, this Br^- dosage will produce an expected baseline Br^- concentration of 258 mg/L.

In the MFT of System 1, the baseline Br^- concentration was below detection limits (<0.5 mg/L, in Base MFT 1), the same baseline Br^- concentration as in the MFT of System 3. In the CT of System 1, the baseline Br^- concentration was 270 mg/L for Base CT 1 and 260 mg/L for Base CT 2 (see Table B-6), similar to 260 mg/L of the baseline Br^- concentration in the CT of System 4. Figure C-21 shows the Br^- concentration in the cap water, MFT, and CT over 1 y of incubation in System 1.

In the MFT, the Br^- concentration increased steadily from a non-detectable concentration at incubation time 0 to 130 mg/L in MFT-U and 210 mg/L in MFT-L at 62 d of incubation. Following this initial increase, the Br^-

concentration in the MFT layer remained quite constant and in the range of 120 to 150 mg/L in MFT-U zone and of 160 to 210 mg/L in MFT-L zone. The consistently higher Br^- concentration in the MFT-L zone than in the MFT-U zone is possibly due to the direct contact of the MFT-L zone with the high Br^- concentration CT layer.

In the CT, it can be seen from Figure C-21 that the Br^- concentration dropped from baseline 270 mg/L (Table B-6) to 210 mg/L in the first 3 d of incubation and then increased steadily to 270 mg/L at 29 d of incubation. Following this, the Br^- concentration in the CT was quite constant and in the range of 220 to 280 mg/L. This Br^- concentration range is close to the baseline Br^- concentrations of 260 mg/L (Base CT 2) or 270 mg/L (Base CT 1) in CT, indicating Br^- is a stable tracer in the CT material, as in System 4. The Br^- concentration in CT-U was slightly lower than in CT-L, possibly due to the direct contact of CT-U zone with the low Br^- concentration MFT layer.

In the cap water, the Br^- concentration increased quickly to 82 mg/L in the first 29 d of incubation, and then showed a slow but steady increase to a concentration in the range of 70 to 110 mg/L over the remaining incubation.

As in System 4, a mass balance of Br^- in the whole column of System 1 was attempted. System 1 contains MFT and CT at time 0, and cap water, MFT, and CT during incubation. The Br^- concentrations in the cap water, and MFT and CT porewaters were measured for each sacrificed column in System 1 (Table B-9). The cap water volume in each sacrificed column of System 1 can be calculated by using the absolute height of cap water at column sacrificing

(see Table B-3). It should be noted that the column ID is 12.1 cm. For the porewater content, Table C-2 provides the empirical estimations of the masses of solids and porewater per unit volume of MFT and CT at specific solids content.

Then using the same procedures as for the mass balance calculation of Br^- in System 4 (see Section 6.3.2.1), Table 6-10 summarises the Br^- mass calculations in the baseline MFT (Base MFT 1), in the baseline CT (Base CT 1 and Base CT 2), in the cap water, and in the MFT and CT porewaters for the sacrificed columns of System 1. It is seen that over 1 y of incubation, the Br^- recovery (relative to the Br^- mass at time 0) in System 1 was for the most part in the range of 92 to 108%. This indicates that the Br^- is a stable tracer with almost 100% recovery in the MFT and CT materials over incubation time.

Table 6-10. The Br^- mass balance calculation in System 1.

Column	t_{incu} (d)	Mass of Br^- at time 0 (mg)			Mass of Br^- at column sacrificing (mg)						Br^- mass recovery (%)
		In MFT	In CT	Total mass of Br^- in the whole column	In cap water	In MFT-U	In MFT-L	In CT-U	In CT-L	Total mass of Br^- in the whole column	
C1-2	3	0	1124	1124	11	29	96	384	369	889	79
C1-3	15	0	1120	1120	64	64	153	366	304	951	85
C1-4	29	0	1115	1115	120	105	204	369	323	1121	101
C1-5	62	0	1115	1115	121	171	275	292	307	1166	105
C1-6	91	0	1124	1124	140	149	248	300	313	1150	102
C1-12	121	0	1082	1082	188	170	231	264	268	1121	104
C1-8	153	0	1111	1111	NA	159	245	255	272	NA	NA
C1-9	182	0	1124	1124	182	150	219	255	276	1082	96
C1-10	213	0	1122	1122	223	191	270	260	256	1200	107
C1-11	244	0	1132	1132	225	175	238	238	282	1158	102
C1-13	267	0	1086	1086	245	185	234	251	261	1176	108
C1-14	303	0	1090	1090	281	NA	NA	NA	NA	NA	NA
C1-15	335	0	1090	1090	235	162	184	206	220	1007	92
C1-16	366	0	1096	1096	258	186	222	246	233	1145	104

1). Br^- mass recovery (%) =((total mass of Br^- at column sacrificing)/(total mass of Br^- at time 0))×100%.
2). NA=not available.

The MFT originally contained no detectable Br^-. The detected concentration of Br^- in the MFT during incubation is the result of Br^- entering the MFT from the underlying CT release water. The concentration drop in Br^- in the MFT layer relative to the Br^- concentration in the CT layer is most likely due to the dilution effect between the MFT water and CT water.

As indicated by the small increase in MFT solids content and the small decrease in MFT tailings volume over time, the MFT in System 1 densified slowly over time. The water content in MFT can therefore be roughly regarded as unchanged over a short time period. Thus, in the MFT layer of System 1, the sum of MFT water and CT release water is a relatively constant amount. As the CT water moves upward through the MFT into the cap water, a fraction of the CT release water will replace the MFT water in the MFT layer and move up together into the cap water layer. Therefore, during the incubation, the water in the MFT layer and the cap water layer contains a mixture of CT water and MFT water.

The volume percents of MFT and CT water (vol%) in the MFT and cap water layers can be calculated simply from the Br^- concentration, by assuming that the Br^- is a conservative species. Table 6-11 shows the percents (vol%) of CT water in the cap water and MFT layers in System 1 over 1 y of incubation, which are calculated by dividing the Br^- concentrations in the cap water and MFT layers by the Br^- concentration in the baseline CT. For example, for cap water at 3 d of incubation, the Br^- concentration is 25 mg/L (see Table B-9), so the CT water percent in this cap water is (25/270)*100=9 vol%. The balance

water in Table 6-11 is the baseline MFT water, in which the Br^- is below detection limits (<0.5 mg/L).

Table 6-11. The volume percent (vol%) of CT water with balance MFT water, based on Br^- analysis in System 1.

t_{incu} (d)	Percent of CT water in cap water and MFT layers (vol%)		
	Cap water	MFT-U	MFT-L
3	9	9	29
15	24	19	44
29	32	30	59
62	26	48	78
91	28	44	74
121	34	52	70
153	NA	48	74
182	36	47	NA
213	41	56	78
244	41	52	70
267	41	56	70
303	44	56	67
335	41	52	59
366	41	56	67

1). Use 270 mg/L as the baseline Br^- concentration in the CT (see Table B-6),
2). The baseline Br^- concentration in the MFT is assumed to be 0 mg/L,
3). NA=not available.

Table 6-11 shows that, as the CT water flows upward to the cap water, the CT water will replace the MFT water in MFT layer and move up together with the MFT water into the cap water. For example, at 366 d of incubation, the CT water replaced 67 vol% of MFT-L porewater, 56 vol% of MFT-U porewater; and the cap water contained 41 vol% of CT water with remaining 59 wt% of MFT water.

The Ca^{2+}, Mg^{2+}, SO_4^{2-}, and electrical conductivity were the major water parameters considered in this study. In System 1, the baseline CT had higher concentrations of Ca^{2+}, Mg^{2+}, SO_4^{2-}, and higher EC than the baseline MFT (see

Table B-6). Thus, the mixing of MFT and CT water in the cap water will reduce the concentrations of these species from the concentrations in the CT simply by dilution effect. Therefore, in the cap water of System 1, the decrease in Ca^{2+}, Mg^{2+}, SO_4^{2-}, and EC relative to the levels in baseline CT might be caused by both simple dilution and other removal mechanisms from the water phase (such as precipitation and microbial reduction).

The dilution effect (P_d) is defined in Equation 6-11:

$$P_d\,(\%) = ((C_{Base\ CT} - C_d)/(C_{Base\ CT} - C_m)) \times 100\% \quad \text{.....(6-11)}$$

where C_d is the ion concentration or EC in the cap water calculated by simple dilution between CT and MFT waters; C_m is the measured ion concentration or EC in the cap water; and $C_{Base\ CT}$ is the baseline ion concentration or EC in the CT.

From the P_d% definition in Equation 6-11, increased P_d% value means increased dilution effect. Based on the percent (vol%) of MFT and CT waters (see Table 6-11), and the Ca^{2+}, Mg^{2+}, SO_4^{2-} concentrations and EC in baseline MFT, in baseline CT, and in the cap water during incubation (see Tables B-6 and B-9), the dilution effect (P_d) at reducing the Ca^{2+}, Mg^{2+}, SO_4^{2-} concentrations and the EC for the cap water can be estimated, as shown in Table 6-12.

Table 6-12. The estimation of dilution effect (P_d) at reducing Ca^{2+}, Mg^{2+}, SO_4^{2-} concentrations, and the EC for the cap water of System 1.

	Makeup of the cap water		Ca^{2+} in the cap water		Mg^{2+} in the cap water		SO_4^{2-} in the cap water		EC in the cap water	
t_{incu} (d)	Vol% of CT water	Vol% of MFT water	C_d (mg/L)	P_d (%)	C_d (mg/L)	P_d (%)	C_d (mg/L)	P_d (%)	C_d (μS/cm)	P_d (%)
3	9	91	26.7	94	16.4	107	67	108	4554.	105
15	24	76	33.7	84	17.8	96	177	112	4757	110
29	32	68	37.2	77	18.5	86	231	100	4857	96
62	26	74	34.4	80	17.9	91	188	82	4777	97
91	28	72	35.5	74	18.1	78	206	72	4811	79
121	34	66	40.7	68	19.0	70	306	73	5006	89
182	36	64	39.0	70	18.8	80	260	71	4911	98
213	41	59	41.2	63	19.3	73	295	64	4975	88
244	41	59	41.2	63	19.3	73	295	73	4975	98
267	41	59	44.2	60	20.0	56	365	75	5118	90
303	44	56	46.2	65	20.0	78	399	80	5181	110
335	41	59	44.2	68	20.0	90	365	81	5118	98
366	41	59	44.2	65	20.0	70	365	85	5118	103

1). The symbols used in Table 6-12 are explained in Equation 6-11.

2). For MFT, the baseline data is from "Base MFT 1" (see Table B-6); For CT, the baseline data is from "Base CT 1" or "Base CT 2" (see Table B-6).

3). Sample calculation for Ca^{2+} at 3 d of incubation:

a). The makeup of this cap water is 9 vol% of CT water and 91 vol% of MFT water (see Table 6-11).

b). The baseline Ca^{2+} concentration was 68.7 mg/L for CT (Base CT 1) and 22.4 mg/L for MFT (Base MFT 1) (see Table B-6).

c). The C_d of Ca^{2+} concentration in the cap water achieved by simple dilution =((68.7×9) + (22.4×91))/100 =26.6 mg/L.

d). The C_m of measured Ca^{2+} concentration in the cap water at 3 d of incubation was 24 mg/L.

e). The dilution effect (P_d %) at reducing the Ca^{2+} concentration for the cap water = ((68.7-26.6)/(68.7-24))*100%=94%.

The estimation of P_d will be severely affected if there are any dissolutions or inputs of these water parameters (i.e. Ca^{2+}, Mg^{2+}, SO_4^{2-} and EC) from the MFT and CT tailings into the porewater during the incubation period. Despite the possible sources of the estimation error, the P_d at Table 6-12 can still show that dilution played a large role at reducing the Ca^{2+}, Mg^{2+}, SO_4^{2-} concentrations and EC for the cap water in System 1. This result indicates that, in the co-disposal of CT beneath MFT system (System 1), a large volume ratio of MFT to CT will be favoured for the purpose of increasing the dilution effects at reducing the Ca^{2+}, Mg^{2+}, SO_4^{2-} concentrations and the EC for the cap water.

6.3.3.2 Calcium and magnesium concentrations

Figure C-22 shows Ca^{2+} concentration in System 1 over 1 y of incubation.

From Table B-6, the baseline Ca^{2+} concentration in the MFT for System 1 (Base MFT 1) was 22 mg/L, similar to 23 mg/L of baseline Ca^{2+} concentration in the MFT for System 3 (Base MFT 2). In the MFT layer of System 1, Figure C-22 shows that the Ca^{2+} concentration decreased slightly and mainly at the beginning of incubation. At 15 d of incubation, the Ca^{2+} concentration in the MFT layer decreased to 17 mg/L in MFT-U and 19 mg/L in MFT-L. After that time, the Ca^{2+} concentration decreased slowly to 13 mg/L in MFT-U and 14 mg/L in MFT-L at 366 d of incubation. The upper zone of MFT had a slightly lower Ca^{2+} concentration than the lower zone of MFT. This slight difference in Ca^{2+} concentration is likely due to the fact that the MFT-L zone was in direct

contact with the CT layer, which had initially high Ca^{2+} concentration. The MFT had consistently lower Ca^{2+} concentration than the CT in System 1 over 1 y of incubation. The Ca^{2+} concentration in the MFT of System 1 was similar to the Ca^{2+} concentration in the MFT of System 3 (see Figure C-8) over 1 y of incubation.

From Table B-6, the baseline Ca^{2+} concentration in the CT was 69 mg/L for columns C1-1 to C1-11 (Base CT 1) and 76 mg/L for columns C1-12 to C1-20 (Base CT 2) in System 1. In comparison, the baseline Ca^{2+} concentration in the CT for System 4 (Base CT 3) was 82 mg/L (see Table B-6). In the CT layer, Figure C-22 shows that the largest drop in Ca^{2+} concentration occurred during the first 30 d of incubation. By 29 d of incubation, the Ca^{2+} concentration in the CT decreased substantially to 29 mg/L in CT-U and 23 mg/L in CT-L. After that time, the Ca^{2+} concentration remained quite constant with 21 mg/L in CT-U and 18 mg/L in CT-L at 366 d of incubation. The upper and lower zones of CT had similar Ca^{2+} concentrations over 1 y of incubation. The Ca^{2+} concentration in the CT of System 1 was similar to the Ca^{2+} concentration in the CT of System 4 (see Figure C-15) during 1 y of incubation.

In the cap water, Figure C-22 indicates that the Ca^{2+} concentration was quite constant with time. During 1 y of incubation, the Ca^{2+} concentration in the cap water was in the range of 23 and 30 mg/L. From Figure C-22, it can be seen that the cap water had a Ca^{2+} concentration close to that in the CT and higher than that in the MFT. This Ca^{2+} concentration difference may be partially due to the pH difference between the cap water and MFT porewater. Compared to

MFT porewater, the cap water had a lower pH over 1 y of incubation (see Figure C-23). This lower pH may contribute to the slightly higher Ca^{2+} concentration in the cap water due to the possible redissolution of $CaCO_3$ under lowered pH conditions.

Using the same procedures as for the Br^- mass balance calculations in Section 6.3.3.1, a mass balance of Ca^{2+} in the whole column of System 1 was attempted. Table 6-13 lists the results of Ca^{2+} mass balance calculations in System 1.

It can be seen from Table 6-13 that, over 1 y of incubation, only less than 50% of the original Ca^{2+} mass still exits in the water, suggesting that more than 50% of the original Ca^{2+} mass was removed from the water by some mechanisms. System 1 showed similar degree of overall Ca^{2+} removal from the water as in System 4 (Table 6-7).

The mechanisms causing Ca^{2+} concentration changes in the MFT and CT of System 1 may include mixing and dilution of high Ca^{2+} concentration CT porewater by low Ca^{2+} concentration MFT porewater, precipitation as $CaCO_3$ at slightly alkaline conditions or redissolution of $CaCO_3$ at lowered pH conditions, and ion exchange between Ca^{2+} and Na^+ on the clays of MFT and CT. The dilution effect in reducing Ca^{2+} concentration is already discussed in Section 6.3.3.1.

Table 6-13. The Ca^{2+} mass balance calculation in System 1.

Column	t_{incu} (d)	Mass of Ca^{2+} at time 0 (mg)			Mass of Ca^{2+} at column sacrificing (mg)						Ca^{2+} mass recovery (%)
		In MFT	In CT	Total mass of Ca^{2+} in the whole column	In cap water	In MFT-U	In MFT-L	In CT-U	In CT-L	Total mass of Ca^{2+} in the whole column	
C1-2	3	57	286	343	10	25	26	93	89	243	71
C1-3	15	56	285	341	26	21	24	55	55	181	54
C1-4	29	57	284	341	39	22	24	40	28	153	45
C1-5	62	57	284	341	44	22	23	32	30	151	45
C1-6	91	56	286	342	44	21	21	26	29	141	41
C1-12	121	56	316	372	50	21	25	35	32	163	43
C1-8	153	56	283	339	NA	18	21	24	23	NA	NA
C1-9	182	56	286	342	49	20	24	28	27	148	43
C1-10	213	57	285	342	51	15	20	26	27	139	41
C1-11	244	57	288	345	51	17	19	28	32	147	42
C1-13	267	57	301	358	51	15	18	23	25	132	37
C1-14	303	57	302	359	71	NA	NA	NA	NA	NA	NA
C1-15	335	57	302	359	63	17	18	23	26	147	41
C1-16	366	57	304	361	63	16	18	21	18	136	38

1). Ca^{2+} mass recovery (%) =((total mass of Ca^{2+} at column sacrificing)/(total mass of Ca^{2+} at time 0))×100%.
2). NA=not available.

The precipitation or redissolution of $CaCO_3$ was discussed previously in Section 6.3.2.2 and Equation 6-8. Figure C-23 shows that the pH in the cap water and MFT and CT porewaters of System 1 were mostly between 7.6 and 8.3, showing slightly alkaline conditions. Due to the high Ca^{2+} concentration and slightly alkaline pH in the CT porewater, the reduction in Ca^{2+} concentration in the CT of System 1 in the first 29 d of incubation was likely due to this $CaCO_3$ precipitation.

Using the same methods as for the calculation of the ratio of $[Ca^{2+}]\times[CO_3^{2-}]$ to Ksp in System 4 (Section 6.3.2.2), Table 6-14 summarises the ratios of $[Ca^{2+}]\times[CO_3^{2-}]$ to Ksp in each zone of System 1 over 1 y of incubation. Table 6-14 shows that the ratios of $[Ca^{2+}]\times[CO_3^{2-}]$ to Ksp in all zones of System 1 over 1 y of incubation are in the range of 3 to 12, indicating that the precipitation of $CaCO_3$ is a possible route for the removal of Ca^{2+} in System 1.

Table 6-14. The ratios of $[Ca^{2+}]\times[CO_3^{2-}]$ to Ksp in the cap water and porewaters of System 1 at column sacrificing.

Column	t_{incu} (d)	The ratio of $[Ca^{2+}]\times[CO_3^{2-}]$ to Ksp				
		In cap water	In MFT-U	In MFT-L	In CT-U	In CT-L
C1-2	3	9		4	11	12
C1-3	15	5	5	5	9	12
C1-4	29	7	5	6	14	12
C1-5	62	NA	6	10	12	6
C1-6	91	5	7	7	7	9
C1-12	121	4	4	7	7	7
C1-8	153		3	4	4	6
C1-9	182	4	5	8	7	9
C1-10	213	4	5	7	5	7
C1-11	244	3	3	5	5	10
C1-13	267	3	3	4	3	5
C1-14	303	NA	NA	NA	NA	NA
C1-15	335	5	5	5	15	14
C1-16	366	10	4	4	10	5

Ion exchange between Ca^{2+} and Na^+ on the clays of the MFT and CT is another important mechanism for Ca^{2+} concentration reduction in MFT and CT, as expressed in the following equation:

$$Ca^{2+} + 2\text{Na-clay} \rightleftharpoons 2Na^+ + \text{Ca-clay} \quad \text{(6-12)}$$

Thus, the drop in Ca^{2+} concentration caused by ion exchange between Ca^{2+} and Na^+ will result in an increase in the Na^+ concentration in the porewater. Figure C-24 shows the Na^+ concentration in System 1 over time. From Figure C-24, it can be seen that the Na^+ concentrations in the cap water and MFT and CT

porewaters increased over time. The increase in Na^+ concentration is a possible indicator of ion exchange between Ca^{2+} and Na^+.

Figure C-25 shows the Mg^{2+} concentration in System 1 over 1 y of incubation. Similar to Ca^{2+}, in System 1, the CT had baseline Mg^{2+} concentration of 25 mg/L for Base CT 1 and 26 mg/L for Base CT 2, higher than 16 mg/L of baseline Mg^{2+} concentration for MFT. In the MFT, the Mg^{2+} concentration was quite constant and in the range of 11 to 16 mg/L over 1 y of incubation. In the CT, the major drop in Mg^{2+} concentration occurred in the 30 d of incubation and reached 14 mg/L in CT-U and 15 mg/L in CT-L at 29 d of incubation. After that time, the Mg^{2+} concentration in the CT was quite constant. In the cap water, the Mg^{2+} concentration was in the range of 16 to 19 mg/L, higher than the concentration in either MFT or CT.

6.3.3.3 Sulphate concentration

Figure C-4 shows the SO_4^{2-} concentration in System 1 over 1 y of incubation.

From Table B-6, in the MFT of System 1, the baseline SO_4^{2-} concentration in the MFT (Base MFT 1) was below detection limits (<0.5 mg/L). In comparison, the baseline SO_4^{2-} concentration in the MFT for System 3 (Base MFT 2) was 14 mg/L. In the MFT, Figure C-4 shows that the SO_4^{2-} concentration increased rapidly at the beginning of incubation and reached 115 mg/L in MFT-U and 226 mg/L in MFT-L at 3 d of incubation. This rapid increase in SO_4^{2-} concentration in the MFT at the early incubation times was

most likely due to the rapid release of the underlying CT water. Following this initial increase, the SO_4^{2-} concentration in the MFT decreased. Most of the SO_4^{2-} concentration drop occurred in the first 30 d of incubation, with the SO_4^{2-} concentration reaching 31 mg/L in MFT-U and 87 mg/L in MFT-L at 29 d of incubation. After that time, the SO_4^{2-} concentration remained relatively constant with 44 mg/L in MFT-U and 60 mg/L in MFT-L at 366 d of incubation. The lower zone of MFT had higher SO_4^{2-} concentration than the upper zone of MFT, likely due to the fact that the MFT-L zone was in direct contact with the underlying CT layer (which had a high SO_4^{2-} concentration).

From Table B-6, it can be seen that the baseline SO_4^{2-} concentration in the CT was 724 mg/L for columns C1-1 to C1-11 (Base CT 1) and 897 mg/L for C1-12 to C1-20 (Base CT 2). In comparison, the baseline SO_4^{2-} concentration in the CT for System 4 (Base CT 3) was 1100 mg/L. In the CT of System 1, Figure C-4 indicates that the largest drop in SO_4^{2-} concentration occurred during the first 30 d of incubation. At 29 d of incubation, the SO_4^{2-} concentration in the CT decreased substantially to 336 mg/L in CT-U and 260 mg/L in CT-L. After that time, the SO_4^{2-} concentration decreased and reached 21 mg/L in CT-U and 23 mg/L in CT-L at 366 d of incubation, corresponding to more than 95% SO_4^{2-} concentration reduction. With the exception of a few data points, the two CT-U and CT-L zones showed similar SO_4^{2-} concentrations over time. Furthermore, the CT had consistently higher SO_4^{2-} concentration than the MFT over 1 y of incubation. At the end of 1 y of incubation, however, both the CT and MFT in System 1 approached similar SO_4^{2-} concentrations in the range of 21 to 60 mg/L.

In the cap water, Figure C-4 shows that the SO_4^{2-} concentration increased rapidly at the beginning of the incubation and reached a maximum value of 235 mg/L at 15 d of incubation. This rapid increase in SO_4^{2-} concentration in cap water at the early incubation was likely from the rapidly released CT water. Following this initial increase, the SO_4^{2-} concentration decreased, and dropped to 73 mg/L at 62 d of incubation. After that time, the SO_4^{2-} concentration remained stable until 213 d of incubation with a SO_4^{2-} concentration of 53 mg/L. From 244 d of incubation, the SO_4^{2-} concentration in the cap water increased with time and reached 277 mg/L at 304 d of incubation and 271 mg/L at 366 d of incubation. These SO_4^{2-} concentrations in the cap water were even higher than in either MFT or CT layer. The reasons causing this increase in SO_4^{2-} concentration in the cap water were unknown.

Using the same procedures as for the Br^- mass balance calculations in Section 6.3.3.1, a mass balance of SO_4^{2-} in the whole column of System 1 was attempted. Table 6-15 lists the results of SO_4^{2-} mass balance calculations in System 1.

Table 6-15. The SO_4^{2-} mass balance calculation in System 1.

Column	t_{incu} (d)	Mass of SO_4^{2-} at time 0 (mg)			Mass of SO_4^{2-} at column sacrificing (mg)						SO_4^{2-} mass recovery (%)
		In MFT	In CT	Total mass of SO_4^{2-} in whole column	In cap water	In MFT-U	In MFT-L	In CT-U	In CT-L	Total mass of SO_4^{2-} in the whole column	
C1-2	3	0	3013	3013	50	159	282	1248	1213	2952	98
C1-3	15	0	3002	3002	230	65	173	749	636	1853	62
C1-4	29	0	2991	2991	318	40	111	459	311	1239	41
C1-5	62	0	2991	2991	126	39	139	321	323	948	32
C1-6	91	0	3013	3013	0	21	78	204	225	528	18
C1-12	121	0	3734	3734	185	50	115	279	75	704	19
C1-8	153	0	2980	2980	NA	15	73	154	154	NA	NA
C1-9	182	0	3013	3013	128	27	64	73	36	328	11
C1-10	213	0	3008	3008	106	24	79	226	253	688	23
C1-11	244	0	3035	3035	272	41	73	119	99	604	20
C1-13	267	0	3748	3748	419	55	81	111	94	760	20
C1-14	303	0	3762	3762	649	NA	NA	NA	NA	NA	NA
C1-15	335	0	3762	3762	507	26	47	50	99	729	19
C1-16	366	0	3782	3782	635	54	74	22	23	808	21

1). SO_4^{2-} mass recovery (%) =((total mass of SO_4^{2-} at column sacrificing)/(total mass of SO_4^{2-} at time 0))×100%.
2). NA=not available.

It is seen from Table 6-15 that, after 1 y of incubation, only less than 20% of the original SO_4^{2-} mass still exits in the water, suggesting that more than 80% of the original SO_4^{2-} mass was removed from the water by some mechanisms in System 1. System 1 removed more SO_4^{2-} than System 4 over same incubation periods.

As discussed previously in Section 2.4, with its high SO_4^{2-} concentration, the conditions in the CT should favour the sulphate reduction by SRB when the environment becomes anaerobic. The MFT in System 1 will receive CT release water, which may also result in a high enough SO_4^{2-} concentration in the MFT to stimulate the SRB activity. The following discussions about the results of HCO_3^-, Eh, and trapped gas analysis are used to determine whether sulphate reduction by SRB was occurring in the CT and MFT of System 1.

As shown in Equation 2-2, the sulphate reduction by SRB will produce HCO_3^-. Figure C-26 shows the HCO_3^- concentration in System 1.

In the CT of System 1, the baseline HCO_3^- concentration for CT was 739 mg/L in Base CT 1 and 806 mg/L in Base CT 2 (see Table B-6). Figure C-26 shows a steady increase in HCO_3^- concentration in the CT over time. At 366 d of incubation, the HCO_3^- concentration reached 1350 mg/L in CT-U and 1310 mg/L CT-L, corresponding to approximately a 65% increase from the baseline data. The increase in HCO_3^- concentration in the CT of System 1 was well matched with the decrease in SO_4^{2-} concentration (see Figure C-4) over 1 y of incubation, indicating the SRB reduction of SO_4^{2-} in the CT layer.

In the MFT of System 1, the baseline HCO_3^- concentration for MFT (Base MFT 1) was 1491 mg/L. As shown in Figure C-26, at the beginning of the incubation, the MFT experienced a slight drop in HCO_3^- concentration, possibly due to the mixing and dilution with the low HCO_3^- concentration upflowing CT water. After 15 d of incubation, the HCO_3^- concentration in the MFT increased slowly until 182 d of incubation. The slight increase in HCO_3^- concentration of MFT was matched with the slight decrease in SO_4^{2-} concentration of MFT (see Figure C-4), implying the activity of sulphate reduction by SRB in the MFT layer. From 210 to 365 d of incubation, the HCO_3^- concentration in MFT dropped slightly. This may be caused by some unknown factors.

The redox potential may also provide an indicator for favourable conditions for SO_4^{2-} reduction by SRB. Figure C-27 shows the Eh in the MFT and CT of System 1 over 1 y of incubation. It can be seen that, after the first 3 to 15 d of incubation, the Eh in the CT was in the range of –178 to –206 mV, and the Eh in the MFT was for the most part in the range of –110 to –182 mV over 1 y of incubation, indicating anaerobic conditions in both MFT and CT. Most of the Eh values in the MFT and CT of System 1 thus support the presence of anaerobic conditions, which favour the SRB activity.

The trapped gas analysis in System 1 (see Table B-12) also showed the presence of low levels of gaseous H_2S in some samples. The presence of H_2S is likely the result of sulphate reduction by SRB.

6.3.3.4 pH and electrical conductivity

The pH in the cap water and porewaters of MFT and CT in System 1 was mostly in the range of 7.6 to 8.3 (see Figure C-23). The cap water had lower pH than the porewaters of MFT and CT over 1 y of incubation.

Figure C-28 shows the electrical conductivity in System 1 over 1 y of incubation. In System 1, the baseline EC was 4430 μS/cm for MFT (Base MFT 1), 5770 μS/cm for CT in columns C1-1 to C1-11 (Base CT 1), and 6120 μS/cm for CT in columns C1-12 to C1-20 (Base CT 2). The baseline CT had a higher EC than the baseline MFT.

Over 1 y of incubation, the EC in MFT increased and reached 4870 μS/cm in MFT-U and 4940 μS/cm in MFT-L at 366 d of incubation. The MFT-L zone showed slightly higher EC than the MFT-U zone, possibly due to the direct contact of the MFT-L zone with the CT layer, which had higher EC.

The EC in the CT showed a rapid decrease in the first 30 d of incubation. This rapid decrease in EC can be attributed to the rapid decrease in Ca^{2+} (see Figure C-22), Mg^{2+} (see Figure C-25), and SO_4^{2-} (see Figure C-4) concentrations in CT at the beginning of incubation. Following this rapid decrease in EC, the EC in the CT increased slightly with time (except for EC data at 153 d of incubation) and reached 5350 μS/cm in CT-U and 5190 μS/cm in CT-L at 366 d of incubation. Both the upper and lower zones of CT showed similar EC values over time.

In the cap water of System 1, the EC was in the range of 4560 to 5330 μS/cm over 1 y of incubation, and between that of MFT and CT. The EC in the cap water increased slightly over time.

6.3.3.5 The possible sinks of SO_4^{2-} reduction by SRB and the AVS analysis

As discussed above, over 366 d of incubation, both the CT and MFT in System 1 had a SO_4^{2-} concentration greater than 20 mg/L in most analyses. The value of 20 mg/L is believed to be the critical SO_4^{2-} concentration, above which SRB will out-compete methanogens for substrates (Fedorak *et al.* 2002). The Eh in the CT and MFT indicated suitable conditions for the SRB, and the decrease in SO_4^{2-} concentrations and the increase in HCO_3^- concentrations indicate the presence of SRB activity in the MFT and CT of System 1.

In the dissimilatory sulphate reduction, SO_4^{2-} acts as electron acceptor during the oxidation of organic matter by SRB and is reduced to sulphide as shown in Equation 2-2.

The MFT and CT in System 1 had pH in the range of 7.6 to 8.3 (see Figure C-23). In this pH range, the predominant form of sulphide is HS^- rather than H_2S (Fedorak *et al.* 2000). Only a small portion of the sulphide may be recovered as H_2S, as shown in Equation 6-13:

$$HS^- + H_2O \rightleftharpoons H_2S_{(g)} + OH^- \quad \text{.....(6-13)}$$

In the presence of heavy metals, such as Fe^{2+}, the HS^- will further react with the metals to precipitate as metal sulphides, such as FeS. FeS may be further converted to pyrite, as shown in the following equations:

$$HS^- + Fe^{2+} \longrightarrow FeS_{(s)} + H^+ \quad \text{(6-14)}$$

$$FeS + S^0 \longrightarrow FeS_{2(s)} \quad \text{(6-15)}$$

As noted by Schlesinger (1997), AVS (mainly the iron sulphides) is an effective trap for H_2S, which might otherwise escape to the atmosphere. Because AVS compounds are metastable and reactive, either by oxidation or by subsequent reduction to FeS_2, it is reasonable to assume that its presence is an indicator of recent SO_4^{2-} reduction (Kennedy *et al.* 1999).

The AVS analysis in this project was performed by the commercial laboratory using 6 M cold HCl and $SnCl_2$ to digest the sample. As discussed in Section 4.2, the analysed sulphur pool was therefore the AVS plus fine-graded (newly formed) synthetic pyrite. The AVS analysis was only conducted on MFT and CT of baseline and after approximately 120 d of incubation, as shown in Table 6-16. Table 6-16 also contains related SO_4^{2-} concentrations (as determined by IC) and S^{2-} concentrations (as determined by CHEMetrics test kit).

Table 6-16. AVS analysis and related SO_4^{2-} and S^{2-} measurements in System 1.

Sample	t_{incu} (d)	AVS (mg/kg of dry sample)	SO_4^{2-} (mg/L)	S^{2-} (mg/L)
Base MFT 1	0	74	BDL	BDL
Base CT 2	0	80	897	4.0
C1-12-CapW	121	NA	90	BDL
C1-12-MFT-U	121	150	41	BDL
C1-12-MFT-L	121	186	94	BDL
C1-12-CT-U	121	29	264	0.1
C1-12-CT-L	121	NA	68	0.1

1). NA=not available,
2). BDL=below detection limit.

The AVS results (see Table 6-16) show that, after approximately 120 d of incubation, the AVS increased in the MFT but decreased in the CT from the baseline data. The increase in AVS of the MFT may be attributed to the formation of sulphides as a result of sulphate reduction by SRB. However, the drop in AVS of the CT is quite unreasonable and suspicious. As discussed above, the high SO_4^{2-} concentration, anaerobic environment (as indicated by the low Eh value), and increased HCO_3^- concentration in the CT all support the sulphate reduction by SRB in the CT. The exact reasons for the decrease in AVS of the CT were unable to be identified.

Sulphite (SO_3^{2-}) and thiosulphate ($S_2O_3^{2-}$) are possible intermediates in the sulphate reduction to sulphide. In a similar project conducted by Fedorak *et al.* (2000), most of the Syncrude MFT and CT samples showed no detectable SO_3^{2-} concentrations, and only occasional detections of $S_2O_3^{2-}$ with a maximum concentration of approximately 50 mg/L in the CT samples. Therefore, $S_2O_3^{2-}$ is a possible sink of sulphur from SO_4^{2-} reduction.

Another possible sink of sulphur from SO_4^{2-} reduction by SRB is dissolved sulphides in the water. As discussed previously in Section 4.2, the S^{2-} analysis on the cap water and porewater was performed using The CHEMetrics test kit. The CHEMetrics test kit measures the total acid soluble sulphides in water after the water is first filtered through a 0.45 μm filter. Thus, the S^{2-} analysis results will include all the components of dissolved H_2S, HS^-, and acid soluble metallic sulphides in suspension.

Table B-9 shows the S^{2-} analysis results on the cap water and porewater of MFT and CT in System 1 over 1 y of incubation. It can be seen from Table B-9 that most of the S^{2-} concentrations in the cap water and porewaters of MFT and CT were non-detectable (<0.05 mg/L), with a few samples having low (0.1 to 6.0 mg/L) concentrations of S^{2-}. These results indicate that the majority of the sulphide from sulphate reduction by SRB was not in the cap water or porewaters in the form of S^{2-}.

6.3.3.6 Solids content

Figure C-29 shows the solids content in the MFT and CT of System 1 over 1 y of incubation. The solids contents of both MFT and CT increased steadily over 1 y of incubation.

In the MFT of System 1, the baseline solids content was 37.9 wt% (Base MFT 1, see Table B-6), similar to 38.0 wt% of the baseline solids content of MFT in System 3. The MFT solids content increased steadily over the entire

year of incubation, and reached 42.5 wt% in MFT-U and 42.9 wt% in MFT-L at 366 d of incubation. This steady increase in the MFT solids content is not consistent with the MFT tailings volume change in System 1 (see Figure C-1). The MFT tailings volume in System 1 did not show a consistent decrease but rather fluctuated over time. The inconsistency between these two data sets can be explained by the following two reasons. First, some measurement error was likely introduced when measuring the Geo-grid position for the calculation of MFT tailings volume change; second, it is possible that gas might be trapped in the MFT, which would affect the data of MFT tailings volume change.

These two factors, however, will not affect the solids content analysis. Therefore, it is assumed that, for the MFT in System 1, the solids content data are more reliable in indicating its consolidation, rather than the data of the MFT tailings volume change.

For the MFT, from its solids content, the released and remaining water percents (vol %) can be empirically estimated. Table C-3 in Appendix C lists the empirical estimation of released and still remaining water contents per litre of original MFT, based on the MFT density and solids content. Table C-3 is adapted from the relevant table provided by Dr. MacKinnon, Syncrude Canada Ltd. Since the baseline MFT in System 1 had solids content of 37.9 wt%, Table C-3 is based on 38 wt% of initial MFT solids content. After 366 d of incubation, the solids content of MFT in System 1 reached 42.5 wt% in MFT-U zone and 42.9 wt% in MFT-L zone (see Table 6-3). At these solids contents, Table C-3

shows that nearly 81 vol% of the original MFT porewater content still remains in the MFT layer.

In the CT of System 1, the baseline solids content was 57.2 wt% for "Base CT 1" and 56.5 wt% for "Base CT 2" (see Table B-6), similar to 56.6 wt% of the baseline solids content in the CT of System 4. Figure C-29 shows that the solids content of CT increased over the entire incubation time, with the most rapid solids content increase occurring in the first 60 d of incubation. The solids content of CT reached 71.4 wt% in CT-U and 69.2 wt% in CT-L at 62 d of incubation, and 73.2 wt% in CT-U zone and 73.5 wt% in CT-L zone at 366 d of incubation. The solids content increase in the CT is consistent with CT tailings volume changes over time (see Figure C-1).

A field study of the CT beneath MFT deposition test conducted by Syncrude Canada Ltd. (Shaw *et al.* 2001) showed that, over about 2.5 y of deposition period, the solids content of CT increased from 55 to 72 wt%, while the solids content of MFT increased from 33 to 41 wt%. In System 1 of this study, over 1 y of incubation, the solids content of CT increased from 56.5 wt% to 73.2 wt% in CT-U zone and to 73.5 wt% in CT-L zone, while the solids content of MFT increased from 37.9 wt% to 42.5 wt% in MFT-U zone and to 42.9 wt% in MFT-L zone (see Table 6-3). This comparison of solids contents between this work and the field study of Shaw *et al.* (2001) implies that further densification of both the MFT and CT in System 1 would be slow.

Figure C-29 shows that the upper and lower zones of CT and MFT in System 1 had similar solids content within individual CT and MFT layers,

indicating uniform densification in the CT or MFT layer. The solids content analysis also shows that no substantial mixing occurred between the MFT and CT layers in System 1. Since the lower MFT zone and upper CT zone samples in System 1 were separated by a 4 cm interval which was discarded when cutting the frozen columns (see Section 4.2), it might still be possible that at the interface of MFT and CT, some degree of mixing have occurred. The field demonstration of the CT beneath MFT deposition conducted by Syncrude Canada Ltd. in 1995 (Shaw *et al.* 2001) provided the similar conclusion; that is, the distinct CT and MFT layers were preserved but there was also a thin size of transition zone between the two layers.

6.3.4 Physical and chemical characteristics in System 2 (Cap water/MFT/CT)

System 2 had six columns and was also a CT beneath MFT system as in System 1. The six columns in System 2 were divided into three groups, each with different chemical amendment in the baseline CT, as shown in Table 4-5. The columns C2-1 to C2-3 had the same chemical composition in the baseline MFT and CT as in System 1, and were comparable to the columns in System 1. Columns C2-4 to C2-6 had elevated Ca^{2+} and SO_4^{2-} amendments in baseline CT, with extra addition of acetate in baseline CT for column C2-6 (see Table 4-5).

As discussed previously, at every cap water sampling, the existing cap water on the top of the MFT layer was completely extracted. Thus, at every sampling, the cap water is newly released water since the previous sampling.

Therefore, the chemical analysis of the cap water in System 2 can provide a time profile of released water composition at different incubation times.

Over 1 y of incubation, 9 in-situ samplings during incubation with 1 sacrificial sampling at the end of 1 y of incubation were conducted. Columns C-1, C-4, and C-6 were sacrificed. Because the tailings settling and cap water producing occurred more rapidly at early incubation times, more frequent in-situ sampling was conducted at early incubation times than at late incubation times.

6.3.4.1 Bromide tracer analysis

As in System 1, approximately 0.22 g NaBr was added to 1 L CT at column filling for System 2 (see Table 4-5). For System 2, the baseline Br^- concentration in the MFT (Base MFT 3) was non-detectable (<0.5 mg/L); the baseline Br^- concentration in the CT was 300 mg/L for columns C2-1 to C2-3 (Base CT 4) and 280 mg/L for columns C2-4 to C2-6 (Base CT 5 and Base CT 6) (see Table B-6). The baseline Br^- concentrations in the MFT and CT of System 2 were similar to those in System 1.

Figure C-30 shows the Br^- concentration in the cap water of System 2 over 352 d of incubation. The Br^- concentration in the cap water of System 2 increased steadily over 352 d of incubation. As discussed in System 1, the cap water Br^- concentration can indicate the proportion of MFT and CT porewaters in the cap water. Increased Br^- concentration in the cap water indicates the increased portion of CT porewater. The data of Br^- concentration in the cap

water of System 2 appear to match that of System 1 (see Figure C-21), which also shows slight Br^- concentration increase in the cap water over time.

6.3.4.2 Calcium and magnesium concentrations

The baseline Ca^{2+} concentration in the MFT of System 2 (Base MFT 3) was 24 mg/L, similar to the baseline Ca^{2+} concentration in the MFT of System 1 (see Table B-6). The baseline Ca^{2+} concentration in the CT for columns C2-1, C2-2, and C2-3 (Base CT 4) was 78 mg/L, similar to the baseline Ca^{2+} concentration in the CT for System 1. The baseline Ca^{2+} concentration in the CT for columns C2-4 and C2-5 (Base CT 5) was 99 mg/L, and for column C2-6 (Base CT 6) was 114 mg/L.

Figure C-31 shows the Ca^{2+} concentration in the cap water of System 2 over 352 d of incubation. Figure C-31 shows that the Ca^{2+} concentration decreased slightly in System 2 over the 352 d of incubation, indicating that the release of Ca^{2+} from the CT water decreased slightly with time. The Ca^{2+} concentration in the cap water of columns C2-1 to C2-3 was in the range of 17 to 32 mg/L over the 352 d of incubation, comparable to the range of 23 to 30 mg/L of Ca^{2+} concentration in the cap water of System 1 over 366 d of incubation. Compared to 78 mg/L of baseline Ca^{2+} concentration in the CT for columns C2-1 to C2-3 (Base CT 4), columns C2-1 to C2-3 in System 2 were effective at reducing the Ca^{2+} concentration for the cap water, as was the case for System 1.

Columns C2-4 to C2-6 had Ca^{2+} concentrations in the cap water ranging from 26 to 41 mg/L over 352 d of incubation, slightly higher than in columns C2-1 to C2-3. These higher concentrations of Ca^{2+} in the cap water are most likely due to the higher baseline Ca^{2+} concentration in the CT. Therefore, the higher Ca^{2+} concentration in the baseline CT will lead to a higher Ca^{2+} concentration in the cap water. Compared to 99 mg/L of baseline Ca^{2+} concentration in CT for columns C2-4 and C2-5 (Base CT 5) and to 114 mg/L of baseline Ca^{2+} concentration in CT for column C2-6 (Base CT 6), columns C2-4 to C2-6 in System 2 were effective at reducing the Ca^{2+} concentration for the cap water.

Figure C-32 shows the Mg^{2+} concentration in the cap water of System 2 over 352 d of incubation. The baseline CT for System 2 had slightly higher Mg^{2+} concentrations (28 mg/L for Base CT 4, 30 mg/L for Base CT 5, and 34 mg/L for Base CT 6) than the baseline MFT for System 2 (16 mg/L for Base MFT 3). The Mg^{2+} concentrations in the baseline CT and MFT for columns C2-1 to C2-3 were close to the Mg^{2+} concentrations in the baseline CT and MFT for System 1.

The release of Mg^{2+} into the cap water over time was quite constant during 352 d of incubation (see Figure C-32). The Mg^{2+} concentration in the cap water was in the range of 14 to 21 mg/L for columns C2-1 to C2-3, and 19 to 27 mg/L for columns C2-4 to C2-6. These cap water Mg^{2+} concentrations in System 2 are similar to the range of 12 to 19 mg/L in the cap water of System 1 during 366 d of incubation. Compared to the Mg^{2+} concentrations in the baseline MFT

and CT, System 2 was effective at reducing the Mg^{2+} concentration for the cap water.

6.3.4.3 Sulphate concentration

From Table B-6, it can be seen that the baseline SO_4^{2-} concentration in the MFT for System 2 (Base MFT 3) was 23 mg/L; the baseline SO_4^{2-} concentration in CT for columns C2-1 to C2-3 (Base CT 4) was 1070 mg/L, for columns C2-4 and C2-5 (Base CT 5) was 1350 mg/L, and for column C2-6 (Base CT 6) was 1660 mg/L. In comparison, the baseline SO_4^{2-} concentration in the MFT of System 1 (Base MFT 1) was non-detectable (<0.5 mg/L); the baseline SO_4^{2-} concentration in the CT of System 1 was 724 mg/L for Base CT 1 and 897 mg/L for Base CT 2.

Figure C-33 shows the SO_4^{2-} concentration in the cap water of System 2 over 352 d of incubation. The SO_4^{2-} concentrations in the cap water of System 2 showed similar trends as the SO_4^{2-} concentrations in the cap water of System 1 (see Figure C-4). The SO_4^{2-} concentration increased quickly at the beginning of the incubation to reach a SO_4^{2-} concentration, after 3 to 7 d of incubation, of the range of 260 to 360 mg/L for columns C2-1 to C2-3, and of the range of 388 to 700 mg/L for columns C2-4 to C2-6. After this initial increase, the SO_4^{2-} concentration decreased steadily to reach a low value at 49 d of incubation. After 49 d of incubation, the SO_4^{2-} concentrations increased over time. The reasons for this SO_4^{2-} concentration increase in the cap water were unknown.

Table B-10 shows the S^{2-} analysis results on the cap water of System 2. All of the S^{2-} concentration in the cap water of System 2 was non-detectable (<0.05 mg/L). In fact, due to the high concentration of O_2 in the headspace, any S^{2-} produced from SO_4^{2-} reduction by SRB would be oxidized and hence disappear from the cap water.

The columns in System 2 had different SO_4^{2-} concentrations in the baseline CT (see Table 4-5). As shown in Figure C-33, the higher SO_4^{2-} concentrations in the CT would likely lead to a higher SO_4^{2-} concentration in the cap water. The addition of acetate in the baseline CT of column C2-6 seemed to have no obvious effect in increasing the removal of SO_4^{2-} by microbial activity over the research period.

6.3.5 Comparisons among Systems 1, 3, and 4

System 1 (Cap water/MFT/CT) was the main research system, while Systems 3 (Cap water/MFT) and 4 (Cap water/CT) served as controls. Because the cap water properties and tailings densification are the foremost important parameters in assessing System 1 of this study, further comparisons of the major cap water parameters (Ca^{2+}, Mg^{2+}, SO_4^{2-} and EC) and tailings solids content among the main system (System 1) and control systems (Systems 3 and 4) will be presented here.

6.3.5.1 Comparisons of Ca^{2+}, Mg^{2+}, and SO_4^{2-} concentrations in the cap water

Figure C-34 shows the comparison of the Ca^{2+} concentrations in the cap water of Systems 1, 3, and 4 over 1 y of incubation. The Ca^{2+} concentration in the cap water of System 1 was in the range of 23 to 30 mg/L over 1 y of incubation. The Ca^{2+} concentration in the cap water of System 1 was only slightly higher than in System 3, and lower than in System 4.

Figure C-35 shows the comparison of the Mg^{2+} concentrations in the cap water of Systems 1, 3, and 4 over 1 y of incubation. The Mg^{2+} concentrations in the cap water of System 1 were in the range of 16 to 19 mg/L over 1 y of incubation. As with Ca^{2+}, the Mg^{2+} concentration in the cap water of System 1 was only slightly higher than in System 3, and lower than in System 4.

Figure C-36 shows the comparison of the SO_4^{2-} concentrations in the cap water of Systems 1, 3, and 4 over 1 y of incubation. The SO_4^{2-} concentration in the cap water of System 1 was in the range of 0 to 277 mg/L over 1 y of incubation. As with Ca^{2+} and Mg^{2+}, the SO_4^{2-} concentrations in the cap water of System 1 were higher than those of System 3 but lower than those in System 4.

It is clear from the comparisons among Figures C-34 to C-36 that, over 1 y of incubation, System 1 was effective at reducing the Ca^{2+}, Mg^{2+}, and SO_4^{2-} concentrations for the cap water and could reach concentrations close to those in the MFT only system.

6.3.5.2 Comparisons of pH and electrical conductivity in the cap water

Figure C-37 shows the comparison of the pH in the cap water of Systems 1, 3, and 4 over 1 y of incubation. The pH in the cap water of all three systems was quite constant over time and was mostly in the range of 7.6 to 8.2.

Figure C-38 shows the comparison of the EC in the cap water of Systems 1, 3, and 4 over 1 y of incubation. The EC in the cap water of all three systems increased slightly with time. Over 1 y of incubation, the EC in the cap water of System 1 was in the range of 4560 to 5270 μS/cm, higher than the range of 4340 to 4670 μS/cm in the cap water of System 3, but lower than the range of 6100 to 6440 μS/cm in the cap water of System 4.

As with Ca^{2+}, Mg^{2+}, and SO_4^{2-}, System 1 was effective at reducing the EC for the cap water, and could reach a level close to that of System 3.

6.3.5.3 Comparison of solids content in MFT and CT

Figure C-39 shows the comparison of the solids content in the MFT between Systems 1 and 3 over 1 y of incubation. The solids content in the MFT of both Systems 1 and 3 increased steadily over the incubation time. The MFT in System 3 had consistently higher solids content than the MFT of System 1, indicating that the MFT in System 1 did not consolidate as fast as the MFT in System 3. The upper and lower zones of MFT showed similar solids content in both Systems 1 and 3 over the 1 y of incubation, indicating the uniform densification over the entire MFT layer in both systems.

Figure C-40 shows the comparison of the solids content in CT between Systems 1 and 4 over 1 y of incubation. The solids content in the CT of both Systems 1 and 4 increased steadily over incubation time, with most rapid increase occurring in the first 60 d of incubation. The CT in both Systems 1 and 4 showed similar solids content increase over 1 y of incubation, indicating the CT in System 1 consolidated as fast as the CT in System 4. The upper and lower zones of CT showed similar solids content in both Systems 1 and 4 over the 1 y of incubation, indicating the uniform densification over the entire CT layer in either system.

6.4 MPN analysis on MFT and CT in System 1

The MPN analyses of methanogens and SRB were conducted on MFT and CT samples of System 1 usually at an interval of every 60 d of incubation. Table B-13 lists the results of MPN analysis. Table B-13 shows that both the MFT and CT in System 1 were rich in methanogens and SRB. The activity of these groups of microorganisms will contribute to the production of CH_4 by methanogens and the reduction of SO_4^{2-} by SRB.

6.4.1 MPN of methanogens

Figure C-41 shows the log (MPN) of methanogens over 1 y of incubation in System 1. For the methanogens in System 1, the MPN was for the most part in the range of 10^3 to 10^5/g (of dry solids) in MFT and of 10^2 to 10^4/g (of dry

solids) in CT. The upper and lower zones of MFT showed similar MPN values of methanogens in System 1 over 1 y of incubation. The MFT had higher MPN of methanogens than the CT over 1 y of incubation. Fedorak *et al.* (2000) reported that the MPN for Syncrude MFT was mostly in the range of 10^5 to 10^7/g (of dry solids) over 1 y of incubation. The MFT in System 1 was placed above a layer of CT, thus different from the MFT in Fedorak *et al.* (2000). The low MPN value of the MFT in System 1 as compared to that in Fedorak *et al.* (2000) may be due to the high SO_4^{2-} concentrations (> 20 mg/L) in the MFT porewater of System 1 (see Figure C-4). The MPN in the CT of System 1 was lower than the MPN of MFT. The high SO_4^{2-} concentration in the CT may account for the low MPN of methanogens (see Figure C-4). As discussed previously, the presence of high concentration of SO_4^{2-} will stimulate the activity of SRB and hence inhibit the methanogen activity.

6.4.2 MPN of SRB

Figure C-42 shows the log (MPN) of SRB over 1 y of incubation in System 1. For the SRB in System 1, the MPN was for the most part in the range of 10^5 to 10^6/g (of dry solids) in MFT and of 10^4 to 10^5/g (of dry solids) in CT. The upper and lower zones of MFT showed similar MPN of SRB in System 1 over 1 y of incubation. As shown in Figure C-4, the CT porewater had consistently higher SO_4^{2-} concentration than the MFT porewater in System 1. From the high SO_4^{2-} concentration, the CT in System 4 should favour the

activity of SRB and have high MPN of SRB. The MFT, however, had consistently higher MPN of SRB than the CT in System 1 over 1 y of incubation. The reasons for the higher MPN of SRB in the MFT than in the CT cannot be identified. The larger MPN values of SRB in the MFT should lead to more SO_4^{2-} reduction in the MFT than in the CT of System 1. This appears to be supported by the AVS analysis, which shows larger AVS values in the MFT than in the CT at 121 d of incubation in System 1 (see Table 6-16). Holowenko (2000) reported that the MPN of SRB was for the most part in the range of 10^5 to 10^7/g (of dry solids) for Syncrude MFT.

7.0 Summary

7.1 Total volume change (Vt) in Systems 3, 4, and 1

For System 3, over 1 y of incubation, the total volume of the MFT only deposit expanded initially and reached a maximum Vt(3) value in the range of 12.3 to 13.5 vol% among the columns at 90 d of incubation, and then the total volume decreased and reached a Vt(3) value of 6.9 vol% at 365 d of incubation.

For System 4, over 1 y of incubation, the total volume change of the CT only deposit was small, with the Vt(4) values in the range of 0.0 to –0.7 vol% among the columns.

For System 1, over 1 y of incubation, the total volume change (Vt(1)) of the CT beneath MFT deposit was between –8.8 vol% and 2.8 vol% among the columns.

7.2 Total tailings volume change (Vtt) in Systems 3, 4, 1, and 2

For System 3, over 1 y of incubation, the total tailings volume of the MFT only deposit increased initially and reached a maximum Vtt(3) value between 3.6 and 4.6 vol% among the columns at 77 d of incubation. After this time, the total tailings volume decreased steadily and reached a Vtt(3) value of 0 vol% at about 110 d of incubation, and of –8.8 vol% at 365 d of incubation.

For System 4, over 1 y of incubation, the total tailings volume of the CT only deposit decreased steadily. The most rapid decrease in total tailings volume occurred in the first 60 d of incubation, with a Vtt(4) value between -27.7 and

-28.6 vol% among the columns at 61 d of incubation and of -31.9 vol% at 365 d of incubation.

For System 1, over 1 y of incubation, the total tailings volume of the CT beneath MFT deposit decreased steadily. The most rapid decrease in total tailings volume occurred in the first 60 d of incubation, with a Vtt(1) value between –17 and –21.2 vol% among the columns at 62 d of incubation and between –22.4 and –26.2 vol% among the columns at 366 d of incubation.

For System 2, the total tailings volume of the CT beneath MFT deposit decreased steadily. The most rapid decrease in total tailings volume occurred in the first 60 d of incubation, with a Vtt(2) value between –18.1 to –21.5 vol% among the columns at 49 d of incubation and between –22.5 to –26.8 vol% among the columns at 352 d of incubation. The total tailings volume change showed no certain effects of the different chemical dosage in CT on the total tailings densification rate over the experiment period.

7.3 Individual MFT and CT tailings volume change (V_{MFT} and V_{CT}) in Systems 1 and 2

The MFT layer in System 1 did not show a definite tailings volume decrease but rather a fluctuating value over 1 y of incubation. The trapped gas bubbles in the MFT and errors caused in determining the Geo-grid position may have contributed to this fluctuating tailings volume data of the MFT.

The CT layer in System 1 consolidated to a larger extent than the MFT layer over 1 y of incubation. Most of the tailings volume decrease of the CT

occurred in the first 60 d of incubation, with a $V_{CT(1)}$ value of -29.7 vol% at 62 d of incubation and of -33.6 vol% at 366 d of incubation.

The MFT layer in System 2 expanded slightly in the first 2 wk of incubation, with a maximum expansion occurring at a $V_{MFT(2)}$ value of 2.9 vol% at 14 d of incubation. Then the MFT started to densify steadily, with a $V_{MFT(2)}$ value in the range of -1.5 to 0.4 vol% at 49 d of incubation and of -6.2 to -14.9 vol% at 352 d of incubation among the columns in System 2. The tailings volume change of the MFT showed no certain effects of the different chemical dosages in baseline CT on the MFT densification rate over the experiment period.

As in System 1, the CT in System 2 consolidated to a larger extent than the MFT. The tailings volume of CT decreased steadily over 1 y of incubation. Most of the CT tailings volume decrease occurred in the first 60 d of incubation, with a $V_{CT(2)}$ value in the range of –28.3 to -31.7 vol% at 49 d of incubation and in the range of –31.8 to -37.4 vol% at 352 d of incubation among the columns in System 2. The tailings volume change of the CT showed no certain effects of the different chemical dosages in baseline CT on the CT densification rate over experiment period.

7.4 Comparisons of total and individual tailings volume changes (Vtt, V_{MFT}, and V_{CT}) among Systems 1, 2, 3 and 4

For the total tailings volume change, over 1 y of incubation, System 4 had the highest total tailings volume reduction with a Vtt(4) value of –31.9 vol%

at 365 d of incubation; then followed by System 1 with a Vtt(1) value of –22.4 to –26.2 vol% among the columns at 366 d of incubation; and System 3 had the lowest total tailings volume reduction with a Vtt(3) of –8.8 vol% at 365 d of incubation. The decrease in total tailings volume of Systems 1 and 4 occurred most rapidly in the first 60 d of incubation and reached a quite stable level after 1 y of incubation, while the total tailings volume in System 3 showed a further trend of decrease after 1 y of incubation.

For the individual MFT tailings volume change, Systems 2 and 3 showed similar MFT tailings volume reduction over incubation, with a $V_{MFT(2)}$ value in the range of –6.2 to –14.9 vol% among the columns at 352 d of incubation in System 2 and a $V_{MFT(3)}$ value of –8.8 vol% at 365 d of incubation in System 3.

For the individual CT tailings volume change, Systems 2 and 4 showed similar CT tailings volume reduction over incubation, with a $V_{CT(2)}$ value in the range of –31.8 to -37.4 vol% among the columns at 352 d of incubation in System 2 and a $V_{CT(4)}$ value of –31.9 vol% at 365 d of incubation in System 4.

7.5 Cap water volume (Vcw) in Systems 3, 4, and 1

In System 3, the cap water was produced steadily over 1 y of incubation. In System 4, most of the cap water was produced in the first 60 d of incubation. In System 1, most of the cap water was produced in the first 60 d of incubation, with a Vcw(1) value in the range of 17.3 to 20.2% at 62 d of incubation and of

17.4 to 24.7 vol% at 365 d of incubation among the columns. Systems 1 and 4 produced more cap water than System 3 over 1 y of incubation.

7.6 Cap water producing rate (Rcw) in Systems 3, 4, and 1

For System 3, the cap water producing rate among the columns reached a maximum value of approximately 17 mL/d in 30 d of incubation, and then decreased slowly to a value of 0.8 mL/d at 365 d of incubation.

For System 4, the cap water producing rate among the columns decreased from an initial value of approximately 200 mL/d to a value between 7.5 and 9.4 mL/d at 61 d of incubation, and to approximately 0 mL/d by 212 d of incubation.

For System 1, the cap water producing rate among the columns decreased from an initial value of approximately 200 mL/d to a value between 6.4 and 9.4 mL/d at 62 d of incubation, and to approximately 0 mL/d by 244 d of incubation, indicating that further dewatering of System 1 would be slow.

7.7 Tedlar bag gas volume in Systems 1, 3, and 4

In Systems 1 and 4, the Tedlar bag gas volumes were small. In System 1, only 10 to 60 mL of Tedlar bag gas was collected in the sacrificed columns over 366 d of incubation. In System 4, 17 to 308 mL of Tedlar bag gas was collected in the sacrificed columns over 365 d of incubation. No obvious gas evolution was visually observed in the columns of Systems 1 or 4.

In System 3, the Tedlar bag gas volume was higher and showed a large variation among the different columns. The Tedlar bag gas volume in the sacrificed columns in System 3 was in the range of 20 to 2030 mL over 365 d of incubation. Obvious gas evolution in the columns of System 3 was visually observed.

7.8 GC analysis on the Tedlar bag gas in Systems 1, 3, and 4

System 1 had for the most part a higher production of CH_4 than System 4, but a lower production of CH_4 than System 3. In System 1, the CH_4 concentration in the Tedlar bag gas increased steadily from 0.04 vol% at 29 d of incubation to 4.57 vol% at 213 d of incubation. In System 3, the CH_4 concentration in the Tedlar bag gas increased steadily from 0.39 vol% at 28 d of incubation to 20.70 vol% at 212 d of incubation. In System 4, the CH_4 concentrations in the Tedlar bag gas were quite low, only between 0 to 0.29 vol% over 1 y of incubation.

The CO_2 concentrations in the Tedlar bag gas of Systems 1, 3, and 4 increased steadily and reached a maximum level of approximately 4 to 8 vol% over 1 y of incubation. The measured CO_2 concentrations by GC in the Tedlar bag gas of System 1 were comparable with the calculated CO_2 concentrations in the column headspace gas of System 1 by Henry's law.

In the column headspaces of Systems 1, 3, and 4, low concentrations (for the most part, <1.0 vol%) of H_2S and C_2H_4 were occasionally detected.

7.9 In-situ headspace gas GC analysis in System 2

Compared to the Tedlar bag gas analysis in System 1, the in-situ headspace gas analysis in System 2 showed low CH_4 and CO_2 concentrations and a high O_2 concentration. Low concentrations (<1.0 vol%) of H_2S and C_2H_4 were detected occasionally.

The in-situ headspace analysis showed that the different chemical amendments in CT had little effects on the production and composition of headspace gases over 1 y of incubation.

Because of the disturbance and air contamination introduced in the in-situ headspace gas analysis, the in-situ gas analysis data of System 2 should be used with caution. The Tedlar bag gas analysis in Systems 1, 3, and 4 will be more reliable and valid in characterising the gas evolution from MFT or CT deposits.

7.10 Bromide tracer analysis and the dilution effect in System 1

In the MFT, over 1 y of incubation, the Br^- concentration increased steadily from initially non-detectable levels (<0.5 mg/L) to 130 mg/L in MFT-U zone and 210 mg/L in MFT-L zone at 62 d of incubation, and remained quite stable in the range of 120 to 150 mg/L for MFT-U zone and 160 to 210 mg/L for MFT-L zone for the remainder of the incubation.

In the CT, over 1 y of incubation, the Br^- concentration was quite constant and for the most part in the range of 220 to 280 mg/L, close to the baseline Br^- concentration in the CT.

In the cap water, the Br^- concentration increased quickly to 82 mg/L in the first 29 d of incubation, and remained in the range of 70 to 110 mg/L over the remaining incubation.

The mass balance calculations of Br^- showed that over 1 y of incubation, the Br^- recovery (relative to the Br^- mass at time 0) in System 1 was for the most part in the range of 92 to 108%. This indicates that the Br^- is a stable tracer with almost 100% recovery in the MFT and CT materials over incubation time.

The Br^- in the MFT and cap water originated from the underlying CT release water. The presence of Br^- in the MFT and cap water indicates the presence of CT water. Based on Br^- concentration analysis, it was shown that both the cap water and MFT porewater contained large percentages of CT water during the incubation, with a CT water portion of 41 vol% in cap water, 56 vol% in MFT-U zone, and 67 vol% in MFT-L zone at 366 d of incubation.

The estimation of dilution effect (P_d%) showed that dilution effect played a large role at reducing the concentrations of Ca^{2+}, Mg^{2+}, SO_4^{2-}, and the EC for the cap water in System 1.

7.11 Calcium and magnesium concentrations in System 1

In the MFT, the Ca^{2+} concentration decreased slightly, with the Ca^{2+} concentration of 17 mg/L in the MFT-U zone and 19 mg/L in the MFT-L zone

at 15 d of incubation, and 13 mg/L in the MFT-U zone and 14 mg/L in the MFT-L zone at 366 d of incubation. The MFT-U zone had slightly lower Ca^{2+} concentrations than the MFT-L zone.

In the CT, the largest drop in Ca^{2+} concentration occurred during the first 30 d of incubation, with a Ca^{2+} concentration of 29 mg/L in CT-U zone and 23 mg/L in CT-L zone at 29 d of incubation, and 21 mg/L in CT-U zone and 18 mg/L in CT-L zone at 366 d of incubation. The two CT-U and CT-L zones had similar Ca^{2+} concentration over 1 y of incubation. The CT had higher Ca^{2+} concentrations than the MFT.

In the cap water layer, the Ca^{2+} concentration was quite constant and in the range of 23 to 30 mg/L over 1 y of incubation. The cap water had Ca^{2+} concentration higher than in the MFT and close to that in the CT.

The mass balance calculations of Ca^{2+} showed that over 1 y of incubation, more than 50% of the original Ca^{2+} mass was removed from the water by some mechanisms. The ratios of $[Ca^{2+}]\times[CO_3^{2-}]$ to Ksp in all zones of System 1 over 1 y of incubation are in the range of 3 to 12, indicating that the precipitation of $CaCO_3$ is a possible route for the removal of Ca^{2+} in System 1.

The Mg^{2+} concentration in the MFT was quite constant (ranging from 11 to 16 mg/L) over 1 y of incubation. The Mg^{2+} concentration in the CT decreased most rapidly in the early incubation and reached 14 mg/L in CT-U zone and 15 mg/L in CT-L zone at 29 d of incubation. After this initial decrease, the Mg^{2+} concentration in the CT was quite stable. The Mg^{2+} concentration in the cap

water was in the range of 16 to 19 mg/L over 1 y of incubation and higher than in either MFT or CT.

7.12 Sulphate concentration in System 1

In the MFT, the SO_4^{2-} concentration increased rapidly from essentially 0 mg/L of baseline concentration to 115 mg/L in MFT-U and 226 mg/L in MFT-L at 3 d of incubation, then decreased mostly in the first 30 d of incubation with 31 mg/L in MFT-U zone and 87 mg/L in MFT-L zone at 29 d of incubation. After that time, SO_4^{2-} concentration remained relatively constant and reached 44 mg/L in MFT-U zone and 60 mg/L in MFT-L zone at 366 d of incubation. The MFT-U zone had for the most part lower SO_4^{2-} concentrations than the MFT-L zone.

In the CT, the largest decrease in SO_4^{2-} concentration occurred during the first 30 d of incubation, with SO_4^{2-} concentrations of 336 mg/L in CT-U zone and 260 mg/L in CT-L zone at 29 d of incubation. After that time, although showing some fluctuation, the SO_4^{2-} concentration for the most part decreased, and reached 21 mg/L in CT-U zone and 23 mg/L in CT-L zone at 366 d of incubation, corresponding to more than 95% SO_4^{2-} concentration reduction. The upper and lower zones of CT showed similar SO_4^{2-} concentration.

The MFT had lower SO_4^{2-} concentration than the CT over 1 y of incubation. However, after 1 y of incubation, both the MFT and CT approached similar SO_4^{2-} concentration in the range of 21 to 60 mg/L.

In the cap water, the SO_4^{2-} concentration increased initially and reached a maximum value of 235 mg/L at 15 d of incubation. The SO_4^{2-} concentration

dropped to 73 mg/L at 62 d of incubation, and then remained quite stable until 213 d of incubation at 52.6 mg/L. After 244 d of incubation, the SO_4^{2-} concentration in the cap water increased unexpectedly.

The mass balance calculations of SO_4^{2-} showed that, after 1 y of incubation, more than 80% of the original SO_4^{2-} mass was removed from the water by some mechanisms in System 1.

7.13 pH and electrical conductivity in System 1

The pH in the cap water and porewaters of MFT and CT was for the most part between 7.6 and 8.3 over 1 y of incubation. The cap water had consistently lower pH values than the MFT and CT porewaters.

In the MFT, the EC increased slightly over time and reached 4870 μS/cm in MFT-U zone and 4940 μS/cm in MFT-L zone at 366 d of incubation. In the CT, the EC showed a rapid decrease in the first 30 d of incubation. Following this initial rapid decrease, the EC in the CT increased slightly over time and reached 5350 μS/cm in CT-U zone and 5190 μS/cm in CT-L zone at 366 d of incubation. The two CT-U and CT-L zones showed similar EC during the incubation. In the cap water, the EC increased with time and was in the range of 4560 to 5330 μS/cm during 1 y of incubation.

7.14 Solids content in System 1

In the MFT, the solids content increased steadily over 1 y of incubation, and reached 42.5 wt% in MFT-U zone and 42.9 wt% in MFT-L zone at 366 d of

incubation. The MFT-U and MFT-L in the MFT showed similar solids content over time, indicating uniform densification over the entire MFT layer. The MFT solids content data are believed to be more reliable than the MFT tailings volume change ($V_{MFT(1)}$) in characterising the densification behaviour of MFT in System 1.

At 366 d of incubation, the solids contents of MFT in System 1 reached 42.5 wt% in upper zone of MFT and 42.9 wt% in the lower zone of MFT. At these solids contents, nearly 81 vol% of porewater (relative to the original porewater content) still remains in the MFT.

In the CT, the solids content increased most rapidly in the first 60 d of incubation, reaching 71.4 wt% in CT-U zone and 69.2 wt% in CT-L zone at 62 d of incubation. After that time, the CT solids content increased continuously over the remaining incubation and reached 73.2 wt% in CT-U and 73.5 wt% in CT-L at 366 d of incubation. The upper and lower zones of CT showed similar solids content over time, indicating uniform densification over the entire CT layer. The solids content analysis also showed that no obvious mixing occurred between the MFT and CT layers in System 1.

7.15 Bromide tracer analysis in System 2

The Br^- concentration in the cap water of System 2 increased over 352 d of incubation, indicating the increased portion of CT porewater in the cap water

over incubation time. At 352 d of incubation, the Br^- concentration in the cap water of System 2 reached 160 to 200 mg/L in the three sacrificed columns.

7.16 Calcium and magnesium concentrations in the cap water of System 2

In the cap water of System 2, the Ca^{2+} concentration decreased slightly in System 2 over 352 d of incubation, indicating that the release of Ca^{2+} from the CT beneath MFT deposit was slightly decreasing over time. The Ca^{2+} concentration in the cap water of columns C2-1 and C2-3 was in the range of 17 to 32 mg/L during 352 d of incubation, comparable to the range of 23 to 30 mg/L of Ca^{2+} concentration in the cap water of System 1 over 366 d of incubation. Compared to the baseline Ca^{2+} concentration in the MFT and CT, as in System 1, columns C2-1 to C2-3 in System 2 were effective at reducing Ca^{2+} concentration for the cap water. The higher concentration of Ca^{2+} in the CT at column filling lead to higher Ca^{2+} concentration in the cap water, as shown in columns C2-4 to C2-6.

The Mg^{2+} concentration in the cap water of System 2 was quite constant during 352 d of incubation and in the range of 14 to 21 mg/L for columns C2-1 to C2-3, similar to the range of 12 to 19 mg/L in the cap water of System 1 during 366 d of incubation. Compared to the baseline Mg^{2+} concentration in the MFT and CT, System 2 was effective at reducing Mg^{2+} concentration for the cap water.

7.17 Sulphate concentration in the cap water of System 2

The SO_4^{2-} concentration during incubation in the cap water of System 2 showed a similar pattern as the SO_4^{2-} concentration in the cap water of System 1. That is, in the cap water of System 2, the SO_4^{2-} concentration increased initially and reached a high SO_4^{2-} concentration in 3 to 7 d of incubation, then decreased and reached the lowest value at 49 d of incubation. After that time, the SO_4^{2-} concentration increased again with time. The reasons for this SO_4^{2-} concentration increase were not clear.

The higher concentration of SO_4^{2-} in the baseline CT caused higher SO_4^{2-} concentration in the cap water. However, the addition of acetate seemed to have no obvious effects on the removal rate of SO_4^{2-} over the experiment period.

7.18 Comparisons of Ca^{2+}, Mg^{2+}, SO_4^{2-} concentrations in the cap water of Systems 1, 3, and 4

The concentrations of Ca^{2+}, Mg^{2+}, and SO_4^{2-} in the cap water of System 1 were slightly higher than in System 3, but much lower than in System 4, indicating that System 1 was effective at reducing Ca^{2+}, Mg^{2+}, and SO_4^{2-} concentrations for the cap water.

7.19 Comparisons of pH and electrical conductivity in the cap water of Systems 1, 3, and 4

The pH values in the cap water of Systems 1, 3, and 4 were similar, and mostly in the range of 7.6 to 8.2 during 1 y of incubation. The EC in the cap

water of Systems 1, 3, and 4 increased slightly over time. During 1 y of incubation, the EC in the cap water of System 1 was in the range of 4560 to 5270 μS/cm, higher than in System 3 with the range of 4340 to 4670 μS/cm, but lower than in System 4 with the range of 6100 to 6440 μS/cm. System 1 was effective at reducing EC for the cap water.

7.20 Comparisons of solids content of MFT and CT among Systems 1, 3, and 4

The solids content in the MFT of both Systems 1 and 3 increased steadily over the incubation time. The MFT in System 3 had consistently higher solids content than in the MFT of System 1, indicating that the MFT in System 1 did not consolidate as fast as the MFT in System 3. The upper and lower zones of MFT showed similar solids content in either System 1 or 3 over 1 y of incubation, indicating the uniform densification rate over the entire MFT layer in either system.

The solids content in the CT of both Systems 1 and 4 increased steadily over incubation time, with largest rapid increase occurred in the first 60 d of incubation. The CT in both Systems 1 and 4 showed similar solids content increase over the 1 y of incubation, indicating that the CT in System 1 consolidated at a rate comparable to the CT in System 4. The upper and lower zones of CT showed similar solids content in either System 1 or 4 over the 1 y of incubation, indicating the uniform densification rate over the entire CT layer in either system.

7.21 MPN analysis on the MFT and CT in System 1

The MFT and CT in System 1 were both rich in methanogens and SRB. The MPN for methanogens was for the most part in the range of 10^3 to 10^5/g (of dry solids) in MFT and 10^2 to 10^4/g (of dry solids) in CT over 1 y of incubation. The MPN for SRB was for the most part in the range of 10^5 to 10^6/g (of dry solids) in MFT and 10^4 to 10^5/g (of dry solids) in CT over 1 y of incubation.

The upper and lower zones of MFT showed similar MPN values of SRB and methanogens.

8.0 Conclusion

In order to optimise tailings management, the oil sands industry has implemented CT process to handle the fluid portion (fine tailings) of its extraction tailings. The co-disposal approach using CT placed beneath MFT was proposed to improve the CT release water quality and the solids densification rates of both CT and MFT. The CT beneath MFT deposit (System 1) was assessed by comparing to the control systems (Systems 3 and 4). In the CT beneath MFT deposit, over 1 y of incubation, the cap water had improved water quality and both the MFT and CT showed steady densifications that were comparable to the control systems, as specified below:

(i) Over 1 y of incubation, the concentrations of Ca^{2+}, Mg^{2+}, SO_4^{2-}, and the electrical conductivity in the cap water of System 1 were only slightly higher than in System 3 but much lower than in System 4, with values of 27 mg/L, 18 mg/L, 271 mg/L, and 5150 μS/cm at the end of 1 y of incubation, respectively. The mass balance calculations of Ca^{2+} and SO_4^{2-} showed that, after 1 y of incubation, over 50% of the original Ca^{2+} mass and 80% of the original SO_4^{2-} mass were removed from the water of System 1. System 1 was therefore effective at reducing the concentrations of Ca^{2+}, Mg^{2+}, SO_4^{2-}, and the EC for the cap water.

(ii) Over 1 y of incubation, the solids content of the MFT in the CT beneath MFT deposit increased steadily from the original 37.9 wt% to 42.5 wt% in the upper zone of MFT and to 42.9 wt% in the lower zone of MFT. This solids content increase was slightly smaller than the solids content increase in

the MFT of control system. The upper and lower zones of the MFT in System 1 showed similar solids content increase over incubation time.

(iii) Over 1 y of incubation, the solids content of the CT in the CT beneath MFT deposit increased from the original 56.5 wt% to 73.2 wt% in the upper zone of CT and to 73.5 wt% in the lower zone of CT. The overall solids content increase of CT in System 1 was slightly larger than the solids content increase in the control system. The upper and lower zones of the CT in System 1 showed similar solids content increase over incubation time.

(iv) Over 1 y of incubation, the MFT and CT in the CT beneath MFT deposit were rich in methanogens and SRB. The activity of the SRB and methanogens in the MFT and CT resulted in SO_4^{2-} reduction and CH_4 production.

(v) In decreasing the concentrations of Ca^{2+}, Mg^{2+}, SO_4^{2-}, and the electrical conductivity for the cap water of the CT beneath MFT deposit, the simple mixing between the CT water and MFT water played a large role due to the dilution effect between the two waters.

The results indicate that the CT beneath MFT deposition is a beneficial disposal scheme for tailings management.

9.0 Recommendations

9.1 In-situ headspace gas analysis in System 2

In System 2, the in-situ headspace gas analysis was accompanied by regular cap water sampling. The void created by the removed cap water was filled with N_2. This procedure will cause severe air contamination in the column headspace. Therefore, the in-situ headspace gas analysis in System 2 should be used with caution.

To avoid the severe air contamination and increase the reliability of the in-situ headspace gas analysis, it is recommended to set up some extra columns to particularly allow for in-situ headspace gas analysis without accompanying the regular cap water extraction.

9.2 AVS analysis

The results of AVS analysis can tell, with some degree of confidence, the sinks of SO_4^{2-} reduction by SRB. The AVS analysis only used approximately 3 g of MFT or CT samples. Due to the heterogeneous nature and large spatial variation of MFT and CT materials, the AVS results should therefore be used with caution. Further, more AVS data at different incubation times may be desired.

9.3 Trapped gas analysis

The trapped gas analysis in this project was designed for qualitative purpose of detecting mainly the presence or absence of CH_4. However, if a

quantitative analysis is required on the trapped gas in MFT and CT, the MFT and CT samples should be sent to the commercial laboratory with the capacity of quantitative analysis of trapped gas. Also a semi-quantitative analysis of trapped gas may be achieved by calibrating the results of this self-developed method with the results of commercial quantitative method.

9.4 The MFT to CT ratio for the CT beneath MFT deposition

System 1 used MFT to CT ratio of 1:2 (by volume). As discussed above, the dilution effect (P_d %, Table 6-12) played a large role at reducing the concentrations of Ca^{2+}, Mg^{2+}, SO_4^{2-}, and the EC for the cap water in System 1. It is thus expected that the increase in MFT to CT ratio will produce cap water with further lowered concentrations of Ca^{2+}, Mg^{2+}, SO_4^{2-}, and EC values. On the other hand, since the concentrations of Ca^{2+}, Mg^{2+}, SO_4^{2-}, and the EC in the cap water of System 1 have already reached a low level close to that in System 3 (the MFT only system), further substantial increase in MFT to CT ratio will not improve the cap water quality to a further large extent. Therefore, the MFT to CT ratios of 1:2 to 1:1 (by volume) may be a suitable range for the CT beneath MFT deposition.

10.0 References

ACR (Alberta Chamber of Resources), 1995. Canada's oil sands industry: yesterday, today and tomorrow. Prepared by National Task Forces on Oil Sands Strategies of the Alberta Chamber of Resources. Alberta.

AERCB (Alberta Energy Resources Conservation Board), 1984. Oil Sands Bitumen Extraction Process Evaluation, Volume 1, Summaries Phases I and II. Calgary. Alberta.

APHA (American Public Health Association), American Water Works Association, and Water Environment Federation, 1995. Standard Methods for the Examination of Water and Wastewater. 19th edition. Washington. D.C.

AWWA (American Water Works Association), 1999. Water Quality and Treatment, McGraw-Hill, Inc. 5th Edition. New York.

Duan W.M., Coleman M.L., and Pye K., 1997. Determination of Reduced Sulfur Species in Sediments---an Evaluation and Modified Technique. Chemical Geology, **141:**185-194.

Fedorak P.M., Coy D.L., Dudas M.J., Renneberg A.J., and Salloum M.J., 2000. Role of Microbiological Processes on Sulfate-enriched Tailings Deposits. Department of Biological Sciences. University of Alberta. Edmonton. Alberta.

Fedorak P.M., Coy D.L., Salloum M.J., and Dudas M.J., 2002. Methanogenic Potential of Tailings Samples from Oil Sands Extraction Plants. Can. J. Microbiol. **48**: 21-33.

FTFC (Fine Tailings Fundamentals Consortium), 1996. Meeting the Challenge-Solutions for Managing Oil Sands Tailings 1989-1995. Edmonton. Alberta.

FTFC (Fine Tailings Fundamentals Consortium), 1995. Advances in Oil Sands Tailings Research. Alberta Department of Energy. Oil Sands and Research Division. Edmonton. Alberta.

Gerard A. B., Loch J.P.G., Heijdt L.M., and Zwolsman J.J.G., 1998. Vertical Distribution of Acid-Volatile Sulfide and Simultaneously Extracted Metals in a Recent Sedimentation Area of the River Meuse in the Netherlands. Environmental Toxicology and Chemistry, **17:** 758-763.

Gray N.F., 1989. Biology of Wastewater Treatment. Oxford University Press. Oxford. England.

Holowenko F.M., 2000. Methanogenesis and Fine Tailings Waste from Oil Sand Extraction: a Microcosm-based Laboratory Examination. M.S. Thesis. University of Alberta. Edmonton. Alberta.

Hopp V. and Hennig I., 1983. Handbook of Applied Chemistry, Hemisphere Publishing Corporation. New York.

Kasperski K.L., 1992. A Review of Properties and Treatment of Oil Sands Tailings. AOSTRA Journal of Research. **8:** 11-53.

Kennedy G. L., Everett J.W., Dewers T., Pickins W., and Edwards D., 1999. Application of Mineral Iron and Sulfide Analysis to Evaluate Natural Attenuation at Fuel Contaminated Site. Journal of Environmental Engineering. **125**: 47-56.

Lasorsa B. and Casas A., 1996. A Comparison of Sample Handling and Analytical Methods for Determination of Acid Volatile Sulphides in Sediment. Marine Chemistry. **52:** 211-220.

Levett P.N., 1991. Anaerobic Microbiology: a Practical Approach. Oxford University Press. Oxford. England.

List B.R. and Lord E.R.F., 1997. Syncrude's Tailings Management Practices from Research to Implementation. CIM Bulletin. **90** (1010): 39-44.

MacKinnon M.D., 1989. Development of the Tailings Pond at Syncrude's Oil Sands Plant: 1978-1987. AOSTRA Journal of Research, **5**: 109-133

MacKinnon M.D., Matthews J.G., Shaw W.H., and Cuddy R.G., 2000. Water Quality Issue Associated with Implementation of Composite Tailings (CT) Technology for Managing Oil Sands Tailings. Proceedings of SWEMP 2000. Calgary. Alberta.

MacKinnon M. D. and Sethi A., 1993. A Comparison of the Physical and Chemical Properties of the Tailings Ponds at the Syncrude and Suncor Oil Sands Plants. Proceedings of Fine Tailings Symposium: "Oil Sands---Our Petroleum Future". Edmonton. Alberta.

Maier R.M., Ian L.P., and Charles P.G., 2000. Environmental Microbiology. Academic press. San Diego. California.

Matthews J.G., Shaw W.H., MacKinnon M.D., and Cuddy R.G., 2000. Development of Composite Tailings Technology at Syncrude Canada. Proceedings of SWEMP 2000. Calgary. Alberta.

Mikula R.J., Kasperski K.L., Burns R.D., and MacKinnon M.D., 1996. Nature and Fate of Oil Sands Fine Tailings. Advances in Chemistry Series 251. American Chemical Society. Washington. DC.

Morse J. W., Millero F.J., Cornwell J.C., and Rickard D., 1987. The Chemistry of the Hydrogen Sulfide and Iron Sulfide Systems in Natural Waters. Earth-Science Reviews, **24:** 1-42.

Nazaroff W.W. and Alvarez-Cohen L., 2001. Environmental Engineering Science. John Wiley & Sons, Inc. New York.

Postgate J.R., 1984. The Sulphate-Reducing Bacteria. Cambridge University Press. Cambridge.

Sawyer C.N., McCarty P.L., and Parkin G.F., 1994. Chemistry for Environmental Engineering. McGraw-Hill, Inc. 4th edition. New York.

Schlesinger H.W., 1997. Biogeochemistry---an analysis of global change. 2nd edition. Academic Press. San Diego. California.

Shaw B., Cuddy G., MacKinnon M., Dawson R., and Kwan K., 2001. Composite Tailings beneath Mature Fine Tailings Deposit: Summary of Laboratory and Field Work 1995 through 2000. Syncrude Canada Ltd. Report.

Shaw B., Cuddy G., McKenna G., and MacKinnon M., 1996. Non-segregating Tailings: 1995 NST Field Demonstration. Syncrude Canada Ltd. Report.

Snoeyink V.L. and Jenkins D., 1980. Water Chemistry. John Wiley & Sons, Inc. New York.

Syncrude Canada Ltd., 2000a. Syncrude Fact Book. Fort McMurray. Alberta.

Syncrude Canada Ltd., 2000b. Securing Canada's Energy Future. Fort McMurray. Alberta.

Tang J., 1997. Fundamental Behaviour of Composite Tailings. M.Sc. Thesis. University of Alberta. Edmonton. Alberta.

VCI (Varian Chrompack International), 1999. User Manual Micro-GC Portable Model CP-2003P. Walnut Creek. California.

Xiaomei L. and Yongsheng F., 1995. Dewatering Fine Tails by Evaporation: a Mathematical Modeling Approach. Report to Syncrude Canada Ltd., Edmonton Research Centre. Edmonton. Alberta.

Appendices

Appendix A. Methods and materials

Table A-1. GC external calibrations (using the GC parameters at Table 4-2).

Gas/GC channel/ Date	t_R (min)	Calibration concentration at each level (vol%)				Calibration curve (linear)	r^2
		Level 1	Level 2	Level 3	Level 4		
O_2/A/27 June-02	0.53	30.0	15.0	5.0	1.0	Y=3.67(e+004) x	0.9998
N_2/A/18 June-02	0.56	100.0	75.0	50.0	25.0	Y=3.63(e+004) x	0.9999
CH_4/A/03 July-02	0.81	80.0	50.0	20.0	1.0	Y=3.58(e+004) x	0.9989
CO_2/B/24 June-02	0.44	20.0	10.0	5.0	1.0	Y=1.81(e+005) x	0.9986
C_2H_4/B/17 Sep.-02	0.55	10.0	5.0	2.0	0.1	Y=1.95(e+005) x	0.9991
H_2S/B/31 Oct.-02	1.30	5.0	3.0	1.0		Y=1.73(e+005) x	0.9934

1). t_R=retention time.
2). r^2=the determination coefficient.
3). Y=the area accounts, and x is the gas concentration (vol%).
4). For H_2S, only three-level calibration was used.

Table A-2. GC verifications (using the GC parameters at Table 4-2).

Date	S/M	Concentration (vol%)/GC channel					
		N_2/A	O_2/A	CH_4/A	CO_2/B	H_2S/B	C_2H_4/B
21 July-02	S	1.01	0.502	0.501	0.504		
	M	2.19	0.849	0.495	0.851		
		0.941	0.538	0.509	0.720		
		0.940	0.539	0.521	0.863		
21 July-02	S	100					
	M	98.7					
		99.9					
		100					
21 July-02	S			100			
	M			103			
				105			
				105			
29 July-02	S		100				
	M		90.2				
			94.0				
			93.4				
19 Sep.-02	S						100
	M						92.0
							98.6
							98.2
21 July-02	S				100		
	M				103		
					103		
					103		
21 July-02	S	54.0	4.01	20	20		
	M	56.9	4.50	18.3	21.4		
		56.6	4.11	18.8	21.7		
		56.6	4.10	18.8	21.4		
7 April-03	S	54.0	4.01	20	20		
	M	58.9	5.10	18.0	19.7		
		58.7	4.89	18.3	19.8		
		58.7	4.92	18.2	20.5		
29 July-02	S			45.1	54.9		
	M			43.2	47.1		
				43.7	47.6		
				43.8	47.5		

1). S=standard concentration.

2). M=measured concentration of standard gas, with triplicate analyses.

Table A-3. The column notations.

System	Number of columns	Column notation
1 (Cap water/MFT/CT)	20	C1-1, ... C1-20
2 (Cap water/MFT/CT)	6	C2-1, ...C2-6
3 (Cap water/MFT)	12	C3-1, ...C3-12
4 (Cap water/CT)	12	C4-1, ...C4-12

Table A-4. The notations for samples in Systems 1, 3, and 4 (using System 1 as illustration).

Sample type		Sample notation
Tedlar bag gas		"C1-1-TGas", ... "C1-20-TGas"
Cap water		"C1-1-CapW", ... "C1-20-CapW"
MFT	For MPN samples	"C1-1-MFT-U, C1-1-MFT-L", ... "C1-20-MFT-U, C1-20-MFT-L"
	For other samples	"C1-1-MFT-U, C1-1-MFT-L", ..."C1-20-MFT-U, C1-20-MFT-L"
CT	For MPN samples	"C1-1-CT-M", ..."C1-20-CT-M"
	For other samples	"C1-1-CT-U, C1-1-CT-L", ... "C1-20-CT-U, C1-20-CT-L"

1). In case of more than one time Tedlar bag samplings from the same column, using suffix (1), (2), ... to indicate the sequence of samplings from the same column. For example, "C1-1-TGas (1)", "C1-1-TGas (2)", "C1-1-TGas (3)",....

2). MFT-U and MFT-L are the upper and lower half zones of MFT in the MFT layer; while CT-U and CT-L are the upper and lower half zones of CT in the CT layer.

3). "M" means the CT sample for MPN analysis is taken from the middle of the CT layer.

Table A-5. The notations for samples in System 2.

Sample type	Sample notation
Regular in-situ headspace gas analysis	"C2-1-OnGas (1), C2-1-OnGas (2), C2-1-OnGas (3), ...", ... "C2-6-OnGas (1), C2-6-OnGas (2), C2-6-OnGas (3), ..."
Regular in-situ cap water sampling	"C2-1-CapW (1), C2-1- CapW (2), C2-1- CapW (3), ...", ... "C2-6- CapW (1), C2-6- CapW (2), C2-6- CapW (3), ..."
MFT at column sacrificing	"C2-1-MFT-U, C2-1-MFT-L", ... "C2-6-MFT-U, C2-6-MFT-L"
CT at column sacrificing	"C2-1-CT-U, C2-1-CT-L", ..."C2-6-CT-U, C2-6-CT-L"

1). The suffix (1), (2), (3), ... means the sequence of sampling times for the same column.
2). MFT-U and MFT-L are the upper and lower half zones of MFT in the MFT layer; while CT-U and CT-L are the upper and lower half zones of CT in the CT layer.

Table A-6. Column fillings and incubation starting times in Systems 1, 3, and 4.

System	Column	Time of filling with MFT	Time of filling with CT
1 (Cap water/MFT/CT)	C1-1	From 2.0 pm to 3.0 pm, 4 Nov.-02	11.30 am, 5 Nov.-02
	C1-2		12.0 noon
	C1-3		12.0 noon
	C1-4		12.30 pm
	C1-5		12.30 pm
	C1-6		1.30 pm
	C1-8		2.0 pm
	C1-9		2.30 pm
	C1-10		2.30 pm
	C1-11		2.45 pm
	C1-12		3.30 pm
	C1-13		4.0 pm
	C1-14		4.0 pm
	C1-15		4.30 pm
	C1-16		4.30 pm
	C1-17		5.0 pm
	C1-18		5.0 pm
	C1-19		5.30 pm
	C1-20		6.0 pm, on 5 Nov.-02
3 (Cap water/MFT)	C3-1, ...C3-12	4.30 pm, 6 Nov.-02	
4 (Cap water/CT)	C4-1, ...C4-12		3.30 pm, 6 Nov.-02

1). For Systems 1 and 4, the time of filling with CT is regarded as the column setup and incubation starting time.
2). For Systems 3, the time of filling with MFT is regarded as the column setup and incubation starting time.
3). Column C1-7 was broken and discarded at column filling.

Table A-7. Column filling and incubation starting time in System 2.

System	Column	Time of filling with MFT	Time of filling with CT
2 (Cap water/MFT/CT)	C2-1	11.0 am, 9 Dec.-02	11.30 am, 10 Dec.-02
	C2-2		11.30 am
	C2-3		11.30 am
	C2-4		2.0 pm
	C2-5		2.0 pm
	C2-6		2.30 pm, 10 Dec.-02

1). The time of filling with CT is regarded as the column setup and incubation starting time.

Appendix B. Results

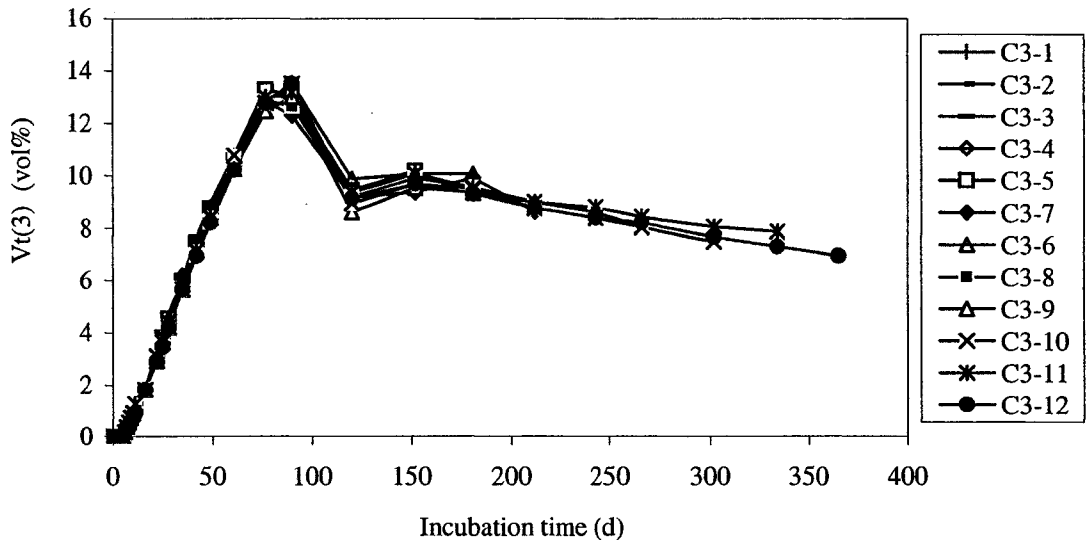

Figure B-1. Total volume changes (Vt) in System 3.

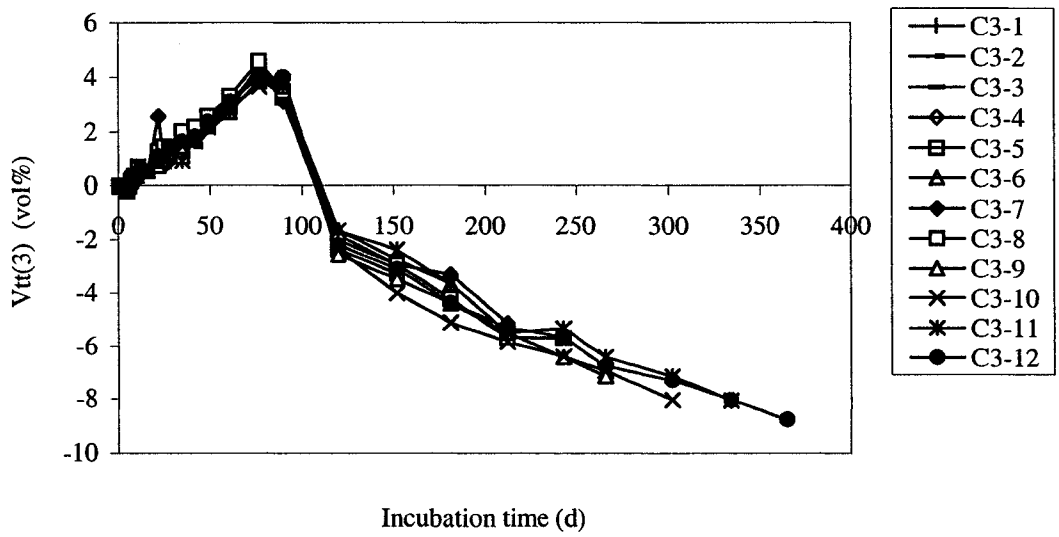

Figure B-2. Total tailings volume changes (Vtt) in System 3.

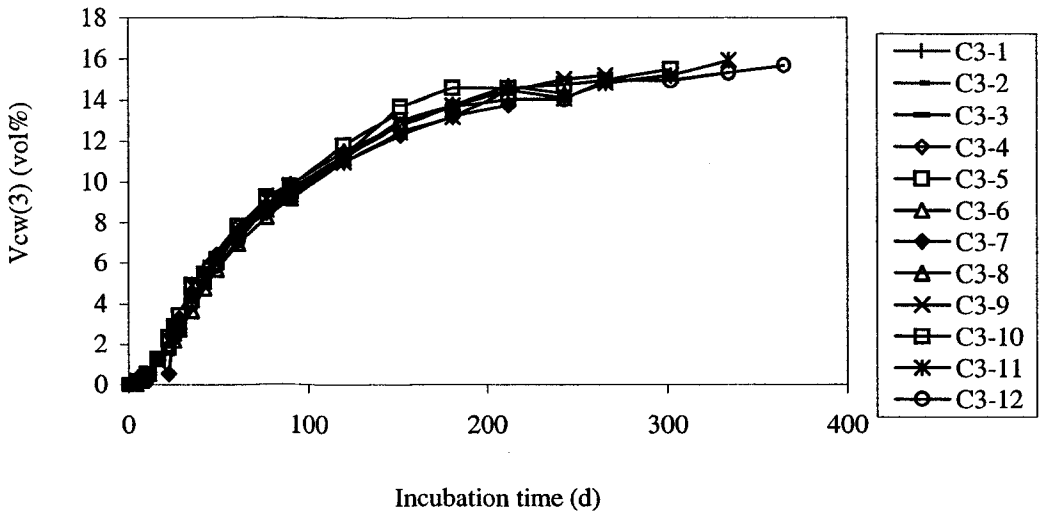

Figure B-3. Cap water volumes (Vcw) in System 3.

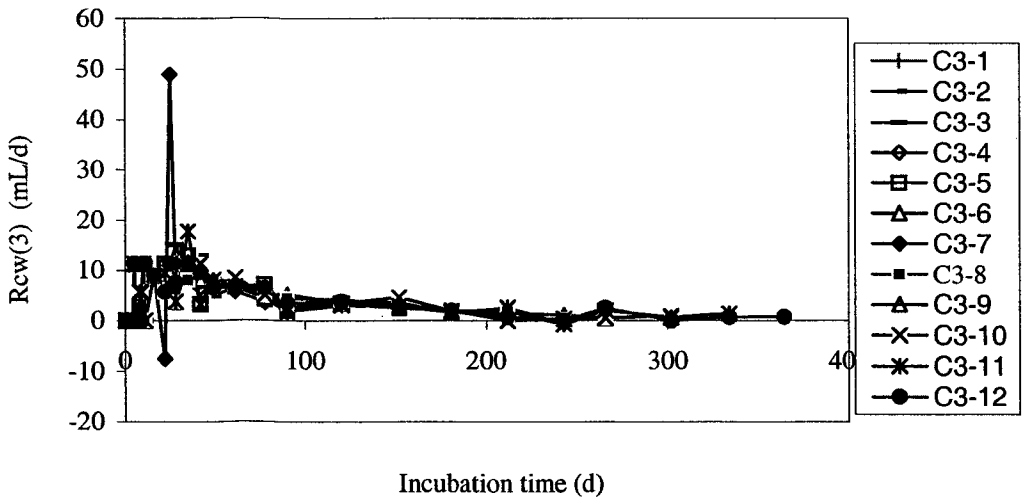

Figure B-4. Cap water producing rates (Rcw) in System 3.

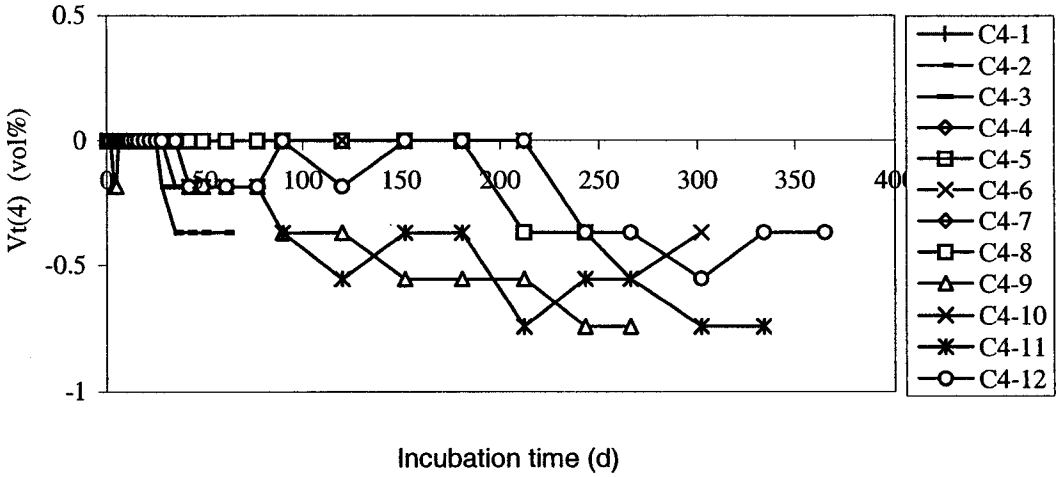

Figure B-5. Total volume changes (Vt) in System 4.

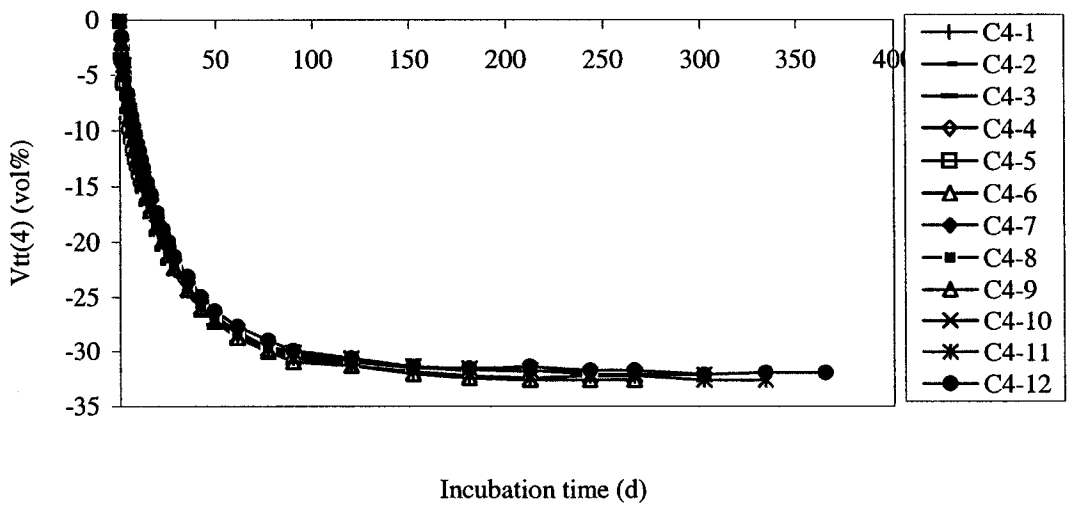

Figure B-6. Total tailings volume changes (Vtt) in System 4.

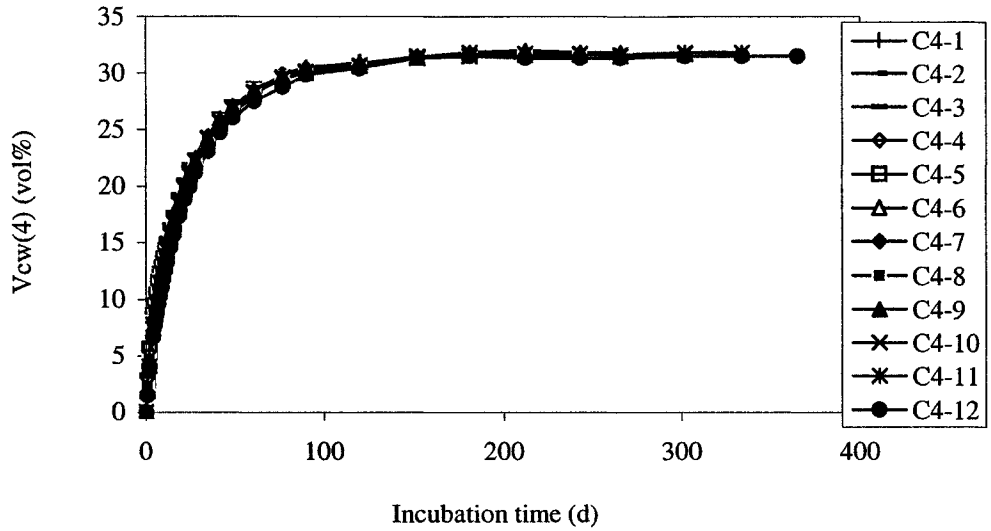

Figure B-7. Cap water volumes (Vcw) in System 4.

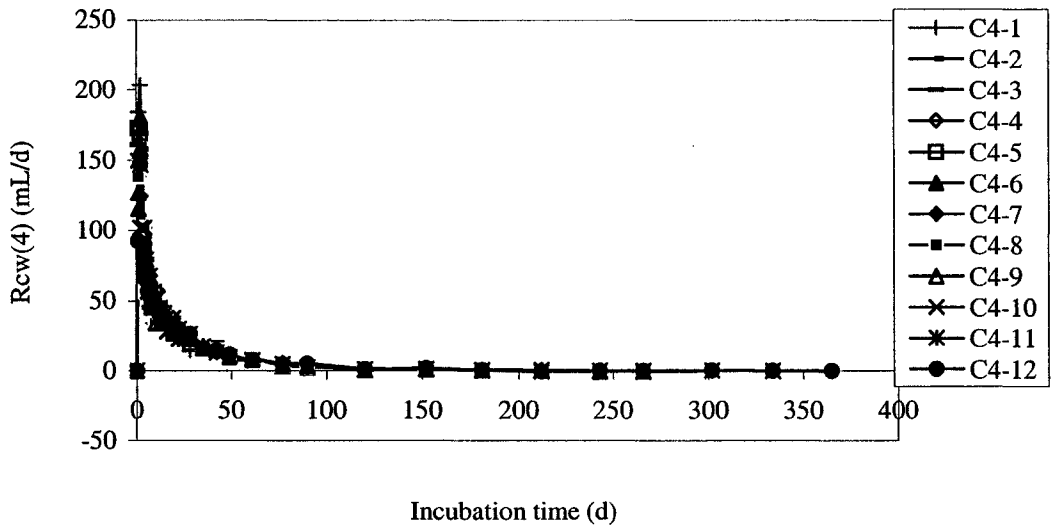

Figure B-8. Cap water producing rates (Rcw) in System 4.

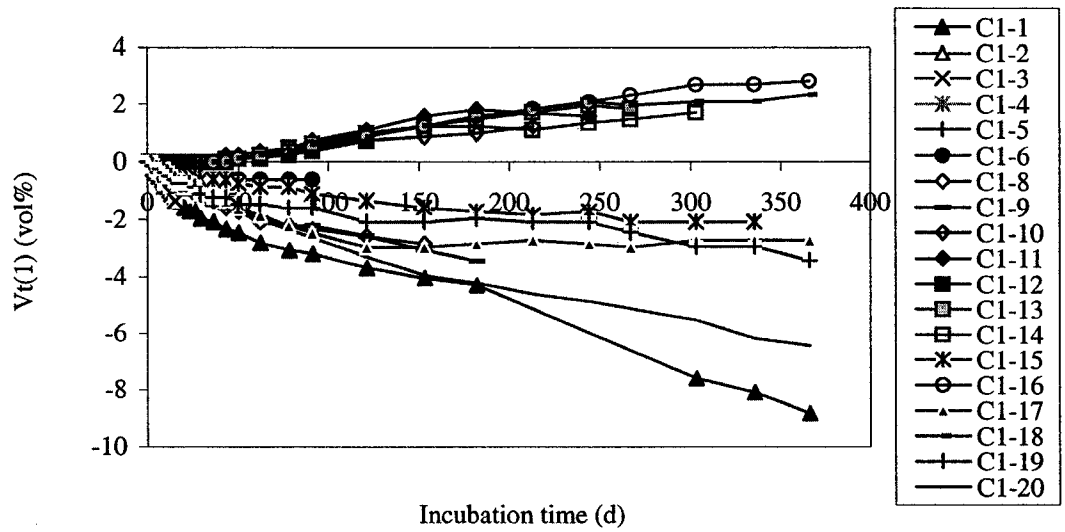

Figure B-9. Total volume changes (Vt) in System 1.

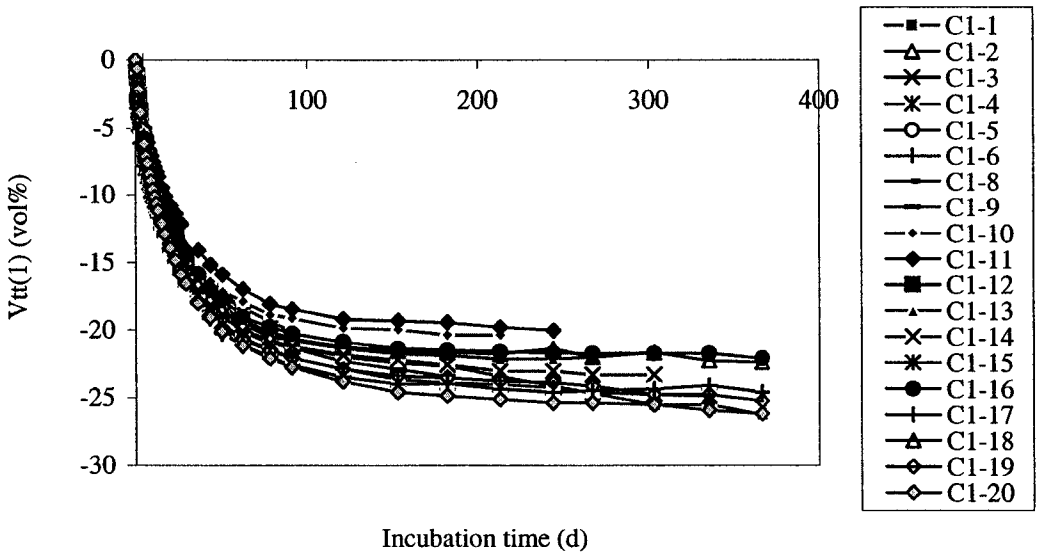

Figure B-10. Total tailings volume changes (Vtt) in System 1.

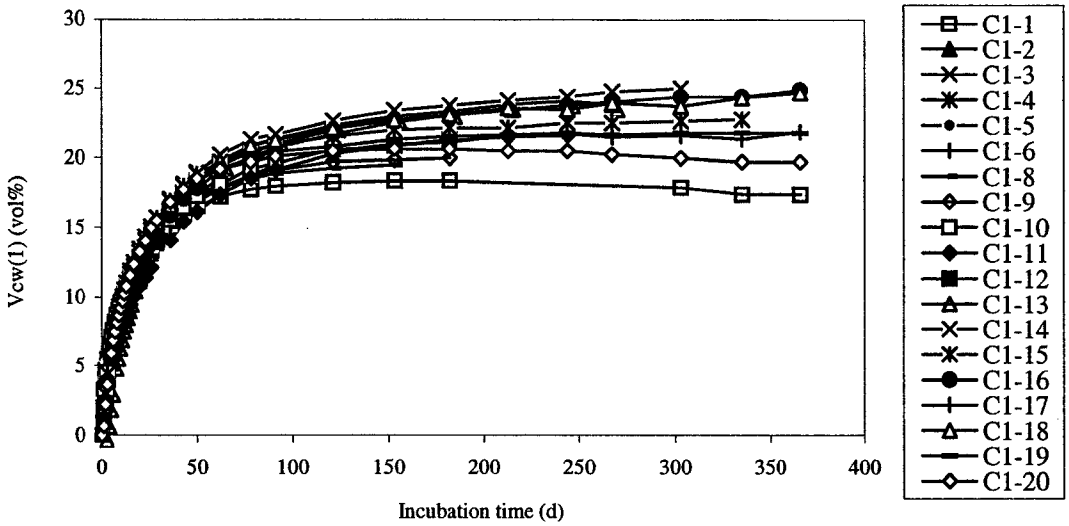

Figure B-11. Cap water volumes (Vcw) in System 1.

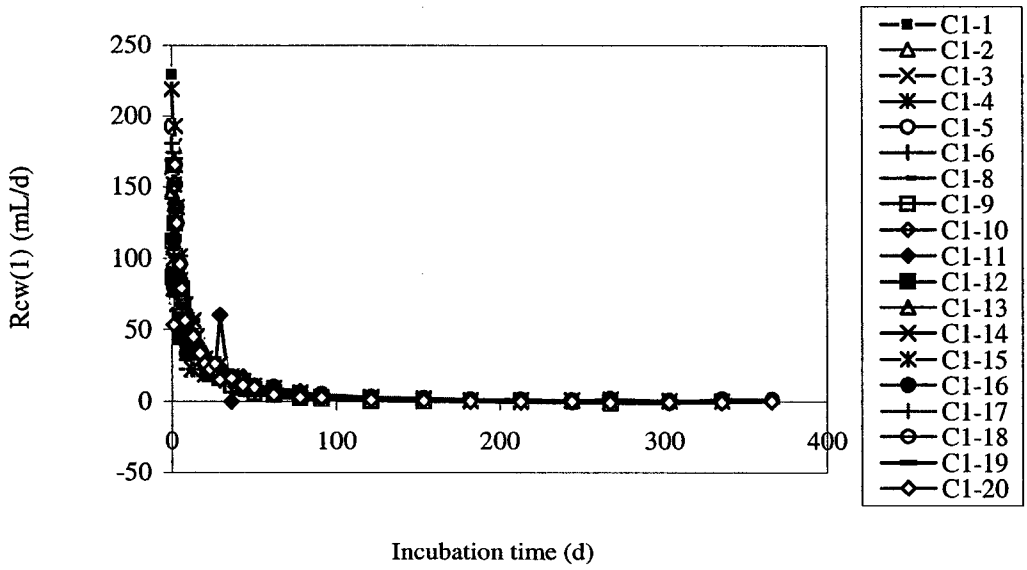

Figure B-12. Cap water producing rates (Rcw) in System 1.

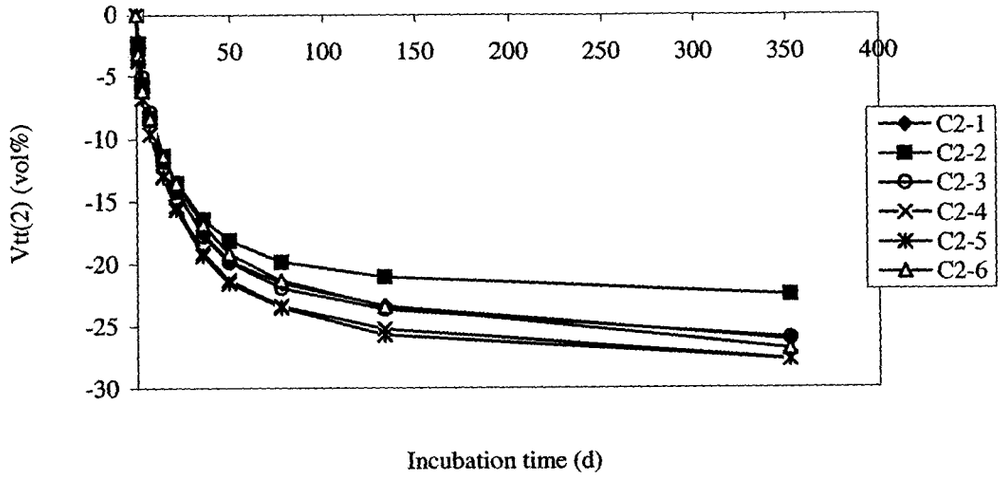

Figure B-13. Total tailings volume changes (Vtt) in System 2.

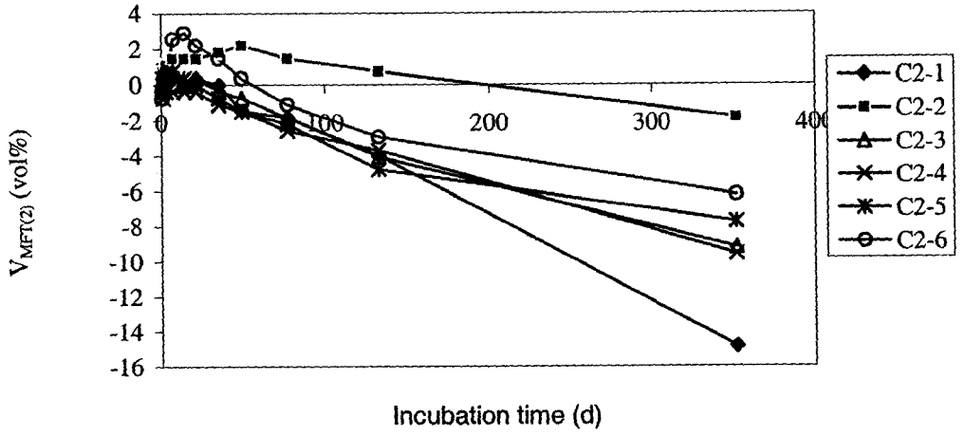

Figure B-14. Individual MFT tailings volume changes (V_{MFT}) in System 2.

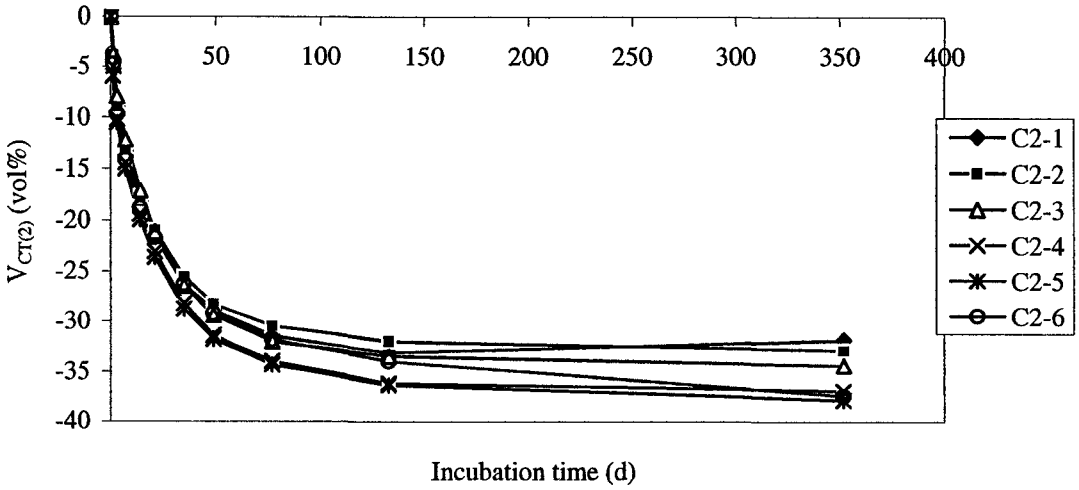

Figure B-15. Individual CT tailings volume changes (V_{CT}) in System 2.

Table B-1. Absolute heights of cap water and MFT in System 3 over 1 y of incubation.

Column	t_{incu} (d)	Height of MFT at time 0 (cm)	Height of cap water at column sacrificing (cm)	Height of MFT at column sacrificing (cm)
C3-1	28	54.5	1.7	55.2
C3-2	61	54.7	4.3	56.2
C3-3	90	54.7	5.1	56.7
C3-4	120	54.9	6.2	53.8
C3-5	152	55.0	7.4	53.2
C3-6	181	54.7	7.5	52.7
C3-7	212	54.5	7.5	51.7
C3-8	243	54.5	7.8	51.4
C3-9	266	54.6	8.3	50.7
C3-10	302	54.8	8.5	50.4
C3-11	334	54.6	8.7	50.2
C3-12	365	54.8	8.6	50.0

Table B-2. Absolute heights of cap water and CT in System 4 over 1 y of incubation.

Column	t_{incu} (d)	Height of CT at time 0 (cm)	Height of cap water at column sacrificing (cm)	Height of CT at column sacrificing (cm)
C4-1	28	54.3	12.2	42.1
C4-2	61	54.2	15.1	38.9
C4-3	90	54.1	16.5	37.6
C4-4	120	54.2	16.8	37.4
C4-5	152	54.2	17.0	37.2
C4-6	181	53.8	17.1	36.7
C4-7	212	54.0	17.2	36.8
C4-8	243	54.1	17.0	36.9
C4-9	266	54.0	17.2	36.4
C4-10	302	54.2	17.2	36.8
C4-11	334	54.0	17.2	36.4
C4-12	365	54.2	17.1	36.9

Table B-3. Absolute heights of cap water, MFT, and CT in System 1 over 1 y of incubation.

		Heights at time 0 (cm)		Heights at column sacrificing (cm)		
Column	t_{incu} (d)	MFT	CT	Cap water	MFT	CT
C1-2	3	27.3	54.6	3.8	27.4	50.6
C1-3	15	26.7	54.4	8.5	27.6	43.9
C1-4	29	27.3	54.2	12.1	27.4	41.5
C1-5	62	27.1	54.2	15.1	28.3	38.1
C1-6	91	27.0	54.6	15.9	26.8	38.4
C1-12	121	26.9	54.1	17.8	26.3	37.5
C1-8	153	27.0	54.0	15.8	26.8	36.1
C1-9	182	27.0	54.6	16.3	25.7	36.8
C1-10	213	27.1	54.5	17.6	28.0	37.0
C1-11	244	27.4	55.0	17.8	27.4	38.5
C1-13	267	27.1	54.3	19.4	26.9	36.6
C1-14	303	27.1	NA	20.4	NA	NA
C1-15	335	27.2	54.5	18.6	25.9	35.5
C1-16	366	27.2	54.8	20.4	27.6	36.3

1). NA=not available.

Table B-4. Tedlar bag gas analyses for the major sacrificed columns in Systems 1, 3, and 4.

Sample	t_{incu} (d)	Tedlar bag gas volume (mL)	GC analysis (vol%)				
			CH_4	N_2	O_2	CO_2	Other gases
System 1 (Cap water/MFT/CT)							
C1-4-TGas	29	45	0.044	77.8	20.7	0.636	H_2S=0.605
C1-5-TGas	62	25	0.476	80.4	18.1	1.29	
C1-6-TGas	91	20	3.66	89.4	4.58	5.23	
C1-12-TGas	121	25	2.93	89.9	5.22	4.03	
C1-8-TGas	153	15	0.132	78.4	20.0	2.10	C_2H_4=0.300; H_2S=0.429
C1-9-TGas	182	12	4.05	92.9	3.06	7.82	H_2S=0.010
C1-10-TGas	213	20	4.57	90.5	4.45	3.88	
C1-11-TGas	244	10	0.662	80.7	17.0	1.96	H_2S=1.25
C1-13-TGas	267	47	0.168	78.5	19.1	1.78	
C1-14-TGas	304	17	0.858	84.5	11.9	4.50	
C1-15-TGas	335	60	0.049	78.8	20.5	0.501	
C1-16-TGas	366	45	0.033	82.4	22.0	0.241	
System 3 (Cap water/MFT)							
C3-1-TGas	28	325	0.393	95.4	3.19	1.43	
C3-2-TGas	61	430	0.443	85.0	13.5	1.77	
C3-3-TGas	90	350	4.72	87.5	6.36	3.06	
C3-4-TGas (1)	90	1020	3.65	93.0	1.69	3.60	
C3-4-TGas (2)	120	400	11.6	79.4	8.00	3.76	
C3-5-TGas	152	45	0.336	77.8	20.8	0.348	C_2H_4=0.115; H_2S=0.932
C3-6-TGas	181	440	20.9	74.3	3.88	5.29	
C3-7-TGas	212	485	20.7	70.60	6.82	5.880	
C3-8-TGas	243	20	0.846	77.0	20.3	0.818	C_2H_4=0.137; H_2S=0.058
C3-9-TGas	266	74	0.557	77.4	20.5	0.559	
C3-10-TGas	303	460	18.0	69.4	10.2	5.45	
C3-11-TGas (1)	90	1030	3.53	93.1	1.59	3.47	
C3-11-TGas (2)	334	1000	34.0	61.3	2.08	6.82	
C3-12-TGas	365	171	7.09	75.3	17.3	3.63	

Table B-4. (*continued*).

Sample	t_{incu} (d)	Tedlar bag gas volume (mL)	GC analysis (vol%)				
			CH_4	N_2	O_2	CO_2	Other gases
System 4 (Cap water/CT)							
C4-1-TGas	28	80	0.040	93.7	5.54	0.885	
C4-2-TGas	61	30	0.061	91.3	8.76	0.646	C_2H_4=0.009 H_2S=0.216
C4-3-TGas	90	60	0.085	95.0	4.76	1.41	
C4-4-TGas	120	40	nd	80.5	17.4	1.85	
C4-5-TGas	152	180	0.109	93.3	4.28	2.65	H_2S=0.440
C4-6-TGas	181	30	0.053	85.7	12.2	4.42	
C4-7-TGas	212	17	0.291	83.0	15.5	0.971	C_2H_4=0.170; H_2S=0.138
C4-8-TGas	243	30	0.129	95.4	3.30	1.19	
C4-9-TGas	266	42	nd	77.8	20.9	0.141	
C4-10-TGas	303	84	0.140	94.7	3.00	3.26	
C4-11-TGas	334	155	0.044	80.0	17.2	2.74	
C4-12-TGas	365	308	0.071	83.4	15.7	2.81	

1). nd=non-detectable.

Table B-5. The regular in-situ headspace gas analyses for the columns in System 2.

Sample	t_{incu} (d)	GC analysis (vol%)				
		CH_4	N_2	O_2	CO_2	Other gases
C2-1-OnGas (1)	1	0.045	83.3	16.3	0.347	C_2H_4=0.092
C2-2-OnGas (1)	1	0.070	83.5	15.8	0.658	C_2H_4=0.278
C2-3-OnGas (1)	1	0.077	85.3	14.1	0.553	C_2H_4=0.024
C2-4-OnGas (1)	1	0.044	82.3	16.8	0.399	C_2H_4=0.007
C2-5-OnGas (1)	1	0.1005	86.2	13.0	0.526	C_2H_4=0.236
C2-6-OnGas (1)	1	0.120	87.4	11.7	0.010	C_2H_4=0.012
C2-1-OnGas (2)	3	0.145	99.0	13.4	0.805	
C2-2-OnGas (2)	3	0.098	82.6	17.3	0.011	C_2H_4=0.020
C2-3-OnGas (2)	3	0.130	85.8	14.0	0.006	C_2H_4=0.072
C2-4-OnGas (2)	3	0.146	86.3	13.2	0.743	C_2H_4=0.013
C2-5-OnGas (2)	3	0.100	84.9	14.7	0.563	C_2H_4=0.016
C2-6-OnGas (2)	3	0.145	87.2	12.1	0.770	C_2H_4=0.022
C2-1-OnGas (3)	7	0.186	83.6	17.8	1.060	H_2S=0.612
C2-2-OnGas (3)	7	0.095	79.7	20.7	0.699	C_2H_4=0.036
C2-3-OnGas (3)	7	0.203	83.1	16.8	0.936	
C2-4-OnGas (3)	7	0.234	83.7	15.9	1.06	C_2H_4=0.012
C2-5-OnGas (3)	7	0.130	81.3	18.3	0.761	
C2-6-OnGas (3)	7	0.031	79.3	20.6	0.577	C_2H_4=0.031
C2-1-OnGas (4)	14	0.298	83.2	18.5	1.71	H_2S=0.006
C2-2-OnGas (4)	14	0.109	78.9	20.8	0.860	
C2-3-OnGas (4)	14	0.382	81.9	16.6	1.80	
C2-4-OnGas (4)	14	0.370	81.8	16.3	1.87	
C2-5-OnGas (4)	14	0.304	80.6	17.7	1.57	
C2-6-OnGas (4)	14	0.573	83.0	14.7	2.03	
C2-1-OnGas (5)	21	0.129	87.5	14.2	1.75	
C2-2-OnGas (5)	21	0.072	80.3	19.7	0.647	
C2-3-OnGas (5)	21	0.166	87.8	11.7	1.12	
C2-4-OnGas (5)	21	0.165	88.8	10.5	1.13	
C2-5-OnGas (5)	21	0.142	86.1	12.9	0.963	
C2-6-OnGas (5)	21	0.263	89.4	9.58	1.23	

Table B-5. *(continued).*

Sample	t_{incu} (d)	Gas GC analysis (vol%)				
		CH_4	N_2	O_2	CO_2	Other gases
C2-1-OnGas (6)	35	0.151	80.1	19.2	2.40	
C2-2-OnGas (6)	35	0.054	77.8	20.7	0.625	C_2H_4=0.033
C2-3-OnGas (6)	35	0.219	80.9	17.3	1.52	C_2H_4=0.010
C2-4-OnGas (6)	35	0.236	81.4	16.3	1.79	
C2-5-OnGas (6)	35	0.181	80.0	18.0	1.29	
C2-6-OnGas (6)	35	0.365	82.8	15.0	1.77	
C2-1-OnGas (7)	49	0.107	79.5	19.8	1.09	
C2-2-OnGas (7)	49	0.045	78.1	20.6	0.621	C_2H_4=0.110
C2-3-OnGas (7)	49	0.195	80.8	18.9	1.90	H_2S=0.009
C2-4-OnGas (7)	49	0.218	79.8	17.8	1.68	
C2-5-OnGas (7)	49	0.147	79.0	18.9	1.31	C_2H_4=0.0079
C2-6-OnGas (7)	49	0.338	80.9	16.7	1.85	H_2S=0.021
C2-1-OnGas (8)	77	0.068	79.2	20.2	1.15	
C2-2-OnGas (8)	77	0.038	78.2	20.8	0.763	C_2H_4=0.093 H_2S=0.057
C2-3-OnGas (8)	77	0.137	78.6	19.4	1.53	
C2-4-OnGas (8)	77	0.158	78.9	18.9	1.67	
C2-5-OnGas (8)	77	0.075	78.5	19.6	1.26	
C2-6-OnGas (8)	77	0.254	79.7	18.0	1.72	
C2-1-OnGas (9)	133	0.047	81.9	20.9	1.19	C_2H_4=0.203
C2-2-OnGas (9)	133	0.030	79.4	21.0	0.685	C_2H_4=0.086; H_2S=0.070.
C2-3-OnGas (9)	133	0.095	79.2	19.5	1.688	
C2-4-OnGas (9)	133	0.100	79.0	19.1	1.84	
C2-5-OnGas (9)	133	0.061	78.8	19.7	1.30	
C2-6-OnGas (9)	133	0.156	79.6	18.1	2.29	
C2-1-OnGas (10)	352	nd	77.2	20.8	0.149	
C2-4-OnGas (10)	352	nd	76.9	20.6	0.275	
C2-6-OnGas (10)	352	0.047	77.4	19.4	1.19	

1). nd=non-detectable.

Table B-6. Physical and chemical analyses in baseline MFT and CT.

		WATER PROPERTIES																	
				(mg/L)			Main Ions (mg/L)								Minor Elements (mg/L)				
Sample	t_{incu} (d)	pH	EC (uS/cm)	Br^-	$N(NH_4^+)$	S^{2-}	Na^+	K^+	Mg^{2+}	Ca^{2+}	F^-	Cl^-	SO_4^{2-}	HCO_3^-	Al	B	Ba	Fe	Si	Sr
Base MFT 1	0	7.96	4430	BDL	9	BDL	1030	16	15.5	22.4	BDL	860	BDL	1491	BDL	3.9	0.58	BDL	4.9	0.953
Base MFT 2	0	7.96	4460	BDL	10.4	BDL	1020	17	15.7	23.1	BDL	890	13.9	1522	BDL	4	0.6	BDL	5.08	0.973
Base MFT 3	0	7.9	4600	BDL	10.1	BDL	1030	15.6	16.2	23.8	BDL	850	22.6	1350	BDL	3.50	0.61	BDL	4.68	0.96
Base CT 1	0	8.22	5770	270	7.5	0.4	1240	19	24.8	68.7	BDL	1000	724	739	BDL	3	0.2	BDL	3.87	1.48
Base CT 2	0	8.17	6120	260	7.9	4	1310	20	26.4	76	BDL	1100	897	806	BDL	3.1	0.13	BDL	3.91	1.61
Base CT 3	0	8.08	6260	260	8.4	10	1400	20	29.5	82	BDL	1000	1100	731	BDL	2.9	0.2	BDL	3.9	1.81
Base CT 4	0	8.0	6350	300	8.4	3	1370	19.0	27.7	77.7	BDL	1100	1070	674	BDL	2.60	0.09	BDL	3.50	1.58
Base CT 5	0	8.1	6770	280	9.0	3	1470	19.2	29.9	98.6	BDL	1100	1350	642	BDL	2.55	0.05	BDL	3.29	1.75
Base CT 6	0	8.0	7900	280	7.9	3	1810	20.9	33.9	114.0	46.0	1100	1660	1160	BDL	2.69	0.08	BDL	3.47	2.06

Table B-6. *(continued).*

Sample	t_{incu} (d)	SOLIDS PROPERTIES									
		Solids content (g/100g)	Oil content (g/100g)	Eh (mV)	AVS (mg/kg of dry sample)	Particle Size Distribution (% of solids less than)					
						44 um	22 um	11 um	5.5 um	2.8 um	1.0 um
Base MFT 1	0	37.92	3.2	-9	73.6	99.8	95	80	57.4	36.2	12.7
Base MFT 2	0	38.03	2.94	2	NA	92	78.9	62.3	44.7	28.3	9.94
Base MFT 3	0	38.63	3.47	-3	NA	86.3	73.4	57.4	41.1	26.3	9.73
Base CT 1	0	57.19	0.81	-202	NA	NA	NA	NA	NA	NA	NA
Base CT 2	0	56.49	0.76	-202	80	34.3	29.3	23.8	16.8	9.73	3.26
Base CT 3	0	56.58	1.13	-196	NA	38.2	31.9	25.2	17.8	10.6	3.59
Base CT 4	0	59.02	1.27	-188	NA	34.2	27.9	21.3	15.0	9.90	4.19
Base CT 5	0	55.65	1.17	-169	NA	37.7	30.9	23.7	16.7	10.90	4.53
Base CT 6	0	54.27	1.2	-172	NA	34.4	28.0	21.5	15.2	10.00	4.21

1). NA=not available.
2). BDL=below detection limits.

Table B-7. Physical and chemical analyses in System 3 .

		WATER PROPERTIES																		
				(mg/L)			Main Ions (mg/L)								Minor Elements (mg/L)					
Sample	t_{incu} (d)	pH	EC (uS/cm)	Br^-	$N(NH_4^+)$	S^{2-}	Na^+	K^+	Mg^{2+}	Ca^{2+}	F^-	Cl^-	SO_4^{2-}	HCO_3^-	Al	B	Ba	Fe	Si	Sr
C3-1-CapW	28	8.2	4420	BDL	NA	BDL	950	15	13.2	19	BDL	1700	11.9	1491	BDL	3.5	0.4	BDL	4.06	0.79
C3-1-MFT-U	28	8.3	4280	BDL	8.7	BDL	939	15	12.8	17	BDL	840	17.3	1430	BDL	1.2	0.8	BDL	3.39	0.73
C3-1-MFT-L	28	8.1	4350	BDL	9.4	BDL	915	14	12.6	16	BDL	850	22.2	1388	BDL	0.9	0.4	BDL	3.06	0.71
C3-2-CapW	61	7.9	4540	BDL	8.8	BDL	1000	15	15.3	22	BDL	900	18.9	NA	BDL	2.7	0.5	BDL	5.12	0.93
C3-2-MFT-U	61	8.1	4300	BDL	9.5	BDL	941	14	11.8	16	BDL	830	9.36	1423	BDL	3	0.4	BDL	3.94	0.7
C3-2-MFT-L	61	8.2	4300	BDL	9.5	BDL	972	15	12.6	17	BDL	830	BDL	1429	BDL	3.1	0.4	BDL	4.28	0.76
C3-3-CapW	90	7.8	4340	BDL	9.0	BDL	906	14	14.4	20	BDL	850	BDL	1525	BDL	3.7	0.4	BDL	5.03	0.9
C3-3-MFT-U	90	8.1	4340	BDL	9.3	BDL	940	15	12.3	17	BDL	840	BDL	1490	BDL	3	0.4	BDL	3.77	0.74
C3-3-MFT-L	90	8	4310	BDL	9.3	BDL	943	15	11.8	16	BDL	840	BDL	1426	BDL	2.9	0.4	BDL	3.55	0.71
C3-4-CapW	120	7.8	4530	BDL	9.1	BDL	977	14	14.8	21	BDL	860	BDL	1547	BDL	3.9	0.4	BDL	5.26	0.91
C3-4-MFT-U	120	7.8	4390	BDL	9.1	BDL	971	14	13.8	19	6.1	830	BDL	1500	BDL	2.9	0.4	BDL	4.09	0.82
C3-4-MFT-L	120	7.8	4370	BDL	9.5	BDL	998	14	14.3	19	5.9	850	BDL	1497	BDL	2.9	0.4	BDL	4.11	0.84
C3-5-CapW	152	NA	NA	NA	NA	BDL	NA	NA	NA	NA	NA	NA	NA	NA	NA	NA	NA	NA	NA	NA
C3-5-MFT-U	152	7.9	4120	BDL	8.7	BDL	881	13	12.6	18	BDL	820	4.68	1514	BDL	2.8	0.4	BDL	4.04	0.76
C3-5-MFT-L	152	8.1	3900	BDL	8.6	BDL	820	13	11.2	16	BDL	740	4.46	1446	BDL	2.7	0.4	BDL	3.69	0.67
C3-6-CapW	181	7.7	4460	BDL	9.7	BDL	1020	15	15.7	23	BDL	840	BDL	1482	BDL	4	0.4	BDL	5.64	0.99
C3-6-MFT-U	181	7.9	4370	BDL		BDL	980	16	13.7	20	BDL	850	BDL	1540	BDL	3.3	0.4	BDL	4.55	0.86
C3-6-MFT-L	181	7.9	4340	BDL		BDL	1040	17	14.6	21	BDL	800	BDL	1530	BDL	3.1	0.5	BDL	4.46	0.91

Table B-7. *(continued).*

Sample	t_{incu} (d)	WATER PROPERTIES																		
				(mg/L)			Main Ions (mg/L)								Minor Elements (mg/L)					
		pH	EC (uS/cm)	Br^-	$N(NH_4^+)$	S^{2-}	Na^+	K^+	Mg^{2+}	Ca^{2+}	F^-	Cl^-	SO_4^{2-}	HCO_3^-	Al	B	Ba	Fe	Si	Sr
C3-7-CapW	212	7.7	4520	BDL	11.7	BDL	1150	16	16	24	BDL	840	BDL	1580	BDL	4.5	0.5	BDL	5.92	1.03
C3-7-MFT-U	212	7.9	4320	BDL	11.3	BDL	1130	15	13	17	BDL	840	BDL	1390	BDL	3.3	0.4	BDL	4.21	0.78
C3-7-MFT-L	212	8	4220	BDL	11.1	BDL	1100	14	13	17	BDL	830	BDL	1390	BDL	3	0.4	BDL	3.96	0.76
C3-8-CapW	243	8.1	4520	BDL	9.2	BDL	1130	15	15	21	BDL	800	BDL	1550	BDL	4.1	0.5	BDL	4.85	0.96
C3-8-MFT-U	243	7.7	4350	BDL	9.7	BDL	1080	14	13	17	BDL	810	BDL	1400	BDL	3.1	0.4	BDL	4.06	0.78
C3-8-MFT-L	243	7.9	4280	BDL	10.0	BDL	1050	14	12	15	BDL	810	BDL	1350	BDL	2.7	0.4	BDL	3.47	0.71
C3-9-CapW	266	8	4530	BDL	7.9	BDL	1040	14	14	20	BDL	840	11.2	1590	BDL	3.7	0.5	BDL	4.42	0.86
C3-9-MFT-U	266	7.9	4330	BDL	10.2	BDL	1010	14	12	16	BDL	820	BDL	1460	BDL	3.1	0.3	BDL	4.15	0.72
C3-9-MFT-L	266	7.7	4280	BDL	10.8	BDL	1020	14	12	15	BDL	810	BDL	1400	BDL	3.1	0.3	BDL	4.02	0.7
C3-10-CapW	302	7.5	4670	BDL	9.4	BDL	1160	16	17	24	BDL	850	9.55	1600	BDL	4.4	0.6	BDL	6.08	1.06
C3-10-MFT-U	302	7.6	4500	BDL	9.5	BDL	1100	15	14	18	BDL	1700	BDL	1400	BDL	3.5	0.4	BDL	4.98	0.82
C3-10-MFT-L	302	7.7	4360	BDL	NA	BDL	1060	14	13	17	BDL	430	11.8	1390	BDL	3.2	0.4	BDL	4.44	0.76
C3-11-CapW	334	8.3	4570	BDL	NA	BDL	1090	17	18	27	BDL	850	11.3	1610	BDL	4.7	0.8	BDL	6.63	1.06
C3-11-MFT-U	334	7.9	4440	BDL	NA	BDL	1030	15	15	19	BDL	850	BDL	1490	BDL	3.3	0.4	BDL	4.36	0.85
C3-11-MFT-L	334	7.9	4310	BDL	NA	BDL	980	15	14	18	BDL	850	BDL	1420	BDL	3	0.4	BDL	4.13	0.79
C3-12-CapW	365	7.8	4630	BDL	8.2	BDL	1150	16	17	24	BDL	850	10.3	1620	BDL	4.6	0.5	BDL	6.19	1.03
C3-12-MFT-U	365	7.8	4490	BDL	8.8	BDL	1110	16	14	18	BDL	860	BDL	1460	BDL	3.5	0.4	BDL	4.76	0.82
C3-12-MFT-L	365	7.8	4410	BDL	10.0	BDL	1090	16	14	19	BDL	840	BDL	1460	BDL	3.6	0.4	BDL	4.88	0.82

Table B-7. *(continued).*

Sample	t_{incu} (d)	SOLIDS PROPERTIES								
					Particle Size Distribution (% of solids less than)					
		Solids content (g/100g)	Oil content (g/100g)	Eh (mV)	44 um	22 um	11 um	5.5 um	2.8 um	1.0 um
C3-1-CapW	28									
C3-1-MFT-U	28	38.3	3.1	21	91.2	77.4	59.9	42.5	27.4	10.7
C3-1-MFT-L	28	39.0	3.37	33	89.6	76.7	60.1	43.1	27.3	9.9
C3-2-CapW	61									
C3-2-MFT-U	61	39.7	3.21	40	95.7	83	66.7	48.6	31.2	11.8
C3-2-MFT-L	61	40.3	3.28	42	88.6	75.5	60.2	43.1	27.2	10.3
C3-3-CapW	90									
C3-3-MFT-U	90	40.9	3.47	21	91.3	78.1	61.5	43.5	27.6	10.4
C3-3-MFT-L	90	41.2	3.48	53	95.2	81.9	65.2	47.1	30.6	12.2
C3-4-CapW	120									
C3-4-MFT-U	120	41.8	3.51	31	95.5	82.2	65.3	46.9	30	11.8
C3-4-MFT-L	120	41.9	3.54	38	91.2	78.4	62.3	44.5	28	10.8
C3-5-CapW	152									
C3-5-MFT-U	152	41.6	3.52	49	90.2	77.7	61.3	44.4	28.4	9.37
C3-5-MFT-L	152	NA	NA	NA	NA	NA	NA	NA	NA	NA
C3-6-CapW	181									
C3-6-MFT-U	181	42.4	3.37	27	83	69.7	52.9	37	22.6	7.89
C3-6-MFT-L	181	43.2	3.65	39	85.9	73.1	57.2	40.2	24.9	8.79

Table B-7. *(continued).*

Sample	t_{incu} (d)	SOLIDS PROPERTIES								
		Solids content (g/100g)	Oil content (g/100g)	Eh (mV)	Particle Size Distribution (% of solids less than)					
					44 um	22 um	11 um	5.5 um	2.8 um	1.0 um
C3-7-CapW	212									
C3-7-MFT-U	212	44.1	3.54	68	86.7	73.4	57.4	40	24.5	9.3
C3-7-MFT-L	212	44.3	3.55	37	91.2	79.4	64.1	46.6	29.5	11.2
C3-8-CapW	243									
C3-8-MFT-U	243	42.5	3.67	33.2	95.7	83.2	66.9	49.4	32.3	12.8
C3-8-MFT-L	243	43.8	3.32	47.1	96	79.8	67.9	47.6	32.0	12.1
C3-9-CapW	266									
C3-9-MFT-U	266	46.8	3.81	67.4	90.3	76.8	59.9	42.3	26.7	8.1
C3-9-MFT-L	266	43.0	3.31	66.6	92	79.6	63.6	45.6	28.3	8.1
C3-10-CapW	302									
C3-10-MFT-U	302	42.7	3.21	41	95.4	82.7	66.6	48.2	30.1	11.0
C3-10-MFT-L	302	43.5	3.69	49	95.4	82.1	65.4	47.7	31.2	12.5
C3-11-CapW	334									
C3-11-MFT-U	334	45.7	3.69	67.6	85.5	73.4	58.1	41.3	25.6	9.1
C3-11-MFT-L	334	46.2	3.93	69.8	89.8	77.5	61.7	44.2	27.6	9.8
C3-12-CapW	365									
C3-12-MFT-U	365	44.3	3.67	69.7	92.0	79.6	63.8	46.0	28.8	10.4
C3-12-MFT-L	365	45.6	3.67	77.1	92.2	79.9	64.2	46.5	29.3	10.7

1). NA=not available.

2). BDL=below detection limits.

Table B-8. Physical and chemical analyses in System 4.

		WATER PROPERTIES																		
				(mg/L)			Main Ions (mg/L)								Minor Elements (mg/L)					
Sample	t_{incu} (d)	pH	EC (uS/cm)	Br^-	$N(NH_4^+)$	S^{2-}	Na^+	K^+	Mg^{2+}	Ca^{2+}	F^-	Cl^-	SO_4^{2-}	HCO_3^-	Al	B	Ba	Fe	Si	Sr
C4-1-CapW	28	7.9	6320	270	NA	BDL	1330	19.2	27.5	60	BDL	1100	1070	642	BDL	2.9	BDL	BDL	3.9	1.57
C4-1-CT-U	28	8.2	6040	280	5.9	BDL	1200	14.7	17.5	34.9	BDL	1100	807	950	BDL	2.3	BDL	BDL	2.9	0.85
C4-1-CT-L	28	8.2	5820	270	8.5	BDL	1260	15.3	16.9	34.1	BDL	1100	659	1010	BDL	2.64	0.10	BDL	3.7	0.85
C4-2-CapW	61	8.1	6230	270	7.8	3	1350	19.2	26.6	34.7	15.0	1100	814	1100	BDL	1.6	BDL	BDL	4.1	1.36
C4-2 CT-U	61	8	5520	260	6.1	0.1	1190	14.5	13.3	26.4	BDL	1000	497	1220	BDL	2.91	0.37	BDL	4.2	0.76
C4-2 CT-L	61	8	5340	260	5.2	0.1	1200	14.2	12.6	25.0	BDL	1000	413	1230	BDL	2.78	0.57	BDL	4.2	0.74
C4-3-CapW	90	8	6360	250	7.3	1	1370	17.7	25.7	39	BDL	1000	1040	1000	BDL	2.82	BDL	BDL	4.1	1.37
C4-3 CT-U	90	8.1	5450	260	4.1	0.1	1170	13.7	12.5	23.5	BDL	1000	355	1140	BDL	2.65	0.34	BDL	3.6	0.70
C4-3 CT-L	90	8.1	5410	260	5.1	0.3	1170	13.7	11.9	22.6	BDL	1000	381	1090	BDL	2.73	0.47	BDL	3.8	0.70
C4-4-CapW	120	7.78	6300	260	6.7	BDL	1320	17.4	25.4	50.3	BDL	1000	927	1080	BDL	2.94	BDL	BDL	4.1	1.36
C4-4-CT-U	120	8.1	5410	260	5.0	0.1	1190	13.2	13.8	27.4	BDL	1000	164	1220	BDL	2.42	0.34	BDL	3.6	0.79
C4-4-CT-L	120	8.1	5390	260	5.0	0.1	1170	13.1	13.5	27.0	BDL	1000	75	1280	BDL	2.61	0.48	BDL	3.9	0.80
C4-5-CapW	152	NA	NA	NA	NA	0.8	NA	NA	NA	NA	NA	NA	NA	NA	NA	NA	NA	NA	NA	NA
C4-5-CT-U	152	8.01	5250	260	5.7	0.4	1090	12.5	12.3	23.7	BDL	1000	404	1144	BDL	2.51	0.29	BDL	3.67	0.70
C4-5-CT-L	152	8.05	5180	250	5.5	0.2	1060	12.3	12.2	23.4	BDL	990	339	1134	BDL	2.60	0.48	BDL	3.94	0.72
C4-6-CapW	181	7.76	6190	260	6.65	BDL	1370	18.6	25.9	55.6	BDL	1000	873	1124	BDL	2.86	BDL	BDL	4.13	1.46
C4-6-CT-U	181	8.05	5420	250	NA	0.8	1210	15.5	13.6	26.5	BDL	1000	348	1044	BDL	2.81	0.35	BDL	4.01	0.81
C4-6-CT-L	181	8.08	5240	250	NA	0.6	1170	14.5	12.6	23.6	BDL	970	61.4	1064	BDL	3.06	0.54	BDL	4.42	0.77

Table B-8. *(continued).*

		WATER PROPERTIES																		
				(mg/L)			Main Ions (mg/L)								Minor Elements (mg/L)					
Sample	t_{incu} (d)	pH	EC (uS/cm)	Br^-	$N(NH_4^+)$	S^{2-}	Na^+	K^+	Mg^{2+}	Ca^{2+}	F^-	Cl^-	SO_4^{2-}	HCO_3^-	Al	B	Ba	Fe	Si	Sr
C4-7-CapW	212	7.9	6240	250	8.7	0.2	1530	18.8	24.5	31.5	BDL	1000	702	1340	BDL	3.28	0.07	BDL	5.00	1.26
C4-7-CT-U	212	8	5320	260	7.6	0.2	1350	13.7	12.6	22.8	BDL	1000	301	1200	BDL	3.08	0.57	BDL	4.47	0.73
C4-7-CT-L	212	8.1	5440	270	6.9	0.1	1400	13.7	13.7	23.2	BDL	1000	310	1230	BDL	2.57	0.27	BDL	3.75	0.74
C4-8-CapW	243	8	6100	260	8.4	1	1450	18.2	21.9	19.7	BDL	1000	490	1480	BDL	3.07	0.02	BDL	4.18	1.09
C4-8-CT-U	243	8.1	5370	260	7.1	BDL	1290	13.6	12.9	23.3	BDL	1000	256	1140	BDL	2.71	0.56	BDL	3.93	0.77
C4-8-CT-L	243	7.9	5450	260	6.9	BDL	1340	14.5	12.7	23.1	BDL	1000	260	1210	BDL	3.09	0.41	BDL	4.36	0.76
C4-9-CapW	266	7.73	6340	270	8.0	BDL	1420	16.6	22.4	35.8	BDL	1000	764	1360	BDL	2.81	BDL	BDL	3.88	1.18
C4-9-CT-U	266	7.90	5620	270	7.1	BDL	1270	12.7	11.9	20.8	BDL	1000	359	1220	BDL	2.66	0.21	BDL	3.44	0.66
C4-9-CT-L	266	8.01	5520	270	7.0	BDL	1280	12.5	11.0	17.9	BDL	1000	305	1260	BDL	2.76	0.37	BDL	4.05	0.63
C4-10-CapW	302	7.6	6240	270	7.7	0.4	1550	18.3	25.1	44.4	BDL	1000	712	1300	BDL	3.16	0.05	BDL	4.52	1.36
C4-10-CT-U	302	8	5540	270	7.1	BDL	1320	13.3	13.3	24.0	BDL	1000	226	1230	BDL	2.41	0.33	BDL	3.77	0.75
C4-10-CT-L	302	8	5340	270	NA	BDL	1300	12.8	12.5	22.7	BDL	1000	192	1230	BDL	2.56	0.44	BDL	3.92	0.72
C4-11-CapW	334	7.9	6300	260	NA	BDL	1420	20.4	29.5	67.7	BDL	1000	965	1120	BDL	3.58	0.11	BDL	5.22	1.66
C4-11-CT-U	334	8.1	5550	260	NA	1	1170	14.0	14.2	27.0	BDL	1000	316	1200	BDL	2.89	0.27	BDL	4.24	0.77
C4-11-CT-L	334	8.2	5290	260	NA	BDL	1110	13.0	12.7	23.0	BDL	1000	172	1270	BDL	2.61	0.46	BDL	4.28	0.70
C4-12-CapW	365	7.7	6440	260	7.6	BDL	1570	19.7	26.7	57.5	BDL	1000	833	1260	BDL	3.48	0.03	BDL	5.07	1.53
C4-12-CT-U	365	8.1	5580	260	5.9	4	1370	15.2	13.9	25.4	BDL	1000	259	1290	BDL	3.15	0.27	BDL	4.87	0.79
C4-12-CT-L	365	8.1	5370	260	6.9	1	1410	15.1	13.5	24.7	BDL	1000	178	1350	BDL	3.34	0.45	BDL	5.34	0.78

Table B-8. *(continued).*

Sample	t_{incu} (d)	SOLIDS PROPERTIES								
		Solids content (g/100g)	Oil content (g/100g)	Eh (mV)	Particle Size Distribution (% of solids less than)					
					44 um	22 um	11 um	5.5 um	2.8 um	1.0 um
C4-1-CapW	28									
C4-1-CT-U	28	65.0	1.31	-197	47.0	41.0	32.5	19.7	10.5	3.7
C4-1-CT-L	28	69.9	1.50	-199	39.2	31.8	24.2	17.2	11.5	5.26
C4-2-CapW	61									
C4-2 CT-U	61	69.3	1.35	-217	41.3	34.3	27.0	19.6	12.9	5.30
C4-2 CT-L	61	70.9	1.36	-210	37.9	31.5	24.9	18.1	11.8	4.68
C4-3-CapW	90									
C4-3 CT-U	90	70.7	1.36	-205	37.3	31.3	24.9	18.2	11.9	4.83
C4-3 CT-L	90	72.6	1.32	-208	36.6	30.9	24.7	18.1	11.5	4.29
C4-4-CapW	120									
C4-4-CT-U	120	71.3	1.15	-209	38.2	31.8	25.1	18.3	11.9	4.72
C4-4-CT-L	120	73.3	1.36	-207	35.4	29.4	23.3	16.9	11.0	4.42
C4-5-CapW	152									
C4-5-CT-U	152	71.2	1.42	-206	48.2	40.1	31.6	22.9	14.7	5.16
C4-5-CT-L	152	73.6	1.33	-201	41.3	34.5	27.2	19.8	12.7	4.57
C4-6-CapW	181									
C4-6-CT-U	181	70.4	1.41	-196	37.4	31.2	24.4	17.6	11.3	4.24
C4-6-CT-L	181	72.8	1.45	-201	39.9	33.3	26.2	18.9	12.2	4.48

Table B-8. *(continued).*

Sample	t_{incu} (d)	SOLIDS PROPERTIES								
		Solids content (g/100g)	Oil content (g/100g)	Eh (mV)	Particle Size Distribution (% of solids less than)					
					44 um	22 um	11 um	5.5 um	2.8 um	1.0 um
C4-7-CapW	212									
C4-7-CT-U	212	75.7	1.44	-205	31	26.5	21.2	15.5	10.3	4.35
C4-7-CT-L	212	74.1	1.50	-194	32	26.2	20.6	14.7	9.6	4.06
C4-8-CapW	243									
C4-8-CT-U	243	74.0	1.43	-204.6	38	30.8	24.0	16.8	10.4	4.08
C4-8-CT-L	243	73.0	1.44	-195.3	38	32.0	25.3	18.5	12.4	5.41
C4-9-CapW	266									
C4-9-CT-U	266	71.5	1.24	-201.1	33	27.6	22.3	16.0	9.8	2.80
C4-9-CT-L	266	73.2	1.24	-204.9	33	27.5	21.8	15.8	10.1	3.06
C4-10-CapW	302									
C4-10-CT-U	302	71.9	1.18	-190	36.7	30.9	24.8	17.9	11.0	4.1
C4-10-CT-L	302	73.5	1.35	-200	30.1	25.5	20.6	15.4	10.2	4.0
C4-11-CapW	334									
C4-11-CT-U	334	74.9	1.52	-184.5	33.0	27.1	21.1	15.0	9.6	3.73
C4-11-CT-L	334	75.9	1.49	-196.7	32.9	27.2	21.2	15.2	9.9	3.89
C4-12-CapW	365									
C4-12-CT-U	365	75.9	0.83	-168	38.4	33.1	27.1	18.7	10.4	3.73
C4-12-CT-L	365	76.4	1.14	-188	39.6	33.6	27.2	19.7	11.9	4.08

1). NA=not available; 2). BDL=below detection limits.

Table B-9. Physical and chemical analyses in System 1.

		WATER PROPERTIES																		
				(mg/L)			Main Ions (mg/L)								Minor Elements (mg/L)					
Sample	t_{incu} (d)	pH	EC (uS/cm)	Br^-	$N(NH_4^+)$	S^{2-}	Na^+	K^+	Mg^{2+}	Ca^{2+}	F^-	Cl^-	SO_4^{2-}	HCO_3^-	Al	B	Ba	Fe	Si	Sr
C1-2-CapW	3	8.1	4610	25	10.2	BDL	1030	16	16.9	24	BDL	880	115	1449	BDL	3.8	0.44	BDL	5	1.01
C1-2-MFT-U	3	8	4490	23	NA	BDL	977	14	14	20	BDL	870	125		BDL	2.7	0.34	BDL	3.7	0.80
C1-2-MFT-L	3	7.9	4730	77	NA	BDL	1000	15	14.7	21	BDL	920	226	1163	BDL	2.4	0.27	BDL	3.2	0.84
C1-2-CT-U	3	8.1	5610	210	NA	BDL	1130	17	19.9	51	BDL	1000	682	752	BDL	2.3	0.11	BDL	3	1.12
C1-2-CT-L	3	8.2	5400	210	NA	BDL	1140	17	19.9	51	BDL	1000	690	690	BDL	2.3	0.11	BDL	3	1.11
C1-3-CapW	15	7.8	4850	66	8.2	BDL	1060	16	17.5	27	BDL	930	235	1338	BDL	3.5	0.43	BDL	4.9	1.10
C1-3-MFT-U	15	8	4460	50	NA	BDL	964	15	12.1	17	BDL	890	51.2	1342	BDL	2.9	0.36	BDL	3.9	0.71
C1-3-MFT-L	15	8	4780	120	NA	BDL	1010	15	13.7	19	BDL	950	136	1235	BDL	2.5	0.34	BDL	3.7	0.80
C1-3-CT-U	15	8.1	5380	240	NA	BDL	1120	15	15.9	36	BDL	1000	491	818	BDL	2.4	0.09	BDL	3.3	0.85
C1-3-CT-L	15	8.2	5380	240	NA	BDL	1110	15	17.9	44	BDL	1000	503	812	BDL	2.5	0.13	BDL	3.7	0.97
C1-4-CapW	29	8	4820	86	NA	BDL	1040	16	17.4	28	BDL	910	229	1301	BDL	3.4	0.41	BDL	BDL	1.07
C1-4-MFT-U	29	8	4570	82	8.1	BDL	997	15.2	12.9	17.5	BDL	940	31	1336	BDL	1.1	0.39	BDL	3.98	0.77
C1-4-MFT-L	29	8.1	4840	160	8.6	BDL	1050	15.3	13.7	18.8	BDL	1000	87	1232	BDL	0.8	0.40	BDL	3.73	0.81
C1-4-CT-U	29	8.4	5090	270	4.7	BDL	1070	14.6	14.2	29.0	6.50	1100	336	938	BDL	0.7	0.67	BDL	3.48	0.73
C1-4-CT-L	29	8.4	5130	270	4.1	BDL	1060	15.0	15.0	23.2	BDL	1000	260	878	BDL	0.9	0.53	BDL	3.69	0.73

Table B-9. *(continued).*

Sample	t_{incu} (d)	WATER PROPERTIES																		
				(mg/L)			Main Ions (mg/L)								Minor Elements (mg/L)					
		pH	EC (uS/cm)	Br^-	$N(NH_4^+)$	S^{2-}	Na^+	K^+	Mg^{2+}	Ca^{2+}	F^-	Cl^-	SO_4^{2-}	HCO_3^-	Al	B	Ba	Fe	Si	Sr
C1-5-CapW	62	7.6	4750	70	9.0	0.0	1060	16.2	17.2	25.6	BDL	900	73	NA	BDL	2.4	0.52	BDL	5.29	1.08
C1-5-MFT-U	62	8.1	4660	130	8.2	0.0	1010	14.2	12.3	16.5	BDL	920	29.6	1380	BDL	2.65	0.36	BDL	4.03	0.74
C1-5-MFT-L	62	8.3	4990	210	8.2	0.0	1040	13.7	13.4	17.8	BDL	990	106.0	1279	BDL	2.28	0.34	BDL	3.58	0.76
C1-5-CT-U	62	8.3	5120	260	5.5	0.0	1070	13.8	13.5	28.6	BDL	1000	286.0	960	BDL	2.56	0.26	BDL	3.79	0.75
C1-5-CT-L	62	8	5140	260	4.3	0.1	1090	13.3	12.9	25.8	BDL	1000	274.0	955	BDL	2.70	0.42	BDL	4.02	0.74
C1-6-CapW	91	7.7	4560	77	NA	0.0	974	14.6	16.3	24.1	BDL	840	BDL	1538	BDL	3.49	0.49	BDL	5.29	1.01
C1-6-MFT-U	91	8.1	4730	120	8.7	0.0	1030	14.5	12.7	16.8	BDL	920	17.3	1397	BDL	2.42	0.38	BDL	3.34	0.75
C1-6-MFT-L	91	8.2	4860	200	8.4	0.0	1060	13.9	12.9	16.6	BDL	970	63.1	1260	BDL	2.18	0.34	BDL	3.15	0.73
C1-6-CT-U	91	8.1	5000	260	5.7	0.0	1050	12.8	12.1	22.8	BDL	1000	177.0	1040	BDL	2.41	0.41	BDL	3.42	0.68
C1-6-CT-L	91	8.2	5090	280	4.3	0.2	1080	13.6	12.7	26.3	BDL	1000	201.0	1020	BDL	2.60	0.42	BDL	3.62	0.74
C1-12-CapW	121	7.71	4870	92	9.0	0.0	1050	14.9	16.8	24.2	BDL	910	90.3	1550	BDL	3.42	0.37	BDL	5.03	1.02
C1-12-MFT-U	121	7.9	4790	140	8.5	0.0	1080	14.0	13.3	16.9	BDL	940	40.7	1405	BDL	2.29	0.34	BDL	3.74	0.77
C1-12-MFT-L	121	8.1	4980	190	7.6	0.0	1150	14.2	15.0	20.3	BDL	990	94.1	1340	BDL	2.28	0.35	BDL	3.75	0.85
C1-12-CT-U	121	8	5230	250	4.2	0.1	1140	13.6	15.1	33.0	BDL	1000	264.0	1120	BDL	2.66	0.38	BDL	4.06	0.87
C1-12-CT-L	121	8	5110	240	5.0	0.1	1110	12.7	13.8	28.3	BDL	1000	67.5	1151	BDL	2.54	0.44	BDL	3.87	0.80
C1-8-CapW	153	NA	NA	NA	NA	BDL	NA	NA	NA	NA	NA	NA	NA	NA	NA	NA	NA	NA	NA	NA
C1-8-MFT-U	153	7.85	4280	130	15.6	0.1	918	13.1	11.5	14.8	BDL	900	12	1382	BDL	2.36	0.32	BDL	3.87	0.68
C1-8-MFT-L	153	7.95	4500	200	8.4	3.0	956	13.0	12.5	17.2	BDL	970	59	1328	BDL	2.31	0.33	BDL	3.79	0.73
C1-8-CT-U	153	7.85	4390	250	5.9	1.0	945	11.9	11.6	23.4	BDL	1000	151	1132	BDL	2.57	0.43	BDL	3.92	0.68
C1-8-CT-L	153	8.03	4650	280	5.3	0.8	950	12.1	11.5	23.8	BDL	1000	159	1076	BDL	2.47	0.45	BDL	3.66	0.69

Table B-9. *(continued).*

Sample	t_{incu} (d)	WATER PROPERTIES																		
				(mg/L)			Main Ions (mg/L)								Minor Elements (mg/L)					
		pH	EC (uS/cm)	Br^-	$N(NH_4^+)$	S^{2-}	Na^+	K^+	Mg^{2+}	Ca^{2+}	F^-	Cl^-	SO_4^{2-}	HCO_3^-	Al	B	Ba	Fe	Si	Sr
C1-9-CapW	182	7.68	4890	97	9.2	1.5	1090	15.9	17.3	26.0	BDL	880	68.3	1596	BDL	3.51	0.45	BDL	5.11	1.08
C1-9-MFT-U	182	7.98	4720	127	NA	0.6	1050	14.1	12.9	16.9	BDL	900	22.6	1421	BDL	2.59	0.36	BDL	4.27	0.77
C1-9-MFT-L	182	8.10	4900	188	NA	3.5	1110	14.8	14.3	20.2	BDL	960	54.6	1382	BDL	2.54	0.41	BDL	4.31	0.85
C1-9-CT-U	182	8.00	4920	245	NA	6.0	1130	14.6	13.1	27.1	BDL	990	70.0	1170	BDL	2.97	0.54	BDL	4.63	0.80
C1-9-CT-L	182	8.15	4920	270	NA	5.5	1110	15.4	13.5	26.0	BDL	1000	35.1	1124	BDL	2.88	0.74	BDL	4.18	0.81
C1-10-CapW	213	7.7	4870	110	11.7	BDL	1230	16.6	17.2	25.1	BDL	900	52.6	1580	BDL	3.92	0.50	BDL	5.59	1.11
C1-10-MFT-U	213	8.2	4550	150	9.2	BDL	1130	13.5	10.6	11.8	BDL	950	18.8	1192	BDL	2.32	0.30	BDL	3.30	0.54
C1-10-MFT-L	213	8.2	4860	210	9.7	3	1230	14.1	12.9	15.9	4.2	1000	61.3	1270	BDL	2.70	0.35	BDL	3.87	0.69
C1-10-CT-U	213	7.9	5270	260	7.1	0.2	1330	14.0	14.3	26.0	BDL	1000	226	1210	BDL	3.11	0.58	BDL	4.37	0.81
C1-10-CT-L	213	8	5260	270	3.3	0.1	1320	14.3	14.8	28.6	BDL	1000	267	1140	BDL	3.09	0.47	BDL	4.48	0.83
C1-11-CapW	244	7.6	4960	110	10.3	BDL	1200	16.4	17.2	25.1	BDL	860	133	1460	BDL	3.68	0.53	BDL	5.34	1.10
C1-11-MFT-U	244	8	4650	140	8.1	2	1150	13.5	11.6	13.4	BDL	910	33	1230	BDL	2.64	0.32	BDL	4.07	0.67
C1-11-MFT-L	244	8.1	4850	190	7.9	5	1170	13.9	12.6	15.2	BDL	950	58	1220	BDL	2.59	0.35	BDL	4.01	0.72
C1-11-CT-U	244	7.9	5140	220	6.5	BDL	1210	13.7	13.6	25.6	BDL	900	110	1159	BDL	2.70	0.55	BDL	4.01	0.80
C1-11-CT-L	244	8.1	5230	270	4.8	BDL	1270	14.5	15.4	30.3	BDL	1000	95	1250	BDL	2.87	0.53	BDL	4.28	0.91
C1-13-CapW	267	7.54	5000	110	10.5	BDL	1150	15.1	16.1	22.9	BDL	900	188	1440	BDL	3.40	0.38	BDL	4.92	1.02
C1-13-MFT-U	267	7.93	4660	150	8.8	3	1110	12.4	10.8	12.3	BDL	940	45	1240	BDL	2.28	0.23	BDL	3.27	0.59
C1-13-MFT-L	267	7.95	4780	190	8.0	4	1130	12.1	11.3	14.5	BDL	970	66	1260	BDL	2.37	0.26	BDL	3.38	0.62
C1-13-CT-U	267	7.76	4970	230	7.1	BDL	1180	12.8	11.9	21.4	BDL	1000	102	1270	BDL	2.87	0.37	BDL	4.31	0.69
C1-13-CT-L	267	7.91	5100	250	7.1	0.4	1180	13.6	12.6	24.2	BDL	1000	90	1260	BDL	3.02	0.41	BDL	4.46	0.75

Table B-9. *(continued).*

Sample	t_{incu} (d)	WATER PROPERTIES																		
				(mg/L)			Main Ions (mg/L)								Minor Elements (mg/L)					
		pH	EC (uS/cm)	Br^-	$N(NH_4^+)$	S^{2-}	Na^+	K^+	Mg^{2+}	Ca^{2+}	F^-	Cl^-	SO_4^{2-}	HCO_3^-	Al	B	Ba	Fe	Si	Sr
C1-14-CapW	303	7.4	5270	120	10.4	BDL	1230	16.3	19.1	30.2	BDL	910	277	NA	BDL	3.54	0.52	BDL	5.37	1.20
C1-14-MFT-U	303	7.8	4910	150	9.1	BDL	1170	13.6	12.9	16.1	BDL	940	45.0	NA	BDL	2.66	0.36	BDL	4.39	0.73
C1-14-MFT-L	303	7.9	4980	180	NA	3	1190	13.3	12.9	16.6	BDL	970	60.3	NA	BDL	2.68	0.35	BDL	4.04	0.73
C1-14-CT-U	303	8	5320	240	7.9	BDL	1360	14.5	14.9	28.4	BDL	1000	156	NA	BDL	2.87	0.46	BDL	4.53	0.85
C1-14-CT-L	303	8.1	5330	260	NA	BDL	1360	14.6	16.1	30.9	BDL	1000	80.3	NA	BDL	2.96	0.60	BDL	4.53	0.95
C1-15-CapW	335	7.7	5100	110	NA	BDL	1080	16.6	19.4	29.3	BDL	920	237	1430	BDL	3.80	0.50	BDL	5.72	1.17
C1-15-MFT-U	335	8.1	4750	140	NA	2	1090	13.7	12.5	14.4	BDL	960	22	1300	BDL	2.70	0.34	BDL	4.46	0.67
C1-15-MFT-L	335	8.1	4810	160	NA	4	1040	13.2	12.5	15.9	BDL	970	41	1310	BDL	2.72	0.33	BDL	4.17	0.67
C1-15-CT-U	335	8.3	5220	220	NA	BDL	1090	14.0	13.3	24.1	BDL	1000	53	1350	BDL	3.26	0.48	BDL	5.14	0.74
C1-15-CT-L	335	8.2	5330	240	NA	BDL	1120	14.5	14.4	28.7	BDL	1000	108	1330	BDL	3.21	0.54	BDL	5.18	0.83
C1-16-CapW	366	8.1	5150	110	9.6	BDL	1280	17.0	17.9	26.8	BDL	910	271	1380	BDL	3.78	0.00	BDL	5.16	1.13
C1-16-MFT-U	366	8	4830	150	7.8	3	1170	13.0	11.8	13.0	BDL	950	44	1320	BDL	2.67	0.26	BDL	3.82	0.64
C1-16-MFT-L	366	8	4940	180	7.9	3.5	1150	12.8	12.1	14.3	BDL	990	60	1320	BDL	2.64	0.27	BDL	3.88	0.65
C1-16-CT-U	366	8.2	5350	240	7.5	BDL	1260	14.1	14.9	20.9	BDL	1000	21	1350	BDL	3.35	0.42	BDL	5.19	0.80
C1-16-CT-L	366	8	5190	230	7.5	BDL	1240	13.9	12.5	18.1	BDL	1000	23	1310	BDL	3.20	0.38	BDL	4.73	0.69

Table B-9. *(continued).*

Sample	t_{incu} (d)	SOLIDS PROPERTIES									
						Particle Size Distribution (% of solids less than)					
		Solids content (g/100g)	Oil content (g/100g)	Eh (mV)	AVS (mg/kg of dry sample)	44 um	22 um	11 um	5.5 um	2.8 um	1.0 um
C1-2-CapW	3			401							
C1-2-MFT-U	3	38.8	3.05	42		91.4	78.4	61.9	44.6	28.60	10.60
C1-2-MFT-L	3	40.9	3.36	33		90.5	77.3	60.1	42.8	27.90	11.30
C1-2-CT-U	3	60.8	1.09	204		34.2	28.0	21.8	15.8	10.30	3.94
C1-2-CT-L	3	63.2	1.10	-41		37.4	30.8	24.0	17.3	11.10	4.26
C1-3-CapW	15			558							
C1-3-MFT-U	15	39.5	3.23	4		90.3	77.2	60.6	43.4	27.90	10.80
C1-3-MFT-L	15	39.2	3.26	-50		92.7	79.3	62.3	44.6	28.70	11.10
C1-3-CT-U	15	63.3	1.23	-184		29.0	24.0	18.7	13.4	8.75	3.50
C1-3-CT-L	15	72.4	1.38	-195		40.3	33.2	25.7	18.3	12.10	5.01
C1-4-CapW	29										
C1-4-MFT-U	29	38.0	2.99	-116		90.7	77.9	61.2	43.9	28.2	10.9
C1-4-MFT-L	29	38.3	3.25	-114		89.8	76.8	60.4	43.1	27.3	10.2
C1-4-CT-U	29	66.2	1.00	-191		40.6	34.1	26.9	19.4	12.5	4.7
C1-4-CT-L	29	72.3	1.30	-190		33.4	27.8	21.6	15.5	10.1	4.1

Table B-9. *(continued).*

Sample	t_{incu} (d)	SOLIDS PROPERTIES									
						Particle Size Distribution (% of solids less than)					
		Solids content (g/100g)	Oil content (g/100g)	Eh (mV)	AVS (mg/kg of dry sample)	44 um	22 um	11 um	5.5 um	2.8 um	1.0 um
C1-5-CapW	62										
C1-5-MFT-U	62	38.3	3.26	-110		99.2	84.5	66.5	48.1	31.6	12.70
C1-5-MFT-L	62	38.8	3.04	-180		95.4	82.6	66.3	48.6	31.3	11.40
C1-5-CT-U	62	71.4	1.36	-194		42.6	35.5	28.0	20.3	13.2	5.29
C1-5-CT-L	62	69.2	1.28	-199		42.9	35.7	28.2	20.4	13.2	5.12
C1-6-CapW	91										
C1-6-MFT-U	91	38.9	3.19	-164		95.7	82.6	65.9	47.9	31.1	12.10
C1-6-MFT-L	91	39.1	3.33	-178		95.2	81.7	64.7	46.8	30.8	12.50
C1-6-CT-U	91	70.7	1.33	-197		39.0	32.3	25.4	18.5	12.1	4.90
C1-6-CT-L	91	72.0	1.36	-197		28.3	23.3	18.3	13.4	8.9	3.69
C1-12-CapW	121										
C1-12-MFT-U	121	38.9	3.18	-135	150.4	92.5	80.3	64.3	46.4	29.1	10.40
C1-12-MFT-L	121	38.8	3.23	-180	185.6	95.0	81.6	65.1	47.2	30.2	11.10
C1-12-CT-U	121	73.3	1.18	-202	28.8	45.1	37.5	30.3	22.1	14.1	5.27
C1-12-CT-L	121	70.9	1.09	-199	NA	41.2	34.4	27.5	20.1	12.9	4.74
C1-8-CapW											
C1-8-MFT-U	153	40.6	3.05	-157		96.0	83.9	68.0	49.9	31.4	10.70
C1-8-MFT-L	153	40.6	3.34	-163		91.8	79.6	64.1	46.5	29.1	10.10
C1-8-CT-U	153	73.1	1.40	-197		35.8	29.7	23.5	17.3	11.3	4.25
C1-8-CT-L	153	75.0	1.33	-183		41.9	35.1	27.8	20.2	12.8	4.52

Table B-9. *(continued).*

Sample	t_{incu} (d)	SOLIDS PROPERTIES									
		Solids content (g/100g)	Oil content (g/100g)	Eh (mV)	AVS (mg/kg of dry sample)	Particle Size Distribution (% of solids less than)					
						44 um	22 um	11 um	5.5 um	2.8 um	1.0 um
C1-9-CapW	182										
C1-9-MFT-U	182	40.1	3.52	-162		84.7	71.9	55.9	39.2	24.6	8.59
C1-9-MFT-L	182	41.3	3.34	-179		88.6	76.3	60.5	43.4	27.2	9.41
C1-9-CT-U	182	73.1	1.43	-202		28.7	23.1	17.7	12.5	8.0	3.14
C1-9-CT-L	182	73.8	1.32	-199		45.2	37.9	30.0	21.7	13.7	4.86
C1-10-CapW	213										
C1-10-MFT-U	213	40.8	3.39	-76		92	80.4	64.7	46.5	29.2	10.90
C1-10-MFT-L	213	39.9	3.37	-182		91	78.4	62.5	45.6	30.0	12.10
C1-10-CT-U	213	74.8	1.49	-206		31	25.8	20.3	14.5	9.5	4.01
C1-10-CT-L	213	76.6	1.45	-195		34	28.7	22.9	16.8	11.3	4.76
C1-11-CapW	244										
C1-11-MFT-U	244	40.4	3.39	-152.2		89	76.1	59.9	42.4	26.5	10.50
C1-11-MFT-L	244	40.5	3.49	-125.9		92	79.6	64.0	46.5	30.0	12.20
C1-11-CT-U	244	73.4	1.46	-193.6		40	33.1	26.2	19.0	12.4	5.30
C1-11-CT-L	244	74.6	1.24	-187.6		37	31.9	25.9	19.3	12.6	5.02
C1-13-CapW	267										
C1-13-MFT-U	267	40.0	3.31	-161.3		92	78.2	63.2	41.0	23.1	8.14
C1-13-MFT-L	267	40.4	3.42	-178.9		90	76.9	60.2	42.5	26.9	8.11
C1-13-CT-U	267	71.0	1.01	-196.6		31	25.2	20.1	14.2	8.4	2.33
C1-13-CT-L	267	72.8	1.24	-196.3		28	23.9	19.2	14.0	9.0	2.77

Table B-9. *(continued).*

Sample	t_{incu} (d)	SOLIDS PROPERTIES									
		Solids content (g/100g)	Oil content (g/100g)	Eh (mV)	AVS (mg/kg of dry sample)	Particle Size Distribution (% of solids less than)					
						44 um	22 um	11 um	5.5 um	2.8 um	1.0 um
C1-14-CapW	303										
C1-14-MFT-U	303	41.9	2.61	-151		91.7	79.6	64.1	45.7	27.9	10.2
C1-14-MFT-L	303	41.2	3.60	-121		95.8	83.1	66.2	48.6	32.5	13.3
C1-14-CT-U	303	72.9	0.73	-192		34.7	29.4	23.8	16.7	9.8	3.7
C1-14-CT-L	303	73.7	1.04	-192		82.7	69.7	56.7	42.0	26.4	9.5
C1-15-CapW	335										
C1-15-MFT-U	335	43.0	3.70	-121.9		88.4	76.0	60.2	43.1	27.1	9.69
C1-15-MFT-L	335	43.9	3.84	-149.8		87.6	74.8	58.7	42.0	26.9	10.10
C1-15-CT-U	335	75.6	1.55	-186.4		28.5	23.4	18.2	13.1	8.6	3.49
C1-15-CT-L	335	76.3	1.34	-188.3		34.3	28.6	22.7	16.5	10.5	3.83
C1-16-CapW	366										
C1-16-MFT-U	366	42.5	3.77	-147		90.9	77.9	61.4	44.3	28.7	11.30
C1-16-MFT-L	366	42.9	3.67	-164		91.8	79.1	62.7	45.5	29.5	11.40
C1-16-CT-U	366	73.2	1.19	-178		46.9	39.8	32.1	22.8	13.5	4.62
C1-16-CT-L	366	73.5	1.47	-181		34.8	28.9	22.7	16.5	10.9	4.47

1). NA=not available.
2). BDL=below detection limits.

Table B-10. Physical and chemical analyses in System 2.

		WATER PROPERTIES																		
				(mg/L)			Main Ions (mg/L)								Minor Elements (mg/L)					
Sample	t_{incu} (d)	pH	EC (uS/cm)	Br^-	$N(NH_4^+)$	S^{2-}	Na^+	K^+	Mg^{2+}	Ca^{2+}	F^-	Cl^-	SO_4^{2-}	HCO_3^-	Al	B	Ba	Fe	Si	Sr
C2-1-CapW(1)	1	7.9	4850	39	11	BDL	1070	17	18.9	28	BDL	910	212	1340	BDL	3.6	0.5	BDL	4.37	1.13
C2-1-CapW(2)	3	8	5130	64	NA	BDL	1150	17	21.1	32	7.7	940	326	1390	BDL	3.5	0.5	BDL	4.74	1.27
C2-1-CapW(3)	7	8	5130	63	10.7	BDL	1150	17	20.6	31	BDL	930	333	1220	BDL	3.5	0.5	BDL	4.82	1.25
C2-1-CapW(4)	14	8.1	5170	72	NA	BDL	1110	17	20.8	32	11	940	346	1230	BDL	2.2	0.5	BDL	4.9	1.31
C2-1-CapW(5)	21	8.1	5070	69	9.8	BDL	1110	17	19	28	8.4	940	252	1050	BDL	2.1	0.5	BDL	4.93	1.19
C2-1-CapW(6)	35	8	5140	85	NA	BDL	1150	16	19.3	29	BDL	930	213	1340	BDL	3.2	0.5	BDL	4.94	1.2
C2-1-CapW(7)	49	8.1	4940	100	8	BDL	1070	15	19.3	28	BDL	920	199	NA	BDL	3.2	0.5	BDL	4.61	1.2
C2-1-CapW(8)	77	8	5330	120	8.13	BDL	1170	16	19.6	27	BDL	930	255	1530	BDL	3.2	0.5	BDL	4.56	1.17
C2-1-CapW(9)	133	8.1	5230	150	8.42	BDL	1090	15	18.9	26	BDL	940	423	1494	BDL	2.9	0.4	BDL	4.05	1.14
C2-1-CapW(10)	352	8.2	5520	160	0.4	BDL	1270	25.0	19.1	25.2	BDL	920	593	1240	BDL	2.98	0.13	BDL	4.52	1.17
C2-1-MFT-U	352	8.1	5010	180	11.0	BDL	1170	14.9	11.8	13.3	BDL	970	96	1360	BDL	2.62	0.24	BDL	3.76	0.64
C2-1-MFT-L	352	8	4950	190	11.0	BDL	1120	13.4	11.5	14.8	BDL	980	110	1320	BDL	2.70	0.27	BDL	3.97	0.65
C2-1-CT-U	352	8.1	5100	210	12.0	BDL	1180	13.6	11.6	21.2	BDL	1000	129	1380	BDL	3.03	0.39	BDL	4.55	0.69
C2-1-CT-L	352	8	5200	220	10.0	BDL	1180	14.9	12.4	24.3	BDL	1000	138	1250	BDL	3.31	0.44	BDL	5.09	0.76

Table B-10. *(continued).*

Sample	t_{incu} (d)	WATER PROPERTIES																		
				(mg/L)			Main Ions (mg/L)								Minor Elements (mg/L)					
		pH	EC (uS/cm)	Br^-	$N(NH_4^+)$	S^{2-}	Na^+	K^+	Mg^{2+}	Ca^{2+}	F^-	Cl^-	SO_4^{2-}	HCO_3^-	Al	B	Ba	Fe	Si	Sr
C2-2-CapW(1)	1	7.9	4760	27	10.8	BDL	1100	17	18.4	27	BDL	880	157	1130	BDL	3.6	0.5	BDL	4.32	1.1
C2-2-CapW(2)	3	8	4960	49	NA	BDL	1130	17	19.6	29	BDL	910	243	1010	BDL	3.5	0.5	BDL	4.64	1.18
C2-2-CapW(3)	7	8	4980	55	10.1	BDL	1130	17	19.2	29	BDL	900	261	860	BDL	3.5	0.5	BDL	4.56	1.16
C2-2-CapW(4)	14	8.2	4920	59	NA	BDL	1070	17	18.7	27	BDL	890	216	1120	BDL	2.1	0.5	BDL	4.64	1.16
C2-2-CapW(5)	21	8.2	4930	69	9.2	BDL	1060	16	17.4	25	BDL	940	168	1220	BDL	2	0.5	BDL	4.85	1.07
C2-2-CapW(6)	35	8.1	4930	78	NA	BDL	1110	16	17.4	25	BDL	940	146	1070	BDL	3.3	0.5	BDL	4.85	1.06
C2-2-CapW(7)	49	8.2	4660	82	7.6	BDL	1010	14	16.4	22	BDL	870	128		BDL	3.3	0.4	BDL	4.57	1
C2-2-CapW(8)	77	8.1	4970	110	8.33	BDL	1090	15	15.9	19	BDL	930	147	1390	BDL	3.3	0.3	BDL	4.52	0.93
C2-2-CapW(9)	133	8.3	4800	130	7.07	BDL	995	14	14.9	17	BDL	910	278	1356	BDL	3	0.3	BDL	4.06	0.87
C2-3-CapW(1)	1	7.9	4890	32	11.2	BDL	1110	17	19.5	29	BDL	890	202	1140	BDL	3.6	0.5	BDL	4.37	1.19
C2-3-CapW(2)	3	8	5060	57	NA	BDL	1160	17	21	32	BDL	910	324	1150	BDL	3.5	0.6	BDL	4.54	1.28
C2-3-CapW(3)	7	8	5140	64	10.6	BDL	1150	17	21	32	BDL	920	360	1080	BDL	3.5	0.5	BDL	4.68	1.27
C2-3-CapW(4)	14	8	5020	58	NA	BDL	1060	16	19.1	29	BDL	920	263	1420	BDL	2.1	0.5	BDL	4.78	1.2
C2-3-CapW(5)	21	8.1	5060	69	9.9	BDL	1070	16	18.7	28	BDL	910	254	1430	BDL	1.9	0.5	BDL	4.74	1.17
C2-3-CapW(6)	35	8	5090	79	NA	BDL	1160	16	18.9	29	BDL	940	145	1080	BDL	3.3	0.5	BDL	5.02	1.18
C2-3-CapW(7)	49	8.1	4780	90	7.8	BDL	1010	15	17.7	27	BDL	890	135	NA	BDL	3.2	0.5	BDL	4.67	1.1
C2-3-CapW(8)	77	8	5150	110	8.2	BDL	1140	16	18.6	28	5	930	170	1510	BDL	3.3	0.5	BDL	4.68	1.12
C2-3-CapW(9)	133	8.1	5090	140	8.9	BDL	1070	15	18.5	28	BDL	930	346	1464	BDL	3	0.4	BDL	4.26	1.14

Table B-10. *(continued).*

Sample	t_{incu} (d)	WATER PROPERTIES																		
				(mg/L)			Main Ions (mg/L)								Minor Elements (mg/L)					
		pH	EC (uS/cm)	Br^-	$N(NH_4^+)$	S^{2-}	Na^+	K^+	Mg^{2+}	Ca^{2+}	F^-	Cl^-	SO_4^{2-}	HCO_3^-	Al	B	Ba	Fe	Si	Sr
C2-4-CapW(1)	1	7.9	5290	69	11.4	BDL	1160	18	23.7	38	BDL	910	476	884	BDL	3.33	0.6	BDL	4.1	1.45
C2-4-CapW(2)	3	7.9	5480	79	NA	BDL	1200	18	24.1	40	BDL	930	560	1120	BDL	3.29	0.5	BDL	4.4	1.47
C2-4-CapW(3)	7	7.9	5330	67	10.6	BDL	1170	17	22.4	37	BDL	910	487	1300	BDL	3.39	0.5	BDL	4.6	1.36
C2-4-CapW(4)	14	8	5230	66	NA	BDL	1130	17	21.5	34	BDL	930	392	1030	BDL	2.11	0.5	BDL	4.8	1.35
C2-4-CapW(5)	21	8.1	5200	74	9.8	BDL	1100	17	19.8	30	BDL	930	333	1160	BDL	1.93	0.5	BDL	4.7	1.24
C2-4-CapW(6)	35	7.9	5260	85	NA	BDL	1200	17	20.4	31	BDL	940	160	1450	BDL	3.32	0.5	BDL	5.1	1.28
C2-4-CapW(7)	49	8.1	4970	97	8.4	BDL	1050	15	19.4	30	BDL	880	158	NA	BDL	3.18	0.5	BDL	4.7	1.2
C2-4-CapW(8)	77	8	5370	120	8.71	BDL	1160	16	19.9	30	BDL	940	198	1660	BDL	3.26	0.5	BDL	4.6	1.2
C2-4-CapW(9)	133	8	5340	150	9.56	BDL	1110	15	20.3	31	BDL	930	411	1526	BDL	2.97	0.5	BDL	4.3	1.25
C2-4-CapW(10)	352	8	5920	190	9.1	BDL	1350	17.0	22.3	30.9	BDL	970	590	1430	BDL	3.08	0.22	BDL	4.30	1.40
C2-4-MFT-U	352	8	5250	210	7.9	BDL	1200	12.8	12.4	12.9	BDL	1000	107	1390	BDL	2.66	0.25	BDL	3.63	0.65
C2-4-MFT-L	352	7.8	5210	210	8.6	BDL	1200	12.2	11.9	14.2	BDL	1000	161	1280	BDL	2.74	0.27	BDL	3.77	0.65
C2-4-CT-U	352	7.8	5440	240	6.9	BDL	1300	13.1	12.0	20.6	BDL	1000	277	1440	BDL	3.10	0.42	BDL	4.31	0.69
C2-4-CT-L	352	8	5560	260	7.3	BDL	1400	14.6	13.2	24.7	BDL	1100	329	1240	BDL	3.48	0.49	BDL	5.06	0.77

Table B-10. *(continued).*

Sample	t_{incu} (d)	WATER PROPERTIES																		
				(mg/L)			Main Ions (mg/L)								Minor Elements (mg/L)					
		pH	EC (uS/cm)	Br^-	$N(NH_4^+)$	S^{2-}	Na^+	K^+	Mg^{2+}	Ca^{2+}	F^-	Cl^-	SO_4^{2-}	HCO_3^-	Al	B	Ba	Fe	Si	Sr
C2-5-CapW(1)	1	7.9	5130	33	11.2	BDL	1150	18	22.5	33	BDL	890	431	1010	BDL	3.4	0.57	BDL	4.3	1.36
C2-5-CapW(2)	3	8.15	5650	70	NA	BDL	1230	18	25.9	40	BDL	900	700	1040	BDL	3.3	0.29	BDL	4.3	1.54
C2-5-CapW(3)	7	8.03	5690	76	11.4	BDL	1280	18	25.7	41	BDL	910	690	964	BDL	3.4	0.34	BDL	4.5	1.55
C2-5-CapW(4)	14	8	5690	87	NA	BDL	1200	18	25.2	40	BDL	920	676	904	BDL	1.9	0.16	BDL	4.6	1.57
C2-5-CapW(5)	21	8.05	5690	98	10.1	BDL	1170	17	23.5	36	BDL	940	627	1330	BDL	1.7	0.28	BDL	4.6	1.45
C2-5-CapW(6)	35	8	5630	110	NA	BDL	1280	18	23.3	36	BDL	940	461	1780	BDL	3.2	0.29	BDL	4.9	1.44
C2-5-CapW(7)	49	7.98	5320	120	8.7	BDL	1170	16	22.3	32	BDL	980	380	NA	BDL	3.1	0.31	BDL	4.6	1.35
C2-5-CapW(8)	77	8	5620	130	8.77	BDL	1230	16	21.4	27	BDL	940	383	1400	BDL	3.2	0.27	BDL	4.5	1.2
C2-5-CapW(9)	133	8.12	5460	150	9.25	BDL	1140	15	20.5	26	BDL	920	438	1606	BDL	2.9	0.27	BDL	4	1.18

Table B-10. *(continued).*

Sample	t_{incu} (d)	WATER PROPERTIES																		
				(mg/L)			Main Ions (mg/L)								Minor Elements (mg/L)					
		pH	EC (uS/cm)	Br^-	$N(NH_4^+)$	S^{2-}	Na^+	K^+	Mg^{2+}	Ca^{2+}	F^-	Cl^-	SO_4^{2-}	HCO_3^-	Al	B	Ba	Fe	Si	Sr
C2-6-CapW(1)	1	7.93	4770	8.9	10.7	BDL	1060	16	18.5	27	BDL	870	142	1410	BDL	3.6	0.48	BDL	4.5	1.1
C2-6-CapW(2)	3	8.01	4950	23	NA	BDL	1110	17	19.8	29	BDL	880	216	1550	BDL	3.6	0.51	BDL	4.8	1.2
C2-6-CapW(3)	7	7.95	5340	47	10.9	BDL	1130	17	21.8	32	BDL	900	388	1520	BDL	3.3	0.57	BDL	4.6	1.3
C2-6-CapW(4)	14	8.01	5320	56	NA	BDL	1120	17	21.5	32	BDL	900	365	1300	BDL	1.9	0.59	BDL	4.7	1.3
C2-6-CapW(5)	21	8.05	5490	75	10.1	BDL	1200	18	22.2	30	BDL	930	367	1200	BDL	1.9	0.58	BDL	4.7	1.4
C2-6-CapW(6)	35	8	5670	96	NA	BDL	1300	18	23	33	BDL	930	320	1520	BDL	3.1	0.59	BDL	4.7	1.4
C2-6-CapW(7)	49	8.05	5450	110	9.5	BDL	1160	16	23	30	BDL	910	289	NA	BDL	2.9	0.56	BDL	4.3	1.4
C2-6-CapW(8)	77	8	5930	140	10.7	BDL	1310	17	23.5	26	BDL	940	284	1820	BDL	3	0.49	BDL	4.4	1.3
C2-6-CapW(9)	133	7.98	6020	170	10.4	BDL	1280	17	25.2	35	BDL	950	583	1858	BDL	2.8	0.23	BDL	4.1	1.5
C2-6-CapW(10)	352	7.88	6800	200	13.0	BDL	1660	18.8	27.4	30.6	BDL	970	868	1750	BDL	3.09	0.13	BDL	4.37	1.64
C2-6-MFT-U	352	7.88	6000	220	8.3	BDL	1450	14.2	14.3	12.5	BDL	1000	282	1770	BDL	2.81	0.24	BDL	3.48	0.70
C2-6-MFT-L	352	7.91	5960	220	7.6	BDL	1440	12.7	12.3	11.1	BDL	1000	288	1690	BDL	2.72	0.25	BDL	3.42	0.60
C2-6-CT-U	352	7.95	6530	250	7.1	BDL	1560	13.4	11.7	12.8	BDL	1000	532	1850	BDL	2.76	0.25	BDL	3.86	0.58
C2-6-CT-L	352	8.07	6620	260	7.0	BDL	1590	13.3	12.0	15.2	BDL	1000	335	2410	BDL	2.85	0.11	BDL	4.05	0.57

Table B-10. *(continued).*

Sample	t_{incu} (d)	SOLIDS PROPERTIES								
					Particle Size Distribution (% of solids less than)					
		Solids content (g/100g)	Oil content (g/100g)	Eh (mV)	44 um	22 um	11 um	5.5 um	2.8 um	1.0 um
C2-1-CapW(10)	352									
C2-1-MFT-U	352	43.0	3.49	-167	91.5	78.8	62.8	45.8	29.2	10.6
C2-1-MFT-L	352	45.5	3.67	-180	90.2	77.9	62.5	45.3	28.1	9.7
C2-1-CT-U	352	76.1	1.26	-187	39.7	33.6	27.1	19.7	12.3	4.4
C2-1-CT-L	352	74.5	0.96	-186	43.3	37.2	30.6	21.5	12.2	4.2
C2-4-CapW(10)	352									
C2-4-MFT-U	352	42.9	3.70	-179	91.6	78.6	62.3	45.2	29.1	10.9
C2-4-MFT-L	352	43.8	3.52	-186	90.2	77.8	62.4	44.9	27.7	9.6
C2-4-CT-U	352	74.9	1.11	-196	38.9	33.0	26.9	19.2	11.3	3.9
C2-4-CT-L	352	75.2	1.51	-203	37.9	31.6	25.0	18.2	11.9	4.7
C2-6-CapW(10)	352									
C2-6-MFT-U	352	41.4	3.34	-197	90.5	77.9	62.1	44.8	28.2	10.2
C2-6-MFT-L	352	44.1	3.51	-199	91.9	79.1	62.8	45.6	29.1	10.8
C2-6-CT-U	352	75.3	0.31	-215	46.0	40.0	32.8	21.8	11.7	4.3
C2-6-CT-L	352	74.5	1.36	-214	38.2	31.8	25.1	18.3	11.8	4.5

1). NA=not available.
2). BDL=below detection limits.

Table B-11. Trapped gas analyses on the baseline MFT and CT samples.

Sample	t_{incu} (d)	Trapped gas analysis (vol%)			
		CH_4	CO_2	C_2H_4	H_2S
Base MFT 1	0	3.48	0.988	nd	nd
Base MFT 2	0	2.85	1.14	nd	nd
Base MFT 3	0	0.046	0.168	0.027	nd
Base CT 1	0	0.072	0.180	nd	nd
Base CT 2	0	0.053	0.211	nd	nd
Base CT 3	0	0.126	0.269	nd	nd
Base CT 4	0	nd	0.158	nd	nd
Base CT 5	0	nd	0.194	0.016	nd
Base CT 6	0	nd	0.066	0.090	nd

1). Using Micro-GC and the GC parameters at Table 4-2 with 30 s of sampling time.
2). nd=non-detectable.

Table B-12. Trapped gas analyses on MFT and CT samples in Systems 1, 2, 3, and 4.

Sample	t_{incu} (d)	Trapped gas analysis (vol%)			
		CH_4	CO_2	C_2H_4	H_2S
System 1 (Cap water/MFT/CT)					
C1-4-MFT-U	29	0.028	0.202	nd	nd
C1-4-MFT-L	29	0.031	0.130	nd	nd
C1-4-CT-U	29	nd	0.007	0.006	nd
C1-4-CT-L	29	nd	0.205	nd	nd
C1-5-MFT-U	62	0.386	0.135	nd	nd
C1-5-MFT-L	62	0.289	0.078	0.076	nd
C1-5-CT-U	62	nd	0.105	0.077	0.418
C1-5-CT-L	62	0.050	0.102	nd	nd
C1-6-MFT-U	91	0.082	0.383	nd	nd
C1-6-MFT-L	91	0.683	0.087	0.097	nd
C1-6-CT-U	91	0.150	0.066	nd	nd
C1-6-CT-L	91	0.069	0.057	0.094	0.246
C1-12-MFT-U	121	0.067	0.266	nd	nd
C1-12-MFT-L	121	0.248	0.263	0.033	nd
C1-12-CT-U	121	0.101	0.256	0.117	0.502
C1-12-CT-L	121	0.205	0.170	0.024	0.009
C1-8-MFT-U	153	0.367	0.390	nd	nd
C1-8-MFT-L	153	0.505	0.116	nd	0.037
C1-8-CT-U	153	0.169	0.320	0.035	0.080
C1-8-CT-L	153	0.094	0.332	nd	0.020
C1-9-MFT-U	182	0.182	0.761	0.577	0.097
C1-9-MFT-L	182	0.074	0.172	nd	nd
C1-9-CT-U	182	nd	0.390	nd	0.035
C1-9-CT-L	182	0.082	0.400	0.110	0.028
C1-10-MFT-U	213	0.053	0.269	nd	
C1-10-MFT-L	213	0.098	0.036	nd	0.425
C1-10-CT-U	213	nd	0.140	nd	0.138
C1-10-CT-L	213	nd	0.121	nd	nd
C1-11-MFT-U	244	0.048	0.0811	nd	nd
C1-11-MFT-L	244	0.072	0.0932	nd	nd
C1-11-CT-U	244	0.049	0.0806	nd	nd
C1-11-CT-L	244	0.034	0.0880	nd	0.050
C1-13-MFT-U	267	0.061	0.063	nd	0.012
C1-13-MFT-L	267	0.091	0.076	nd	0.036
C1-13-CT-U	267	nd	0.086	nd	nd
C1-13-CT-L	267	0.045	0.088	nd	0.054

Table B-12. *(continued).*

Sample	t_{incu} (d)	Trapped gas analysis (vol%)			
		CH_4	CO_2	C_2H_4	H_2S
System 1 (Cap water/MFT/CT) *(continued)*					
C1-14-MFT-U	303	0.050	0.083	nd	nd
C1-14-MFT-L	303	0.036	0.118	nd	nd
C1-14-CT-U	303	0.310	0.115	nd	nd
C1-14-CT-L	303	0.075	0.118	nd	nd
C1-15-MFT-U	335	0.257	0.070	nd	nd
C1-15-MFT-L	335	0.222	0.074	nd	nd
C1-15-CT-U	335	0.148	0.079	nd	nd
C1-15-CT-L	335	0.042	0.072	nd	nd
C1-16-MFT-U	366	1.13	1.39	nd	nd
C1-16-MFT-L	366	0.752	0.120	nd	nd
C1-16-CT-U	366	0.482	0.175	nd	nd
C1-16-CT-L	366	0.412	0.115	nd	nd
System 2 (Cap water/MFT/CT)					
C2-1-MFT-U	352	1.04	0.090	nd	nd
C2-1-MFT-L	352	1.64	0.114	nd	nd
C2-1-CT-U	352	1.02	0.064	nd	nd
C2-1-CT-L	352	0.674	0.060	nd	nd
C2-4-MFT-U	352	1.66	0.161	nd	nd
C2-4-MFT-L	352	1.71	0.149	nd	nd
C2-4-CT-U	352	0.730	0.092	nd	nd
C2-4-CT-L	352	0.228	0.075	nd	nd
C2-6-MFT-U	352	1.12	0.148	nd	nd
C2-6-MFT-L	352	1.62	0.108	nd	nd
C2-6-CT-U	352	1.08	0.057	nd	nd
C2-6-CT-L	352	0.718	0.043	nd	nd

Table B-12. *(continued)*

Sample	t_{incu} (d)	Trapped gas analysis (vol%)			
		CH_4	CO_2	C_2H_4	H_2S
System 3 (Cap water/MFT)					
C3-1-MFT-U	28	0.383	0.196	nd	nd
C3-1-MFT-L	28	0.139	0.154	0.049	nd
C3-2-MFT-U	61	0.857	0.104	nd	nd
C3-2-MFT-L	61	1.06	0.122	nd	0.011
C3-3-MFT-U	90	0.457	0.164	nd	nd
C3-3-MFT-L	90	1.24	0.130	0.012	nd
C3-4-MFT-U	120	1.14	0.202	0.060	nd
C3-4-MFT-L	120	0.631	0.025	0.030	0.072
C3-5-MFT-U	152	0.399	0.291	0.357	0.102
C3-5-MFT-L	152	0.051	0.275	0.099	nd
C3-6-MFT-U	181	0.033	0.180	nd	nd
C3-6-MFT-L	181	0.149	0.524	0.119	nd
C3-7-MFT-U	212	0.058	0.284	nd	nd
C3-7-MFT-L	212	0.070	0.136	0.031	0.046
C3-8-MFT-U	243	nd	0.107	nd	nd
C3-8-MFT-L	243	0.101	0.117	nd	nd
C3-9-MFT-U	266	0.161	0.089	nd	nd
C3-9-MFT-L	266	0.150	0.103	nd	0.011
C3-10-MFT-U	302	0.138	0.143	nd	nd
C3-10-MFT-L	302	0.142	0.137	nd	nd
C3-11-MFT-U	334	0.585	0.129	nd	nd
C3-11-MFT-L	334	0.513	0.114	nd	nd
C3-12-MFT-U	365	0.233	0.129	nd	nd
C3-12-MFT-L	365	nd	0.603	nd	nd

Table B-12. *(continued).*

Sample	t_{incu} (d)	Trapped gas analysis (vol%)			
		CH_4	CO_2	C_2H_4	H_2S
System 4 (Cap water/CT)					
C4-1-CT-U	28	nd	0.021	0.023	nd
C4-1-CT-L	28	0.034	0.242	nd	0.062
C4-2-CT-U	61	0.037	0.277	0.255	nd
C4-2-CT-L	61	nd	0.133	nd	nd
C4-3-CT-U	90	0.031	0.311	0.071	0.010
C4-3-CT-L	90	nd	0.143	0.020	nd
C4-4-CT-U	120	0.135	0.082	nd	nd
C4-4-CT-L	120	0.277	0.093	nd	nd
C4-5-CT-U	152	0.085	0.387	0.090	nd
C4-5-CT-L	152	nd	0.152	0.025	nd
C4-6-CT-U	181	nd	0.343	0.089	0.018
C4-6-CT-L	181	nd	0.332	0.008	nd
C4-7-CT-U	212	0.078	0.293	0.193	nd
C4-7-CT-L	212	nd	0.316	0.052	1.10
C4-8-CT-U	243	0.069	0.086	nd	nd
C4-8-CT-L	243	nd	0.088	nd	nd
C4-9-CT-U	266	nd	0.104	nd	nd
C4-9-CT-L	266	0.041	0.103	nd	nd
C4-10-CT-U	302	0.051	0.127	nd	nd
C4-10-CT-L	302	0.047	0.125	nd	nd
C4-11-CT-U	334	0.084	0.068	nd	nd
C4-11-CT-L	334	0.195	0.053	nd	nd
C4-12-CT-U	365	1.12	0.165	nd	nd
C4-12-CT-L	365	0.171	0.369	nd	nd

1). Using Micro-GC and the GC parameters at Table 4-2 with 30 s sampling time.
2). nd=non-detectable.

Table B-13. MPN analyses on MFT and CT samples of System 1.

Sample	t_{incu} (d)	Methanogen MPN/g of dry solids	SRB MPN/g of dry solids
Base CT 1	0	1.57E+02	1.57E+05
Base CT 2	0	1.40E+01	1.50E+06
Base MFT 1	0	2.24E+03	1.97E+03
C1-3-CT-M	15	1.15E+03	6.80E+04
C1-3-MFT-U	15	5.04E+03	5.42E+05
C1-3-MFT-L	15	2.28E+03	4.83E+05
C1-4-CT-M	29	5.44E+03	3.09E+05
C1-4-MFT-L	29	5.75E+03	4.98E+05
C1-4-MFT-U	29	8.14E+03	2.00E+06
C1-5-CT-M	62	1.16E+03	1.22E+05
C1-5-MFT-L	62	1.95E+05	9.86E+05
C1-5-MFT-U	62	2.11E+05	5.09E+05
C1-12-CT-M	121	1.14E+04	2.84E+04
C1-12-MFT-L	121	5.22E+04	5.48E+05
C1-12-MFT-U	121	2.94E+03	8.46E+05
C1-9-CT-M	182	4.96E+03	2.75E+04
C1-9-MFT-L	182	4.67E+03	9.16E+05
C1-9-MFT-U	182	5.99E+05	1.08E+06
C1-11-CT-M	244	5.26E+04	2.81E+04
C1-11-MFT-L	244	8.62E+04	2.14E+06
C1-11-MFT-U	244	1.99E+05	5.36E+05
C1-14-CT-M	303	2.95E+04	2.51E+03
C1-14-MFT-L	303	5.18E+04	1.92E+06
C1-14-MFT-U	303	2.61E+05	2.34E+05
C1-16-CT-M	366	2.67E+04	9.76E+02
C1-16-MFT-L	366	4.96E+05	4.44E+06
C1-16-MFT-U	366	4.89E+05	4.09E+04

Appendix C. Discussion

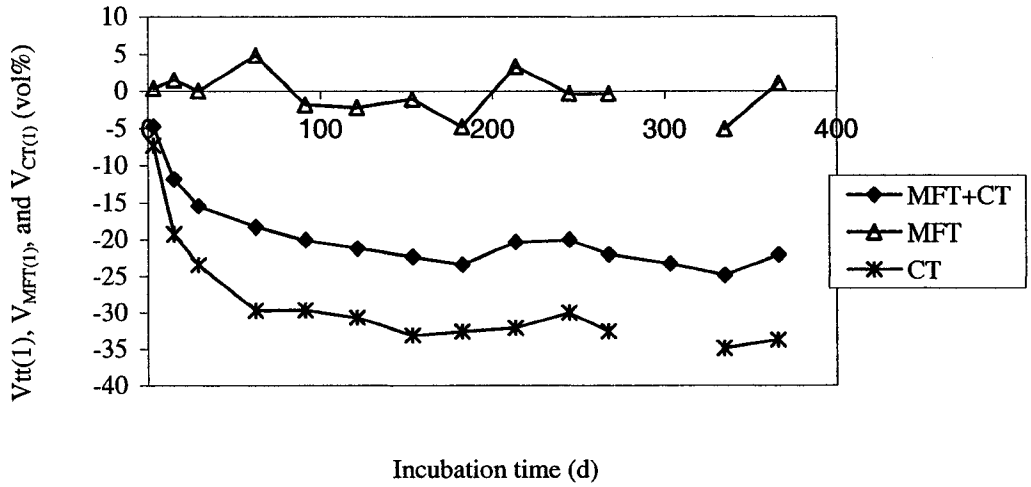

Figure C-1. Total and individual tailings volume changes (Vtt, V_{MFT}, and V_{CT}) in System 1.

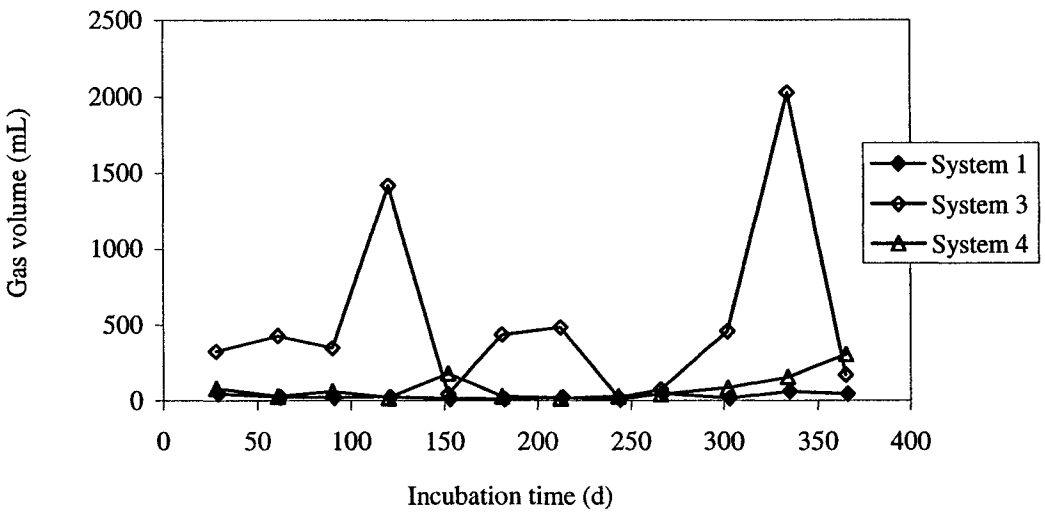

Figure C-2. Tedlar bag gas volumes in Systems 1, 3, and 4.

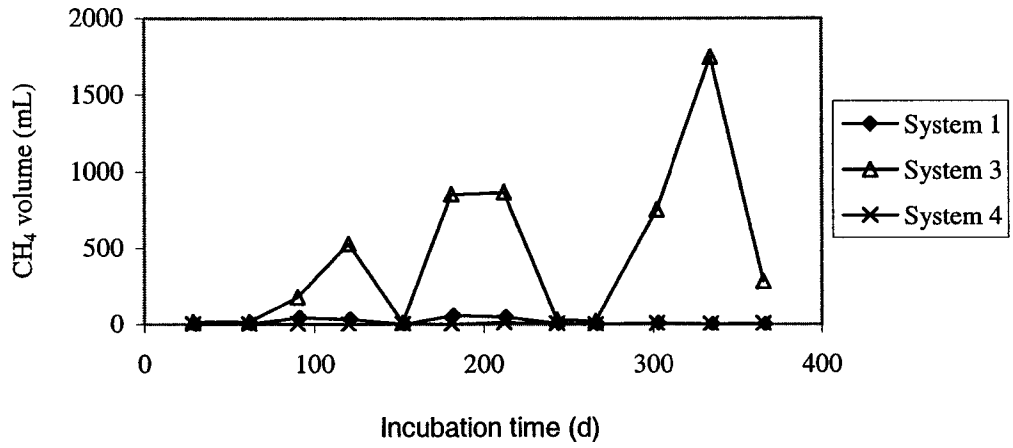

Figure C-3. Total CH_4 volumes in the Tedlar bag and column headspace of Systems 1, 3, and 4.

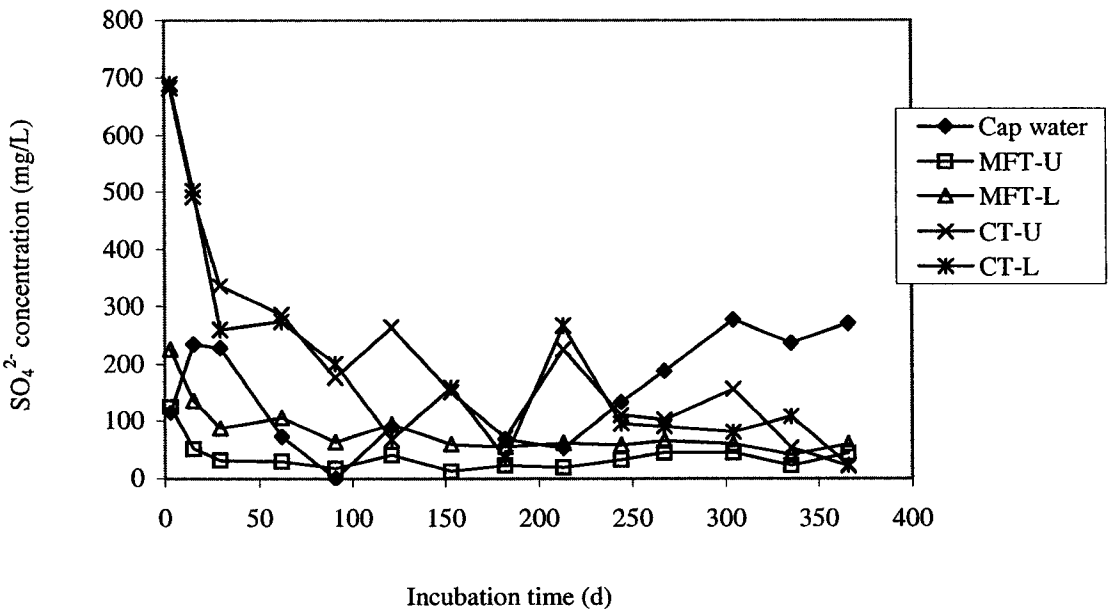

Figure C-4. SO_4^{2-} concentrations in System 1.

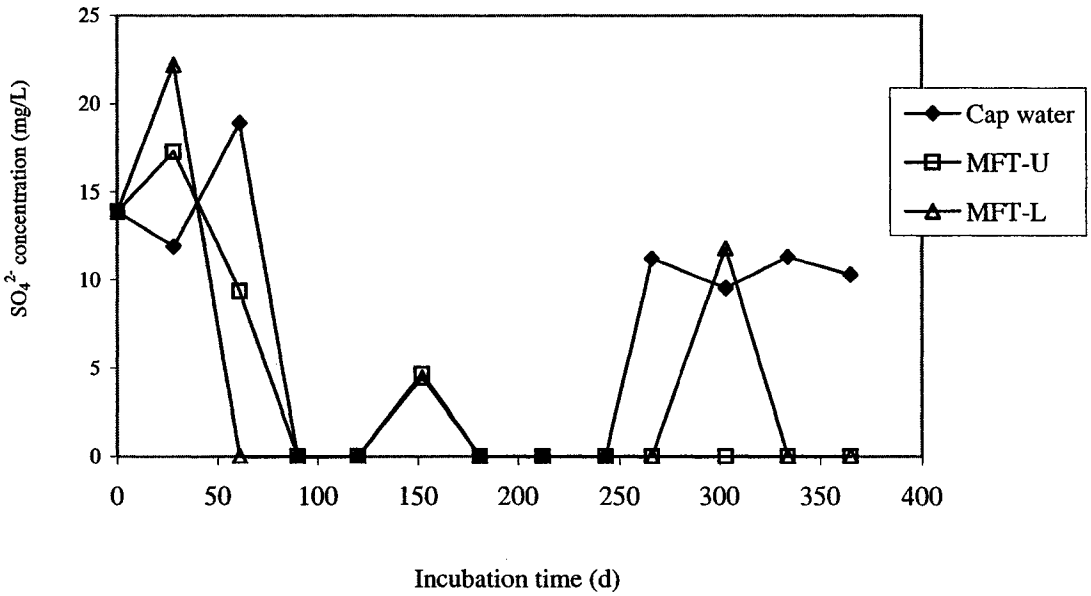

Figure C-5. SO_4^{2-} concentrations in System 3.

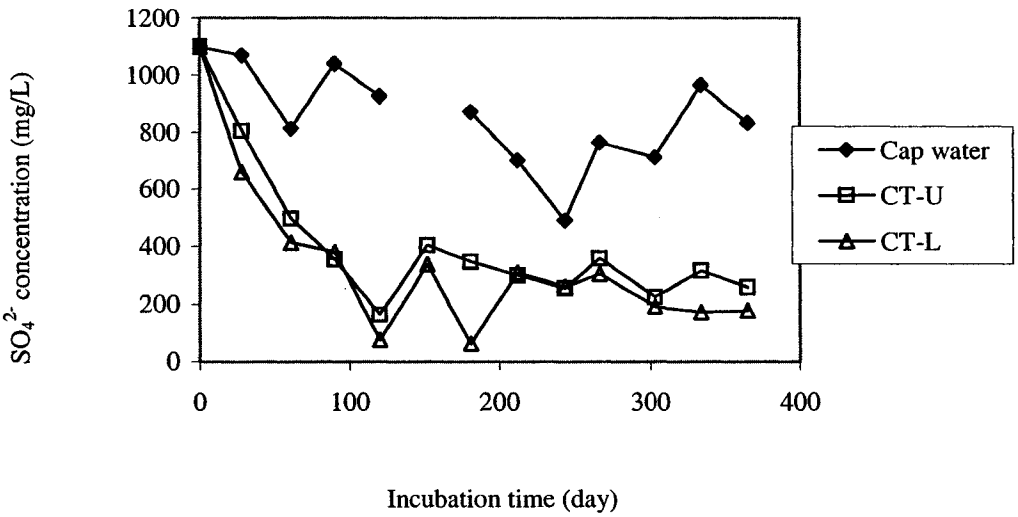

Figure C-6. SO_4^{2-} concentrations in System 4.

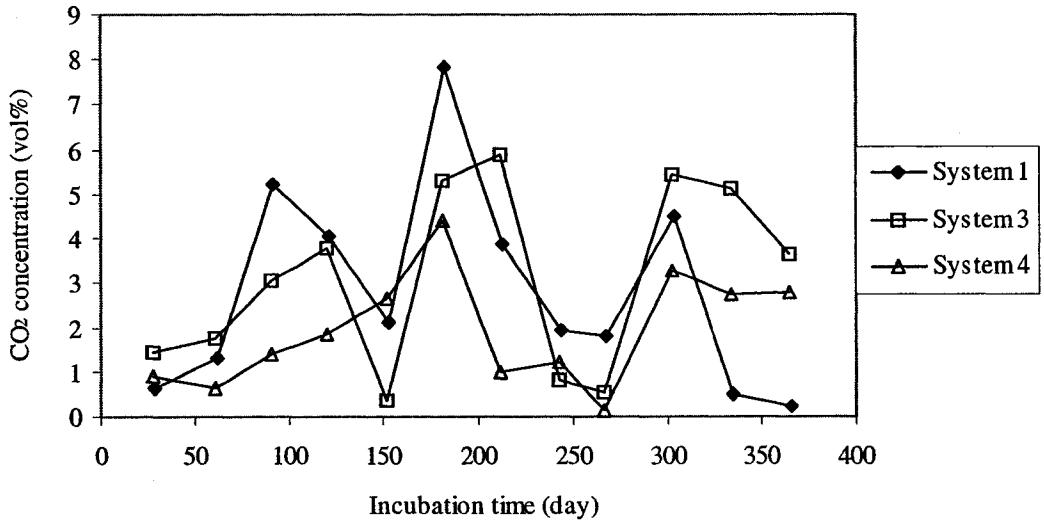

Figure C-7. CO_2 concentrations in the headspace of Systems 1, 3, and 4.

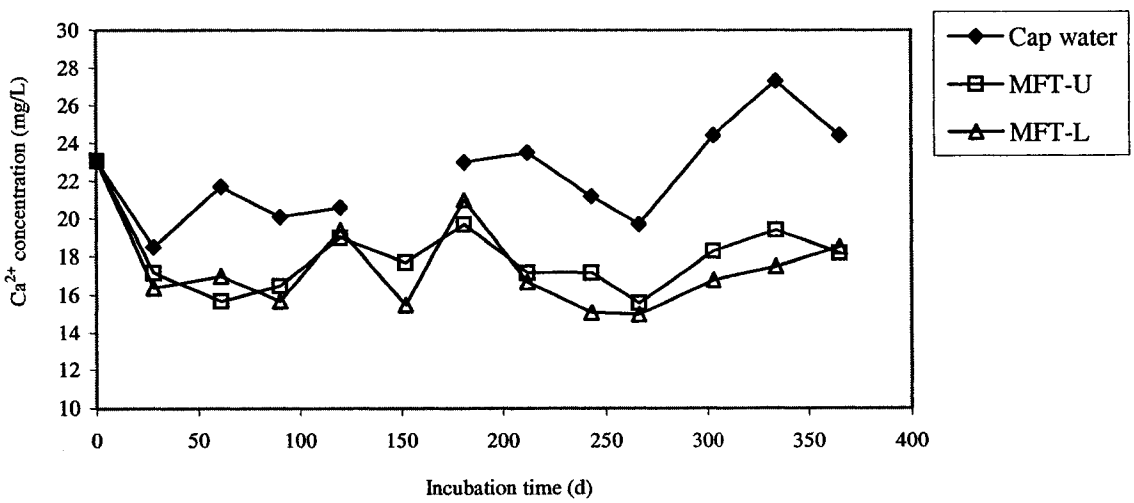

Figure C-8. Ca^{2+} concentrations in System 3.

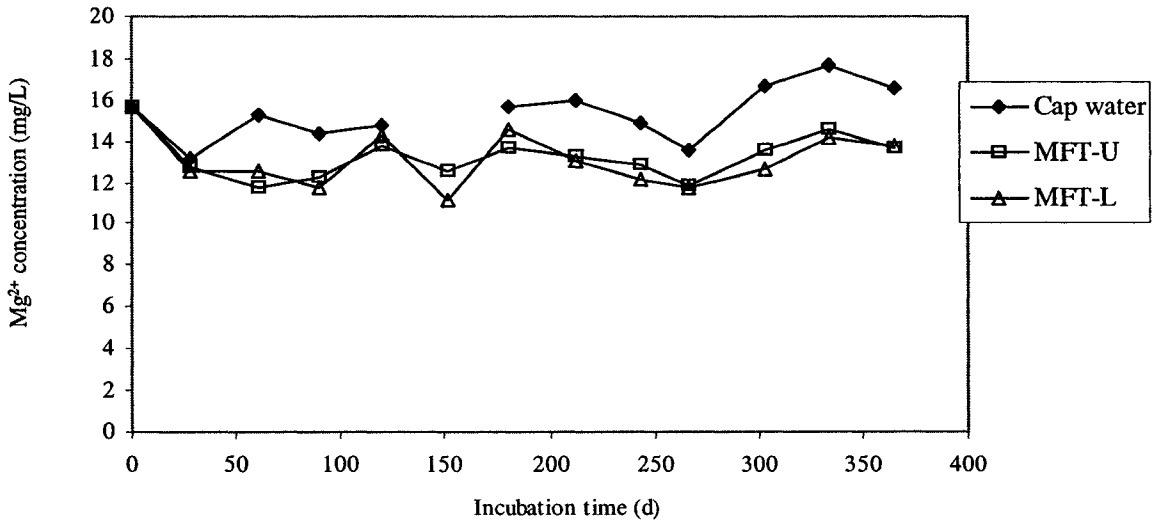

Figure C-9. Mg^{2+} concentrations in System 3.

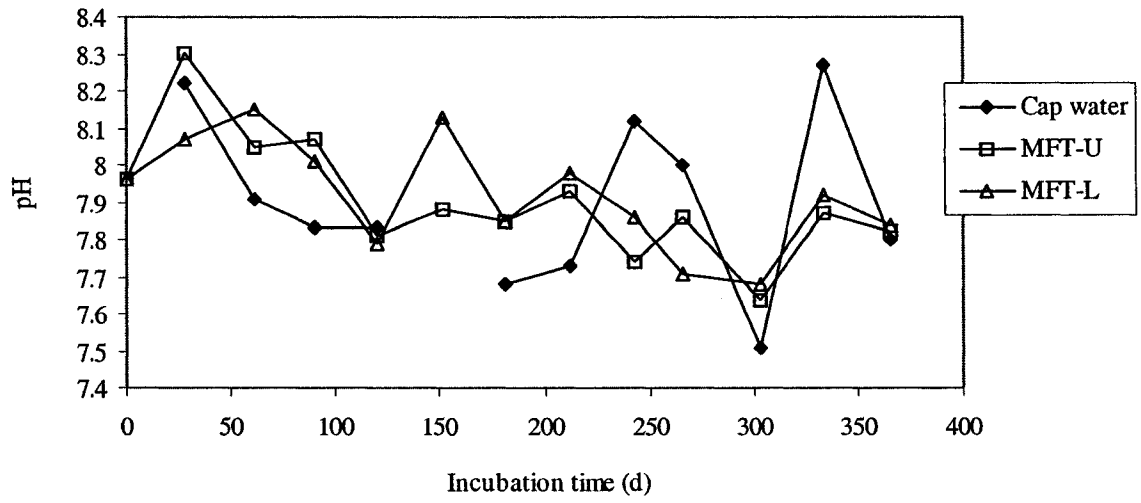

Figure C-10. pHs in System 3.

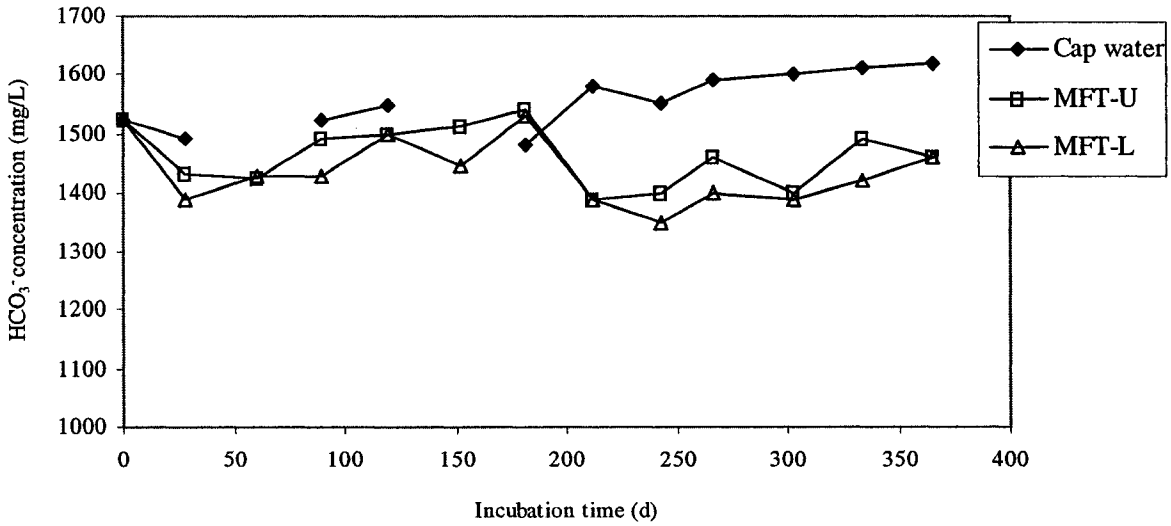

Figure C-11. HCO_3^- concentrations in System 3.

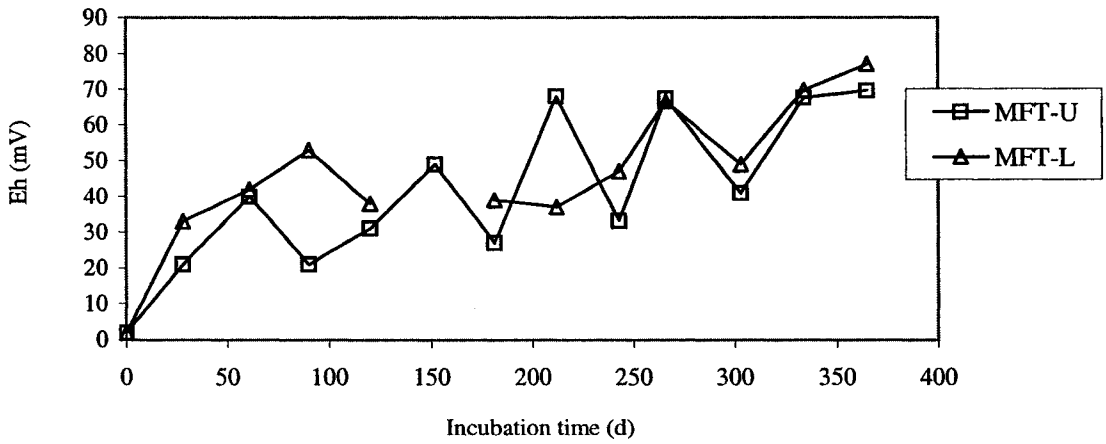

Figure C-12. Redox potentials in System 3.

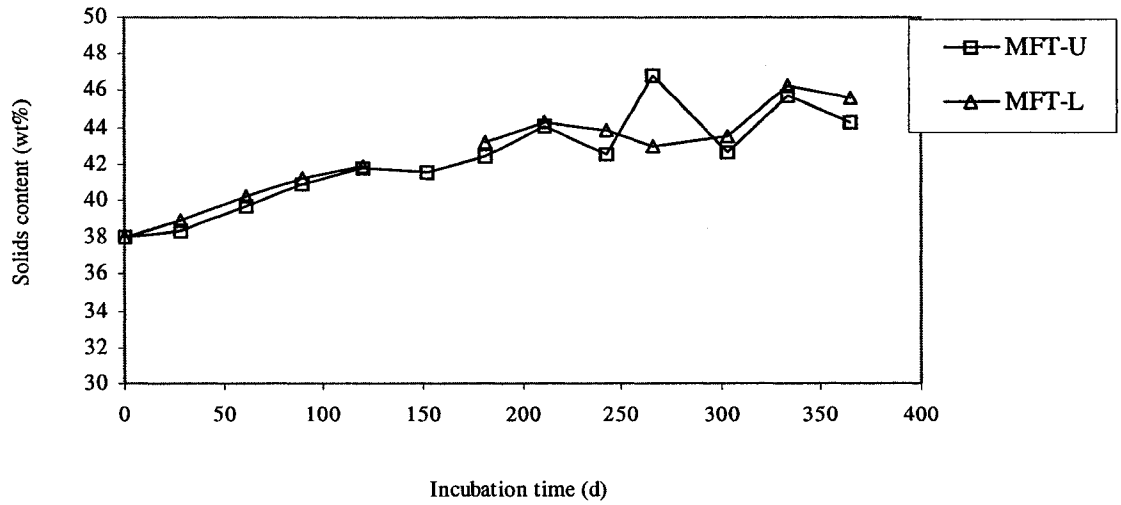

Figure C-13. Solids contents in System 3.

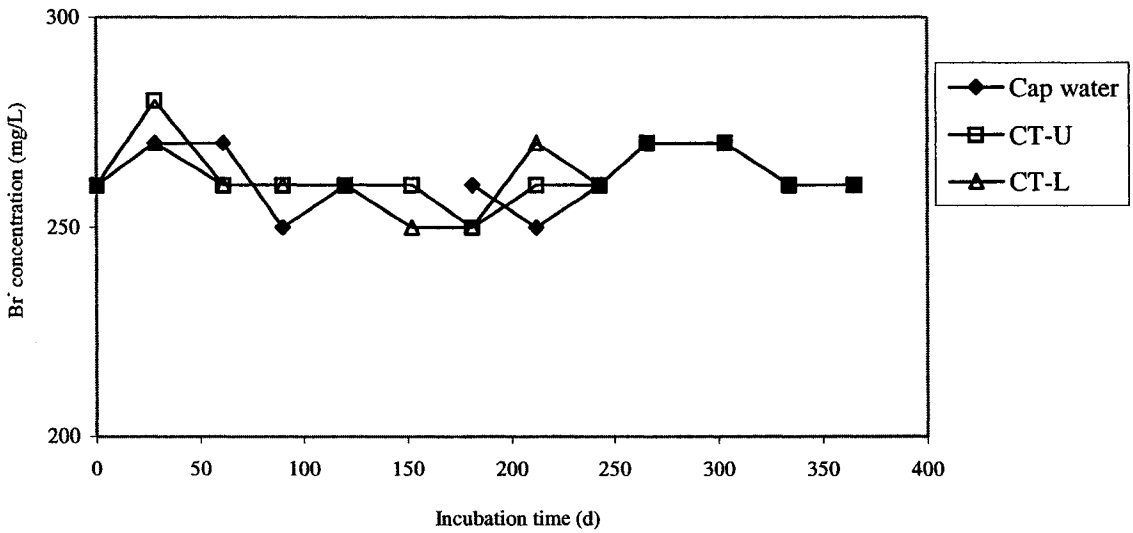

Figure C-14. Br^- concentrations in System 4.

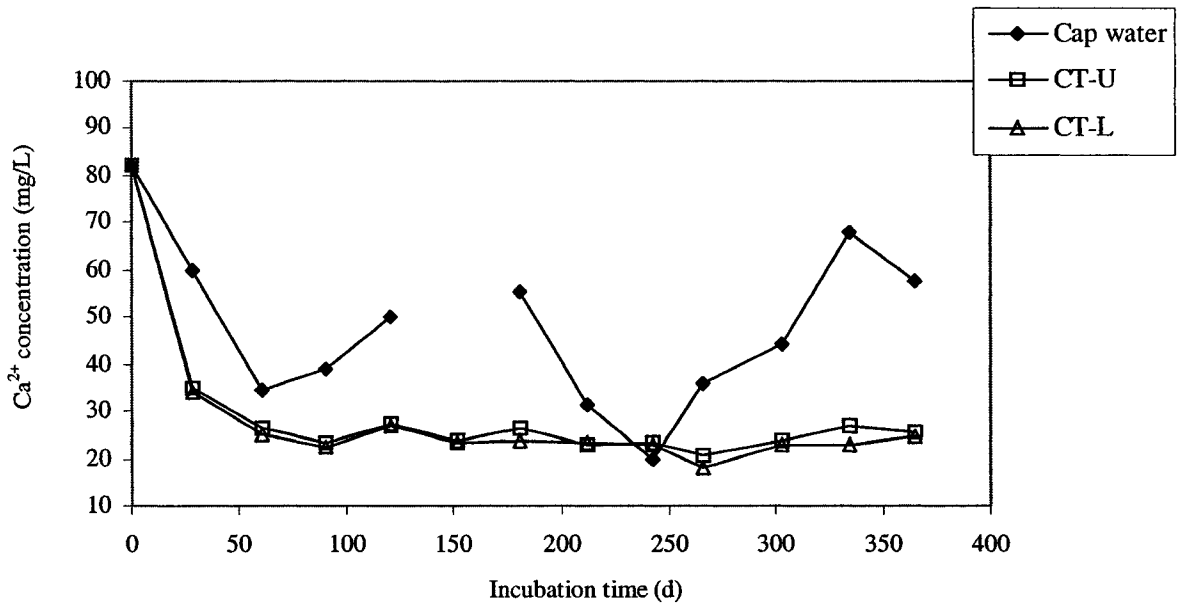

Figure C-15. Ca^{2+} concentrations in System 4.

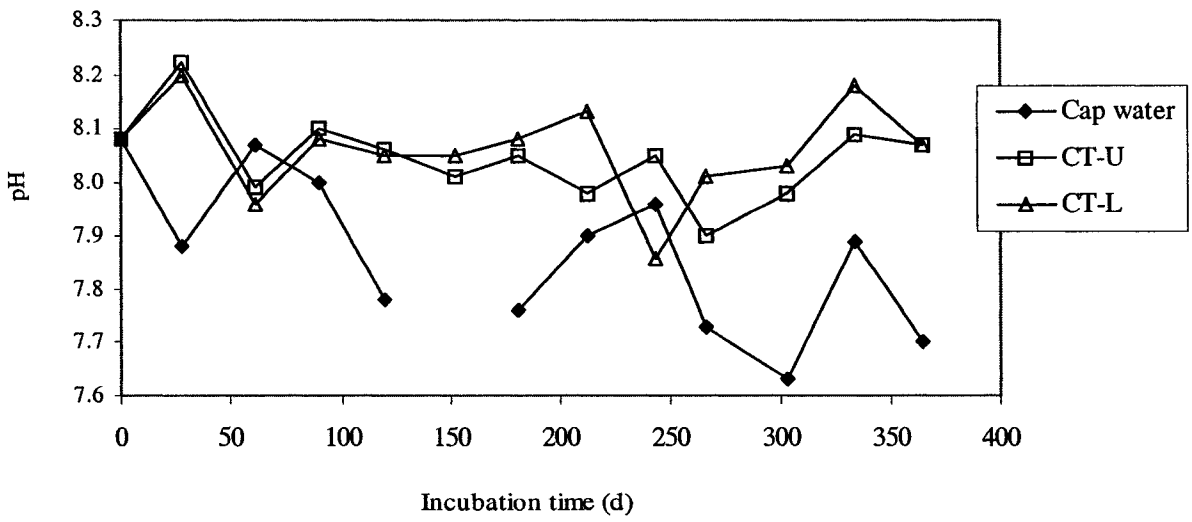

Figure C-16. pHs in System 4.

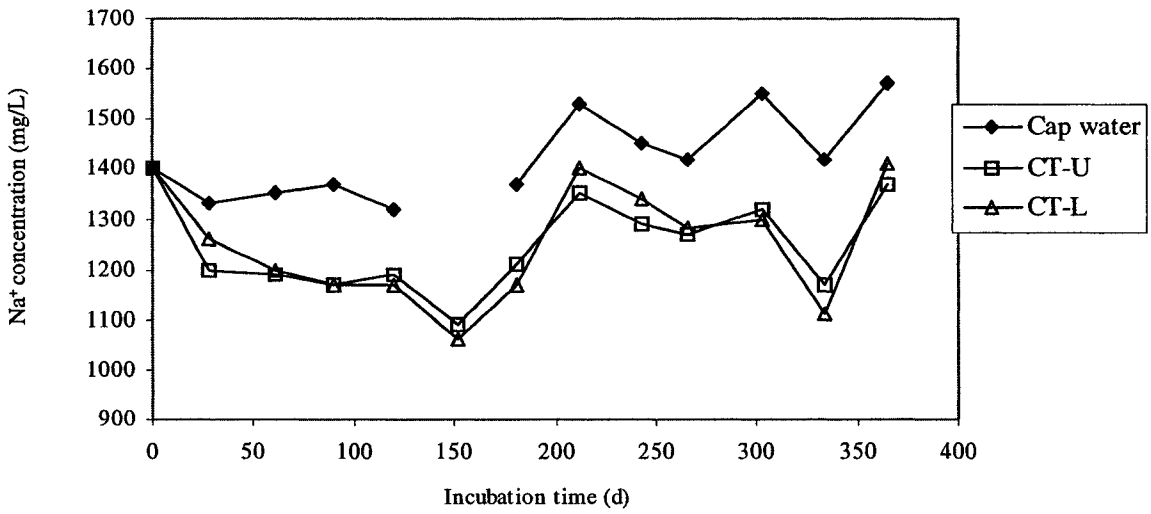

Figure C-17. Na^+ concentrations in System 4.

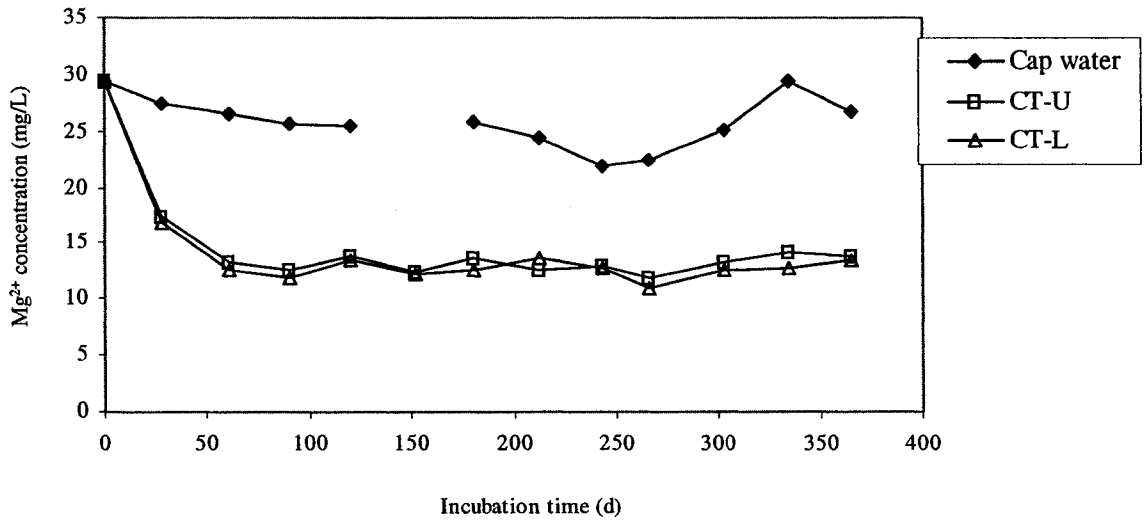

Figure C-18. Mg^{2+} concentrations in System 4.

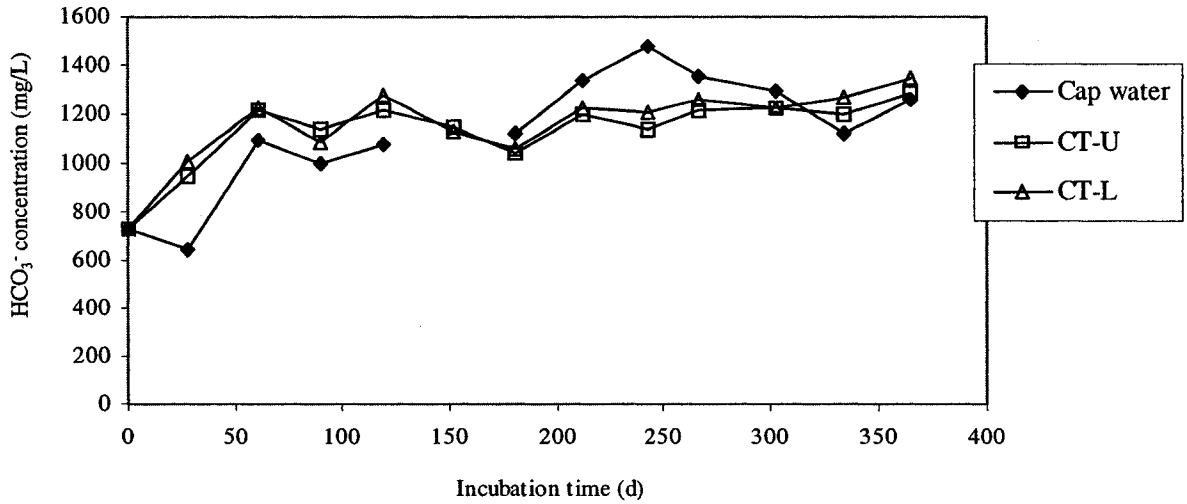

Figure C-19. HCO_3^- concentrations in System 4.

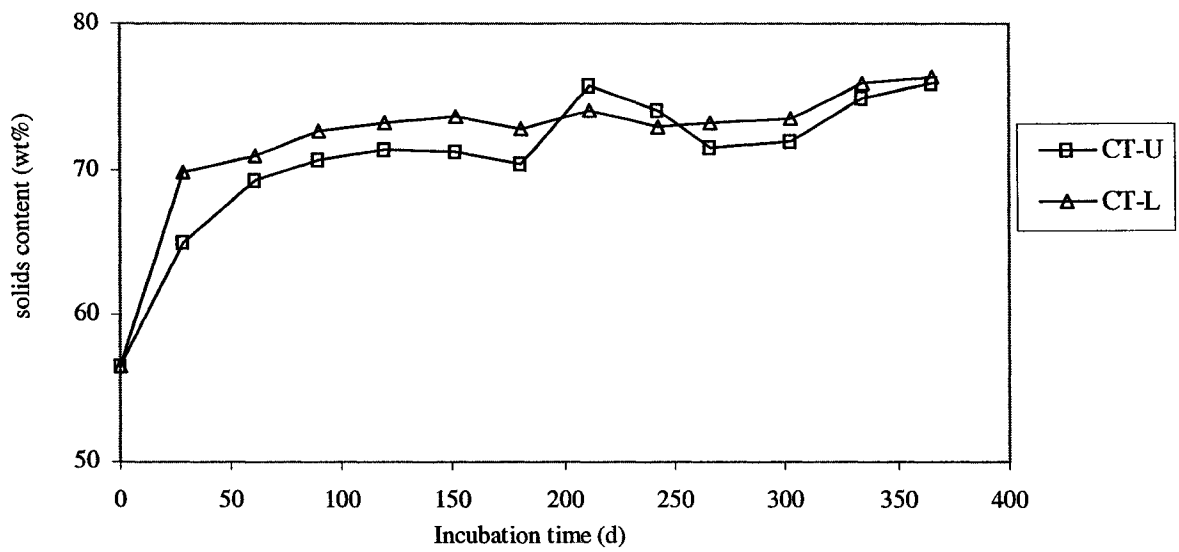

Figure C-20. Solids contents in System 4.

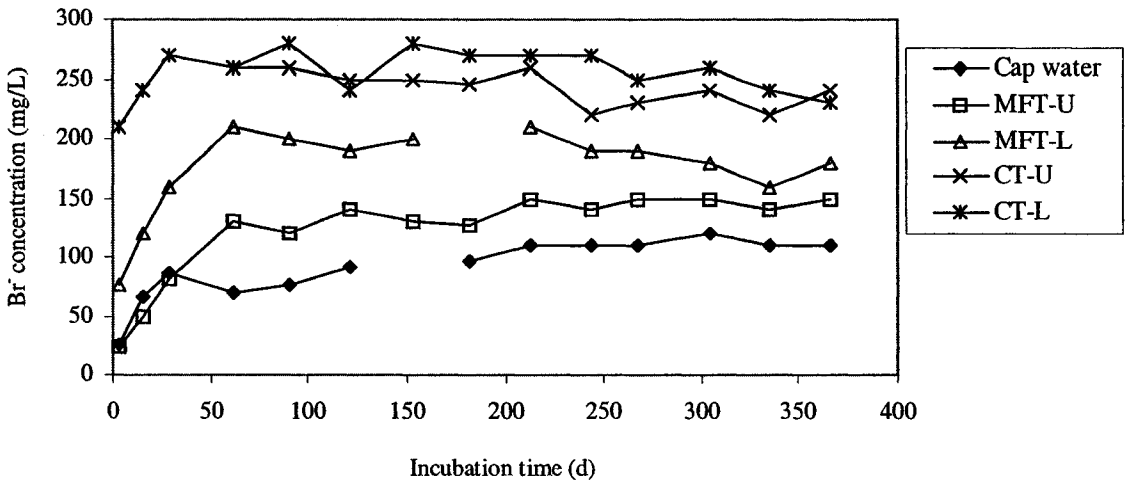

Figure C-21. Br^- concentrations in System 1.

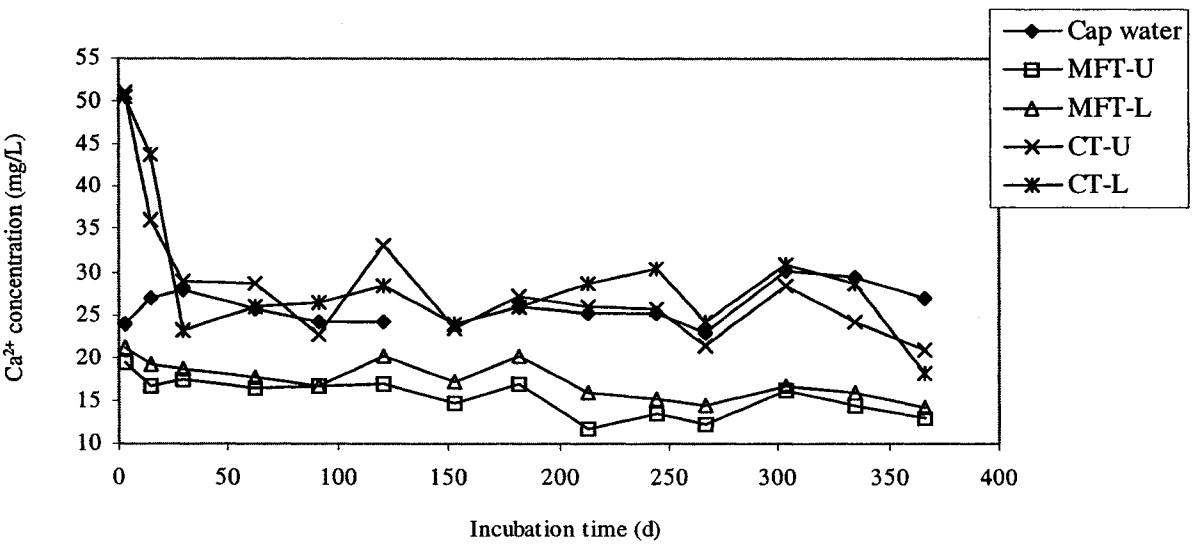

Figure C-22. Ca^{2+} concentrations in System 1.

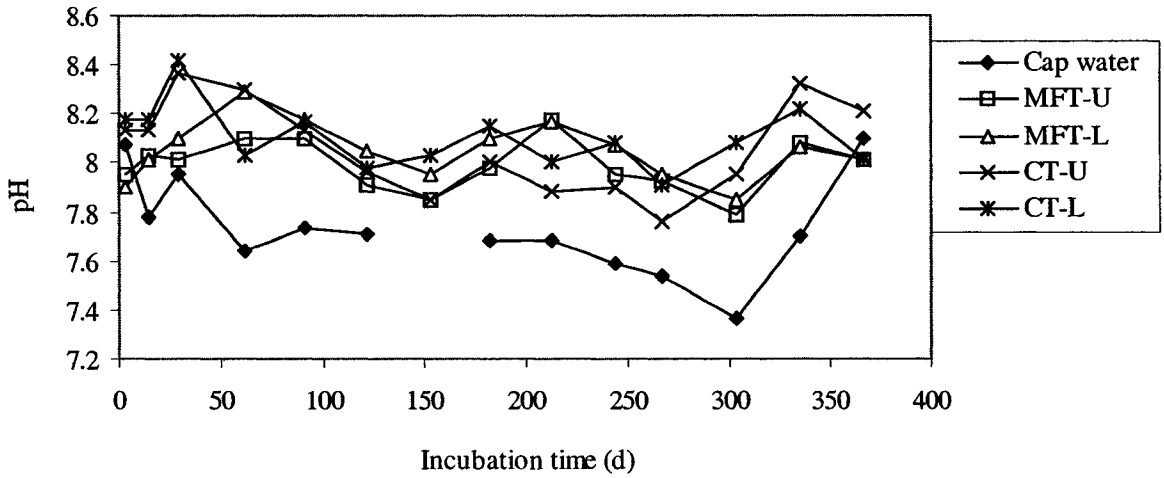

Figure C-23. pHs in System 1.

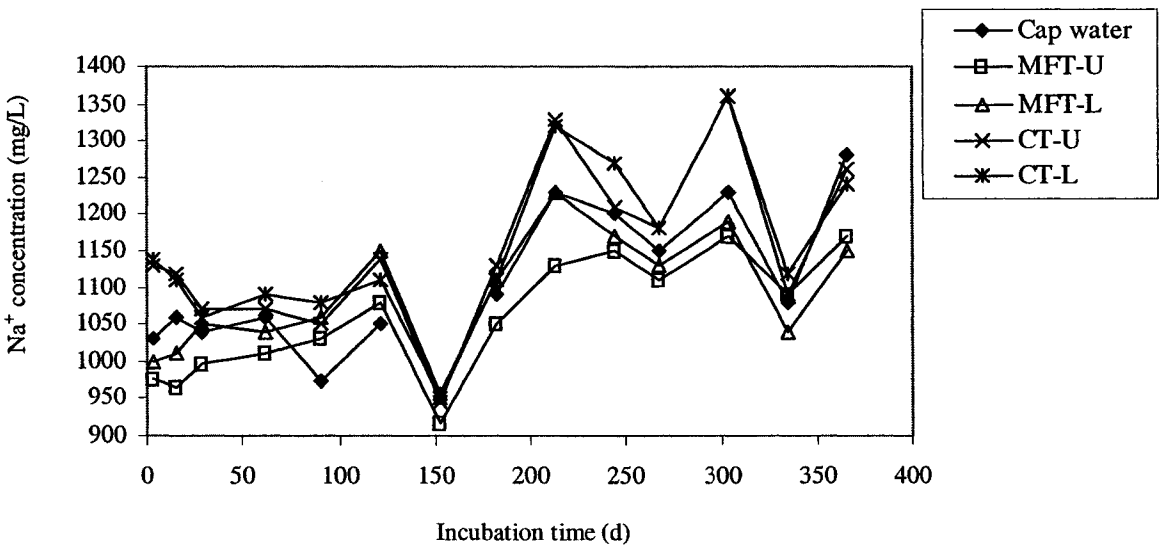

Figure C-24. Na^+ concentrations in System 1.

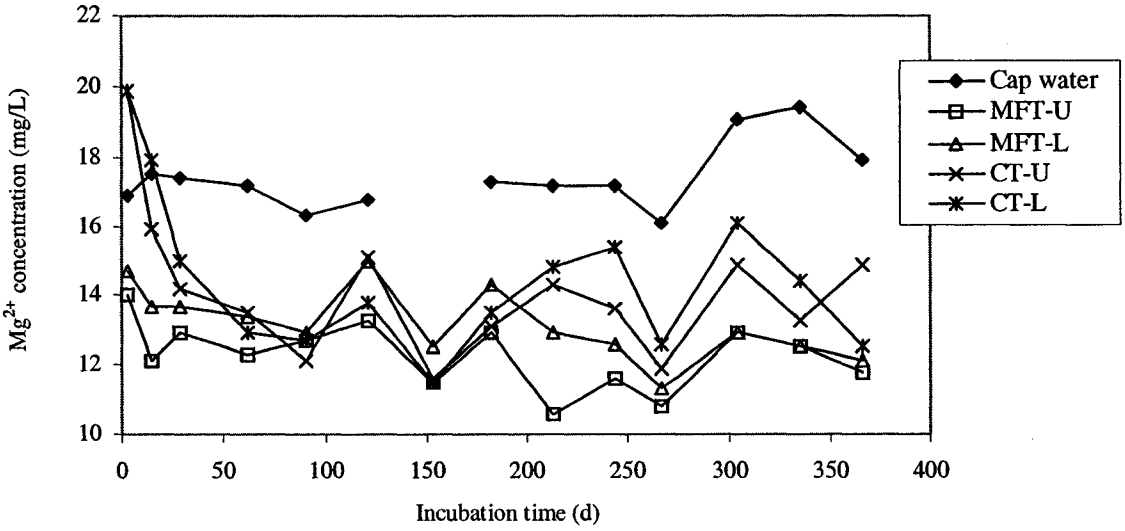

Figure C-25. Mg^{2+} concentrations in System 1.

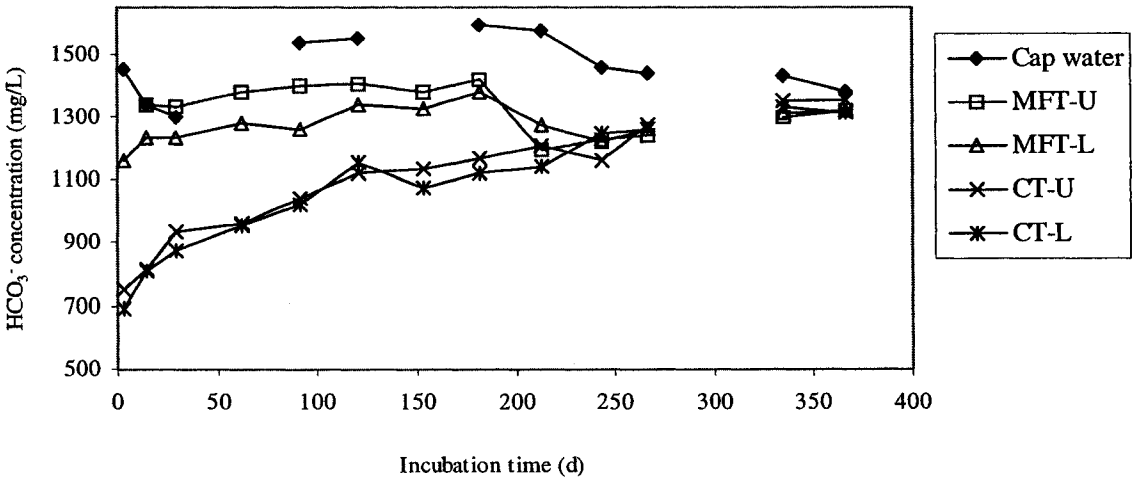

Figure C-26. HCO_3^- concentrations in System 1.

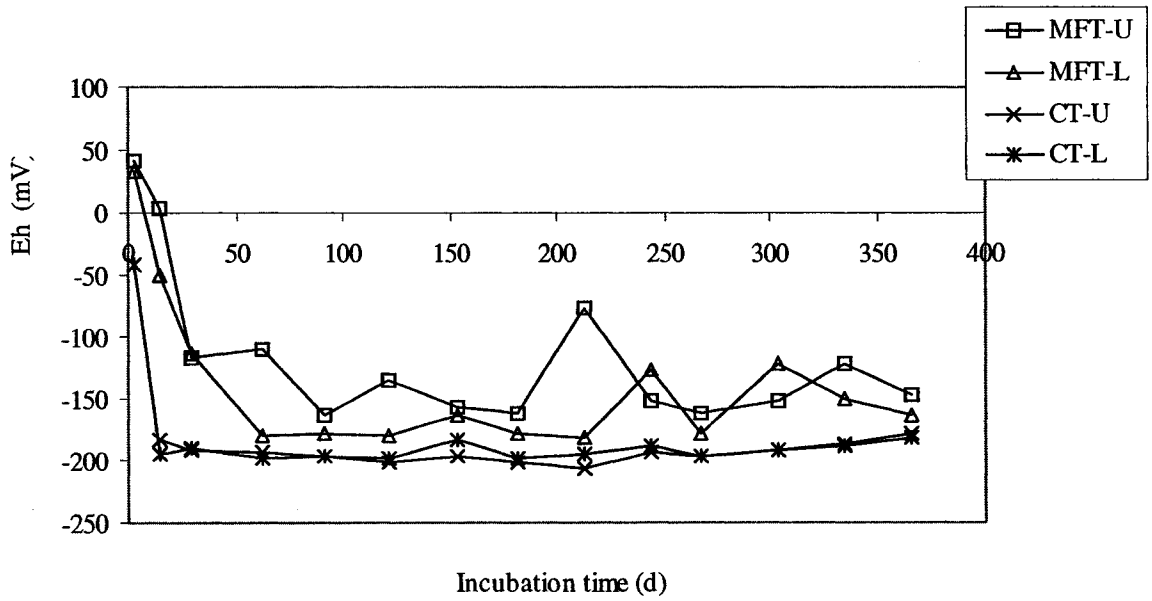

Figure C-27. Redox potentials in System.

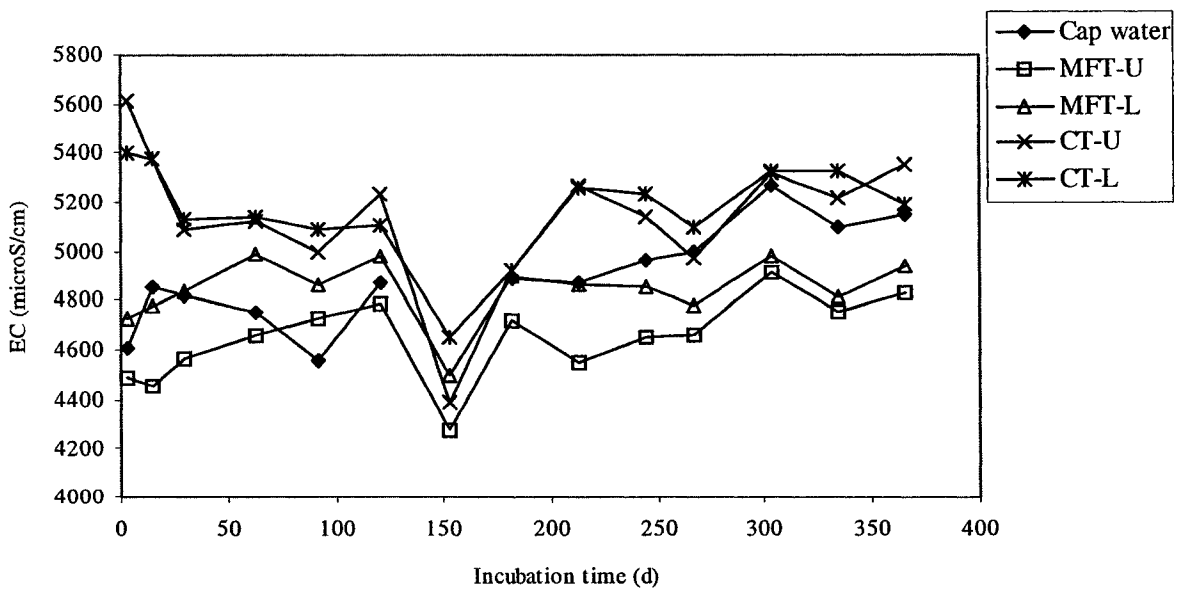

Figure C-28. Electrical conductivities in system 1.

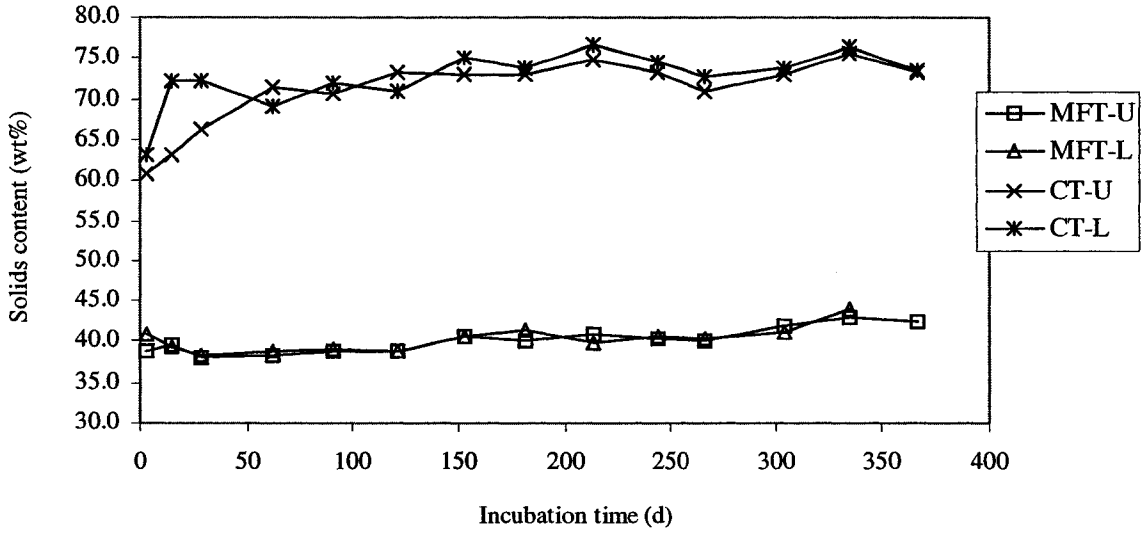

Figure C-29. Solids contents in System 1.

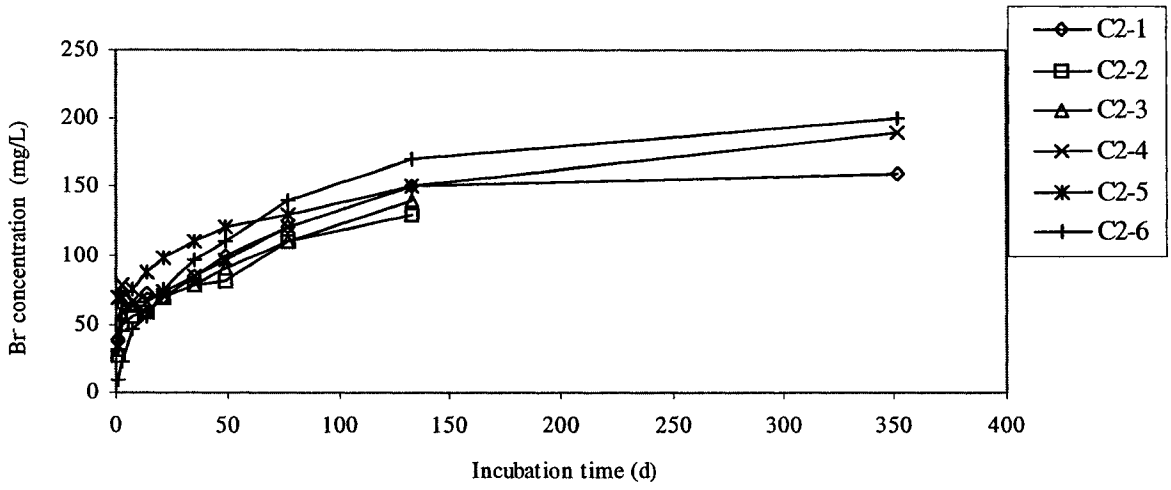

Figure C-30. Br^- concentrations in the cap water of System 2.

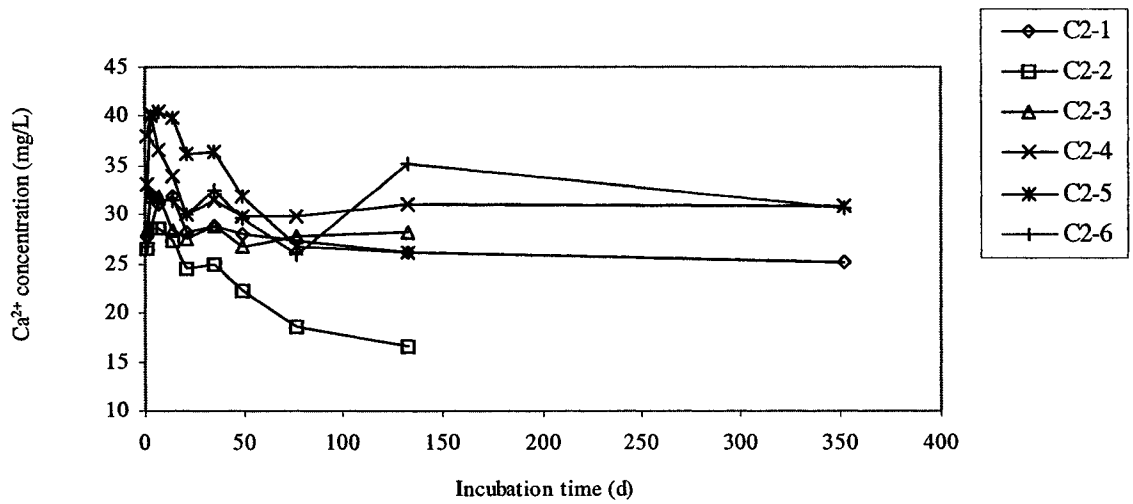

Figure C-31. Ca^{2+} concentrations in the cap water of System 2.

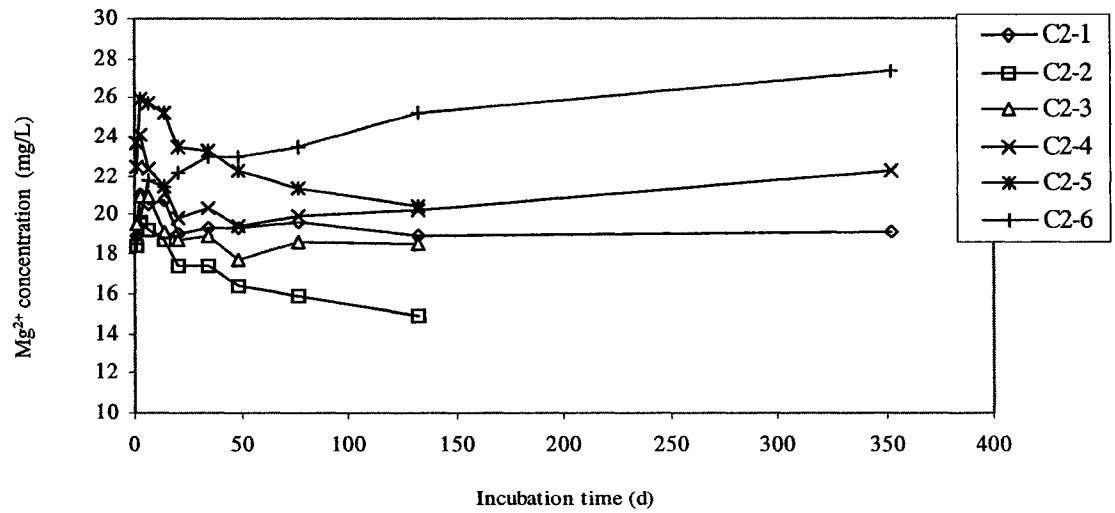

Figure C-32. Mg^{2+}concentrations in the cap water of System 2.

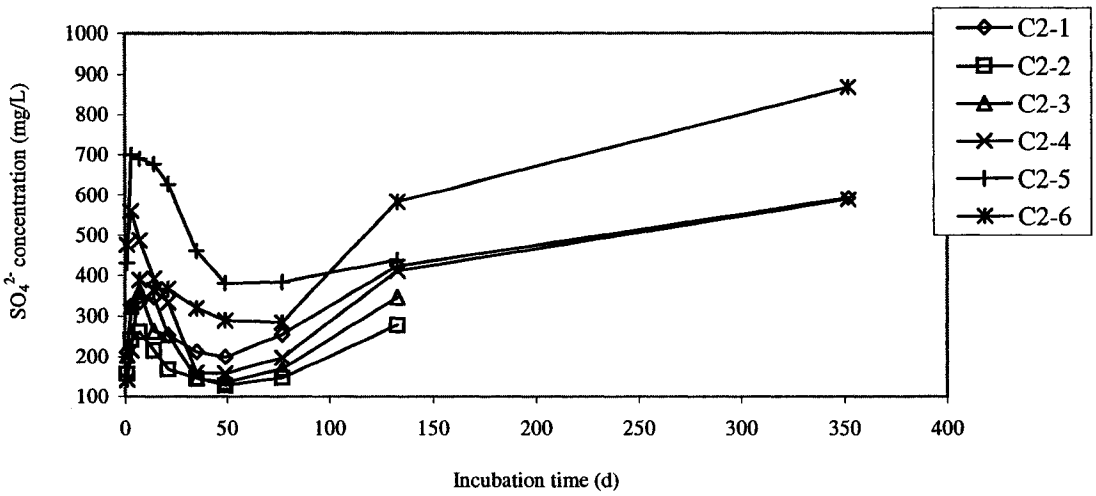

Figure C-33. SO_4^{2-} concentrations in the cap water of System 2.

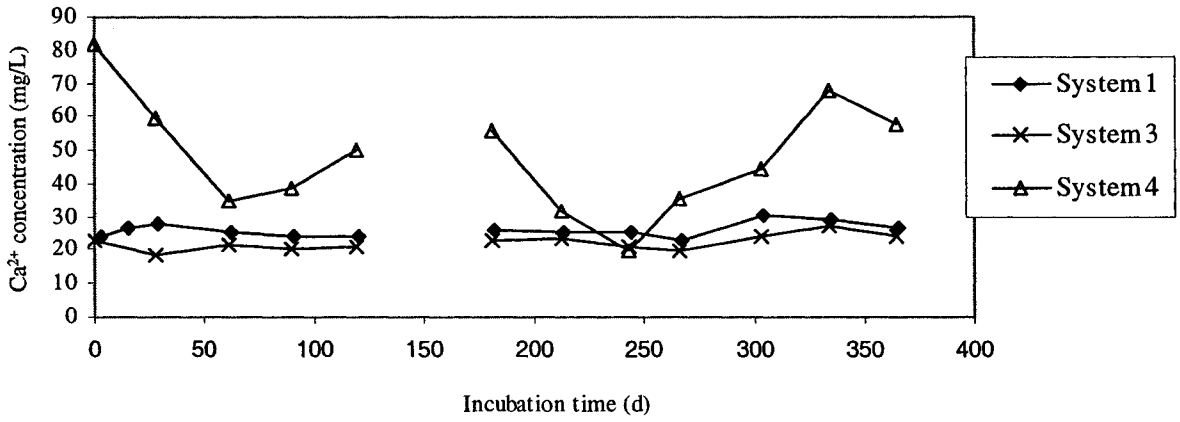

Figure C-34. Ca^{2+} concentrations in the cap water of Systems 1, 3, and 4.

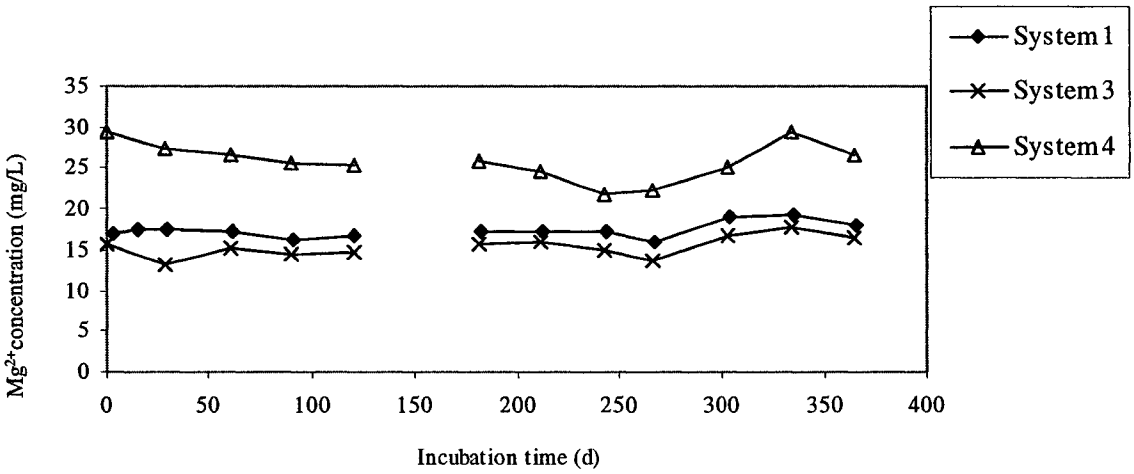

Figure C-35. Mg^{2+} concentrations in the cap water of Systems 1, 3, and 4.

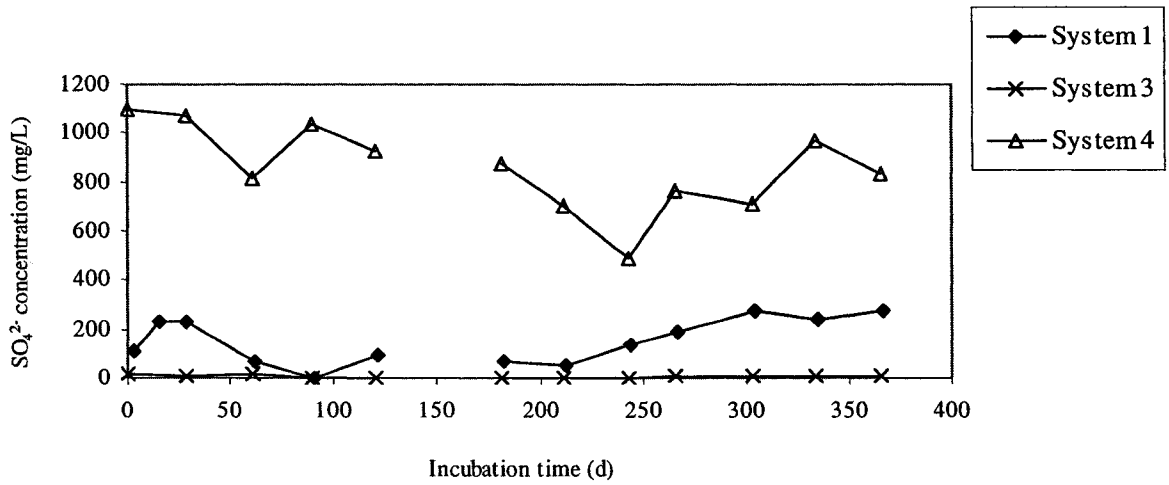

Figure C-36. SO_4^{2-} concentrations in the cap water of Systems 1, 3, and 4.

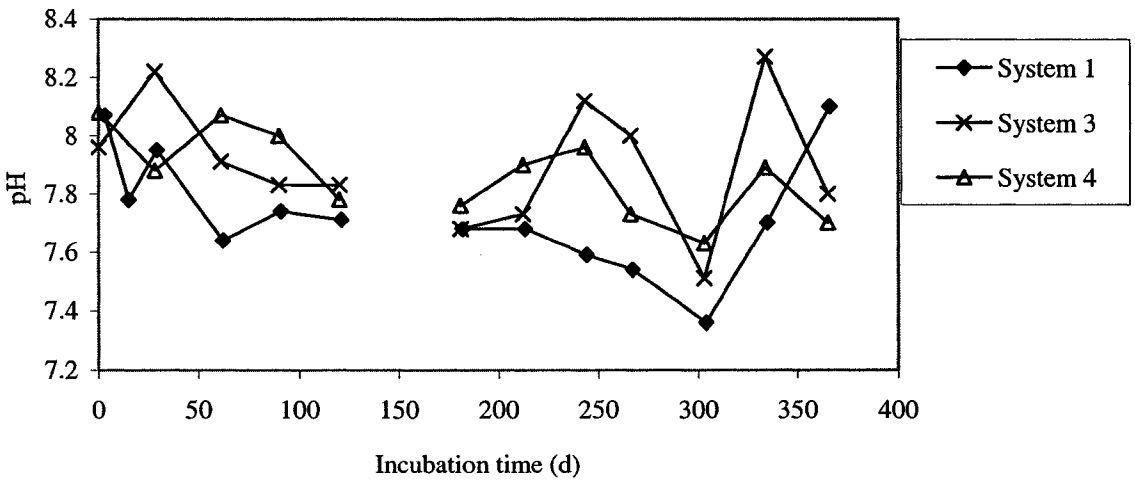

Figure C-37. pHs in the cap water of Systems 1, 3, and 4.

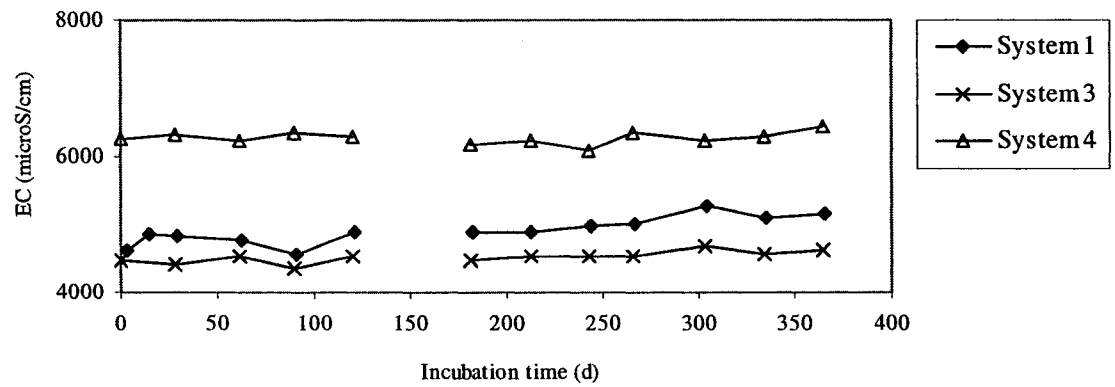

Figure C-38. Electrical conductivities in the cap water of Systems 1, 3, and 4.

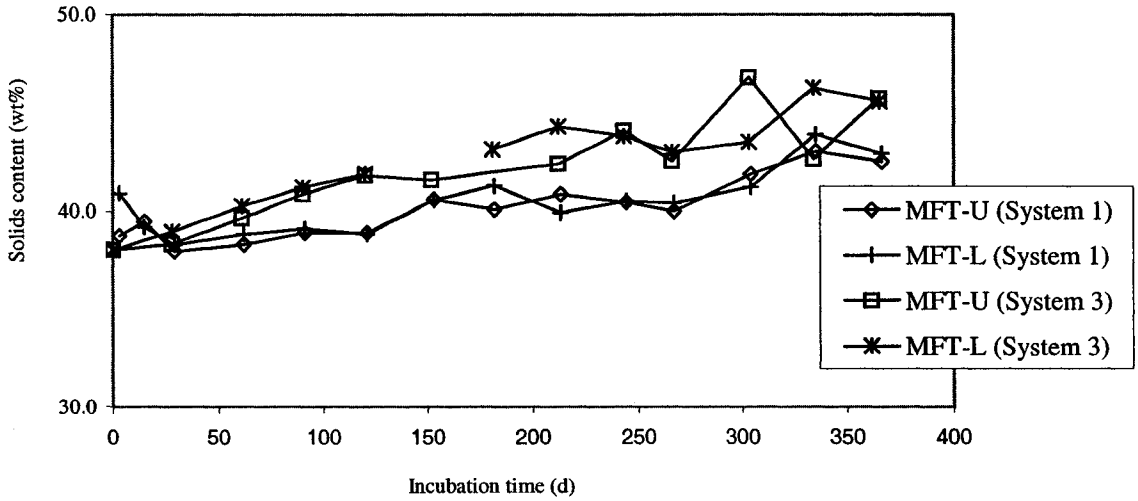

Figure C-39. Solids contents of MFT in Systems 1 and 3.

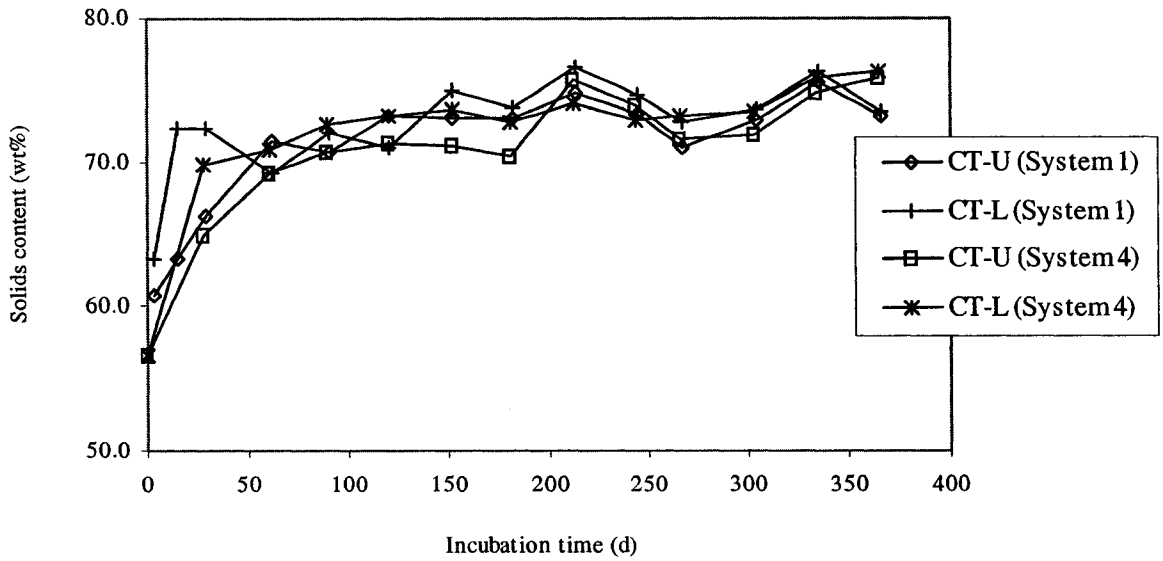

Figure C-40. Solids contents of CT in Systems 1 and 4.

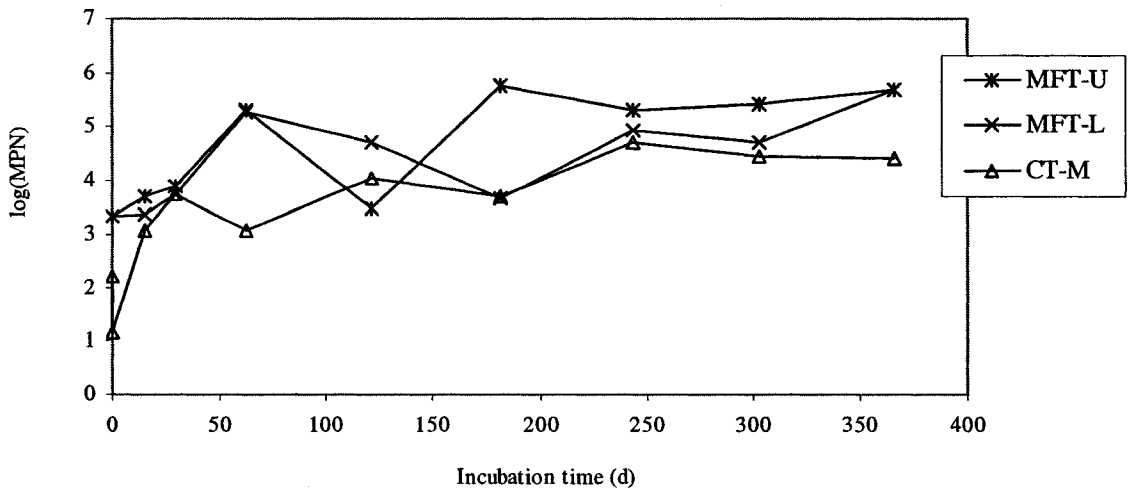

Figure C-41. MPN of Methanogens in System 1.

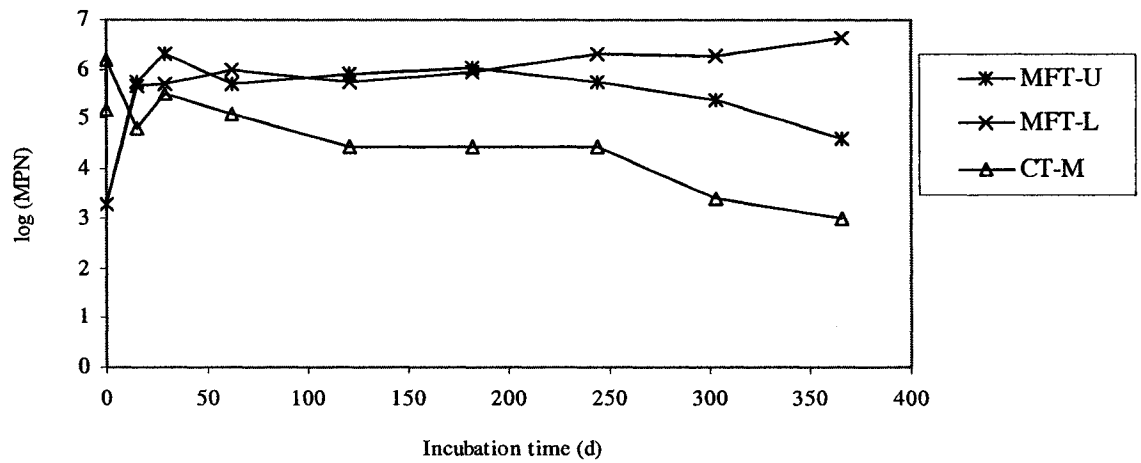

Figure C-42. MPN of SRB in System 1.

Table C-1. Comparison of CO_2 concentrations in the headspace of System 1 between the calculated concentrations by Henry's law and the measured concentrations by GC.

Column	t_{incu} (d)	$[H_2CO_3^*]$ in cap water (M)	Calculated Pco_2 in headspace (atm)	Calculated CO_2 concentration in headspace (vol%)	Measured CO_2 concentration in headspace (vol%)
C1-4	29	5.6E-04	1.8E-02	1.76	0.64
C1-5	62	NA	NA	NA	1.29
C1-6	91	1.1E-03	3.4E-02	3.38	5.23
C1-12	121	1.2E-03	3.6E-02	3.64	4.03
C1-8	153	NA	NA	NA	2.10
C1-9	182	1.3E-03	4.0E-02	4.02	7.82
C1-10	213	1.3E-03	4.0E-02	3.98	3.88
C1-11	244	1.4E-03	4.5E-02	4.52	1.96
C1-13	267	1.6E-03	5.0E-02	5.01	1.78
C1-14	304	NA	NA	NA	4.50
C1-15	335	1.1E-03	3.4E-02	3.44	0.50
C1-16	366	4.2E-04	1.3E-02	1.32	0.24

1). Assuming the total gas pressure in the headspace is 1 atm.
2). NA=not available.

Table C-2. Empirical estimations of masses of solids and porewater per unit volume of MFT or CT at specific solids content.

Solids content of MFT or CT (wt%)	ρ (density of MFT or CT) (g/L)	Mass of solids (g/L of MFT or CT)	Volume of porewater (mL/L of MFT or CT)	Solids content of MFT or CT (wt%)	ρ (density of MFT or CT) (g/L)	Mass of solids (g/L of MFT or CT)	Volume of porewater (mL/L of MFT or CT)
38	1308	497	811	58	1562	906	656
39	1319	514	805	59	1577	930	647
40	1330	532	798	60	1592	955	637
41	1341	550	791	61	1608	981	627
42	1352	568	784	62	1624	1007	617
43	1364	586	777	63	1641	1034	607
44	1375	605	770	64	1658	1061	597
45	1387	624	763	65	1675	1089	586
46	1399	644	756	66	1693	1117	576
47	1411	663	748	67	1711	1146	565
48	1424	683	740	68	1729	1176	553
49	1436	704	733	69	1748	1206	542
50	1449	725	725	70	1767	1237	530
51	1462	746	717	71	1786	1268	518
52	1476	767	708	72	1806	1301	506
53	1489	789	700	73	1827	1334	493
54	1503	812	692	74	1848	1367	480
55	1517	835	683	75	1869	1402	467
56	1532	858	674	76	1891	1437	454
57	1547	882	665	77	1914	1473	440

1). Assuming:

a). The density of water is 1 g/mL.

b). The mass of MFT or CT is the sum of the masses of solids and porewater.

c). $\rho = (1/(1-0.0062 \times wt\%)) \times 1000$ (g/L of MFT or CT).

2). Sample calculation (at solids content of 38 wt%):

a). The mass of solids = $\rho \times wt\% = 1308 \times 38\% = 497$ (g/L of MFT or CT).

b). The mass of porewater = 1308-497=811 (g/L of MFT or CT).

c). The volume of porewater =811 (mL/L of MFT or CT).

Table C-3. Empirical estimation of released and still remaining MFT waters, in originally 1 L MFT with initial MFT solids content of 38 wt%.

MFT			Waters		
Solids content (wt%)	ρ (density) (g/mL)	Volume (mL)	MFT porewater (mL)	Released MFT water (mL)	Remaining MFT porewater (vol%)
38	1.308	1000	811	0	100
39	1.319	967	778	34	96
40	1.330	935	746	65	92
41	1.341	904	715	96	88
42	1.352	876	687	125	85
43	1.364	848	659	152	81
44	1.375	822	633	178	78
45	1.387	797	608	204	75
46	1.399	773	584	228	72
47	1.411	750	561	251	69
48	1.424	728	539	273	66
49	1.436	706	517	294	64
50	1.449	686	497	314	61

1). Percent of remaining porewater (vol%) is relative to the total MFT porewater volume at solids content of 38wt%,

2). Table C-3 is adapted from the relevant table, which is provided by Dr. MacKinnon in Syncrude.